HIGHLY SELECTIVE RHODIUM–CATALYZED C–H BORYLATIONS IN PREPARATION OF SUBSTRATES FOR SUZUKI–MIYAURA CROSS–COUPLINGS: MONO– AND CHEMOSELECTIVE FORMATION OF AROMATIC COMPOUNDS

by

Brandon Dario Moore

A thesis submitted to the Department of Chemistry

In conformity with the requirements for

the degree of Master of Science

Queen's University

Kingston, Ontario, Canada

March, 2015

Abstract

The advent of the Suzuki–Miyaura cross–coupling reaction and its significance to the synthesis of new carbon–carbon bonds has increased the demand for efficient routes to organoboron starting materials. C–H borylation (activation) has provided an interesting approach to alleviate the requirement for prefunctionalized molecules such as aryl halides to obtain these desired organoboron substrates.

We report the first use of a rhodium *N*–heterocyclic carbene (NHC) complex for the catalytic C–H borylation. The reaction is found to proceed under very mild conditions (room temperature, short reaction times) and is applicable to a variety of 2–phenylpyridine (2–Ph–pyr) derivatives. Additionally, exclusive selectivity for the monoborylated product is observed with no bisborylation occurring in the reaction, which was found to be attributable to the key nitrogen–boron coordination.

The selective monoborylation was further united with a Suzuki–Miyaura cross–coupling in a one–pot reaction to produce monoarylated phenylpyridines in good overall yields with no formation of the bisarylated compounds. Commonly, metal–catalyzed direct arylations require the use of steric blocking groups in order to obtain the desired monoselectivity and prevent bisarylation from occurring. However, these sterically biased substrates are avoided with the system described herein.

Further, the chemoselectivity of the Suzuki–Miyaura cross–coupling of secondary boronic esters was investigated in intermolecular competition reactions with Mizoroki–Heck acceptors. Interestingly, the conditions of the reaction could be easily tuned to chemoselectively produce either the Suzuki–Miyaura or the Mizoroki–Heck cross–coupled product in good yields. This

knowledge was then applied to an intramolecular competition reaction on a substrate containing both Suzuki–Miyaura and Mizoroki–Heck acceptor sites. Excitingly, the Suzuki–Miyaura cross–coupled product was obtained in good yield leaving the alkene substituent unreacted in the reaction. This chemoselectivity pathway opens the door for the preparation of polysubstituted aromatic compounds without the additional need for protection and deprotection steps which could result in a reduced overall yield of the desired product.

Co-Authorship

I hereby declare that this thesis incorporates material that is the result of a joint research project as follows:

This thesis incorporates the outcome of research undertaken with the assistance of doctoral student Eric C. Keske and postdoctoral research fellow Dr. Olena V. Zenkina. In all cases, the primary contributions, a majority of the experimental efforts and data analysis were performed by the author. All data contained in the experimental section were acquired by the author.

I certify that, with the above qualification, this thesis and the research to which it encompasses is the product of my own work.

Acknowledgements

First and foremost I am greatly indebted to my supervisor Dr. Cathleen Crudden. The time spent working with you helped me to better understand the trade while growing both as a scientist and a person. Leaving the lab, I feel my training and experiences have best prepared me for any future challenges I may come across. You challenged me to be better every day and for that, I am deeply grateful and fortunate to have studied with such an influential chemist.

To the past and present members of the Crudden lab, I'd like to express my appreciation for everything along the way. Ya'll definitely made my time and failed reactions, much easier to deal with. Specific props goes out to Eric "E–Funk" Keske, who was influential in furthering my knowledge in many areas of chemistry, whisky and introducing me to sweet delicious bourbon, brownest of the brown. As well, thank you Olena, Patty "2–Sheds", Mike, Smitha and Cristina "Ooley–Mooley" for guidance, expanding my knowledge and sharing delicious beverages. Also thanks to Alphonse for opening your heart…and your liquor cabinet.

In addition to those mentioned above, thank you to everyone whom I crossed paths with during my time here at Queen's. Particularly, shout out to Boniface, Bachus, Fraser, Fowler, Anthony and Gurpaul amongst many others who were there to cheers a glass, play a game of puck, toss the ball around or stomp the boots and giddy up to some good 'ol country tunes.

Deepest thanks goes out to my family who were always standing beside me along the way. I would not have been able to make it this far without your reassurance and inspiration. It is not lost how instrumental you were in achieving this goal. I hope you're as proud of me as I am of you. And to my best friend Brittany. Everything just seems to have gotten a little brighter since you came into my life. I can't begin to think how lucky I am to have such a great companion to

spend my time with and count on. You're always there for support and I'm so lucky and grateful to have you beside me along the way. You light up my life and I love you.

This is for Grandma, Nonno and Nonna, whom were always a large part of my life. You always wished for great things for me and I wish you could be here to celebrate this accomplishment.

Table of Contents

List of Figures

List of Tables

List of Schemes

List of Abbreviations

σCAM	σ–Complex assisted metathesis
2–Ph–pyr	2–Phenylpyridine
9–BBN	9–Borabicyclo[3.3.1]nonane
Ac	Acetyl
Ar	Aryl
B_2neop_2	Bis(neopentyl glycolato)diboron
B_2pin_2	Bis(pinacolato)diboron
Bdan	1,8–Diaminonaphthyl boronamide
BDE	Bond dissociation energy
Bipy	2,2'–Bipyridine
Bn	Benzyl
Boc	*tert*–Butoxycarbonyl
BQ	1,4–Benzoquinone
Bu	Butyl
^oC	Celsius
C–C	Carbon–Carbon bond
C–H	Carbon–Hydrogen bond
C_{Ar}–H	Aromatic Carbon–Hydrogen bond
Cat.	Catalyst
CO	Carbonyl (C=O)
COD	1,5–Cyclooctadiene

COE	Cyclooctene
CMD	Concerted metalation–deprotonation
Cp	Cyclopentadiene
Cp*	1,2,3,4,5–Pentamethylcyclopentadiene
d, D, ^{2}H	Deuterium
dba	Dibenzylideneacetone
Cy	Cyclohexyl
DCM	Dichloromethane (CH_2Cl_2)
DG	Directing group
DME	1,2–Dimethoxyethane
D*o*M	Directed *ortho*–metalation
DMG	Directed metalating group
dppb	1,4–Bis(diphenylphosphino)butane
dtbpy	4,4'–^{t}butyl–2,2'–bipyridine
E	Electrophile
EA	Elemental analysis
EAS	Electrophilic aromatic substitution
EBA	Electrophilic bond activation
Eq.	Equation
eq.	Equivalent(s)
Et	Ethyl
eV	Electron volt
Fc	Ferrocene

FG	Functional group
HBcat	Catecholborane (4,5–Benzo–1,3,2–dioxaborolane)
HBpin	Pinacolborane (4,4,5,5–Tetramethyl–1,3,2–dioxaborolane)
hr	Hour(s)
HRMS	High–resolution mass spectrometry
hv	Ultraviolet light
Hz	Hertz
IAd	1–Adamantyl
IMes	1,3–Bis(2,4,6–trimethylphenyl)imidazol–2–ylidene
IPr	1,3–Bis(2,6–diisopropylphenyl)imidazol–2–ylidene
I^{t}Bu	1,3–Bis(*tert*–butyl)imidazol–2–ylidene
J	Coupling Constant
kJ	kilojoule
L	Ligand
M	Metal
Me	Methyl
MeCN	Acetonitrile
MeOH	Methanol
MI	Migratory insertion
MIDA	*N*–Methyliminodiacetic acid ($(CH_3)N(CH_3CO_2H)_2$)
min	Minute(s)
mol, mmol	Mole/millimole
Ms	Mesityl

MTBE	Methyl *tert*–butyl ether ($C(CH_3)_3OCH_3$)
NHC	*N*–Heterocyclic carbene
NMR	Nuclear magnetic resonance
NR	No reaction
Nu	Nucleophile
OA	Oxidative addition
MOM	Methoxymethyl ether ($–CH_2OCH_3$)
pK_a	Acid dissociation constant
PKC	Protein kinase C
Ph	Phenyl
ppm	Parts per million
Pr	Propyl
Py, Pyr	Pyridine or Pyridyl
R, R', R^1	Organic functional group
(*R*,*S*)–Josiphos	(*R*)–1–[(*S*)–2–(diphenylphosphino)ferrocenyl]ethyldicyclohexylphosphine
RE	Reductive elimination
RT, rt	Room temperature
SIMes	1,3–bis(2,4,6–trimethylphenyl)imidazolin–2–ylidene
SIPr	1,3–bis(2,6–diisopropylphenyl)imidazolin–2–ylidene
Si–SMAP	Silicon–supported silicon constrained monodentate trialkylphosphine
Si–TRIP	Silicon–supported triptycene–type phosphine
Si–TPP	Silicon–supported 4–(diphenylphosphino)–dimethylsiloxane
SPhos	2–Dicyclohexylphosphino–2',6'–dimethoxybiphenyl

$S_{RN}1$	Radical nucleophilic substitution
T	Temperature
Tf	Trifluoromethylsulfonate ($–SO_2CF_3$)
TLC	Thin layer chromatrography
Ts, Tos	Tosyl ($–SO_2(C_6H_4–p–CH_3)$)
THF	Tetrahydrofuran ($(CH_2)_4O$)
TIPS	Triisopropylsilyl ($–Si(CH(CH_3)_2)_3$)
TMEDA	Tetramethylethylenediamine ($(CH_3)_2NC_2H_4N(CH_3)_2$)
TMS	Trimethylsilyl ($–Si(CH_3)_3$)
XPhos	2–Dicyclohexylphosphino–2’,4’,6’–triisopropylbiphen

Chapter 1

Mild and Regioselective Synthesis of Polysubstituted Aromatics

1.1 Synthesis of Polysubstituted Aromatic Compounds

Aromatic and heteroaromatic compounds are important structural moieties with an extensive history of diverse applications in a variety of fields.[1-3] Of particular note, many chemical compounds requiring multistep synthesis, particularly those sought by pharmaceutical, agrochemical and materials science industries, consist of aromatic and heteroaromatic building blocks.[4-6] Polysubstituted aromatic molecules have long presented a challenge to synthetic chemists as regiospecificity can often be challenging. As such, there are currently many transformations which can be used to derivatize commercially available aromatics and are applicable to obtain polysubstituted aromatic compounds both on laboratory and industrial scales.[7]

A number of transformations are possible for the synthesis of polysubstituted aromatic compounds including: electrophilic aromatic substitution (EAS), nucleophilic substitution reactions (including $S_{RN}1$), sigmatropic rearrangements, cycloaddition reactions (including Diels–Alder) and aromatic ring construction starting from acyclic precursors[8] as well as transition metal–catalyzed carbocyclizations[9-10] (Figure 1–1). Although these methods are commonly employed for the construction of aromatic rings,

utilizing these reactions in a mild manner is not a trivial process. Synthesis of 1,2–disubstituted aromatics present significant challenges primarily due to the sterics preventing reagents from reacting with the *ortho*–position while also leaving pre–existing functionalities unabridged by the reagents involved in the reaction. Accordingly, harsh reaction conditions, regioselectivity issues, protection and deprotection steps, stoichiometric amounts of reagents and formation of hazardous byproducts are not uncommon in synthesizing these molecules under electrophilic substitution conditions. As a result, the use of these procedures tends to be very inconvenient in large scale laboratory and industrial processes. Thus several strategies such as directed *ortho*–metalation (D*o*M)[8,10] have been developed to address these synthetic challenges.

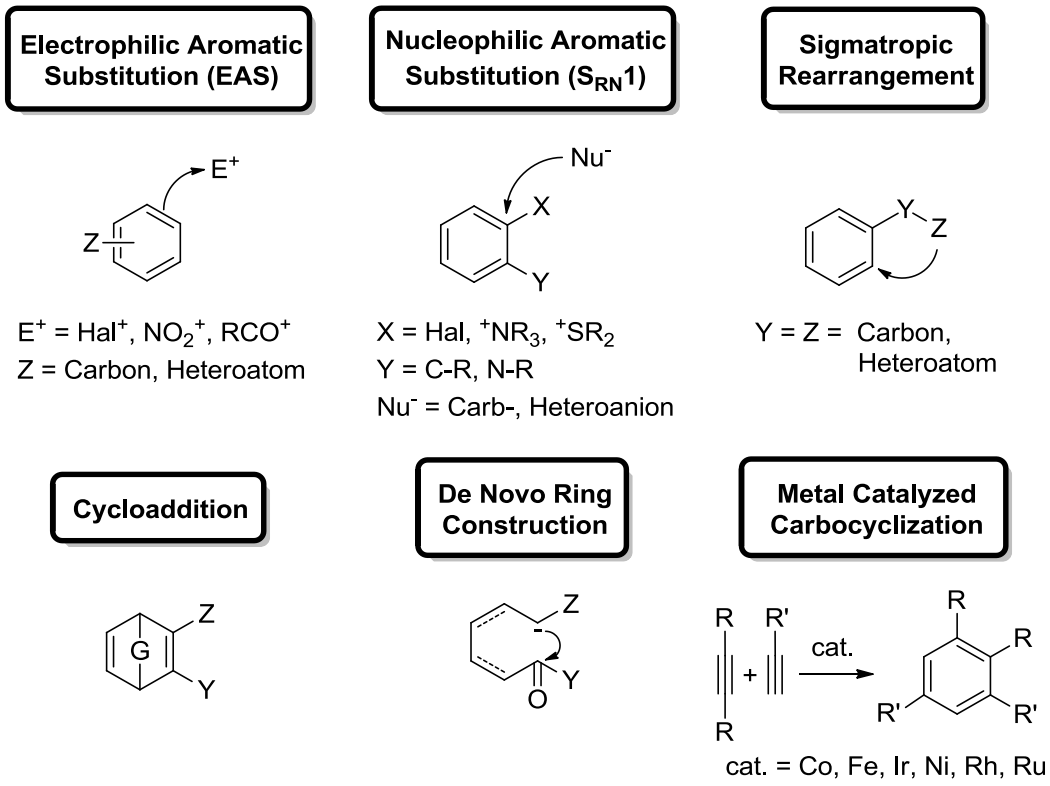

Figure 1-1. Common approaches to construction of aromatic rings

1.2 Directed *ortho*–Metalation (D*o*M)

One of the most successful regioselective preparations of 1,2–disubstituted aromatics is directed *ortho*–metalation (D*o*M). In this process, a heteroatom–derived directed metalating group (DMG) **1–1**, coordinates to an organolithium reagent (**TS–1**) and 'directs' it to the *ortho*–position allowing the site–selective deprotonation of the aromatic C–H bond thus forming the *ortho*–lithiated intermediate **1–2**. Subsequent treatment of **1–2** with an appropriate electrophile results in the formation of 1,2–disubstituted aromatic compounds of type **1–3** (Scheme 1–1).

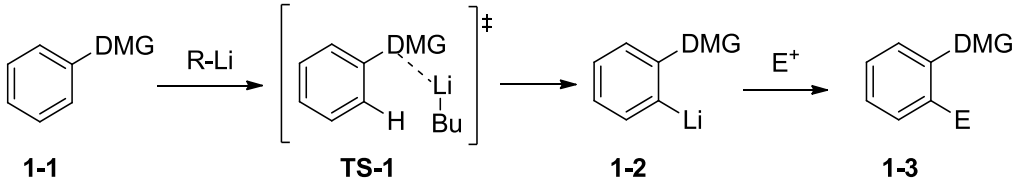

Scheme 1-1. General process of directed *ortho*–Metalation (D*o*M)

The simultaneous pioneering reports of Gilman[11] in 1939 and Wittig[12] in 1940, can be attributed to sparking the birth of the D*o*M reaction in synthetic organic chemistry. Over the course of the last seventy years, systematic studies by Gilman[13] and subsequently Hauser[14-15] in the 1960's resulted in the expansion of DMGs (Figure 1–2) to include both carbon–based and heteroatom–based directing groups.[16] The intermediate organolithium compound, **1–2**, is able to react with a large range of electrophiles (Figure 1–2) both inter– and intramolecularly. Taking advantage of the high regioselectivity and the compatibility

with a broad range of electrophiles, the library of available 1,2–disubstituted and higher order functionalized aromatic compounds has undergone significant expansion.

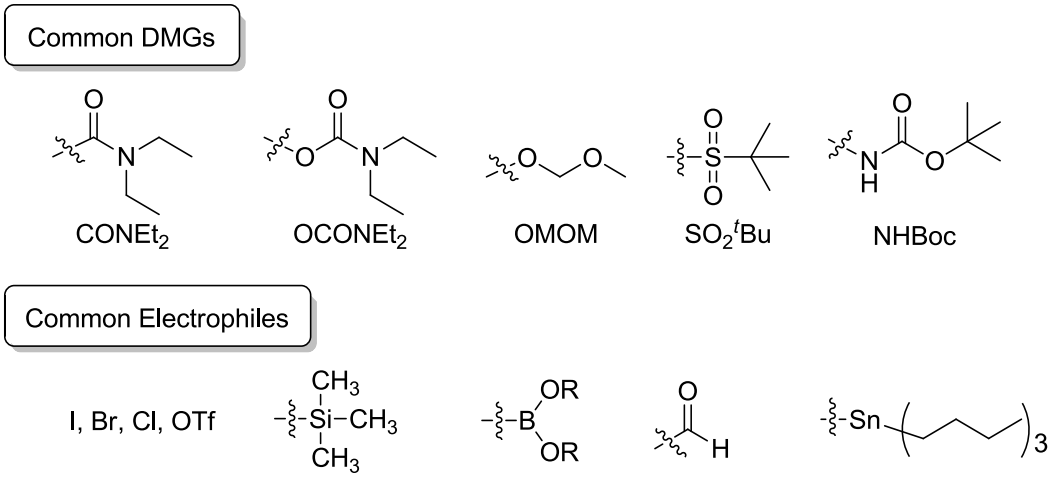

Figure 1-2. Common DMGs and electrophiles in D*o*M reactions

One of the most significant advances over the past decade is the use of D*o*M chemistry to generate main–group organometallic electrophiles for metal–catalyzed cross–couplings, producing new methodology for synthesizing *ortho*–substituted biaryl and higher order aromatic compounds.[16-17] These cross–coupling reactions typically produce biaryl compounds and are generally catalyzed by palladium or nickel based catalysts (Figure 1–3). Introduction of halide or pseudohalide (Cl, Br, I, OTf, OMs), silyl (SiR_3), stannyl (SnR_3) and boryl ($B(OR)_2$) functional groups by D*o*M reactions have allowed the subsequent use of metal–catalyzed processes such as Suzuki–Miyaura, Stille, Negishi and Kumada–Corriu cross–couplings in a combinatory approach with D*o*M chemistry. As an example, Snieckus and coworkers[18] have applied the sequential D*o*M/Suzuki cross–coupling for making substituted biphenyls (Scheme 1–2).

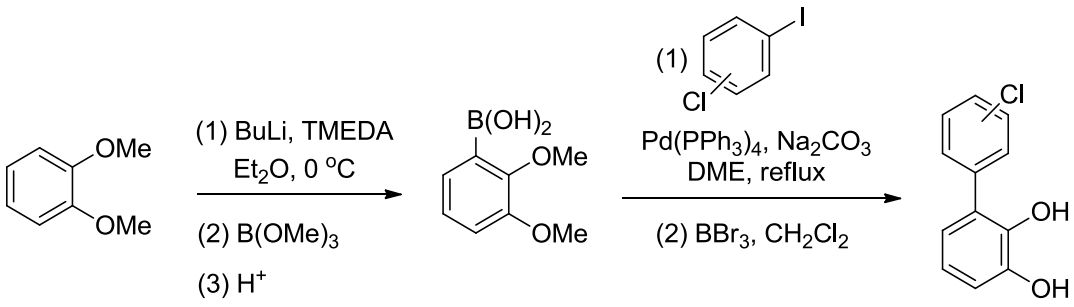

Scheme 1-2. Sequential D*o*M/Suzuki–Miyaura cross–coupling for synthesis of 1,2–disubstituted biaryls by Snieckus and coworkers

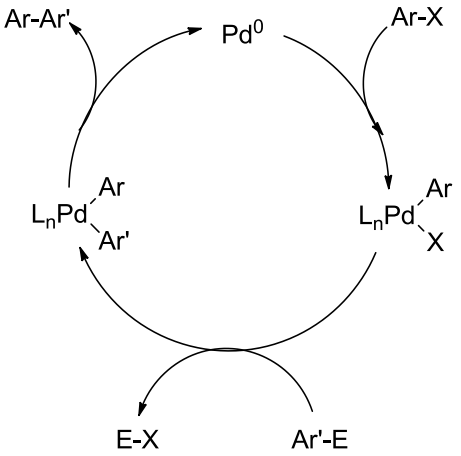

E	X	Cross-Coupling
$B(OR)_2$	Hal, OTf	Suzuki-Miyaura
SnR_3	Hal, OTf	Stille
ZnX	Hal, OTf	Negishi
MgX	OTf, $OCONEt_2$ $SCONEt_2$	Kumada-Corriu

Figure 1-3. Common catalytic cycle for palladium–catalyzed cross–couplings

Although it provides viable routes to functionalized and highly regiospecific 1,2–substituted aromatic compounds, D*o*M chemistry has the following limitations in industrial processes: 1) D*o*M reactions require stoichiometric amounts of alkyllithium species, which can be difficult to handle; 2) reactions require cryogenic conditions which is expensive on large scale; 3) functionalized aromatics need to be compatible with the alkyllithium species. Acidic functional groups, such as carboxylic acids (–CO_2H) and hydroxyls (–OH) are incompatible with the highly basic lithiating reagents utilized in D*o*M procedures. While these drawbacks are minimized on the laboratory scale, industrial scale requirements can in turn limit the synthetic utility of D*o*M chemistry. Thus more user friendly, environmentally benign and cost effective alternatives are highly sought after.

1.3 Modes of Cyclometalation *via* C–H Activation

As described previously, the most significant advance in the field of transition metal–catalyzed C–H activation has been the use of directing groups in order to dramatically improve regioselectivity. Whereas D*o*M pathways typically incorporate the metal (Li) *via* coordination to the DMG and deprotonation of the *ortho*–C_{Ar}–H bond, C–H activation pathways tend to proceed *via* a cyclometalation process between the C–H bond and the metal center. Cyclometalation refers to the metal mediated activation of a C–H bond to form a metallacycle containing a new M–C σ–bond (Scheme 1–3).[19] The two steps common to the cyclometalations are the initial coordination of the metal to the organic molecule and cleavage of the C–H to produce the metallacyle. The mechanistic pathway

of metal insertion into the C–H bond to produce the cyclometalated complex in C–H activation reactions tends to be system dependent and not unique to all C–H activations in general. Electronic configuration at the metal center as well as the hybridization of the C–H bond can lead to differences in the cyclometalation step occurring between the metal complex and the organic substrate.[20] Currently, four main pathways have been established for the cleavage of the C–H bond: oxidative addition, electrophilic bond activation, concerted metalation–deprotonation and σ–bond metathesis.

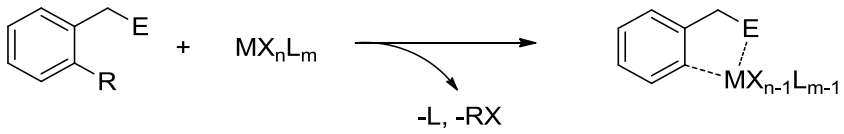

Scheme 1-3. Cyclometalation in C–H activation

1.3.1 Oxidative Addition

Oxidative addition is a commonly encountered mechanism for the cyclometalation of C–H bonds with low valent late transition metal complexes[21] including $Ru^{0,II}$, Os^{II}, Rh^{I}, Ir^{I} and $Pt^{0,II}$. Upon coordination of the metal to the organic substrate to form the chelated complex **1–5** (Figure 1–4), the metal centre inserts into the antibonding σ^* orbital of the C–H bond and undergoes a $2e^-$ transfer forming a new metal complex, **1–6**, with the oxidation state of the metal increasing by +2. After oxidative addition occurs, reductive elimination can occur either spontaneously (such as elimination of H_2 from the metal center) or induced by base (example with elimination of H–X or R–X) to produce the cyclometalated complex **1–7** (Scheme 1–4).[20] In most cases, C–H activation is facile in

catalytic pathways and not rate limiting. The difficulty in catalytic pathways often involves the reductive elimination of the product from the higher metal oxidation state. Stability of this intermediate complex as well as the rigidity of the system can require increased temperatures or the presence of base in order to facilitate the reductive elimination process. It is important to note that while the oxidative addition is believed to be a concerted process, the intermediate agostic complex (Scheme 1–7 Pathway B), may be considered as a transition state of the oxidative addition.

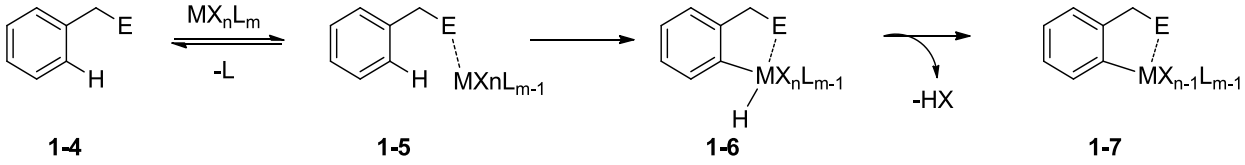

Scheme 1-4. Oxidative addition of C–H bond towards cyclometalation

Seminal examples of oxidative addition of unactivated C–H bonds to metal centers were reported by Bergman[22-24] and Jones[25] utilizing complexes of general formula [Cp*(PMe_3)MH_2] (M = Rh, Ir) (Scheme 1–5). In these reactions, photolysis of the metal complex **1–8** in hydrocarbon solvents resulted in the loss of H_2 from the complex followed by the oxidative addition of the hydrocarbon to the metal formally cleaving the C–H bond producing the new metal hydride complex **1–9**. Upon monitoring the reaction by ^{1}H NMR, new metal hydride peaks were easily observable as evidence of oxidative addition to the metal complex.[26] Similarly, Graham[27] also reported the photolysis of an [Cp*Ir$(CO)_2$] complex with loss of carbon monoxide (CO) to achieve the C–H activated product.

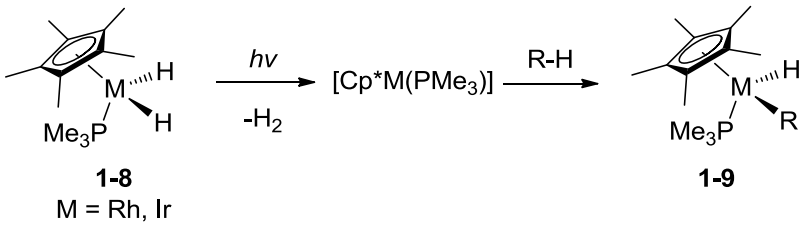

1-8
M = Rh, Ir

1-9

Scheme 1-5. Photolytic oxidative addition of metal to alkyl C–H bond

1.3.2 Electrophilic Bond Activation

In an alternative mechanism, electrophilic bond activation (EBA) is commonly observed in highly electrophilic late transition metal systems such as Pd^{II}, Pt^{II}, Pt^{IV}, Hg^{II}, Rh^{III}, Ir^{III} and Tl^{III}.[21] With EBA, metal insertion into the C–H bond on the aromatic ring to form the *ortho*–C–M bond does not form a metal hydride intermediate leaving the oxidation state of the metal unchanged. EBA generally occurs in systems with late transition metals which feature basic type ligands attached to the metal. Cyclometalation *via* EBA (Scheme 1–6, Pathway A) is initiated by coordination of the metal to a nucleophilic directing group on the organic species, producing **1–5**, followed by bond activation through the formation of a σ–complex with the metal to produce the arenium intermediate **1–10**. This step is often rate limiting and loss of H–X from **1–10** generates the cyclometalated product **1–12**. Work by van Koten and coworkers[28] indicated that formation of the Pt σ–complex proceeds *via* an arenium intermediate, supported by increases in the C–C bonds lengths of the characterized intermediate (Figure 1–4). In the final step, presence of acetate type ligands assist in removing the hydrogen from the arenium species to form the metallacycle.

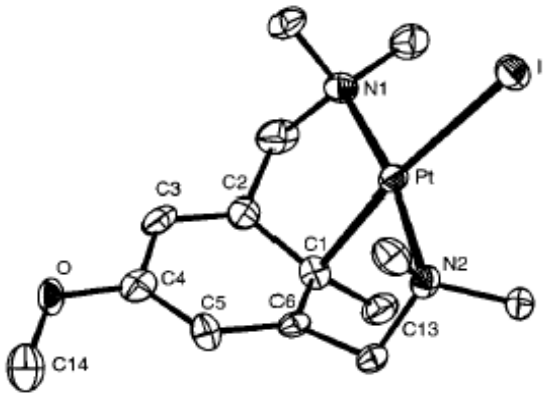

Bond	Length
Pt-I	2.625
Pt-N1	2.100
Pt-N2	2.103
Pt-C1	2.127
C1-C13	1.541
C1-C2	1.443
C2-C3	1.365
C3-C4	1.381
C4-C5	1.399
C5-C6	1.384
C6-C1	1.440
C4-O	1.339

Figure 1-4. Crystal structure for arenium intermediate as determined by van Koten[28]

1.3.3 Concerted Metalation–Deprotonation

Concerted metalation–deprotonation (CMD)[29-32] (Scheme 1–6, Pathway B) has been suggested as an alternative mechanism to EBA for cyclometalation with C_{Ar}–H bonds. CMD mechanisms have been implicated for Pd^{II}, Ru^{II}, Rh^{III} and Ir^{III} based systems,[33-36] which commonly incorporate coordinating bases such as acetates or carbonates in the reaction. These coordinating bases play an integral part in the CMD pathway as they assist the deprotonation of the proximal C–H bond of the substrate.[37-41] Though some reports indicate that EBA and CMD pathways are almost identical, they vary from one another in the intermediate steps of the cyclometalation. Specifically, while the EBA mechanism proceeds through an arenium intermediate, the CMD pathway suggests that during the metalation of the aryl ring, the C–H bond is deprotonated by aid of a pendant basic ligand (**1–11**) in a concerted fashion without the formation of an arenium intermediate. After this, the protonated ligand can eliminate from the coordination sphere of the metal, resulting in

the cyclometalated product **1–12**. Development of the CMD mechanism was brought forth in large part due to the observation that electronically biased substituents on the aromatic ring showed little to no effects in the observed reaction rates. This observation is inconsistent with the idea of an arenium intermediate being formed though an electrophilic activation–type pathway, which should display drastically different rate profiles depending on the electronic character of the substrates.

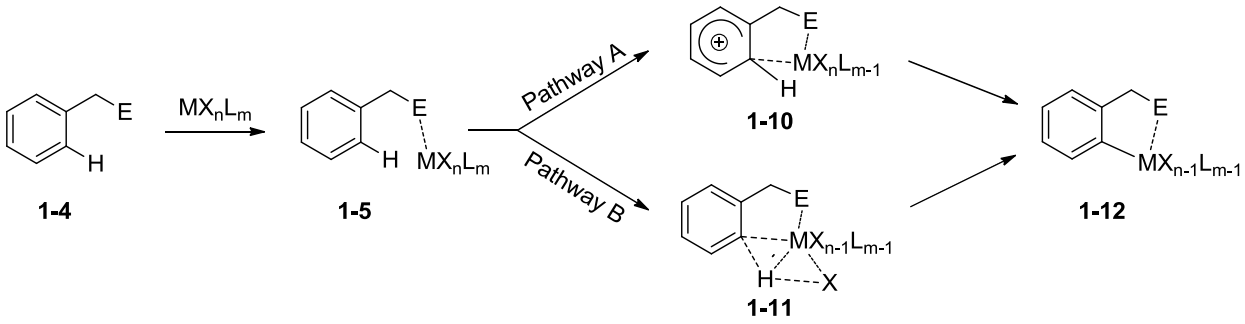

Scheme 1-6. Pathways for the cyclometalation process *via* electrophilic bond activation (EBA) (Pathway A) and concerted metalation–deprotonation (CMD) (Pathway B)

1.3.4 σ–Bond Metathesis

Cyclometalation occurring *via σ*–bond metathesis is another possible mechanism which is generally only viable for low oxidation state metals with a d^0 configuration. The concerted process involves a four–membered transition state for the deprotonation of the hydrogen from the aromatic ring.[42] This mechanism has been commonly described for early transition metal systems of type Cp_2MR (M = Sc, Ln) or Cp_2MR_2 (M = Ti, Zr, Hf), as these metals are in their highest oxidation state and thus cannot undergo oxidative

addition nor reductively eliminate to lower their oxidation state. The electron density at the metal center of **TS–2** helps to stabilize the incoming hydride leading to the new M–C σ–bond (Scheme 1–7).[43-46] This hydride stabilization by the metal center is often referred to as σ–complex assisted metathesis (σCAM).[42] While commonly applied to metal complexes containing alkyl ligands, this mechanistic pathway has also been proposed for late transition metal hydride complexes of rhenium, ruthenium and osmium in select cases.[20]

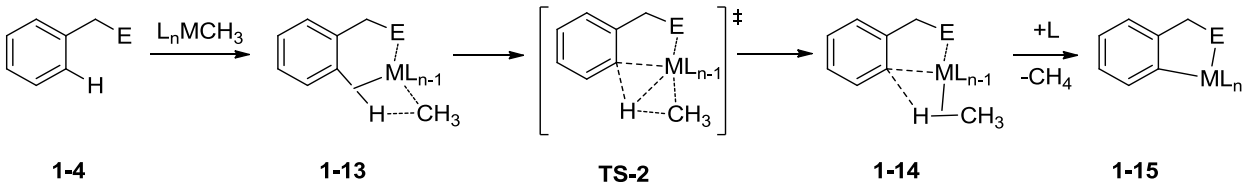

Scheme 1-7. General pathway for ***σ***CAM pathway

1.4 Transition Metal–Catalyzed C–H Activation

C–H bonds are ubiquitous in organic molecules though their low reactivity makes direct functionalization non–trivial.[47] The desire for more efficient, environmentally friendly processes, calls for alternative approaches to the classical methods or D*o*M chemistry previously discussed, especially in those processes requiring large–scale, multi–step syntheses. The direct functionalization of aromatic C–H bonds catalyzed by transition metals provides an interesting and exciting alternative approach to producing C–X bonds (X = carbon, heteroatom, halogen). As the substrates generally require no

preactivation, employing a C–H activation protocol provides an atom economical[48-49] approach to synthesis that does not require the formation of halogenated or otherwise prefunctionalized substrates.[50] As a result, the field of transition metal–catalyzed C–H activation has undergone an explosive and unparalleled growth over the last few years.[51]

A major breakthrough reported by Fujiwara[52] was revolutionary to the field of C–H activation. In his seminal report, stoichiometric amounts of a $[PdCl_2 \cdot Styrene]_2$ dimer were coupled with benzene for the formation of *trans*–stilbene (Scheme 1–8) marking one of the first examples of aromatic C–H bond activation by transition metal complexes. Unfortunately, the process was stoichiometric in palladium and the yields were low though curiously, the presence of the acetic acid was found to be crucial for the reaction. Substitution of the benzene solvent for toluene resulted in the desired *trans*–4–methylstilbene in a similar yield, negating the possibility of styrene decomposition in the reaction to produce the *trans*–stilbene products. The reaction was later optimized by replacement of $[PdCl_2 \cdot Styrene]_2$ with $Pd(OAc)_2$ leading to synthetically useful yields (up to 90%) while increasing the scope of olefins and aromatics capable of undergoing the coupling reaction.[53] Most importantly, the addition of oxidants to the reaction mixture such as copper or silver salts allowed for the catalytic use of $Pd(OAc)_2$, which reoxidizes Pd^0 back to Pd^{II}.[54]

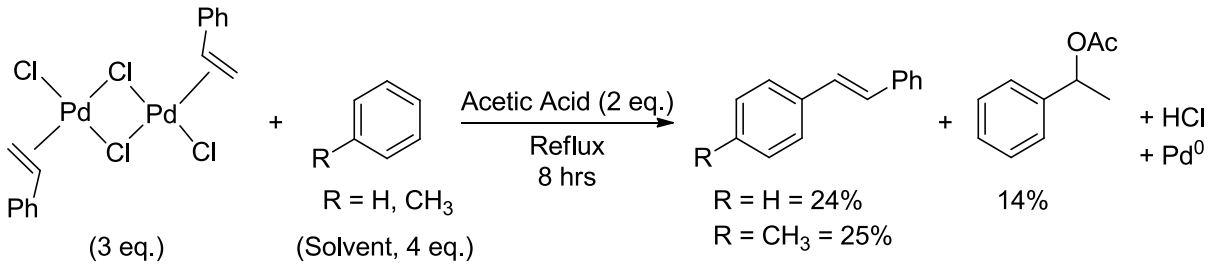

Scheme 1-8. Fujiwara coupling of benzene and toluene with styrene[52]

Although the above example detailing the use of transition metal–catalyzed C–H activation provides an advantageous alternative to more traditional metal–catalyzed cross–coupling reactions, this strategy is not without its limitations. Aromatic C–H bonds characteristically have high bond dissociation energies (465 kJ/mol)[55] as well as relatively low acidities (pK_a of C_6H_5–H ≈ 40 in H_2O). Though they are not completely inert as previously thought, these characteristics render the activation of C–H bonds significantly difficult. As a result, C–H bond activation reactions often require high temperatures and can also call for oxidants as well as highly basic or acidic additives.[56] While these conditions may be required to activate the C–H bond, functional groups on the molecule may also be affected and as a result may oxidize, decompose or be cleaved under the conditions required to achieve the metal–catalyzed C–H activation. Consequently, conducting the reactions regioselectively under mild conditions presents a great challenge in C–H bond activation chemistry; particularly cases in which directing groups are absent, leading to mixtures of regioisomers (*vide infra*).[56]

It has been long known that a variety of transition metals are capable of inserting into C–H bonds.[20, 57-59] This concept was pioneered extensively by Shaw, Milstein, van Koten[60-63] and coworkers towards the synthesis of cyclometalated ligands on transition metals. In a similar vein to D*o*M chemistry, these transformations often require the presence of a proximal basic ligand such as phosphines or amines to facilitate coordination of the ligand with the metal center. Equation 1–1 exemplifies this with the use of chelating pincer ligands. Conversely, these transformations were exploited for the formation of new transition metal complexes and as such, these processes were not investigated in a catalytic sense towards the synthesis of functionalized organic molecules. However, the compounds which are synthesized by this method can be used as efficient complexes in a variety of metal–catalyzed reactions.[64]

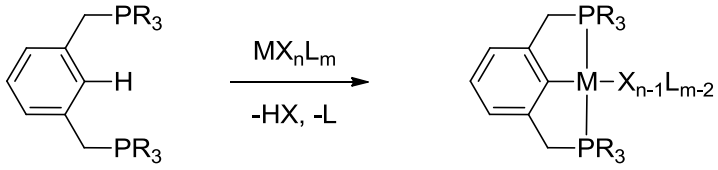

(1-1)

More relevant to C–H functionalization chemistry, Horino and Inoue[65] demonstrated the ability to selectively functionalize acetanilide derivatives in the *ortho*–position *via* formation of an *ortho*–palladated complex. This complex was formed under remarkably mild conditions utilizing $Pd(OAc)_2$ and could also be isolated. Subsequent reactions with carbon monoxide and olefins resulted in C–C bond formation (Scheme 1–9). While these reactions required the stoichiometric use of $Pd(OAc)_2$, this report was a major advance in the field as it demonstrated the capability of transition metals to not only

insert into C–H bonds, but to mediate synthetically interesting reactions with high regioselectivity in the presence of directing groups. Through their studies, it was observed that *ortho*–substituted acetanilides were unable to form the cyclopalladated complex. While at the time no suggestion was given for the lack of reactivity of *ortho*–substituted acetanilides, Glorius[66] later provided evidence that steric repulsion of the directing group with the catalyst was responsible for the lack of reactivity.

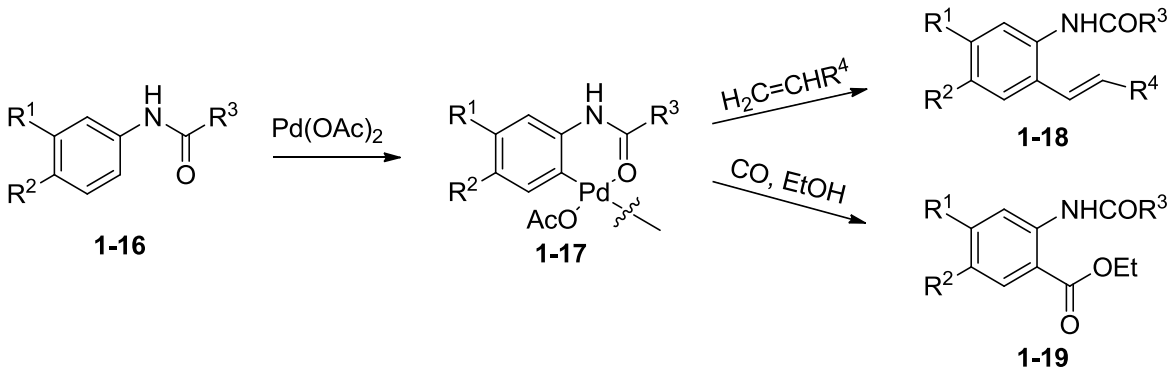

Scheme 1-9. Synthesis of *ortho*–substituted aromatics *via* cyclopalladation of $Pd(OAc)_2$[65]

By the early 1990's, C–H bond cleavage was widely studied and known for a variety of metals.[57] While these processes occur with stoichiometric amounts of metal, catalytic attempts at C–H cleavage were met with low yields and low catalyst turnovers. A major breakthrough was reported by Murai and coworkers[67] who described the use of $RuH_2(CO)(PPh_3)_3$ to catalyze the *ortho*–alkylation of aromatic ketones (Scheme 1–10). This catalytic process overcame many of the previously reported issues with *ortho*–mediated alkylations.[68] Specifically, the reaction proceeds with catalyst loadings of

the $RuH_2(CO)(PPh_3)_3$ as low as 2 mol%, avoiding use of stoichiometric metal in the reaction. Selectivity was dramatically improved as regioisomers were avoided in cases of where multiple *ortho*–sites were available for alkylation leading to the formation of only one regioisomer as the dominant product. As well, the generality of the alkylation is applicable to a wide variety of aromatic and heteroaromatic compounds and a variety of olefins could be incorporated, dramatically increasing the scope of the reaction.

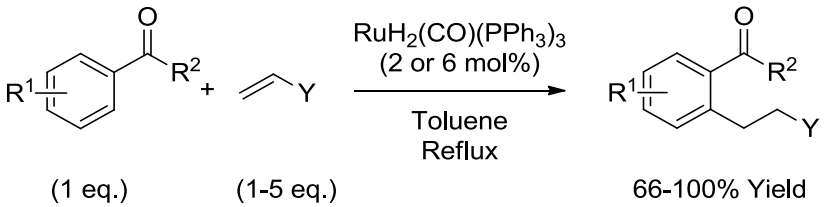

Scheme 1-10. Catalytic C–H alkylation by Murai and coworkers[67]

Detailed mechanistic studies on the reaction were conducted to elucidate the catalytic cycle for the ruthenium–catalyzed C–H alkylation depicted in Figure 1–5.[69] Initially, the olefin coordinates to the pre–catalyst $RuH_2(CO)(PPh_3)_3$, **1–E**, and is hydrogenated leading to the formation of the active catalyst, **1–F**. Introduction of the aryl substituent, **1–20**, allows for coordination of the low valent Ru^0 to the ester, forming coordinated complex **1–G**. Insertion of the ruthenium into the C_{Ar}–H bond likely occurs *via* an oxidative addition to the Ru^0 complex resulting in the formation of the ruthenium hydride **1–H**. The olefin then coordinates to the cyclometalated ruthenium complex and displaces one of the labile ligands forming intermediate **1–I**. Hydride insertion from the ruthenium centre can proceed to the internal or terminal carbon leading to the formation of branched, **1–J**, or linear, **1–K**, complexes respectively. Since no branched isomer of the

alkylated product is observed, complex **1–J**, if formed, does not undergo reductive elimination and thus must revert back to complex **1–I**. Upon formation of complex **1–K**, reductive elimination occurs to generate the product **1–21** and regenerate the active catalyst **1–F**. ^{13}C kinetic isotope effect (KIE) and deuterium labeling studies conducted on the reaction indicated that the C–H activation step (formation of **1–H**) is facile and occurs readily and reversibly, strongly suggesting that the rate limiting step is the reductive elimination to form the C–C bond.

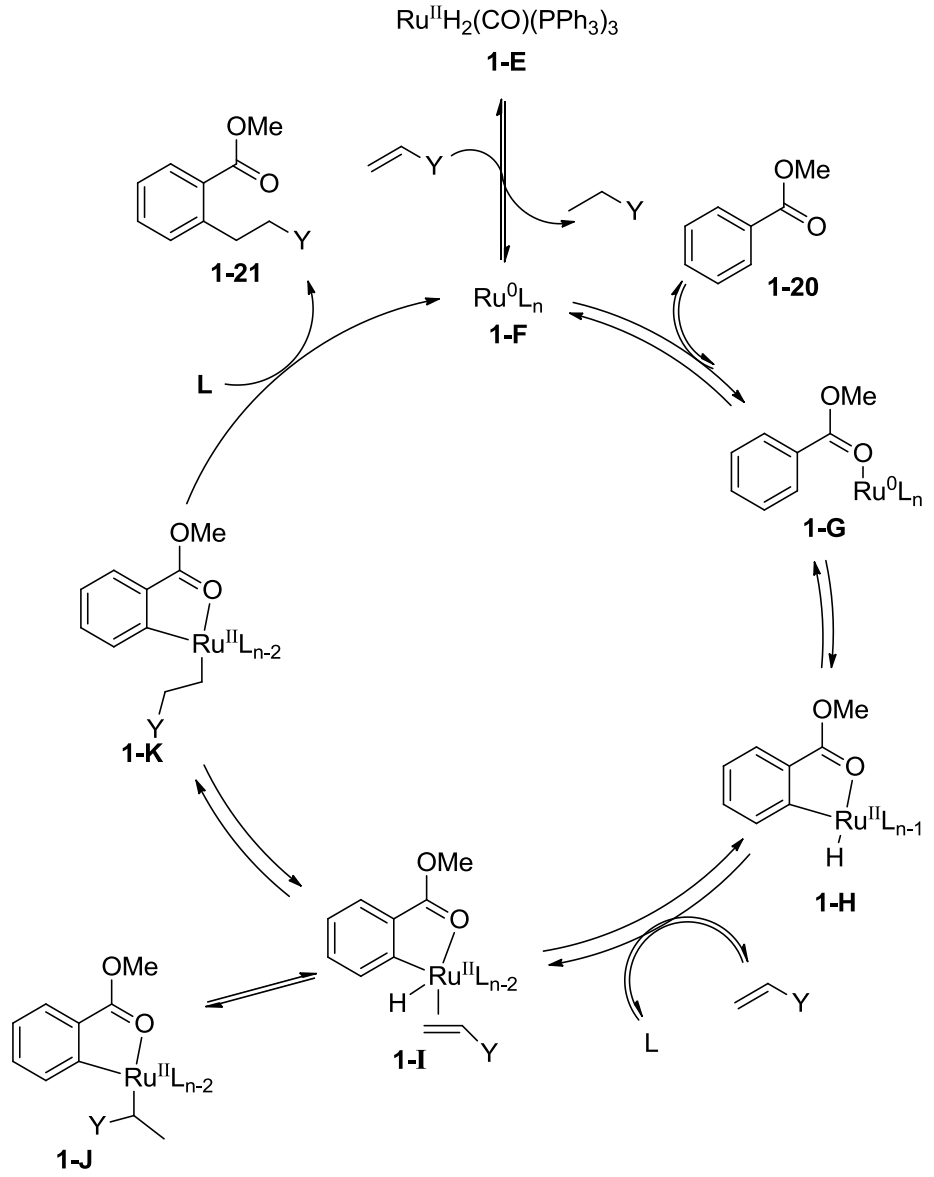

Figure 1-5. Murai's proposed catalytic cycle of Ru–catalyzed *ortho*–alkylation

1.5 Metal–Catalyzed C–H Borylation

1.5.1 Synthesis of Arylboronic Esters

Organoboron compounds (Figure 1–6) have played a pivotal role in the development of organic, inorganic and materials chemistry over the past 30 years due in large part to the discovery of the Suzuki–Miyaura cross–coupling reaction and their use therein.[70-71] These applications include optical materials,[72-73] neutron capture therapy,[74-75] as well as in the synthesis of medicinal compounds and precursors.[76] Additionally, arylboronates are capable of undergoing many essential bond forming reactions including metal–catalyzed cross–couplings, 1,2– and 1,4–addition to carbonyls, oxidative aminations, oxidative Heck reactions, additions to imines and iminium ions.[77-82]

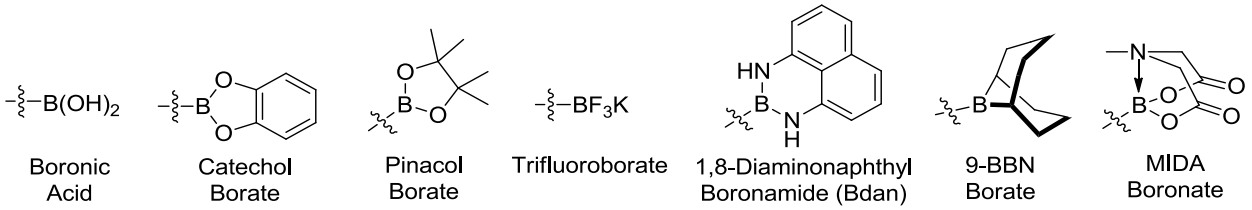

Figure 1-6. Common boron functional groups used in Suzuki–Miyaura cross–couplings

Conventionally, a handful of methodologies are commonly employed to synthesize arylboronic esters. Most commonly these species are synthesized by reacting organometallic reagents such as Grignard or organolithium reagents available either through lithium–halogen exchange, or by D*o*M chemistry with molecules such as trimethyl borate ($B(OMe)_3$). Unfortunately however, these methods have inherent limitations involving the handling of the highly reactive organometallic reagents (*vide supra*).

More recent developments have involved the use of transition metal–catalyzed cross–coupling reactions. These catalytic transformations take place more commonly under palladium–catalyzed[83] conditions while Marder[84] has since reported an alternative route based on copper–catalyzed conditions. In both cases, aryl halides are coupled with diboron reagents such as bis(pinacolato)diboron (B_2Pin_2) or bis(neopentyl glycolato)diboron (B_2neop_2), to form the target arylboronate while the former method also proved applicable to pinacolborane (HBpin) (Scheme 1–11). While the desired arylboronates are easily prepared, the procedures are stepwise, time consuming and draw on the need for prefunctionalized aryl species. As a result, the ability to directly functionalize molecules, particularly aromatic compounds, to form organoboron compounds with exclusive selectivity is highly advantageous.

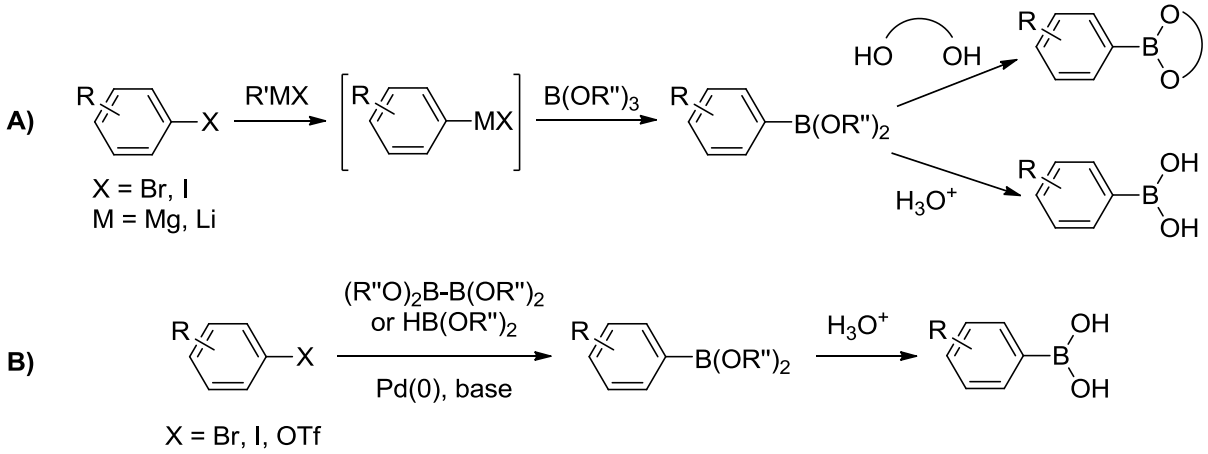

Scheme 1-11. Common strategies for synthesis of arylboronate esters by A) lithium halogen exchange, Grignard reagents or D*o*M and B) palladium–catalyzed routes

1.5.2 From Stoichiometric to Catalyzed C–H Borylation Reactions

A seminal report on the C–H borylation of aromatic molecules appeared in 1995 by Hartwig[85] describing the irradiation of [CpFe(CO)$_2$(Bcat)] in aromatic solvents producing arylboronic esters (Scheme 1–12). In their studies, the photochemical borylation of benzene with catecholborane (HBcat) was achieved resulting in C_6H_5BCat in 87% yield. Although only the monoborylated product was obtained, the reaction was poorly selective in reactions employing substituted aromatic molecules where multiple isomers are possible. For example, when the reaction is conducted with toluene, a 1.1:1 mixture of *meta*– and *para*–substituted products are observed while reaction in anisole yields a 1:1.6:1.1 ratio of *ortho*–, *meta*– and *para*–substituted products. Despite its novelty, the poor selectivity observed with substituted arenes and the stoichiometric use of the metal boryl complex severely hampers the utility of this reaction.

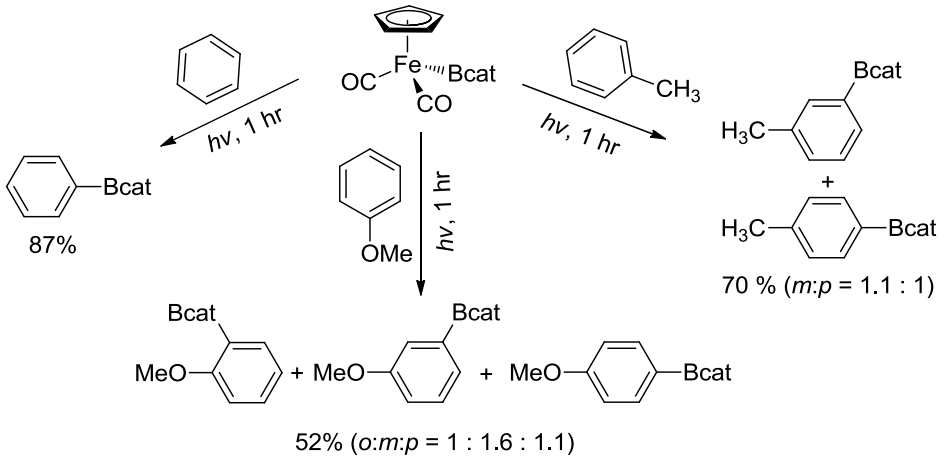

Scheme 1-12. Photolysis of [(CpFe(CO)$_2$(Bcat)] complex to yield arylboronate esters

In 1999, Hartwig and Chen[86] introduced the first catalytic C–H borylation of alkanes under photochemical conditions using [Cp*Re(CO)$_3$] as the catalyst and B_2Pin_2 as the boron source leading to high yields of alkylboronate esters. A variety of alkanes were borylated at the least sterically hindered position in excellent yields (75–100% of the borylated alkane). Stoichiometric studies with [Cp*Re(CO)(Bpin)$_2$] indicated that the first step of the catalytic cycle was the oxidative addition of B_2Pin_2 to the metal centre with the subsequent loss of CO and that the [Cp*Re(CO)(Bpin)$_2$] complex is a viable intermediate in the process.

Prior to 2000, C–H borylations were conducted under photochemical conditions and while efficient, were not practical outside of laboratory settings. While Smith and coworkers[87] originally reported the first thermal C–H borylation of benzene mediated by [Cp*Ir(PMe)$_3$H$_2$], these reactions were stoichiometric in metal and still not overly practical outside of the laboratory. In 2000, Hartwig[88] and coworkers introduced the first catalytic C–H borylation reactions under thermal conditions utilizing Rh^I catalysts. At elevated temperatures (150 ^oC) various alkanes could be borylated with exclusive selectivity for the terminal position in moderate to good yields (up to 88%). Smith and coworkers[89] subsequently reported the borylation of benzene was also achieved with excellent yields under thermal conditions producing solely the monoborylated product (Scheme 1–13). The catalyst loading could be significantly decreased to 0.5 mol% with only a small loss in the yield, though the reaction time had to be significantly increased. Unfortunately, benzene was the only aromatic compound which was borylated under these conditions and other substituted arenes were not investigated at the time. Needless to say, this discovery was a

major breakthrough for the application of C–H borylation chemistry, but significant progress was still needed to make this procedure more practical.

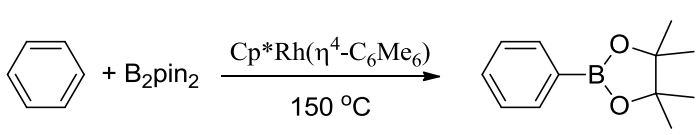

Cat. (mol %)	Time (hr)	Yield (%)
5.0	2.5	92
0.5	45	82

Scheme 1-13. C–H borylation of benzene under thermal conditions

1.5.3 Undirected C–H Borylation of Arenes

To date, iridium catalysts have been the most investigated for the C–H borylation of arenes. Hartwig and Miyaura[90] described a convenient and highly effective catalytic system for the undirected C–H borylation of a wide variety of aromatic compounds. The bench stable, and commercially available $[Ir(COD)Cl]_2$ was demonstrated to be an effective precatalyst in the presence of chelating nitrogen donors such as 2,2'–bipyridine (bipy). The iridium–catalyzed system utilized B_2Pin_2 in stoichiometric amounts with various substituted arenes (including heteroarenes) which produced arylboronate esters in high yield. Use of the more reactive $[Ir(COE)_2Cl]_2$ even allowed this reaction to take place at room temperature (Scheme 1–14). Stoichiometric studies under these conditions demonstrated that, a trisboryl complex $[Ir(bipy)(COE)(BPin)_3]$ was formed (**1–L**).[91] This complex was isolated and characterized by X–ray crystallography and subsequent studies demonstrated this species to be a chemically and kinetically competent intermediate in the

overall reaction (Figure 1–7) as dissolution of the trisboryl complex in C_6D_6 yielded three equivalents of C_6D_5Bpin (**1–22**) in 80% yield (Scheme 1–15). These studies led the authors to propose the catalytic cycle depicted in Figure 1–7.

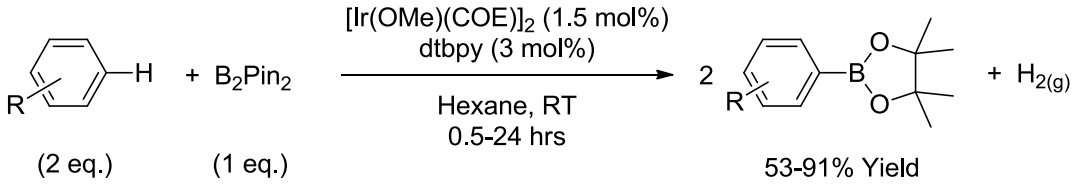

Scheme 1-14. Undirected borylation of arenes with B_2Pin_2 using $[Ir(OMe)(COE)]_2$/dtbpy

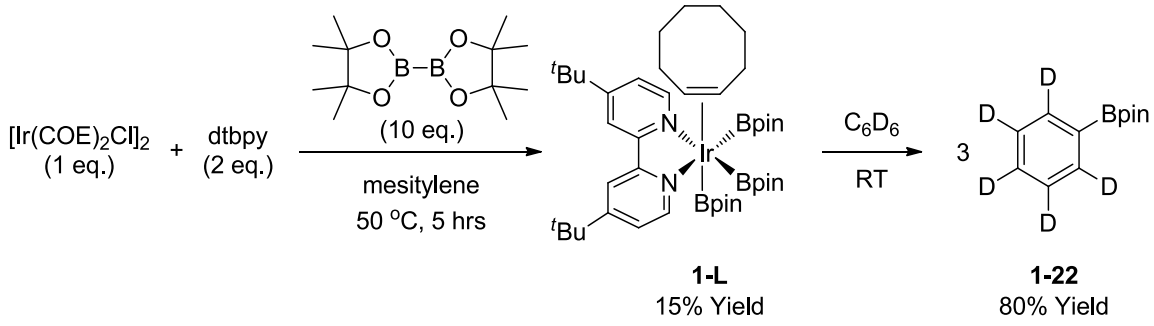

Scheme 1-15. Isolation of iridium trisboryl intermediate **1–L**

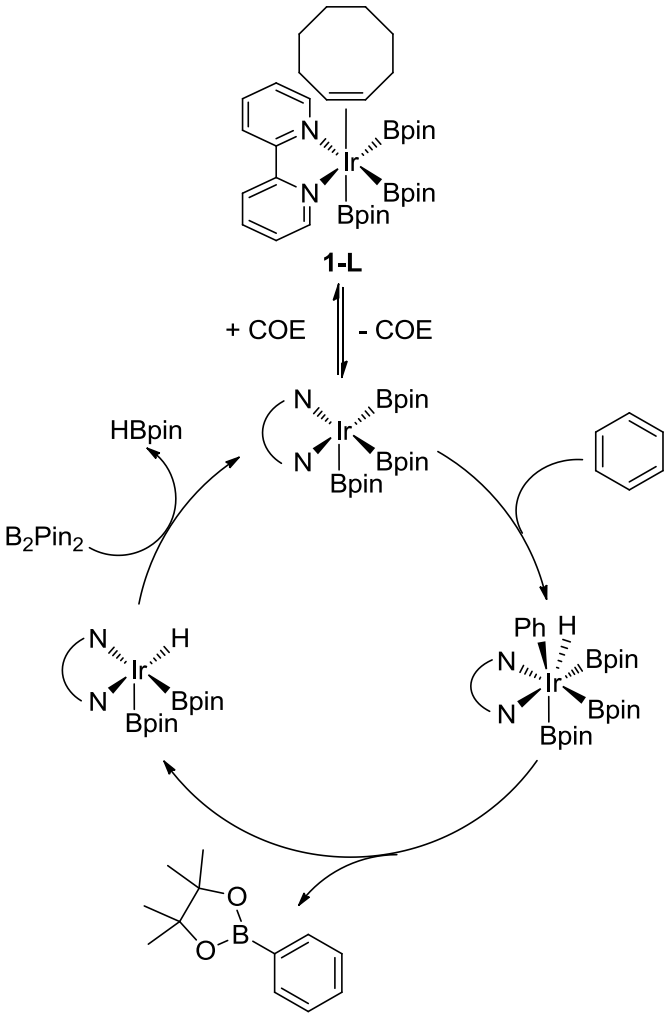

Figure 1-7. Catalytic cycle of undirected borylation of benzene with [Ir(bipy)(COE)(Bpin)$_3$]

The nature of the ligands on the iridium precatalysts were extensively investigated[90] and it was determined that highly basic anionic ligands such as –OMe were found to dramatically increase the reactivity of the catalyst system. Initial studies of less basic systems of IrCl(COD)]$_2$ or [Ir(OAc)(COD)]$_2$ with derivatives of the bipy ligand showed no borylation. Ultimately the commercially available, air and moisture stable precatalyst

$[Ir(OMe)(COD)]_2$ was found to display excellent reactivity for the borylation in presence of the electron rich and bulky 4,4'–ditertbutyl–2,2'–bipyridine (dtbpy) ligand. The role of the basic additive appears to be related to the facile formation of the trisboryl intermediate (**1–L**) which is thought to occur *via* oxidative addition of B_2Pin_2 to the $[Ir(OR)(COD)]_2$ species followed by reductive elimination of alkoxy boronate (ROBpin).

The C–H borylation of substituted benzenes was investigated[90] utilizing the $[Ir(OMe)(COD)]_2$/dtbpy system (Scheme 1–16). Borylation of 1,2– and 1,3–substituted symmetrical substrates yielded a single product while unsymmetrical substrates also yielded a single product due to the steric accessibility of one C–H position over the others in the molecule. 1,4–Dichlorobenzene was the only substrate which was able to undergo borylation at the *ortho*–position though the steric hindrance of the chloro groups significantly slowed the reaction and the yield of the borylated substrate was significantly lower than the other substrates investigated in the study. Importantly, common functional groups were tolerated under the reaction conditions and borylations were selective for C–H bonds over C–heteroatom bonds in the substrates studied. Similarly, Smith and coworkers[92] also demonstrated the viability of the chelating ligands such as bisphosphines in accelerating the borylation reactions. Like Hartwig's initial study with chelating bipy ligands,[91] the reactions required a large excess of the arene and long reaction times were observed. Studies on the reaction mechanism and isolation of potential intermediates suggested that the increased reaction times were a result of the induction period leading to the formation of the Ir^{III} trisboryl intermediate complex.[91, 93]

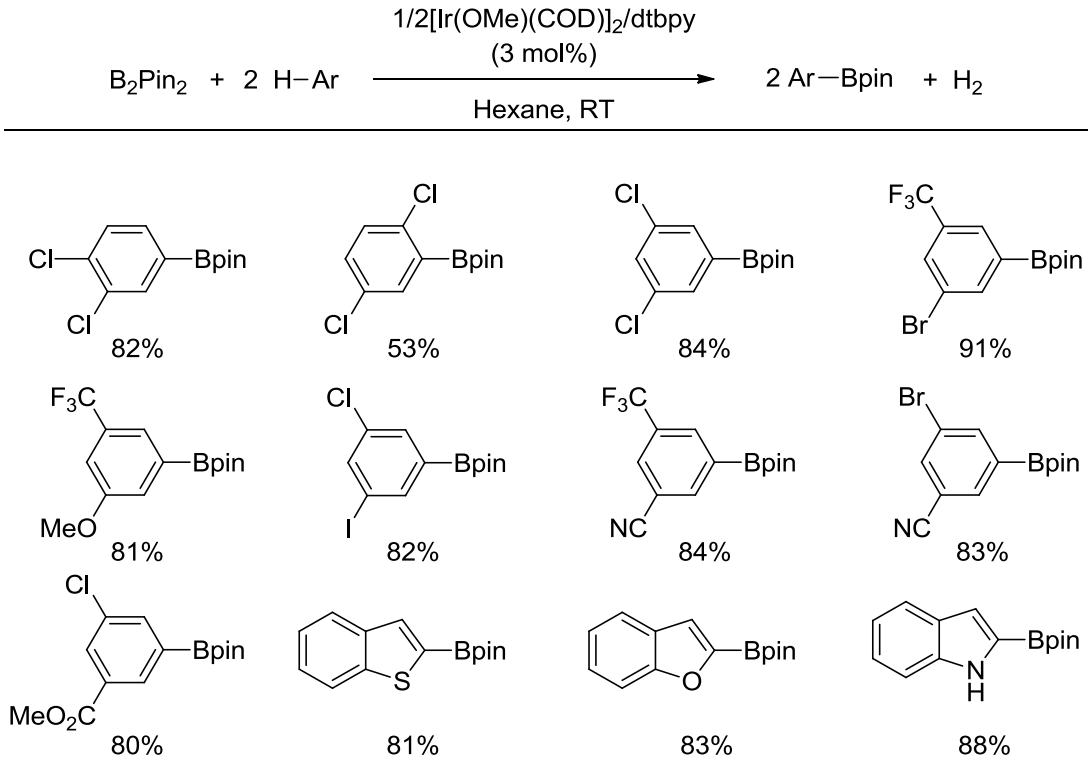

Scheme 1-16. Undirected aromatic borylation with B_2Pin_2 of disubstituted arenes and heteroaromatics[90]

Heteroaromatics provide a unique reactivity for undirected C–H borylation reactions differing from the reactivities seen with aromatic substrates. While regioselectivity can often be an issue with organic aromatic substrates, regioselectivity in heteroaromatics is generally controlled by selective functionalization of the most acidic C–H bond in the substrate allowing the borylation to occur *alpha* to the heteroatom. This reactivity is frequently observed with furan, pyrrole and thiophene species with the electronics of the ring largely dictating the reactivities of these heteroaromatic compounds.[93-94] Unsubstituted 5–membered heteroaromatic rings (Eq. 1–2) undergo borylation at the 2– and 5–positions while 2–substituted heteroaromatics undergo

borylation at the 5–position (Eq. 1–3).[95-96] Remarkably, when bulky groups such as triisopropylsilyl (TIPS) are directly bonded to the nitrogen of a pyrrole, borylation occurs at the 3–position of the ring rather than the 2–position (Eq. 1–4).[96-98] Heteroatoms fused with benzene rings (benzothiophene, benzofuran or indole) undergo monoborylation with the –Bpin group adding to the 2–position with no competing borylation on the arene ring (Eq. 1–5).[90, 99]

The reactivity of pyridine based aromatics in iridium–catalyzed C–H borylation differs slightly from the reactivities observed with the 5–membered heterocycles. Pyridine rings which are substituted at the 2–position generally undergo competitive borylation at the 4–position and 5–positions relative to the nitrogen heteroatom, likely for steric reasons (Eq. 1–6).[100] Meanwhile, pyridine rings with a substituent at the 3–position typically undergo borylation at the 5–position (Eq. 1–7) while 2,6–disubstituted pyridine rings undergo borylation at the 4–position (Eq. 1–8).[101] Interestingly, bipyridine rings joined at the 2–position which contain large substituents at their respective 4–positions (such as *tert*–butyl groups) will undergo borylation with 1 eq. of B_2Pin_2 at the 6– and 6'–positions of the bipyridine (Eq. 1–9).[100]

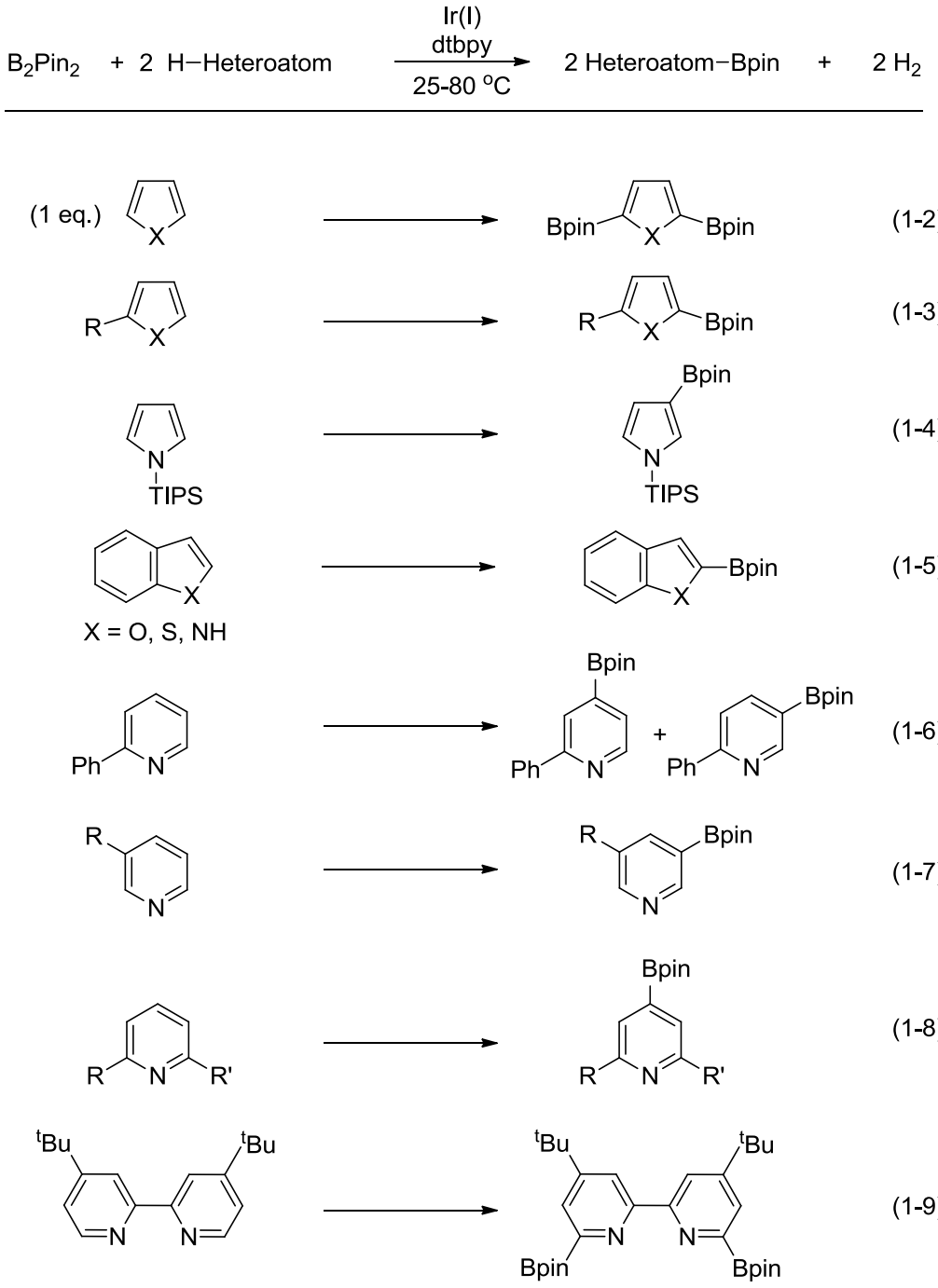

Shortly following Hartwig's thermal C–H borylation of benzene, Smith[89] reported C–H borylations of substituted arenes using [Cp*Ir(PMe_3)(H)(Bpin)] and [Cp*Rh(η^4–

C_6Me_6)] catalysts under thermal conditions. Importantly, it was found that anisole (Eq. 1–10) reacts preferentially at the *meta*–position while *N*,*N*–dimethylaniline (Eq. 1–11) promotes borylation at the *para*–position (Scheme 1–17). This selectivity was speculated to largely be due to electronic arguments with regard to the aniline derivative since reaction with cumene (Eq. 1–12) yielded a statistical distribution of the *meta*– and *para*–products. Arenes bearing amide and ester functionalities which display potential competing reactions were also competent substrates and the reduction of the carbonyls was not observed. Interestingly, the amide (Eq. 1–13) was found to promote *ortho*–borylation in a ratio of 4.17:1.98:1.00 (*ortho*:*meta*:*para*). Importantly, the borylations were found to be fully compatible with various heteroatoms without degradation of the product and the transformations were carried out under thermal conditions in relatively short reaction times. Unfortunately, the reaction still failed to be completely selective to one position on the aromatic ring. Although *meta*– and *para*–substituted borylated products were obtained, the amide functional group showed promising ability as a directing group towards selective *ortho*–borylation on the aromatic ring.

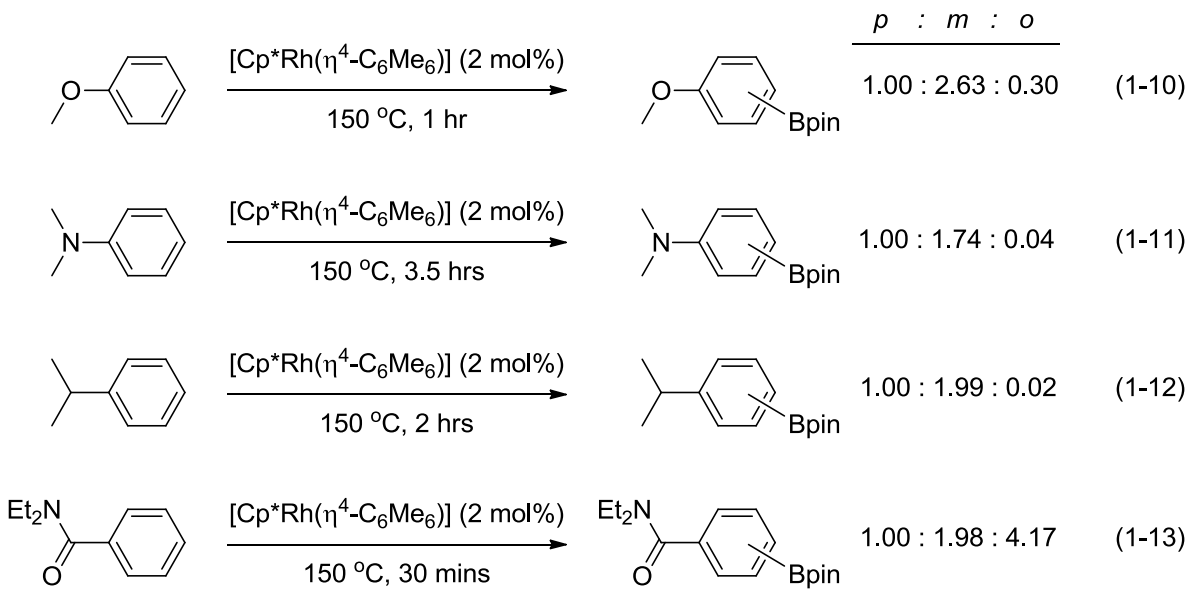

Scheme 1-17. Selectivities of borylated arenes by Smith and coworkers[89]

1.5.4 Iridium–Catalyzed Functional Group Directed C–H Borylation of Arenes

With mixtures of *ortho*–, *meta*– and *para*–borylated products, C–H borylation of monosubstituted phenyl rings fails to achieve the regioselectivity of their heteroaromatic counterparts. Specifically, selective *ortho*–borylation of substituted aromatics still presents a significant challenge in synthetic chemistry. As described above, Hartwig's catalytic system consisting of $[Ir(COD)OMe]_2$ and dtbpy typically results in products whose regioselectivity is dominated by steric effects. This lack of selectivity is likely a result of the intermediate $[Ir(COE)(dtbpy)(Bpin)_3]$, which is thought to be the catalytically active species which undergoes C–H activation, is coordinatively saturated and cannot accommodate additional ligands such as a directing group. To address this, several

research groups have investigated the possibility of using similar catalytic systems but instead employing monodentate ligands.

The site selective borylation for the *ortho*–position of aromatic rings was achieved by Ishiyama and Miyaura[102] in 2010 with the use of benzoate ester derivatives. Implementing the same iridium source as Hartwig $[Ir(\mu–OMe)(COD)]_2$, the biscoordinated dtbpy ligand was replaced with the electron poor tris[3,5–bis(trifluoromethyl)phenyl]phosphine monodentate ligand. This resulted in the borylation of benzoates in high yields with near exclusive selectivity for the *ortho*–position (Scheme 1–18). The reaction was tolerant of functional group substitution at the *meta*– and *para*–positions. Amazingly, 1,2–disubstituted benzoates were also borylated at the vacant *ortho*–position with no loss in yield or selectivity of the reaction. The reaction tolerated methyl (95%), ethyl (92%) isopropyl (89%) and *tert*–butyl (83%) esters as functional groups showing only a minor decrease in the yield with an increase in the sterics of the directing group. The directed *ortho*–borylation was later extended to utilizing ketone directing groups[103] however increased temperatures were required and the yields were significantly lower. Yields were increased upon the use of triphenylarsine ($AsPh_3$) as the ligand which significantly increased the reactivity of the system and yields over 100% (relative to 0.5 eq. of B_2Pin_2) were observed. The authors speculated that this was largely due to the ability of HBpin to act as the borylation source which could occur once full consumption of the B_2Pin_2 was achieved.

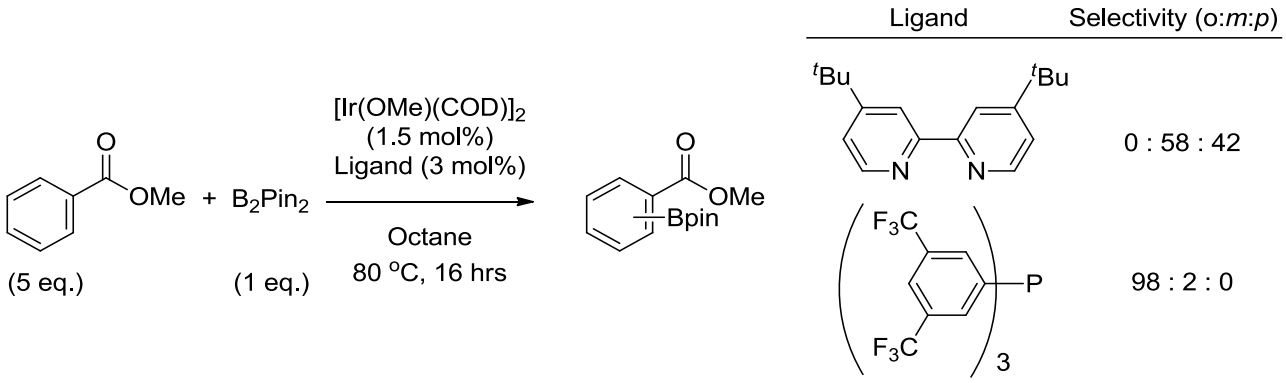

Scheme 1-18. Selectivity in benzoate–directed borylation with dtbpy and P(3,5–$(F_3C)_2C_6H_3)_3$ ligands

The scope of directing groups was significantly expanded in 2009 by Sawamura and coworkers[104] whose alternative approach to C–H borylation involved the use of Ir^I catalysts coordinated to heterogeneous silica–supported ligands (Figure 1–8). While previous C–H borylations were catalyzed by homogeneous systems, this marked the first heterogeneous system used for such a process. This catalytic system was effective for the *ortho*–borylation of aryl species with an assortment of directing groups including esters ($–CO_2R$), amides ($–CONR_2$), sulfonates ($–SO_3R$), acetals ($–C(OR)_2$) as well as benzyl methoxymethyl ether (Bn–OMOM) to produce the *ortho*–borylated products with exclusive regioselectivity in excellent yields (Scheme 1–19). Impressively, chlorine was found to be a competent directing group though the selectivity for the *ortho*–position was slightly decreased (92:8 *ortho*:(*meta*+*para*)). However, addition of the $–CF_3$ substituent *para* to the chlorine provided complete selectivity for the *ortho*–position (>99:1 *ortho*:(*meta*+*para*)). Significantly, immobilization of the phosphine ligands proved to be crucial to the reaction as attempts to conduct the reaction under homogeneous

conditions with $[Ir(OMe)(COD)]_2$ and Ph–SMAP or other phosphine ligands (PPh_3, P^tBu_3, PCy_3, PMe_3) were found to produce at best only trace amounts of *ortho*–borylated product. This has proven to be a major limitation of the borylation reaction and unfortunately the heterogeneous catalyst could not be recycled in the process.

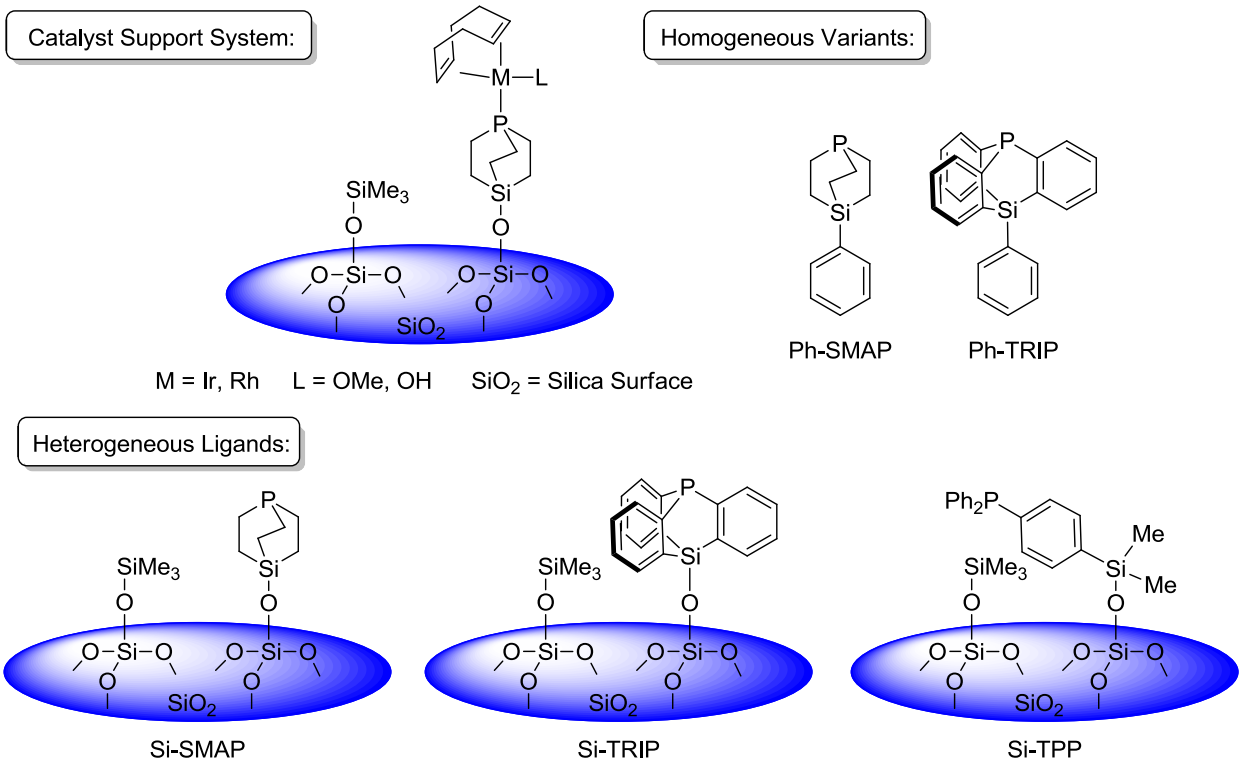

Figure 1-8. Sawamura's heterogeneous silica supported ligands

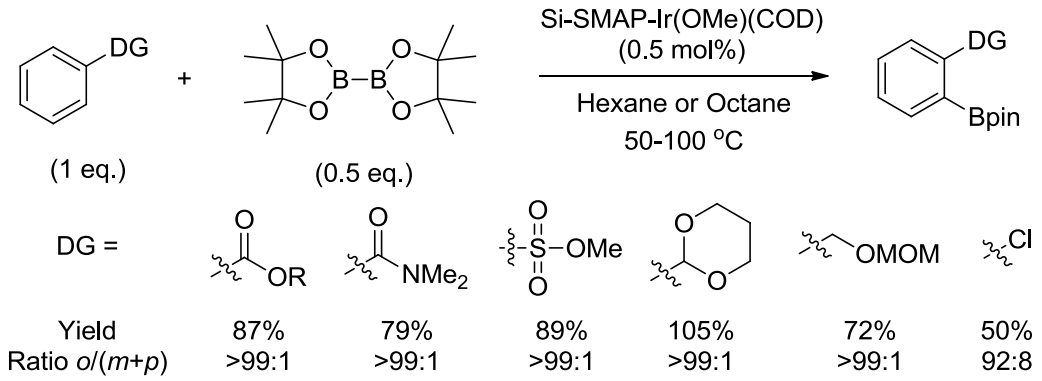

Scheme 1-19. Scope of directing groups for *ortho*–C–H borylation with Si–SMAP–Ir(OMe)(COD)

The Si–SMAP–Ir(OMe)(COD) catalysts can also been applied to systems utilizing phenol derivatives as directing groups, however carbamates were the only functional group which provided good yields and exclusive selectivity for the *ortho*–position.[105] Heteroatoms (particularly furan, pyrrole, thiophene, benzothiophene, benzofuran and indole) could also be regioselectively borylated at the 3–position using 2–methoxycarbonyl directing groups which allowed borylation at a more sterically hindered position in comparison to the $[Ir(OMe)(COD)]_2$/dtbpy systems.[106]

The scope of the metal–catalyzed directed *ortho*–borylation has been largely dominated by oxygen–based directing groups including esters, ketones carbamates and amides. Aside from carbonyl groups, Hartwig has shown the reactivity of the methylsilyl functionality (–$C(CH_3)SiMe_3H$) towards *ortho*–borylation of arenes (Eq. 1–14).[107] In cases where the α–methyl group was not present, regioselectivity issues were encountered and bisborylation was observed in a 2.3:1 ratio (*mono*:*bis*). Similarly, siloxy groups (–$OSiEt_2H$) (Eq. 1–15) were also capable of directing *ortho*–borylation of arenes.

However, only arenes bearing steric blocking groups at one of the *ortho*–positions were investigated, likely to prevent mixtures of mono– and bisborylated products.

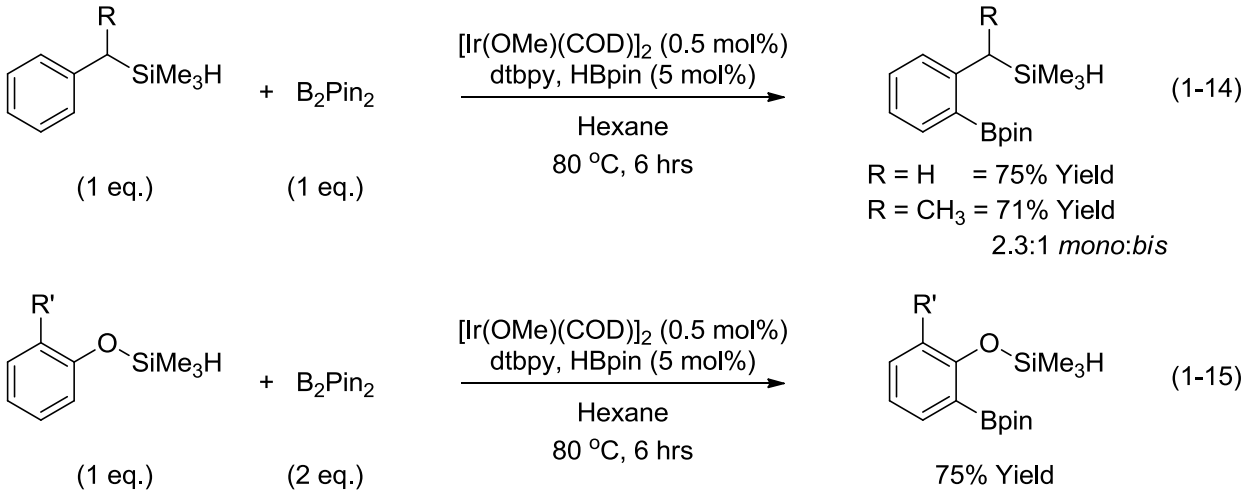

Preliminary reports of selective nitrogen–directed borylation primarily occurred with 2–substituted indoles which showed borylation to occur selectively at the 7–position (Eq. 1–16).[108] Important to the study was the investigation of the mechanism as the selectivity for the 7–position of indole was unexpected. Through deuterium labelling studies on the diborylation of indole and the isosteric analogue benzofuran (minus the heteroatom bound hydrogen), Smith and coworkers[108] postulated that the nitrogen is capable of coordinating to the iridium metal and directing borylation to the C–7 position (Scheme 1–20, B). It was first speculated that the NH bond could be responsible for the coordinating to an acidic –Bpin moiety on the metal *via* hydrogen bonding (Scheme 1–20, A). However, when benzofuran was employed in place of indole, C–7 borylation was still observed as the major product thus ruling out the requirement for a

hydrogen bond donor in this position. Thus it is predicted that this mechanism proceeds *via* the pathway seen in B (Scheme 1–20). Similarly, Steen, Marder and Sawamura[109] have shown that the borylation of quinolines selectively occurs at the 8–position using the Si–SMAP–$[Ir(OMe)(COD)]_2$ system (Eq. 1–17). Although the mechanism of the reaction was not investigated, it is plausible to suggest a similar pathway to that observed in the borylation of indoles at the C7–position is present (Scheme 1–20).

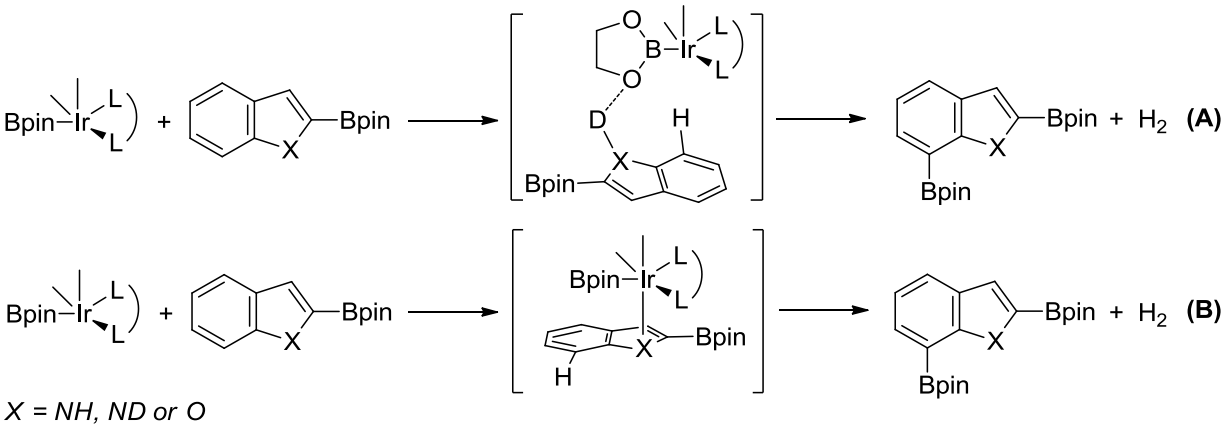

Scheme 1-20. Potential *N*–directed mechanisms for C7–borylation *via* A) NH hydrogen bonding of the substrate with acidic moieties on the metal and B) lone pair of nitrogen chelating with the metal

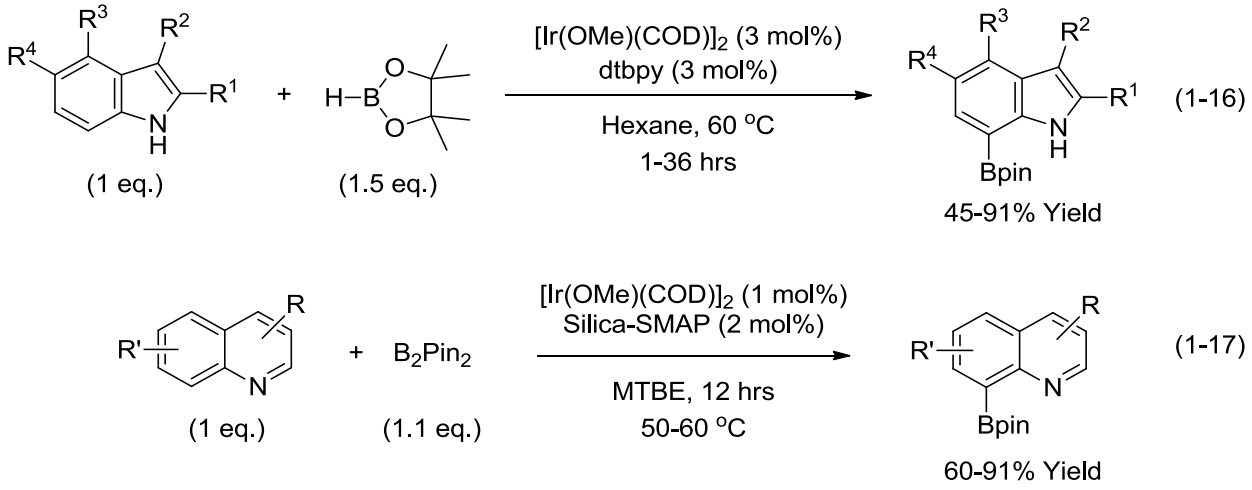

Expanding on the incorporation of nitrogen functionalities as directing groups for directed borylation reactions, Fernández and Lassaletta[110] employed the traditional $[Ir(OMe)(COD)]_2$ catalyst with hemilabile picolinaldehyde *N*,*N*–dibenzylhydrazone ligand (**1–23**) for the borylation of 2–arylpyridines and 1–naphthalisoquinolines with B_2Pin_2. Inspired by the high reactivity of Hartwig's system, their investigation into the use hemilabile ligands was to replace dtbpy with an unsymmetrical biscoordinated *N*,*N*–ligand which contains one weaker nitrogen donor. Investigating the reaction with 1–naphthalisoquinoline, they found that various pyridine hydrazones were competent ligands providing site selective borylation to the 2–position of the naphthyl ring which overcame regioselectivity issues experienced with the dtbpy ligand (Scheme 1–21). As a result, a variety of isoquinoline and 2–arylpyridine derivatives were borylated under relatively mild conditions.

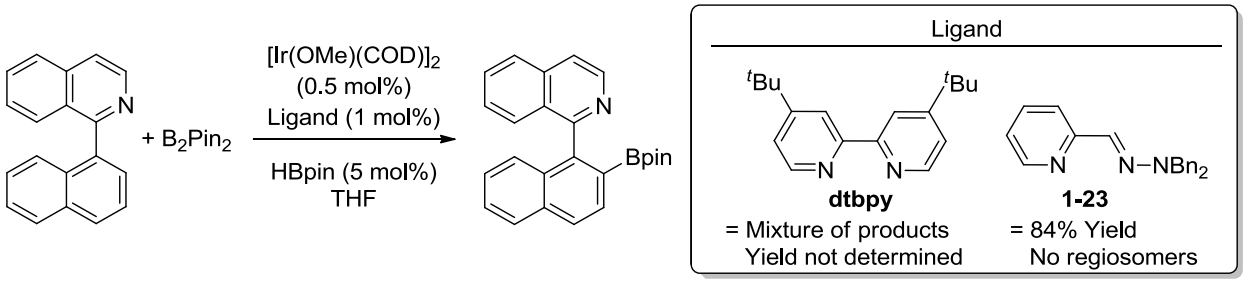

Scheme 1-21. Reactivity of 1–naphthylisoquinoline borylation with dtbpy and **1–23**

A mechanistic interpretation of the reaction is provided in Figure 1–9 which exemplifies the borylation of 2–phenylpyridine. Upon formation of **1–M**, which contains an open coordination site, 2–phenylpyridine can coordinate *via* the nitrogen atom to the metal center producing **1–N**. Subsequently, **1–N** is in equilibrium with **1–O** in which the weaker nitrogen donor can dissociate from the metal center producing a vacant site at the metal center. Upon formation of this product, the phenyl ring adjacent to the pyridine on 2–phenylpyridine can undergo oxidative addition to the metal producing species **1–P**. Reductive elimination of the borylated aryl ring produces intermediate **1–Q**, which is promoted by the coordination of the dissociated nitrogen ligand back to the metal center. Lastly, the borylated 2–phenylpyridine ring is expelled producing the 16e^- species **1–R** which undergoes transmetalation with B_2Pin_2 to regenerate the catalytically active trisboryl species **1–M**, which had been previously suggested.[110-112]

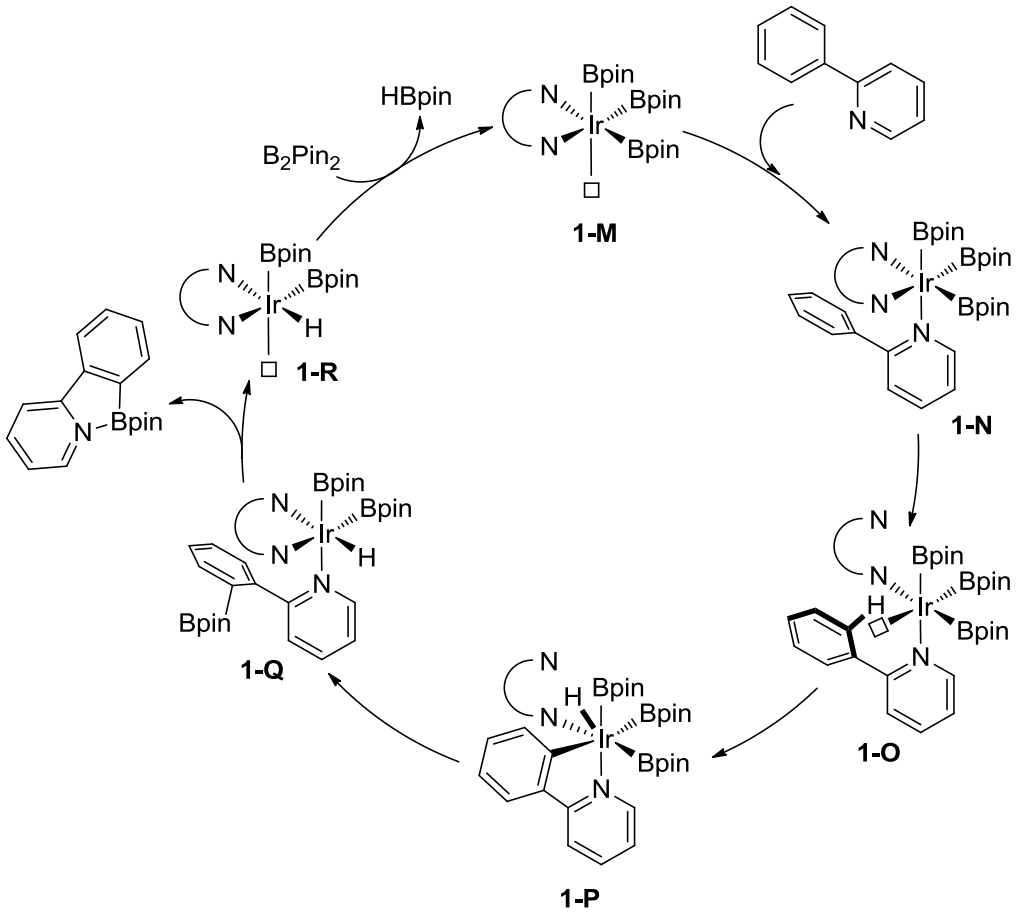

Figure 1-9. Catalytic cycle for the directed borylation of 2–phenylpyridine with hemilabile *N*,*N*–ligands

Similarly, Fernández and Lassaletta have also proven *N*,*N*–dimethylhydrazones to be viable directors for the site selective *ortho*–borylation of an adjacent phenyl ring with B_2Pin_2[110] as well as the more atom economical HBpin.[113] Diborations have also been carried out with the hydrazone directing group and B_2Pin_2 forming selectively diborated product with no monoborylation observed.[114] Furthermore, Clark and coworkers[115] have carried out selective *ortho*–borylations using benzylamines as directing groups. Using

[Ir(OMe)(COD)]$_2$ with picolylamine as the ligand, a variety of substituted benzylamines were borylated using B_2Pin_2 as the boron source. Unfortunately, mixtures of mono– and bisborylated products were obtained in substrates which did not present a steric blocking group at one *ortho*–position (Scheme 1–22).

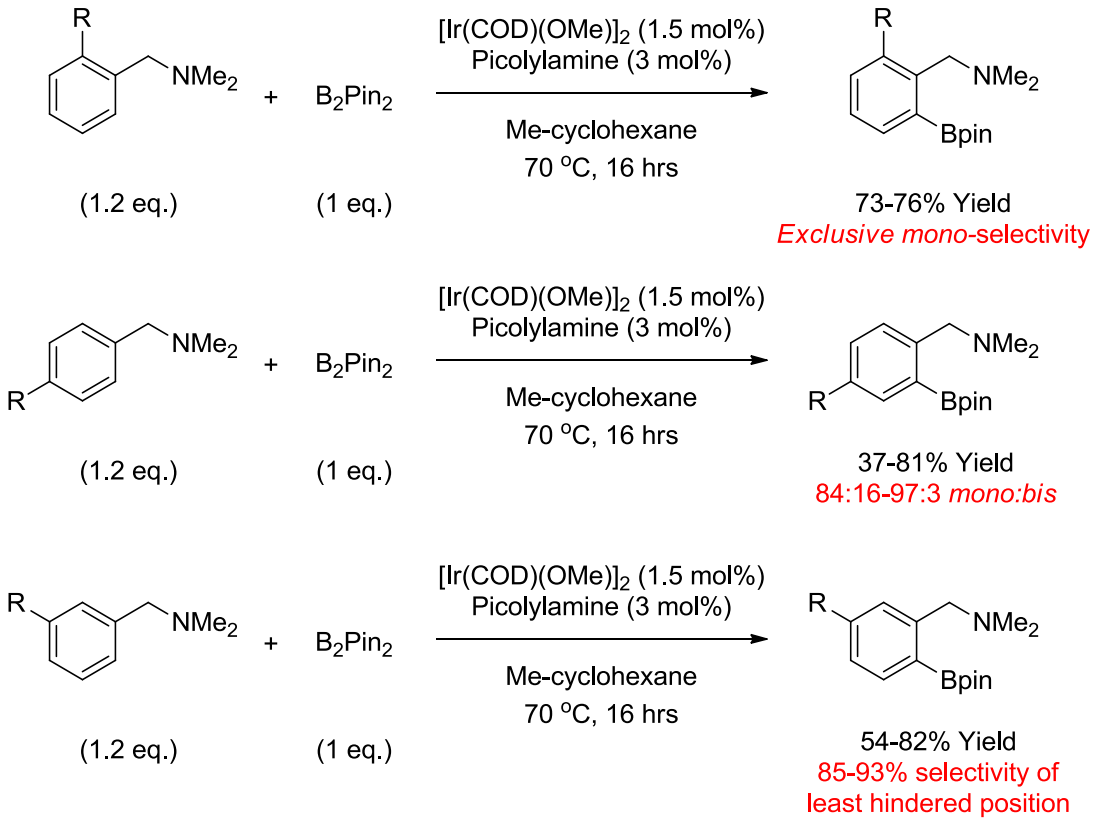

Scheme 1-22. Ir–catalyzed *ortho*–borylation directed by benzylamines

1.5.5 Palladium–Catalyzed Functional Group Directed C–H Borylation of Arenes

Although the field of C–H borylation chemistry has been largely dominated by iridium–catalyzed reactions (specifically [Ir(OMe)(COD)]$_2$ systems), select examples do exist for other metal–catalyzed processes. Examples of palladium–catalyzed systems exist

for $Pd(OAc)_2$ using B_2Pin_2 as the boron source in the site selective *ortho*–borylation of acetanilides by Fu[116] and benzamides by Yu[117] (Eq. 1–18 & 1–19). These processes are thought to go through Pd^{II} systems and require stoichiometric amounts of oxidants such as 1,4–benzoquinone (BQ) or potassium persulfate ($K_2S_2O_8$) in order to regenerate the active Pd^{II} catalyst from Pd^0. More recently, Kuninobu, Takai and coworkers[118] have utilized $Pd(OAc)_2$ for the borylation of 2–phenylpyridine with 9–borabicyclo[3.3.1]nonane (9–BBN) as the boron source (Eq. 1–20). Impressively, these reactions proceed at room temperature through a Pd^0 route thus not requiring oxidants to regenerate the active catalyst.

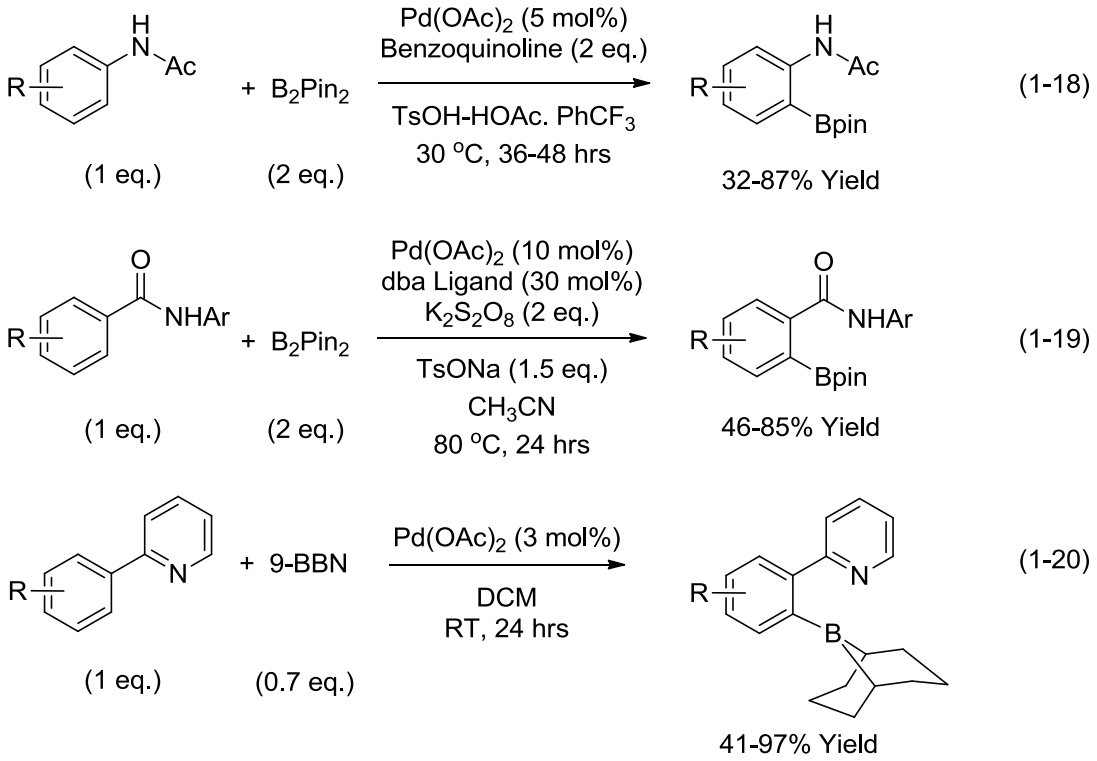

1.5.6 Rhodium–Catalyzed Functional Group Directed C–H Borylation of Arenes

Rhodium has typically been used as an alternative to iridium–catalyzed systems in the undirected borylation of arenes (*vide supra*, Scheme 1–18). However, their utility as viable C–H borylation catalysts has been limited due to the harsh conditions as well as the propensity for rhodium to catalyze the borylation of alkylarenes at the benzylic position, causing major issues with regioselectivity and thus mixtures of borylated products.[89, 119-120] As such, their use as catalysts in directed C–H borylation has not been extensively investigated.

The first directed, site selective *ortho*–borylation with rhodium catalysts was reported by Sawamura[121] with the use of $[Rh(OH)(COD)]_2$ and the Si–SMAP ligand (Figure 1–8) (1:1 Rh:L) to create the SMAP–[Rh(COD)(OH)] active catalyst. Using B_2Pin_2 as the boron source, *N*–functionalized arenes were borylated under mild conditions using various sp^2–nitrogen directing groups including pyridine, imidazole and pyrazole as well as sp^3–directing groups including NMe_2, pyrrolidine and 1,3–dimethyl–imidazolidine (Scheme 1–23). These reactions proceed at room temperature and 0.5 eq. of B_2Pin_2 is required to prevent exclusive bisborylation from occur at the 2– and 6–positions. While majority of the reactions results in the monoborylated product, some bisborylation is encountered. Some substrates containing a *meta*–substituent on the borylated ring reacted without bisborylation and while sterics may play a factor in the regioselectivity, the flexibility of the directing group allowing coordination of the nitrogen to the –Bpin group cannot be ignored.[110] Although the reactions proved to be very efficient for the borylation reactions (very low loading of catalyst, substoichiometric B_2Pin_2 and mild temperatures

<85 °C), the heterogeneity of the system somewhat limits the utility as no comment to recycling of the catalyst was stated. Likewise, attempts to use soluble variants of the ligand to make the reaction homogeneous failed to produce the desired borylated products in significant yields.[121] The same authors have recently extended this system to the borylation of sp^3 C–H bonds with comparable yields and selectivities.[122-124]

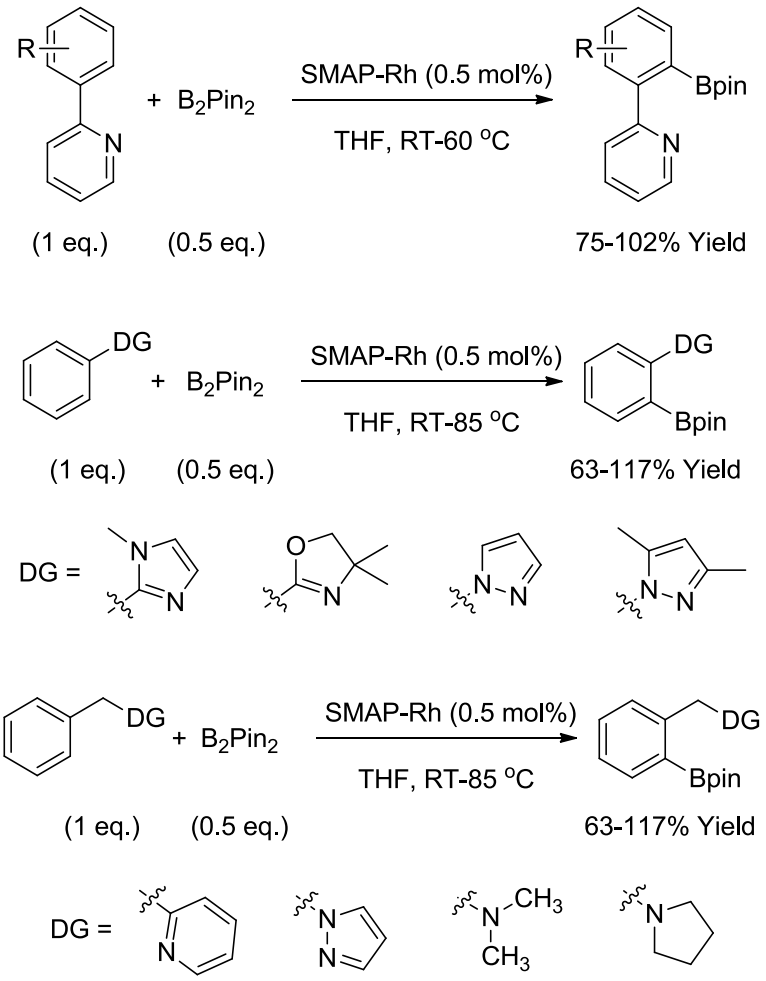

Scheme 1-23. Rh–catalyzed C–H borylation with silica supported ligands[125]

Thus far, the only reported *ortho*–directed C–H borylation of arenes to occur in a homogeneous system has been reported by Chen and Yan[126] in the borylation–amination resulting in the synthesis of carbazoles (Scheme 1–24). This reaction employs the Rh^{III} catalyst [$RhCp^*(OTf)_2$] using an *ortho*–aniline ($–C_6H_5NH_2$) directing group to regioselectively borylate the *ortho*–position of the adjacent ring with B_2Pin_2. Initial studies on the reaction indicated borylation of the *ortho*–position, and the product was isolated in 30% yield even in the presence of $Cu(OAc)_2$ oxidant. However, upon addition of K_2CO_3 base to the reaction, the borylated product is rapidly coupled with the amino group to produce the carbazole product. Interestingly, removal of Rh^{III} catalyst, $Cu(OAc)_2$, B_2Pin_2 or K_2CO_3 from the reaction, or swapping B_2Pin_2 for $BF_3{\cdot}OEt$ hinders any formation of the carbazole product indicating the generation of the C–B *in situ* is essential to the carbazole formation.

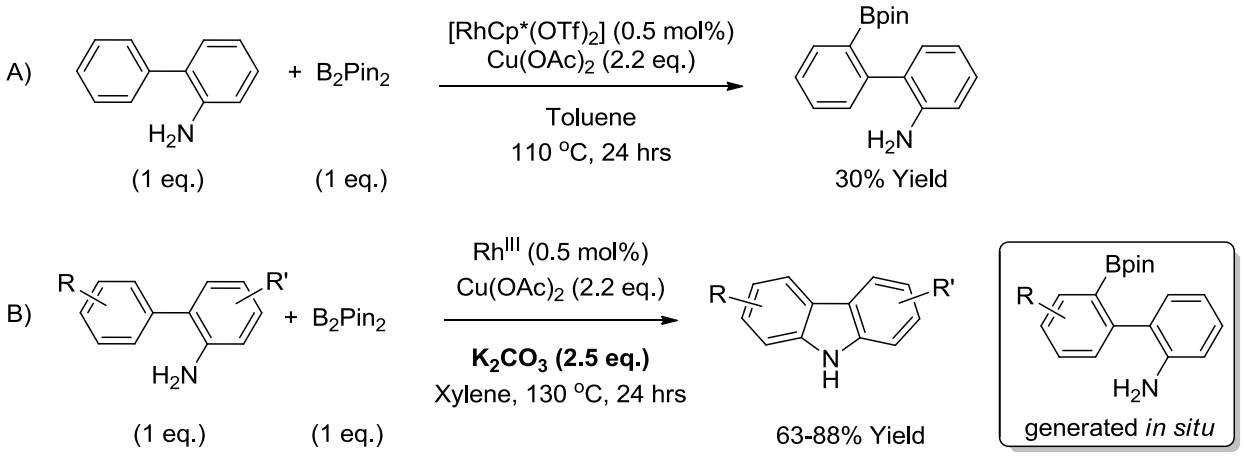

Scheme 1-24. Rh^{III}–catalyzed borylation with amino directing group in A) absence of K_2CO_3 and B) presence of K_2CO_3 producing the carbazole

1.6 Conclusions and Outlook

The increased synthetic utility of metal–catalyzed cross–coupling reactions, particularly Suzuki–Miyaura cross–couplings is a measure of the importance of discovering efficient routes to arylboronate starting materials.[56, 125, 127] In the realm of synthesizing polysubstituted aromatic compounds, C–H activation has pushed towards the forefront as a beneficial alternative to traditional approaches such as D*o*M and standard cross–coupling reactions. C–H activation is an ever expanding field with many diverse applications, the incorporation of this methodology towards directed C–H borylation provides a gateway to arylboronates with exclusive regioselectivites observed. Primarily, conducting C–H borylation reactions under mild conditions with high selectivities will provide extremely advantageous synthetic routes to valuable aromatic substrates.

1.7 References

1. Pan, S.; Ryu, N.; Shibata, T. *J. Am. Chem. Soc.* **2012**, *134*, 17474-17477.
2. Constable, D. J. C.; Dunn, P. J.; Hayler, J. D.; Humphrey, G. R.; Leazer, J. J. L.; Linderman, R. J.; Lorenz, K.; Manley, J.; Pearlman, B. A.; Wells, A.; Zaks, A.; Zhang, T. Y. *Green Chem.* **2007**, *9*, 411-420.
3. Bouffard, J.; Itami, K. *Top. Curr. Chem.* **2010**, *292*, 231-280.
4. Carey, J. S.; Laffan, D.; Thomson, C.; Williams, M. T. *Org. Biomol. Chem.* **2006**, *4*, 2337-2347.
5. Grondal, C.; Jeanty, M.; Enders, D. *Nature Chemistry* **2010**, *2*, 167-178.
6. Newman, D. J.; Cragg, G. M. *J. Nat. Prod.* **2012**, *75*, 311-335.
7. Nicolaou, K. C.; Vourloumis, D.; Winssinger, N.; Baran, P. S. *Angew. Chem. Int. Ed.* **2000**, *39*, 44-122.
8. Bamfield, P.; Gordon, P. F. *Chem. Soc. Rev.* **1984**, *13*, 441-488.
9. Ojima, I.; Tzamarioudaki, M.; Li, Z.; Donovan, R. J. *Chem. Rev.* **1996**, *96*, 635-662.
10. Inglesby, P. A.; Evans, P. A. *Chem. Soc. Rev.* **2010**, *39*, 2791-2805.
11. Gilman, H.; Bebb, R. L. *J. Am. Chem. Soc.* **1939**, *61*, 109-112.
12. Wittig, G.; Fuhrmann, G. *Chem. Ber.* **1940**, *73*, 1197-1218.
13. Gilman, H.; Morton, J. W. The Metalation Reaction with Organolithium Compounds. In *Org. React.*, John Wiley & Sons, Inc.: **1954**; Vol. 8, p 258.
14. Puterbaugh, W. H.; Hauser, C. R. *J. Org. Chem.* **1964**, *29*, 853-856.
15. Slocum, D. W.; Sugarman, D. I. Directed Metalation. In *Polyamine-Chelated Alkali Metal Compounds*, Adv. Chem. Ser.: **1974**; Vol. 130, pp 222-247.
16. Hartung, C. G.; Snieckus, V. The Directed ortho Metalation Reaction - A Point of Departure for New Synthetic Aromatic Chemistry. In *Modern Arene Chemistry*, Astruc, D., Ed. Wiley-VCH Verlag GmbH & Co. KGaA: Weinheim, **2002**; pp 330-367.
17. Board, J.; Cosman, J. L.; Rantanen, T.; Singh, S. P.; Snieckus, V. *Platinum Metals Rev.* **2013**, *57*, 234-258.
18. Nerdinger, S.; Marchhart, R.; Riebel, P.; Kendall, C.; R. Johnson, M.; Yin, C. F.; Snieckus, V.; D. Eltis, L. *Chem. Commun.* **1999**, 2259-2260.
19. Trofimenko, S. *Inorg. Chem.* **1973**, *12*, 1215-1221.
20. Albrecht, M. *Chem. Rev.* **2010**, *110*, 576-623.
21. Labinger, J. A.; Bercaw, J. E. *Nature* **2002**, *417*, 507-514.
22. Janowicz, A. H.; Bergman, R. G. *J. Am. Chem. Soc.* **1982**, *104*, 352-354.
23. Janowicz, A. H.; Bergman, R. G. *J. Am. Chem. Soc.* **1983**, *105*, 3929-3939.
24. Periana, R. A.; Bergman, R. G. *Organometallics* **1984**, *3*, 508-510.
25. Jones, W. D.; Feher, F. J. *J. Am. Chem. Soc.* **1984**, *106*, 1650-1663.
26. Kaesz, H. D.; Saillant, R. B. *Chem. Rev.* **1972**, *72*, 231-281.
27. Hoyano, J. K.; McMaster, A. D.; Graham, W. A. G. *J. Am. Chem. Soc.* **1983**, *105*, 7190-7191.
28. Albrecht, M.; Spek, A. L.; van Koten, G. *J. Am. Chem. Soc.* **2001**, *123*, 7233-7246.

29. González, J. J.; García, N.; Gómez-Lor, B.; Echavarren, A. M. *J. Org. Chem.* **1997**, *62*, 1286-1291.
30. Campeau, L. C.; Parisien, M.; Leblanc, M.; Fagnou, K. *J. Am. Chem. Soc.* **2004**, *126*, 9186-9187.
31. Campeau, L. C.; Parisien, M.; Jean, A.; Fagnou, K. *J. Am. Chem. Soc.* **2005**, *128*, 581-590.
32. Lapointe, D.; Fagnou, K. *Chem. Lett.* **2010**, *39*, 1118-1126.
33. Davies, D. L.; Al-Duaij, O.; Fawcett, J.; Giardiello, M.; Hilton, S. T.; Russell, D. R. *Dalton Trans.* **2003**, 4132-4138.
34. Davies, D. L.; Donald, S. M. A.; Macgregor, S. A. *J. Am. Chem. Soc.* **2005**, *127*, 13754-13755.
35. Davies, D. L.; Donald, S. M. A.; Al-Duaij, O.; Macgregor, S. A.; Pölleth, M. *J. Am. Chem. Soc.* **2006**, *128*, 4210-4211.
36. Boutadla, Y.; Davies, D. L.; Macgregor, S. A.; Poblador-Bahamonde, A. I. *Dalton Trans.* **2009**, 5820-5831.
37. García-Cuadrado, D.; Braga, A. A. C.; Maseras, F.; Echavarren, A. M. *J. Am. Chem. Soc.* **2006**, *128*, 1066-1067.
38. Lafrance, M.; Rowley, C. N.; Woo, T. K.; Fagnou, K. *J. Am. Chem. Soc.* **2006**, *128*, 8754-8756.
39. Lafrance, M.; Fagnou, K. *J. Am. Chem. Soc.* **2006**, *128*, 16496-16497.
40. García-Cuadrado, D.; de Mendoza, P.; Braga, A. A. C.; Maseras, F.; Echavarren, A. M. *J. Am. Chem. Soc.* **2007**, *129*, 6880-6886.
41. Gorelsky, S. I.; Lapointe, D.; Fagnou, K. *J. Am. Chem. Soc.* **2008**, *130*, 10848-10849.
42. Perutz, R. N.; Sabo-Etienne, S. *Angew. Chem. Int. Ed.* **2007**, *46*, 2578-2592.
43. Watson, P. L.; Parshall, G. W. *Acc. Chem. Res.* **1985**, *18*, 51-56.
44. Jones, W. D. *Science* **2000**, *287*, 1942-1943.
45. Sadow, A. D.; Tilley, T. D. *J. Am. Chem. Soc.* **2004**, *127*, 643-656.
46. Balcells, D.; Clot, E.; Eisenstein, O. *Chem. Rev.* **2010**, *110*, 749-823.
47. Bergman, R. G. *Nature* **2007**, *446*, 391-393.
48. Trost, B. M. *Science* **1991**, *254*, 1471-1477.
49. Trost, B. M. *Angew. Chem. Int. Ed. Engl.* **1995**, *34*, 259-281.
50. Colby, D. A.; Bergman, R. G.; Ellman, J. A. *Chem. Rev.* **2010**, *110*, 624-655.
51. Yamaguchi, J.; Yamaguchi, A. D.; Itami, K. *Angew. Chem. Int. Ed.* **2012**, *51*, 8960-9009.
52. Moritani, I.; Fujiwara, Y. *Tetrahedron Lett.* **1967**, *8*, 1119-1122.
53. Fujiwara, Y.; Noritani, I.; Danno, S.; Asano, R.; Teranishi, S. *J. Am. Chem. Soc.* **1969**, *91*, 7166-7169.
54. Fujiwara, Y.; Moritani, I.; Matsuda, M.; Teranishi, S. *Tetrahedron Lett.* **1968**, *9*, 3863-3865.
55. Luo, Y. R.; Cheng, J. P. Bond Dissociation Energies. In *Handbook of Chemistry and Physics*, 94th ed.; Haynes, W. M., Ed. CRC Press/Taylor and Francis: Boca Raton, **2014**; pp 65-96.

56. Wencel-Delord, J.; Droge, T.; Liu, F.; Glorius, F. *Chem. Soc. Rev.* **2011**, *40*, 4740-4761.
57. Ryabov, A. D. *Chem. Rev.* **1990**, *90*, 403-424.
58. Shilov, A. E.; Shul'pin, G. B. *Chem. Rev.* **1997**, *97*, 2879-2932.
59. Niu, J. L.; Hao, X. Q.; Gong, J. F.; Song, M. P. *Dalton Trans.* **2011**, *40*, 5135-5150.
60. Moulton, C. J.; Shaw, B. L. *J. Chem. Soc., Dalton Trans.* **1976**, 1020-1024.
61. Albrecht, M.; van Koten, G. *Angew. Chem. Int. Ed.* **2001**, *40*, 3750-3781.
62. Singleton, J. T. *Tetrahedron* **2003**, *59*, 1837-1857.
63. van der Boom, M. E.; Milstein, D. *Chem. Rev.* **2003**, *103*, 1759-1792.
64. van Koten, G. *J. Organomet. Chem.* **2013**, *730*, 156-164.
65. Horino, H.; Inoue, N. *J. Org. Chem.* **1981**, *46*, 4416-4422.
66. Patureau, F. W.; Glorius, F. *J. Am. Chem. Soc.* **2010**, *132*, 9982-9983.
67. Murai, S.; Kakiuchi, F.; Sekine, S.; Tanaka, Y.; Kamatani, A.; Sonoda, M.; Chatani, N. *Nature* **1993**, *366*, 529-531.
68. Snieckus, V. *Chem. Rev.* **1990**, *90*, 879-933.
69. Kakiuchi, F.; Ohtaki, H.; Sonoda, M.; Chatani, N.; Murai, S. *Chem. Lett.* **2001**, *30*, 918-919.
70. Miyaura, N.; Suzuki, A. *J. Chem. Soc., Chem. Commun.* **1979**, 866-867.
71. Miyaura, N.; Suzuki, A. *Chem. Rev.* **1995**, *95*, 2457-2483.
72. Entwistle, C. D.; Marder, T. B. *Angew. Chem. Int. Ed.* **2002**, *41*, 2927-2931.
73. Entwistle, C. D.; Marder, T. B. *Chem. Mater.* **2004**, *16*, 4574-4585.
74. Hawthorne, M. F.; Maderna, A. *Chem. Rev.* **1999**, *99*, 3421-3434.
75. Soloway, A. H.; Tjarks, W.; Barnum, B. A.; Rong, F. G.; Barth, R. F.; Codogni, I. M.; Wilson, J. G. *Chem. Rev.* **1998**, *98*, 1515-1562.
76. Hall, D. G. Structure, Properties, and Preparation of Boronic Acid Derivatives. In *Boronic Acids*, Wiley-VCH Verlag GmbH & Co. KGaA: **2011**; pp 1-133.
77. Hayashi, T.; Yamasaki, K. *Chem. Rev.* **2003**, *103*, 2829-2844.
78. Beccalli, E. M.; Broggini, G.; Martinelli, M.; Sottocornola, S. *Chem. Rev.* **2007**, *107*, 5318-5365.
79. Alberico, D.; Scott, M. E.; Lautens, M. *Chem. Rev.* **2007**, *107*, 174-238.
80. Tobisu, M.; Chatani, N. *Angew. Chem. Int. Ed.* **2009**, *48*, 3565-3568.
81. Crudden, C. M.; Glasspoole, B. W.; Lata, C. J. *Chem. Commun.* **2009**, 6704-6716.
82. Lennox, A. J. J.; Lloyd-Jones, G. C. *Chem. Soc. Rev.* **2014**, *43*, 412-443.
83. Miyaura, N. *Top. Curr. Chem.* **2002**, *11*, 10-59.
84. Kleeberg, C.; Dang, L.; Lin, Z.; Marder, T. B. *Angew. Chem. Int. Ed.* **2009**, *48*, 5350-5354.
85. Waltz, K. M.; He, X.; Muhoro, C.; Hartwig, J. F. *J. Am. Chem. Soc.* **1995**, *117*, 11357-11358.
86. Chen, H.; Hartwig, J. F. *Angew. Chem. Int. Ed.* **1999**, *38*, 3391-3393.
87. Iverson, C. N.; Smith, M. R. *J. Am. Chem. Soc.* **1999**, *121*, 7696-7697.
88. Chen, H.; Schlecht, S.; Semple, T. C.; Hartwig, J. F. *Science* **2000**, *287*, 1995-1997.
89. Cho, J. Y.; Iverson, C. N.; Smith, M. R. *J. Am. Chem. Soc.* **2000**, *122*, 12868-12869.
90. Ishiyama, T.; Takagi, J.; Hartwig, J. F.; Miyaura, N. *Angew. Chem. Int. Ed.* **2002**, *41*, 3056-3058.

91. Ishiyama, T.; Takagi, J.; Ishida, K.; Miyaura, N.; Anastasi, N. R.; Hartwig, J. F. *J. Am. Chem. Soc.* **2002**, *124*, 390-391.
92. Cho, J. Y.; Tse, M. K.; Holmes, D.; Maleczka, R. E.; Smith, M. R. *Science* **2002**, *295*, 305-308.
93. Hartwig, J. F. *Acc. Chem. Res.* **2012**, *45*, 864-873.
94. Vanchura, I. I. B. A.; Preshlock, S. M.; Roosen, P. C.; Kallepalli, V. A.; Staples, R. J.; Maleczka, J. R. E.; Singleton, D. A.; Smith, M. R. *Chem. Commun.* **2010**, *46*, 7724-7726.
95. Ishiyama, T.; Takagi, J.; Yonekawa, Y.; Hartwig, J. F.; Miyaura, N. *Adv. Synth. Catal.* **2003**, *345*, 1103-1106.
96. Takagi, J.; Sato, K.; Hartwig, J. F.; Ishiyama, T.; Miyaura, N. *Tetrahedron Lett.* **2002**, *43*, 5649-5651.
97. Tse, M. K.; Cho, J. Y.; Smith, M. R. *Org. Lett.* **2001**, *3*, 2831-2833.
98. Beck, E. M.; Hatley, R.; Gaunt, M. J. *Angew. Chem. Int. Ed.* **2008**, *47*, 3004-3007.
99. Ishiyama, T.; Nobuta, Y.; Hartwig, J. F.; Miyaura, N. *Chem. Commun.* **2003**, 2924-2925.
100. Mkhalid, I. A. I.; Coventry, D. N.; Albesa-Jove, D.; Batsanov, A. S.; Howard, J. A. K.; Perutz, R. N.; Marder, T. B. *Angew. Chem. Int. Ed.* **2006**, *45*, 489-491.
101. Murphy, J. M.; Liao, X.; Hartwig, J. F. *J. Am. Chem. Soc.* **2007**, *129*, 15434-15435.
102. Ishiyama, T.; Isou, H.; Kikuchi, T.; Miyaura, N. *Chem. Commun.* **2010**, *46*, 159-161.
103. Itoh, H.; Kikuchi, T.; Ishiyama, T.; Miyaura, N. *Chem. Lett.* **2011**, *40*, 1007-1008.
104. Kawamorita, S.; Ohmiya, H.; Hara, K.; Fukuoka, A.; Sawamura, M. *J. Am. Chem. Soc.* **2009**, *131*, 5058-5059.
105. Yamazaki, K.; Kawamorita, S.; Ohmiya, H.; Sawamura, M. *Org. Lett.* **2010**, *12*, 3978-3981.
106. Kawamorita, S.; Ohmiya, H.; Sawamura, M. *J. Org. Chem.* **2010**, *75*, 3855-3858.
107. Boebel, T. A.; Hartwig, J. F. *J. Am. Chem. Soc.* **2008**, *130*, 7534-7535.
108. Paul, S.; Chotana, G. A.; Holmes, D.; Reichle, R. C.; Maleczka, R. E.; Smith, M. R. *J. Am. Chem. Soc.* **2006**, *128*, 15552-15553.
109. Konishi, S.; Kawamorita, S.; Iwai, T.; Steel, P. G.; Marder, T. B.; Sawamura, M. *Chem. Asian J.* **2014**, *9*, 434-438.
110. Ros, A.; Estepa, B.; López-Rodríguez, R.; Álvarez, E.; Fernández, R.; Lassaletta, J. M. *Angew. Chem. Int. Ed.* **2011**, *50*, 11724-11728.
111. Tamura, H.; Yamazaki, H.; Sato, H.; Sakaki, S. *J. Am. Chem. Soc.* **2003**, *125*, 16114-16126.
112. Boller, T. M.; Murphy, J. M.; Hapke, M.; Ishiyama, T.; Miyaura, N.; Hartwig, J. F. *J. Am. Chem. Soc.* **2005**, *127*, 14263-14278.
113. López-Rodríguez, R.; Ros, A.; Fernández, R.; Lassaletta, J. M. *J. Org. Chem.* **2012**, *77*, 9915-9920.
114. Ros, A.; López-Rodríguez, R.; Estepa, B.; Álvarez, E.; Fernández, R.; Lassaletta, J. M. *J. Am. Chem. Soc.* **2012**, *134*, 4573-4576.
115. Roering, A. J.; Hale, L. V. A.; Squier, P. A.; Ringgold, M. A.; Wiederspan, E. R.; Clark, T. B. *Org. Lett.* **2012**, *14*, 3558-3561.

116. Xiao, B.; Li, Y. M.; Liu, Z. J.; Yang, H. Y.; Fu, Y. *Chem. Commun.* **2012**, *48*, 4854-4856.
117. Dai, H. X.; Yu, J. Q. *J. Am. Chem. Soc.* **2012**, *134*, 134-137.
118. Kuninobu, Y.; Iwanaga, T.; Omura, T.; Takai, K. *Angew. Chem. Int. Ed.* **2013**, *52*, 4431-4434.
119. Shimada, S.; Batsanov, A. S.; Howard, J. A. K.; Marder, T. B. *Angew. Chem. Int. Ed.* **2001**, *40*, 2168-2171.
120. Mertins, K.; Zapf, A.; Beller, M. *J. Mol. Catal. A: Chem.* **2004**, *207*, 21-25.
121. Kawamorita, S.; Miyazaki, T.; Ohmiya, H.; Iwai, T.; Sawamura, M. *J. Am. Chem. Soc.* **2011**, *133*, 19310-19313.
122. Kawamorita, S.; Miyazaki, T.; Iwai, T.; Ohmiya, H.; Sawamura, M. *J. Am. Chem. Soc.* **2012**, *134*, 12924-12927.
123. Kawamorita, S.; Murakami, R.; Iwai, T.; Sawamura, M. *J. Am. Chem. Soc.* **2013**, *135*, 2947-2950.
124. Iwai, T.; Murakami, R.; Harada, T.; Kawamorita, S.; Sawamura, M. *Adv. Synth. Catal.* **2014**, *356*, 1563-1570.
125. Ros, A.; Fernandez, R.; Lassaletta, J. M. *Chem. Soc. Rev.* **2014**, *43*, 3229-3243.
126. Jiang, Q.; Duan-Mu, D.; Zhong, W.; Chen, H.; Yan, H. *Chem. Eur. J.* **2013**, *19*, 1903-1907.
127. Mkhalid, I. A. I.; Barnard, J. H.; Marder, T. B.; Murphy, J. M.; Hartwig, J. F. *Chem. Rev.* **2010**, *110*, 890-931.

Chapter 2

Regioselective Rh^{I}–Catalyzed Directed *ortho*–Borylation of 2–Phenylpyridines for the Preparation of Mono–Arylated Compounds

2.1 Introduction

2.1.1 Rh–Catalyzed C–H Activation

Rhodium catalysts are known to effect a variety of C–H activation reactions in both undirected and directed systems and are employed in such transformations as alkylations, alkenylations, arylations, carbonylations and borylations.[1] Mechanistically speaking, the C–H activation can occur at either Rh^{I}, which typically occurs by oxidative addition of the C–H bond resulting in a Rh^{III} hydride complex; or at Rh^{III}, typically by a CMD mechanism (*vide supra*). Additionally, C–H activation can occur at Rh^{II} metal centres.[2-4] The activity of these oxidation states towards the desired C–H activation, indicate the possibility of using these catalysts in a wide variety of viable transformations, making rhodium species exciting catalysts in C–H activation chemistry.

A seminal publication on rhodium mediated C–H activation appeared from the Diamond group[5] on the synthesis of quinaldine derivatives. The authors utilized simple anilines as starting materials and catalytic amounts of $RhCl_3 \cdot 3H_2O$ under 100 atm of ethylene at 200 ^{o}C (Scheme 2–1). It was determined that the Rh^{III} precursor was readily

reduced to Rh^{I} under the reaction conditions and that this was likely the active metal complex undergoing C–H activation. The authors suggested that the rhodium–complex undergoes cyclometalation at the *ortho*–position through insertion into the C_{Ar}–H bond producing **2–3** and is directed to that position by the amine functional group on the aromatic ring.

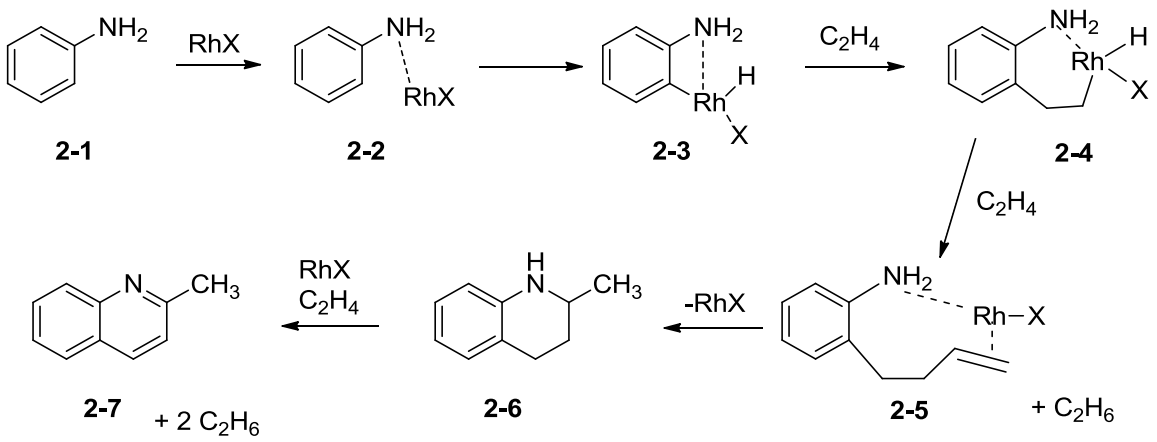

Scheme 2-1. Amine directed *ortho*–functionalization to form quinaldine

Since this seminal report, numerous accounts of metal promoted C–H bond cleavage employing stoichiometric metal complexes have appeared, but few were apparent before the early 1990's. Rhodium–catalyzed C–H bond activation was largely dormant until 1994 when Kim and coworkers[6] reported the catalytic alkylation of 2–phenylpyridine (2–Ph–pyr) and 3–methyl–2–phenylpyridine utilizing Rh^{I} systems (Scheme 2–2). The alkylations were achieved using terminal alkenes and were selective for the *ortho*–position

on the ring adjacent to the pyridine. With 2–Ph–pyr, regioselectivity was an issue and mixtures of mono– and bisalkylated products were obtained. This was overcome by sterically biasing the starting material, installing a steric blocking group at the 3–position of in the pyridine ring. As such, 3–methyl–2–phenylpyridine selectively produced the monosubstituted products in good yields with exclusive selectivity.

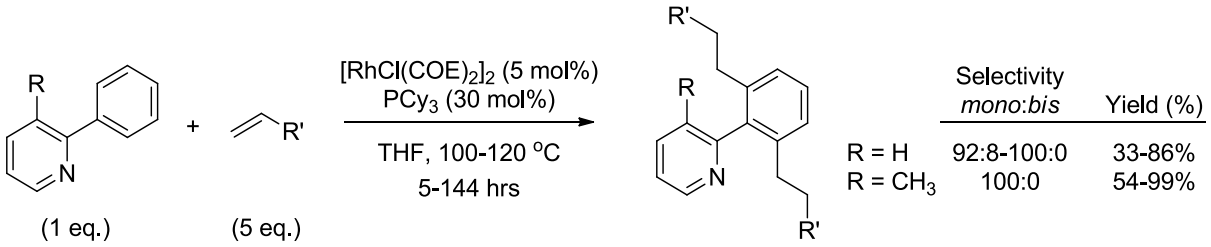

Scheme 2-2. Rh–catalyzed *ortho*–alkylation of 2–Ph–pyr and 3–methyl–2–phenylpyridine

This pioneering work was further improved by Jun and coworkers[7] showing that imines were capable of directed *ortho*–alkylation (formally a hydroarylation across the alkene) using Wilkinson's catalyst [$RhCl(PPh_3)_3$] with isomerisable terminal olefins (Scheme 2–3). Impressively, the reaction proceeds with complete regioselectivity for the *ortho*–position while olefin isomerization is also avoided. Interestingly, these conditions displayed a more comprehensive scope in place of the previously reported ruthenium–catalyzed system reported by Murai (Scheme 1–10).[8] After the directed C–H alkylation, hydrolysis of the imine to the ketone yields similar products to Murai's ketone directed system, rendering the two systems essentially analogous to one another. However, the rhodium–catalyzed alkylation improves upon the Murai system as it does not require the

use of steric groups, such as methyl substitution at the 6–position to block over alkylation and does not require non–isomerisable olefins to prevent further regioisomers, nor require excess of the olefin to promote the reaction. Mechanistically speaking, the reaction is believed to go by a similar mechanistic route to the one depicted in Figure 2–1.

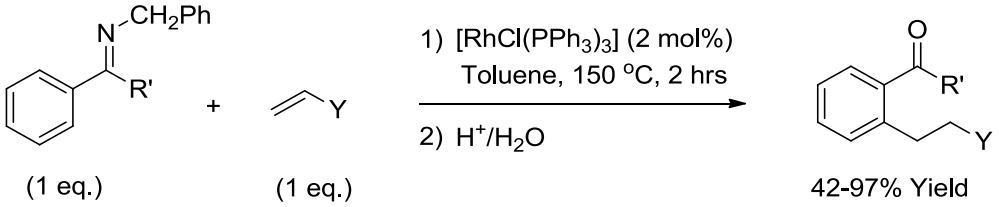

Scheme 2-3. Imine directed *ortho*–alkylation catalyzed by Wilkinson's catalyst

These processes are proposed to proceed through a Rh^{I}–catalyzed route wherein the catalyst undergoes cyclometalation with the substrate by oxidative addition of the C–H bond. Generally, the mechanistic cycle seen in Figure 2–1 can be applied to these alkylation regardless of the directing group used. Initially, the metal coordinates to the substrate, **2–A**, promoting dissociation of one of the ligands producing **2–B**. The metal coordinated substrate undergoes facile oxidative addition into the C_{Ar}–H bond producing metallacycle **2–C**. Ligand exchange with the vinyl substrate and subsequent migratory insertion produces intermediate metallacycle **2–E**, which reductively eliminates to generate product **2–F** and regenerate the catalytically active species **2–B**.

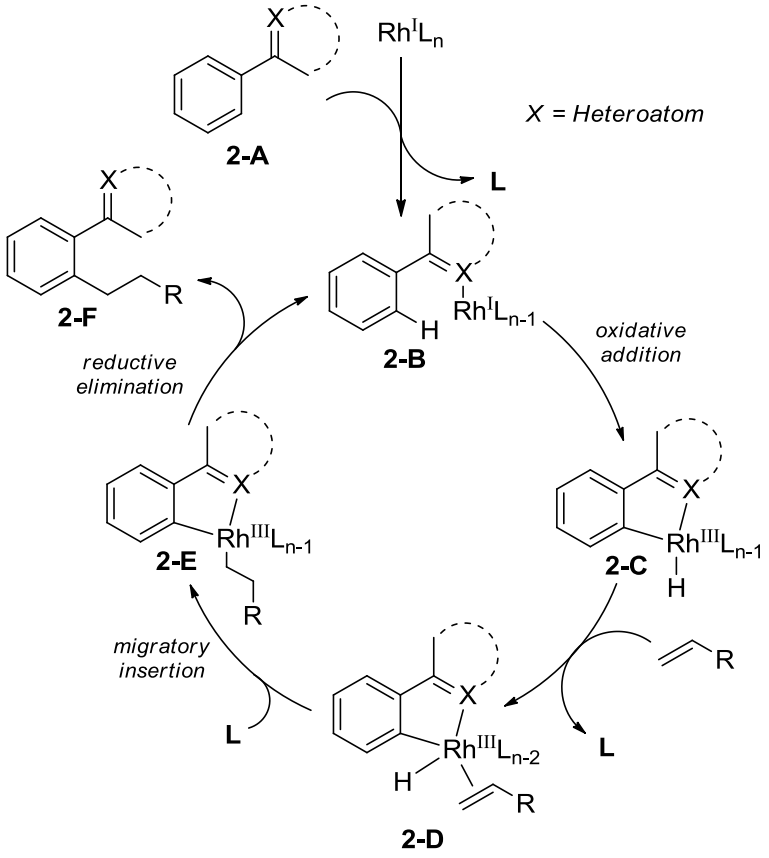

Figure 2-1. General chelation–assisted *ortho*–alkylation *via* Rh^{I} pathway

The previous examples demonstrate that Wilkinson's catalyst is a competent catalyst for the rhodium–catalyzed C–H activation reactions, in particular in the context of C–H alkylation reactions. This catalyst has proven to be highly reactive while also being relatively air and moisture stable making it easy to employ. However, the reported systems typically require harsh conditions (>130 ºC) and a limited scope of directing groups. As a result, development of more suitable catalytic systems utilizing milder conditions was highly desired.

Bergman and Ellman[9] improved the scope of the possible substrates in directed alkylation reactions by using α,β–unsaturated *N*–benzyl aldimines (Scheme 2–4). Initial investigation found that Wilkinson's catalyst was not suitable for the alkylation to occur prompting the authors to find an alternative rhodium catalyst. Bergman and Ellman's system instead utilized a catalytic system consisting of $[RhCl(COE)_2]_2$ along with 4 equivalents of a more sterically bulky and electron rich phosphine ligand such as tricyclohexylphosphine (PCy_3) or (dicyclohexylphosphinyl)ferrocene ($FcPCy_2$).[9] The ratio of phosphine to rhodium is lowered from 3:1 (as in Wilkinson's catalyst) to 2:1 and the reaction proceeds at much milder temperatures (50 °C), although an excess of alkene (or alkyne) was required. While hydroacylation is avoided (as seen with Wilkinson's catalyst)[7] the reaction is not completely chemoselective with regard to the stereochemistry of the double bond *beta* to the imine producing the small amounts of the *E*–isomer (overall *Z*:*E* selectivity 5:1). Likewise, terminal alkynes were also compatible and yielded the alkenylated product with minimal formation of the *E*–isomer (*Z*:*E* = 20:1).

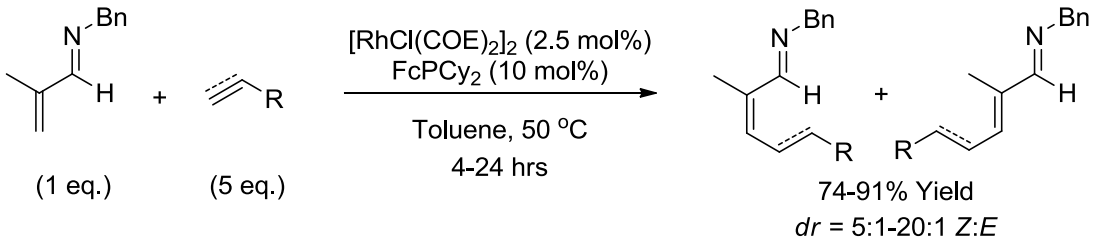

Scheme 2-4. Selective alkylation of imines using $[RhCl(COE)_2]_2/FcPCy_2$

Bergman and Ellman further demonstrated the viability of the $[RhCl(COE)_2]_2/PCy_3$ catalytic system for a plethora of C–H activation reactions including alkylations, alkenylations and arylations.[1, 10-13] This significant expansion in the reaction scope has shown viable synthetic utility of C–H activation reactions catalyzed by Rh^I systems which the authors have applied to the synthesis of biologically active natural products and drug targets including (+)–lithospermic acid[14], vasicoline[15] and a protein kinase C (PKC) inhibitor[16].

2.1.2 N–Heterocyclic Carbenes

Recently, *N*–heterocyclic carbenes (NHCs) have emerged as attractive alternatives to phosphines for ligands in transition metal catalysis. Carbenes were first introduced as ligands on transition metal complexes in 1964 when Fischer and Maasböl[17] isolated a tungsten carbonyl complex with a methoxymethylene based carbene $[W(CO)_5(C(OCH_3)CH_3)]$ **2–8**. Individual reports by Öfele[18] and Wanzlick[19] in 1968 demonstrated the first NHC–based metal complexes (**2–9** and **2–10**) which were obtained from imidazolium salts and metal precursors. Although observed as ligands in transition metal complexes, the free carbenes were unstable and only seen as fleeting intermediates. It was not until years later that the first stable free carbene, **2–11**, was isolated and characterized by Bertrand and coworkers[20] in 1988. Shortly following this discovery, Arduengo and coworkers[21] reported the isolated NHC variant, **2–12**, adding to the utility of these moieties as ligands in the chemical industry (Figure 2–2).

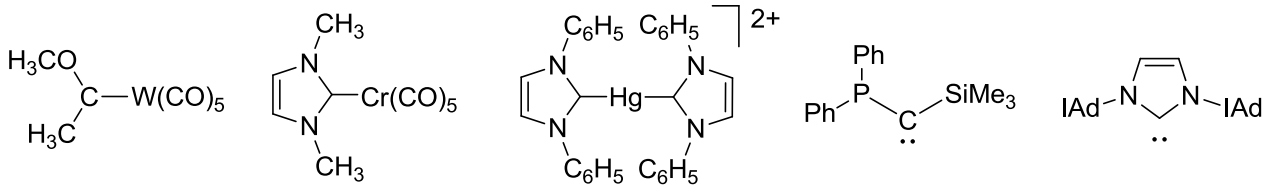

2-8 Fischer & Maasbol 1964 | **2-9** Ofele 1968 | **2-10** Wanzlick 1968 | **2-11** Bertrand 1988 | **2-12** Arduengo 1991

Figure 2-2. Brief history of carbenes from discovery as metal complexes (1964) to isolation (1988 and 1991)

A study by Nolan and coworkers[22] investigated the electron donating properties of NHCs by measuring the vibrational frequencies of carbonyl ligands in nickel complexes of general formula [Ni(CO)$_3$NHC], in comparison to complexes containing PR$_3$ ligands. This study demonstrated the significant increase in σ–donor ability of NHCs over phosphines. Consequently, the use of NHCs provides much more electron rich metal centers which can promote more facile oxidative addition of less reactive bonds with the metal center.[23] NHCs form strong bonds with metal centres producing higher bond dissociation energies (BDEs) than seen with phosphines. As a result, equilibrium favours carbenes in the metal bound form preferentially over the free carbene. This in turn can reduce the amount of free carbene found in solution leading to more robust catalytic systems.

Accordingly, NHCs provide interesting alternatives to phosphines as ligands in transition metal complexes. The first use of these ligands in catalysis was demonstrated by Herrmann and coworkers[24] who utilized Pd–NHC complexes for the Heck reaction of bromobenzene derivatives with *n*–butyl acrylate. The complexes displayed incredibly high reactivity with high turnover numbers indicating the potential for these ligands in catalysis.

Excellent reactivity of transition metal–NHC complexes has sparked a large interest and has led to the exploration into a wide range of transition metal–catalyzed reactions.[25-28]

Indeed the field of NHCs in transition metal catalysis has been largely dominated by palladium and ruthenium complexes as these species have been demonstrated to be highly active for cross–coupling[29-30] and olefin metathesis[31-32] reactions respectively. To a lesser extent, Rh–NHCs have also been described, but investigation into their catalytic activity has been rather modest and has been primarily restricted to hydrosilylation, hydrogenation and hydroformylation reactions.[27, 33] While Rh–NHC complexes are well known to the literature, the diversity of the actual complexes has been surprisingly limited, as the majority of these complexes exist as Rh^{I} species of general formula [Rh(NHC)(COD)Cl] (COD = 1,5–cyclooctadiene). These complexes can be synthesized by a variety of methods, are typically air and moisture stable and are typically stable to column chromatography, while also resistant to other decomposition reactions.

Largely influenced by the abundance of Ru–NHC and Pd–NHC complexes reported in the literature, our group sought to build upon the field of known Rh–NHC complexes, with interest to expand the scope of catalytic transformations these complexes were capable of effecting. Our group had previously utilized Rh–NHC complexes for the catalytic hydroformylations[34-35] and hydrogenations[36] showing excellent reactivity in both systems. We have also prepared various Rh–*bis*(NHC) systems for the activation of small molecules such as O_2, H_2, N_2 and CO.[37-38]

Recently we reported the synthesis of dimeric Rh–NHC complexes, where each rhodium was bound to one NHC, and one ethylene molecule while retaining the dimeric

structure of the complex. The structure of these complexes was also confirmed by single crystal X–ray crystallography.[37, 39] The synthesis of these complexes appears to be general and kinetically accessible for all NHCs analyzed, thus we successfully synthesized complexes of this nature for 1,3–*bis*(2,4,6–trimethylphenyl)imidazol–2–ylidene (IMes, **2–13**); 1,3–*bis*(2,4,6–trimethylphenyl)imidazolin–2–ylidene (SIMes, **2–14**); 1,3–*bis*(2,6–diisopropylphenyl)imidazol–2–ylidene (IPr, **2–15**) and 1,3–*bis*(2,6–diisopropylphenyl)imidazolin–2–ylidene (SIPr, **2–16**) (Figure 2–3) in high yield. The stability of the resulting complexes appeared to be dictated by the steric properties of the NHC ligand with more bulky carbenes being less stable.

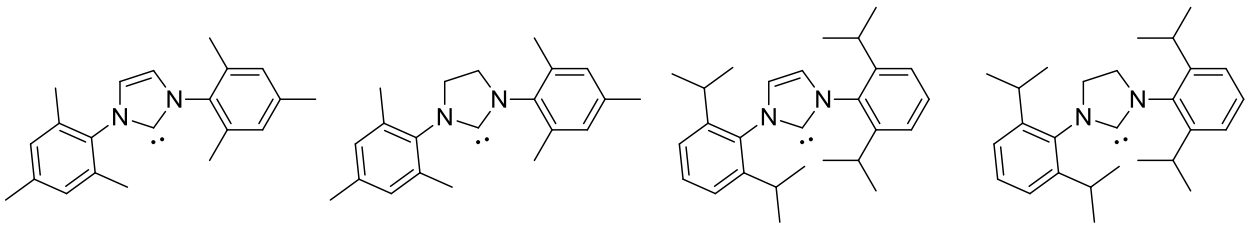

Figure 2-3. *N*–heterocyclic carbenes used in our rhodium systems ranging from smallest (IMes) to largest (SIPr)

Nolan and coworkers[40] first reported the synthesis of the related dimeric complex $[Rh(COE)(I^tBu)Cl]_2$ (I^tBu = 1,3–bis(*tert*–butyl)imidazol–2–ylidene) from $[Rh(COE)_2Cl]_2$ and the free I^tBu carbene in pentane (Scheme 2–5). However, these complexes were found to be very unstable upon treatment with benzene or hexanes, thus resulting in spontaneous cyclometalation of the *tert*–butyl wingtip groups to the rhodium metal centre forming complex **2–17**. While the degradation was found to be rapid with these complexes in the

solution state, crystal structures of the isolated solids clearly demonstrated the formation of the dimeric structure **2–18**.

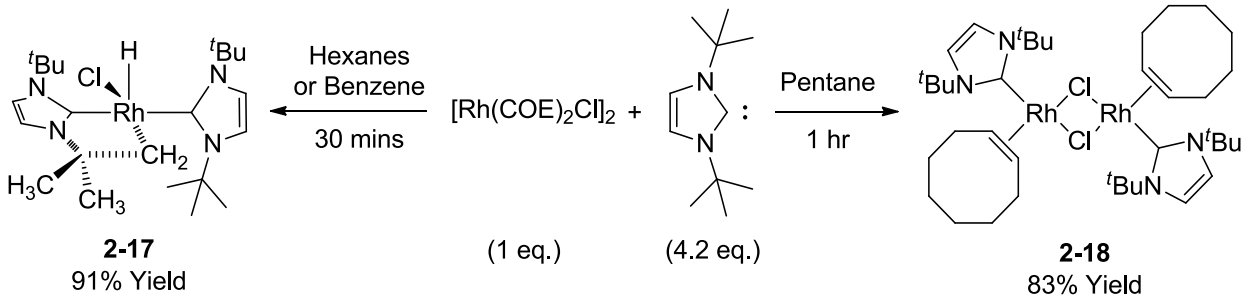

Scheme 2-5. Cyclometalation of wingtip groups of I^{t}Bu with Rh–metal centre

Later James and coworkers[41-43] reported [Rh(NHC)(COE)Cl]$_2$ (NHC = IMes or IPr) complexes (Scheme 2–6) which were isolated and stable, however the authors did not further investigate the complexes for catalytic applications.

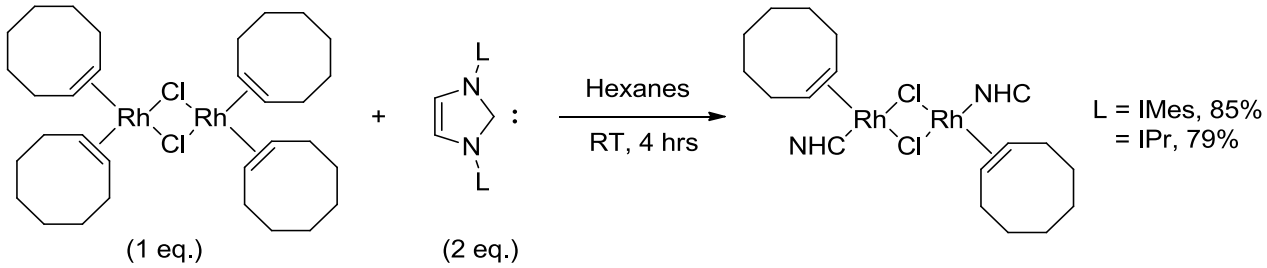

Scheme 2-6. Decreased sterics of wingtip groups circumventing cyclometalation with Rh–metal centre

Building upon this, our lab explored the reactivity of both ethylene and COE dimers towards a variety of other ligands. Reaction with neutral $2e^-$ donors resulted in the formation of *tetra*–heteroleptic compounds containing ethylene (C_2H_4) as the labile olefin ligand.[39] Similarly, the $[Rh(C_2H_4)(IPr)Cl]_2$ complex, **2–20**, can be easily prepared by reaction of the free carbene with $[Rh(C_2H_4)_2Cl]_2$, **2–19**, producing the dimeric rhodium carbene complex in near quantitative yield (Scheme 2–7). Preparation of the initial dimeric rhodium complex **2–19** is achieved by reacting commercially available $RhCl_3{\cdot}3H_2O$ under an atmosphere of ethylene gas in an alcoholic solvent.

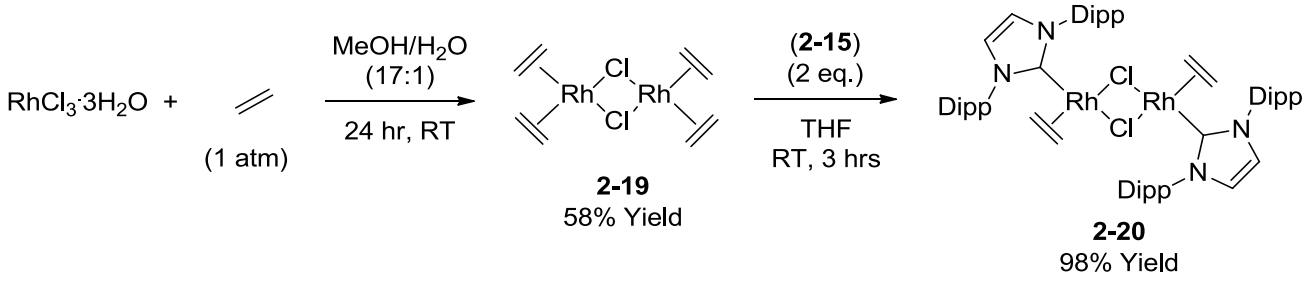

Scheme 2-7. Synthesis of $[Rh(IPr)(C_2H_4)Cl]_2$ dimer **2–20** (Dipp = 2,6–diisopropylaniline)

2.2 Results and Discussion

2.2.1 Direct Borylation of Benzene

Rhodium complexes have a long history in C–H borylation reactions as the facile activation of Rh^I complexes towards the oxidative addition of boron species such as HBpin and B_2Pin_2 make these ideal complexes for catalysis involving these reagents (*vide supra*, Chapter 1.5.6). In 2001, Marder and coworkers[44] reported the use of $[RhCl(P^iPr_3)_2(N_2)]$,

2–21, as a precatalyst in the direct C–H borylation of simple arenes using pinacolborane (HBpin) at high temperature. The proposed catalytic cycle involves formation of Rh^{I}–H, **2–G**, by oxidative addition of the HBPin to the metal centre of complex **2–21**, followed by reductive elimination of ClBPin (Figure 2–4). We proposed that a similar mechanism may be possible instead utilizing catalyst **2–20**, and sought to investigate its activity in C–H borylation reactions.

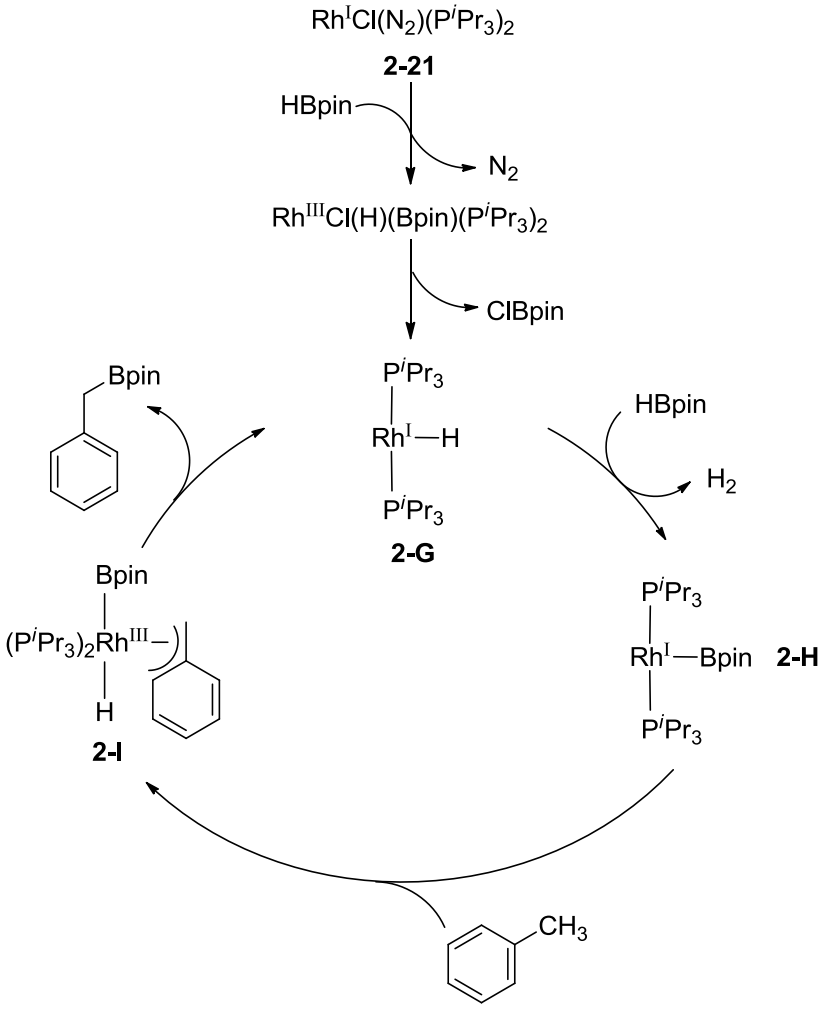

Figure 2-4. Catalytic cycle proposed by Marder for the borylation of toluene

Thus complex **2–20** was tested for the direct borylation of benzene at elevated temperatures (140 ^{o}C) (Scheme 2–8). Mixing 1 mol% of **2-20** with HBpin in a 0.2 M solution of benzene yielded the desired Ph–Bpin in 56% isolated yield. Monitoring the crude reaction mixture by ^{11}B NMR indicated a significant amount of B_2Pin_3 decomposition product at δ 22 ppm[45] along with the desired borylated product **2–22**, observed at δ 30 ppm. While the desired product was achieved, the catalyst was found to be less active than that reported by Marder, who observed the desired product in 62% and 86% yields by gas chromatography (GC) after 14 and 58 hrs respectively. Since our catalyst was likely to be more sensitive to decomposition based on the higher degree of coordinative unsaturation, we attempted the undirected borylation under milder conditions, conducting the reaction at 100 ^{o}C and 85 ^{o}C. Unfortunately, HBpin remained unreacted at milder temperatures, with the ^{11}B NMR showing only minor formation of the desired product **2–22**.

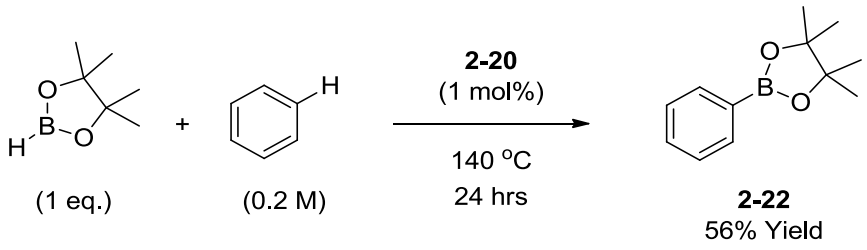

Scheme 2-8. Direct borylation of benzene with $[Rh(IPr)(C_2H_4)Cl]_2$

Since the borylation of benzene itself was not highly effective, we studied the reactivity of compounds containing directing groups to aid in the C–H activation process catalyzed by **2–20**.

2.2.2 Directed Borylation

The Crudden group has previously shown that the rhodium dimer **2–20** reacts with a variety of neutral 2e^- ligands including NHCs, phosphines and small molecules producing stable 16 e^- monomeric rhodium complexes.[37, 39, 46] The reactivity of complex **2–20** with the bidentate ligand 2,2'–bipyridine (bipy) resulted in the clean formation of the 16e^- [Rh(IPr)(bipy)Cl] complex with both nitrogen atoms coordinating to the metal centre at room temperature. Interestingly, the more common [Rh(IPr)(COD)Cl] precatalyst displayed no activity towards bipy under identical conditions suggesting that loss of COD is not facile. The IMes variant of complex **2–20** was recently suggested by Chang and coworkers[47] in their studies for rollover C–H activation of bipy derivatives. This complex was proposed to form in–situ from a system containing [Rh(acac)$_3$]/IMes–HCl under basic conditions. However, the presumed active catalytic species was never isolated. In addition, complex **2–20** reacted with 2–Ph–pyr giving the C–H activated compound **2–23**, that was observed by ^{1}H NMR (Figure 2–5). Based on these results, we were confident that C–H borylation would take place with complex **2–20**.[48]

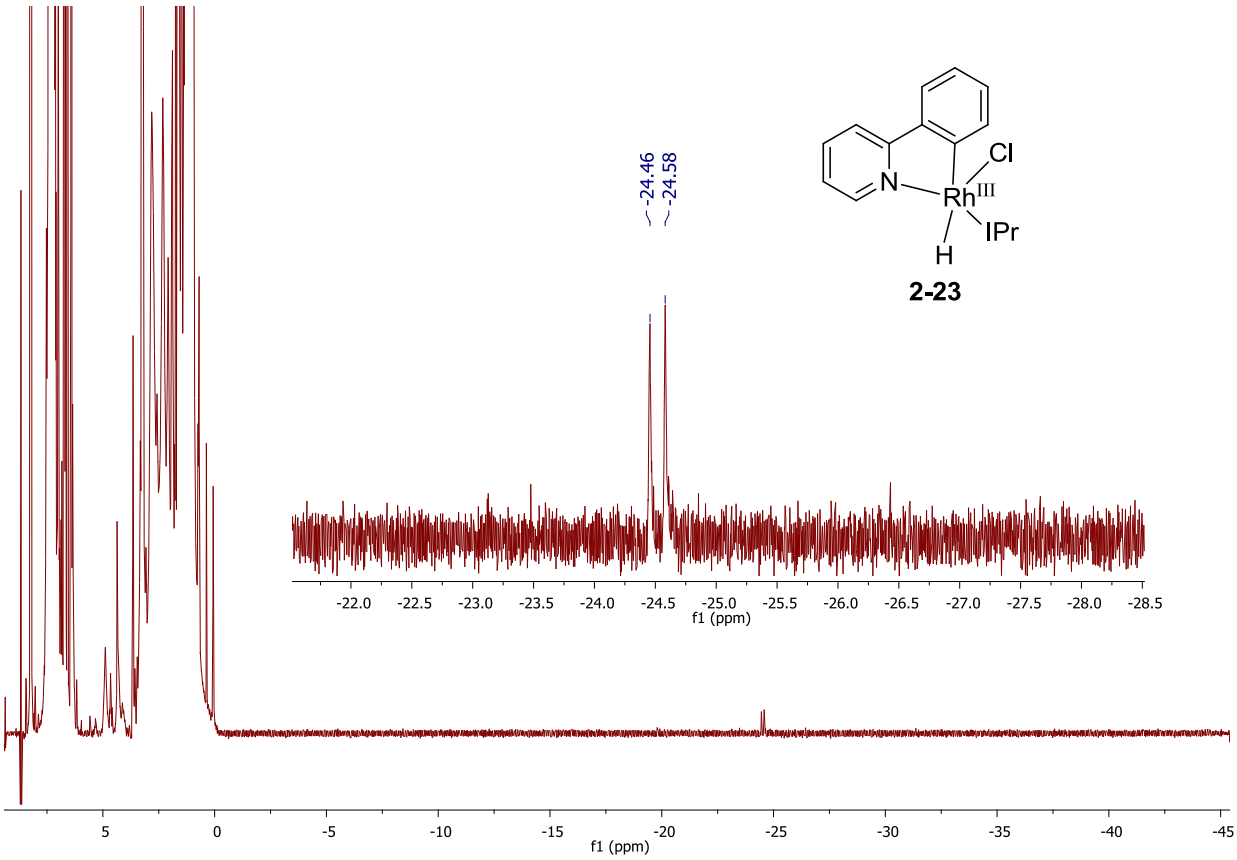

Figure 2-5. ^{1}H NMR observation of Rh^{III}–H (**2–23**) formation after 3 hours

2.2.3 Nitrogen Directed C–H Borylation

Reaction of complex **2–20** with 2–Ph–pyr and HBpin in benzene gave no product at room temperature. From stoichiometric studies by Eric Keske in the Crudden group, however, oxidative addition of the C_{Ar}–H bond appeared to occur at least to some extent at room temperature. We hypothesized that if a catalytic cycle similar to Figure 2–4 was in effect, reductive elimination of Cl–Bpin species may be rate limiting. To investigate this, KO^{t}Bu was added to the reaction in order to facilitate the reductive elimination of Cl–Bpin

from the rhodium complex. Upon addition of the base, bubbling in the reaction mixture was observed and the borylated 2–Ph–pyr product, **2–24**, was observed in 32% yield by ^{1}H NMR (Scheme 2–9).[48]

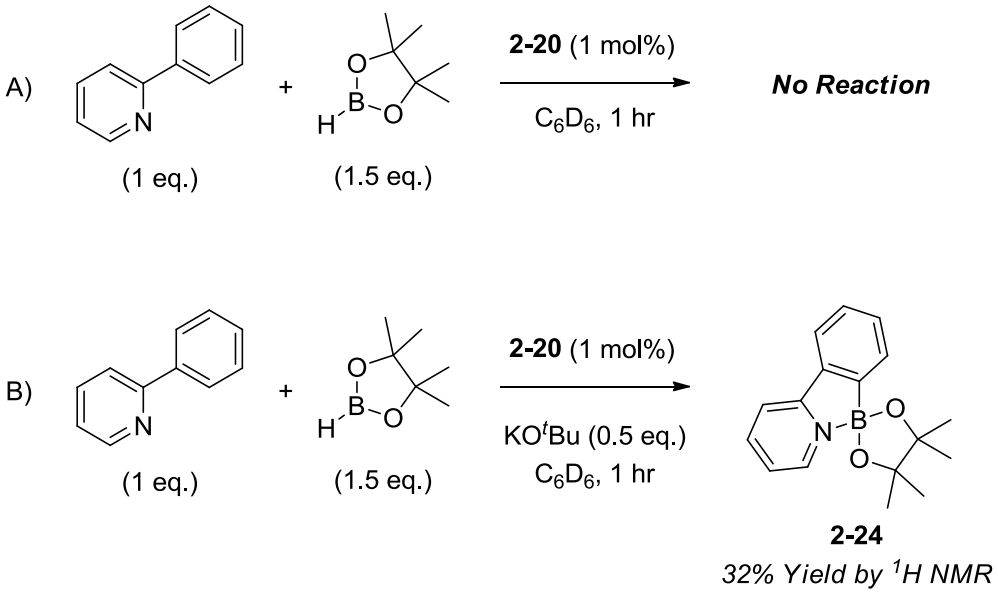

Scheme 2-9. Reaction of **2–20** with 2–Ph–pyr A) without KO^{t}Bu and B) with KO^{t}Bu

Early investigation into the reaction conducted in our group found that alkoxide bases such as sodium isopropoxide (NaO^{i}Pr) and potassium *tert*–butoxide (KO^{t}Bu) in substoichiometric amounts (0.25 equivalents relative to the 2–Ph–pyr) were most efficient for the borylation reaction. It was also found that coordinating solvents such as THF were less effective, while non–polar aromatic solvents, namely benzene, were most efficient for the borylation. Increasing the catalyst loading was found to have no increase on the yield of the desired product while an alternative Rh^{I}–NHC complex [Rh(COD)(IPr)Cl] did not facilitate the borylation of 2–Ph–pyr. In a collaborative effort with Eric Keske and Dr.

Olena Zenkina, the C–H borylation of 2–Ph–pyr was optimized in a 91% yield by ^{1}H NMR. (Scheme 2–10).

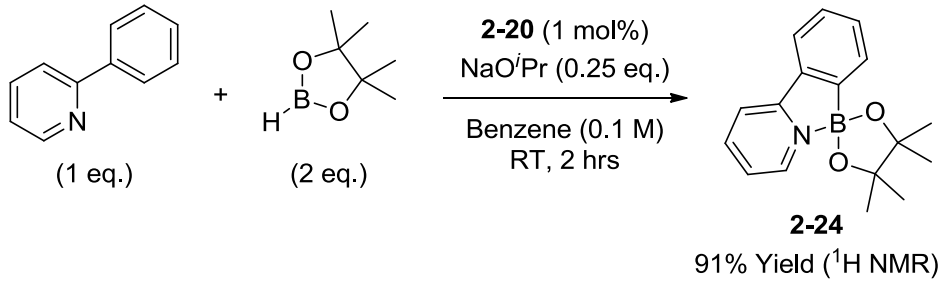

Scheme 2-10. Optimized reaction conditions for the C–H borylation of 2–Ph–pyr

2.2.4 Scale–up and Isolation of Borylated 2–Phenylpyridine, ***2–24***

With optimized conditions in hand, we scaled up the reaction and attempted the isolation of **2–24**. Repeating the optimized conditions at 0.5 mmol of starting material, we found incomplete conversion to the desired product when monitoring the reaction by ^{1}H NMR with conversion only reaching 50%. Eventually the discrepancy between this and the previous results was traced to the batch of NaO^{i}Pr employed. The base is not commercially available and was synthesized from sodium metal and reagent grade isopropanol (Scheme 2–11).

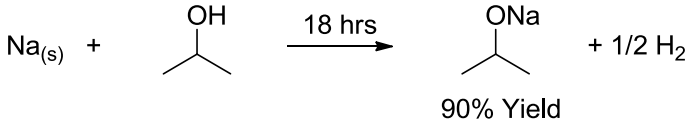

Scheme 2-11. Synthesis of NaO^{i}Pr base

After preparing various batches of NaO^iPr, we were not able to reproducibly obtain high yields of the borylation and thus we turned to commercially available bases under our previously optimized conditions (Eq. 2–1). Sodium acetate was completely ineffective (Table 2–1, entry 1).[48] Switching to cesium carbonate (Cs_2CO_3) provided the borylated product **2–24**, however the reaction was significantly slower than previously seen with the alkoxide bases (entries 2 and 3), likely due to its decreased solubility C_6H_6. Finally, commercially available sodium ethoxide (NaOEt) was discovered to be efficient for promoting the borylation of 2–Ph–pyr using 0.25 equivalents of the base. Using 2 equivalents of HBpin and conducting the reaction for 2 hours, near quantitative conversion of the 2–Ph–pyr to the borylated product **2–24** was observed, with complete consumption of HBpin (entry 7).

Table 2-1. Reoptimization of the base[a]

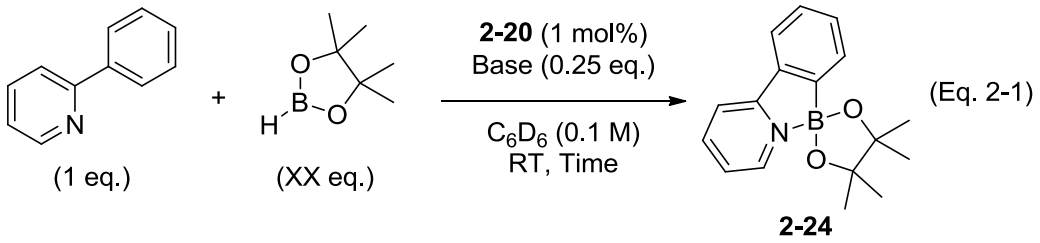

Entry	Base	HBpin (equiv.)	Time (hrs)	Conversion (%)[b]
1	NaOAc	1.5	2	NR[c]
2	Cs_2CO_3	1.5	2	10
3	Cs_2CO_3	1.5	18	60
4	NaOEt	1.5	2	>90
5	NaOEt	1	1	63
6	NaOEt	1.5	2	71[d]
7	NaOEt	2	2	93
8	NaOEt	2	2	78[d]

[a]Reactions performed in a glovebox under inert atmosphere and transferred directly to a J–Young tube to measure ^{1}H NMR conversion. [b]Conversion determined by ^{1}H NMR. [c]NR = no reaction. [d]Isolated yield after column chromatography on basic alumina.

After obtaining significant conversion as determined by ^{1}H NMR, the desired borylated product was isolated by column chromatography using basic alumina as the stationary phase. Original attempts to isolate the product on silica gel resulted in dramatic decreases in the isolated yield of **2–24** (less than 50% isolated from 90% according to ^{1}H NMR yield calculations). Analysis of the TLC plates (Figure 2–6) from the collected fractions of the columned product on silica gel suggested that the product decomposed in the presence of the silica. This likely results from the protic nature of the silica gel assisting the well-known protodeboronation[49] of the borylated 2–Ph–pyr promoting cleavage of the C_{Ar}–Bpin bond and regenerating the starting material.

The major issues surrounding isolation were circumvented when basic alumina was used as the stationary phase in the column allowing **2–24** to be isolated in 78% yield.

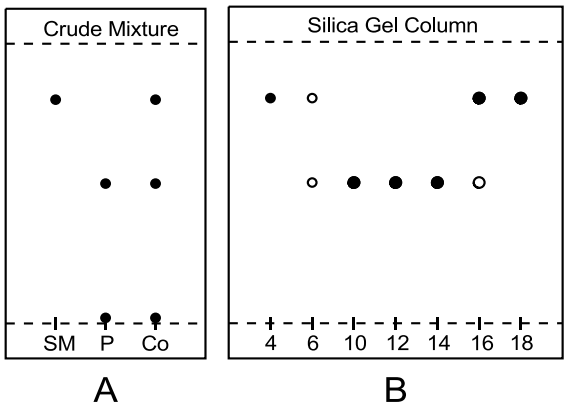

Figure 2-6. Representative TLC plates using 3:1 EtOAc/Hexanes eluent mixture indicating A) crude mixture on silica backed TLC and B) collected fractions indicating decomposition of borylated product on silica gel column. (SM = 2–Ph–pyr; P = **2–24**; Co = cospot; #s = column fraction)

2.2.5 Substrate Scope of Rh–Catalyzed C–H Borylation

Resolving isolation issues with the borylated product **2–24**, the rhodium–catalyzed C–H borylation was scaled up to 0.5 mmol and the substrate scope of the reaction was investigated (Table 2–2 & Table 2–3).[48] While reactions analyzed on the NMR scale (0.13 mmol of 2–Ph–pyr) required 2 hours to reach completion, scale up to 0.5 mmol required additional time (4 hours) for the reaction to reach completion. This is most likely due to the limited solubility of the NaOEt base in benzene. Using optimized conditions, a variety of 2–phenylpyridine derivatives were prepared and isolated with a range of steric (Table 2–2) and electronic (Table 2–3) properties.

Table 2-2. Steric effects for the Rh–catalyzed C–H borylation[a,b]

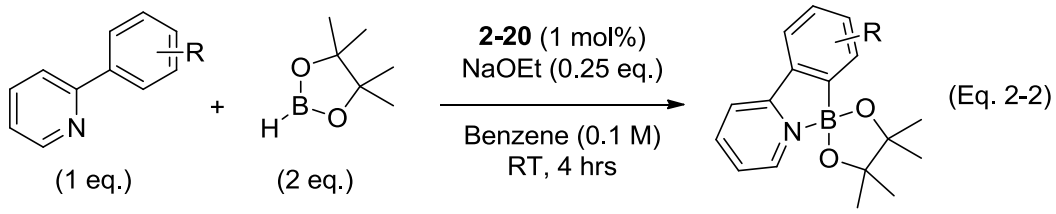

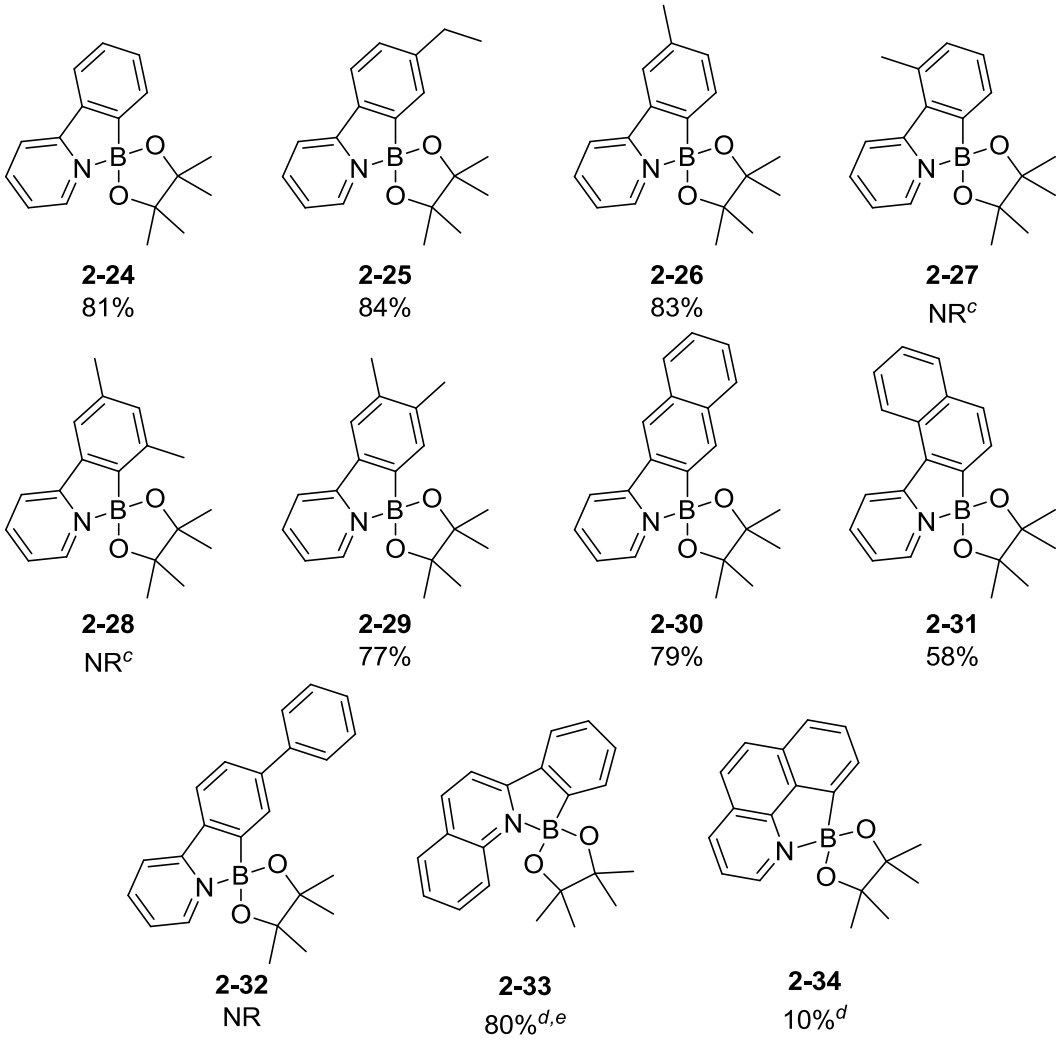

[a]Reactions conducted using substrate (0.5 mmol), HBpin, (1 mmol), NaOEt (0.125 mmol) and **2–20** (0.005 mmol) in benzene (0.1 M) for 4 hours. [b]Isolated yields by basic alumina column chromatography. [c]NR = no reaction. [d]Conversion to product based on ^{1}H NMR. [e]Product not isolated due to instability.

Table 2-3. Electronic effects for the Rh–catalyzed C–H borylation[a,b]

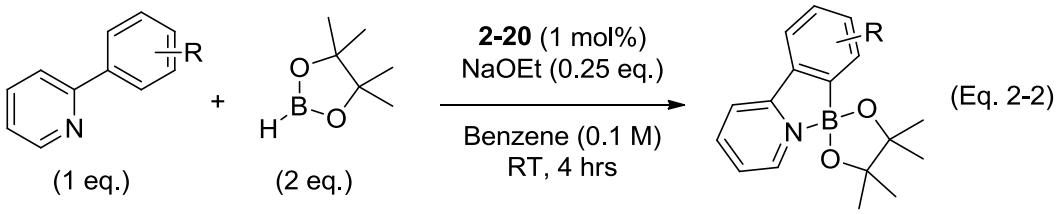

(Eq. 2-2)

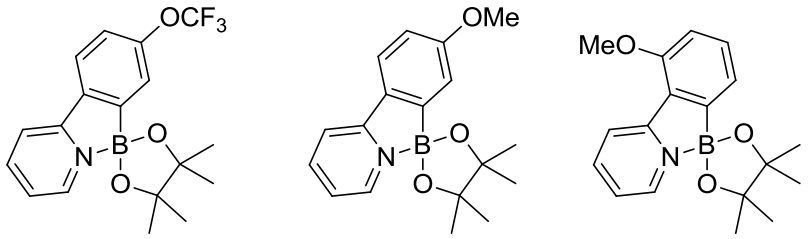

2-35
15%[c]

2-36
81%

2-37
NR[d]

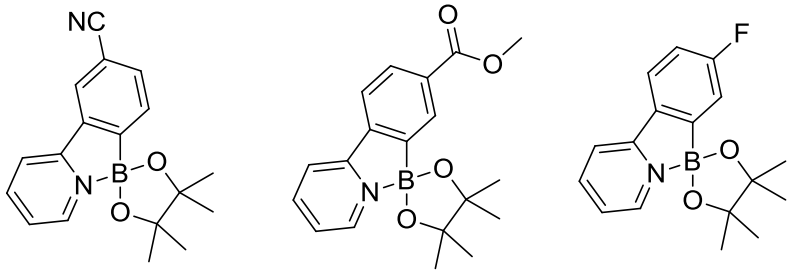

2-38
NR[d]

2-39
NR[d]

2-40
33%[c]

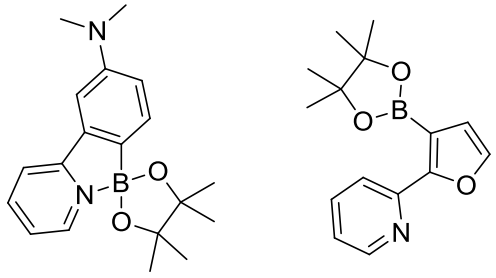

2-41
20%[c]

2-42
99%[c,e]

[a]Reactions conducted using substrate (0.5 mmol), HBpin, (1 mmol), NaOEt (0.125 mmol) and **2–20** (0.005 mmol) in benzene (0.1 M) for 4 hours. [b]Isolated yields by basic alumina column chromatography. [c]Conversion to product based on ^{1}H NMR. [d]NR = no reaction. [e]Product not isolated due to instability.

The C–H borylation tolerates phenylpyridines which contain alkyl substituents in the *meta*– and *para*–positions on the phenyl ring adjacent to the pyridine producing the desired borylated product in excellent yields (Table 2–2, entries **2–24** to **2–26**). However, *ortho*–substituted phenylpyridines failed to produce the desired borylated products (entry **2–27**). While the 3,5–disubstitution pattern failed to react (**2–28**), a 3,4–disubstitution pattern had no effect on the reaction and produced the desired product **2–29**. Substituted naphthyl rings were also borylated providing the desired compounds **2–30** and **2–31** while the isoquinoline derivative showed no effect on the reaction borylating the desired product **2–33**. While alkyl substituents in the *para*–position did not hinder the borylation reaction, *para*–biphenyl is unreactive under the mild conditions used to produce the desired borylated product **2–32**. It is speculated that the sterics around the phenyl ring adjacent the pyridyl ring largely dominate the reactivity of the C–H borylation reaction as can be easily summarized by Figure 2–7. Rigid systems such as benzo[*h*]quinoline also failed to produce the desired borylated compound, **2–34**, in substantial yields which is likely attributed to hindered ability of the **2–20** forming the Rh^{III}–H bond.

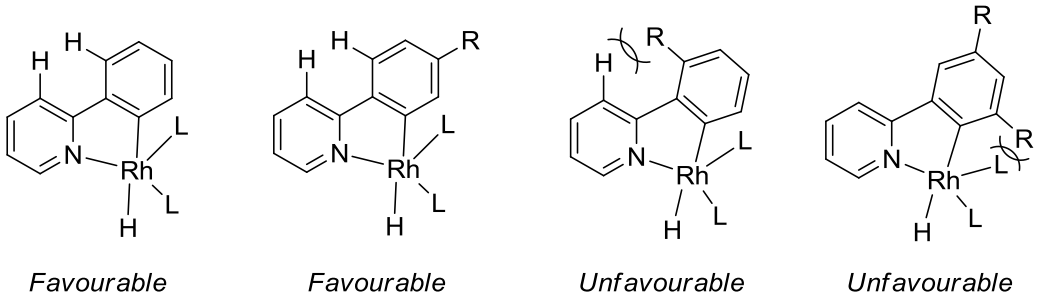

Figure 2-7. Sterics affecting C–H borylation with phenylpyridine substrates

Electron neutral and electron donating substituents (Table 2–3) are tolerated in the rhodium–catalyzed C–H borylation reaction when at the 3– and 4–positions. While electron donating 4–methoxy was found to have no effect on the reaction (**2–36**), the *ortho*–substituted methoxy yielded no C–H borylation product (**2–37**). An electron donating group such as dimethylamino in the *meta*–position caused the reaction to become sluggish with only minor formation to the borylated product **2–41** observed by ^{1}H NMR. It is likely that the nitrogen from the amino group coordinates with the rhodium metal centre creating a stable intermediate resulting in a slow turnover. Alternatively, amines can with HBpin which could hinder the C–H borylation from occurring as well.[50]

Complete conversion of 2–furylpyridine to the C–H borylated product was observed (**2–42**), however stability issues arose and the product could not be isolated by chromatography (silica gel or alumina). However, the crude mixture was fully characterized indicating the desired product **2–42** had been formed. Similarly, 2–phenylquinoline was also found to produce the desired borylated product **2–33** (Table 2–2), which was observed by ^{1}H NMR. Again the product was fairly unstable and attempts to isolate the product by column chromatography failed to yield the desired product.

Interestingly, when strongly electron withdrawing substituents are introduced in the *meta*– or *para*–position, no C–H borylation occurred (Table 2–3, entries **2–38** and **2–39**). These two substrates are highly basic and postulated to undergo facile coordination with the rhodium metal centre competitively with the pyridyl unit. To probe the possibility of slow oxidative addition of either substrate with **2–20**, studies were conducted with stoichiometric amounts of each substrate. Mixing 0.5 equivalents of **2–20** with each

substrate for 3 hours and analyzing the reaction by ^{1}H NMR revealed a doublet at δ –23 ppm ($^{1}J_{Rh–H}$ = 45 Hz) for 2–(3–nitrile)phenylpyridine (Figure 2–8) and a doublet at δ –24.8 ppm ($^{1}J_{Rh–H}$ = 50 Hz) for 2–(4–methoxycarbonyl)phenylpyridine (Figure 2–9). In both cases, the Rh^{III}–H signal observed, which is indicative of products **2–43** and **2–44**, appeared more intense than that observed with 2–Ph–pyr seen in Figure 2–5. Accordingly, the oxidative addition of the C_{Ar}–H bond with the rhodium metal centre appears to be facile in all cases. It is possible that the electron withdrawing substituents on the aromatic ring to help stabilize the Rh^{III}–H bond thus prolonging the lifetime of the intermediate. Interestingly, unlike with unsubstituted 2–Ph–pyr, an additional pair of doublets were also observed with the nitrile and methoxycarbonyl derivatives which were shifted further downfield relative to the characteristic peak. Presumably, these doublets also indicate Rh^{III}–H peaks in a different environment, although nothing more can be determined about their structure at this point.

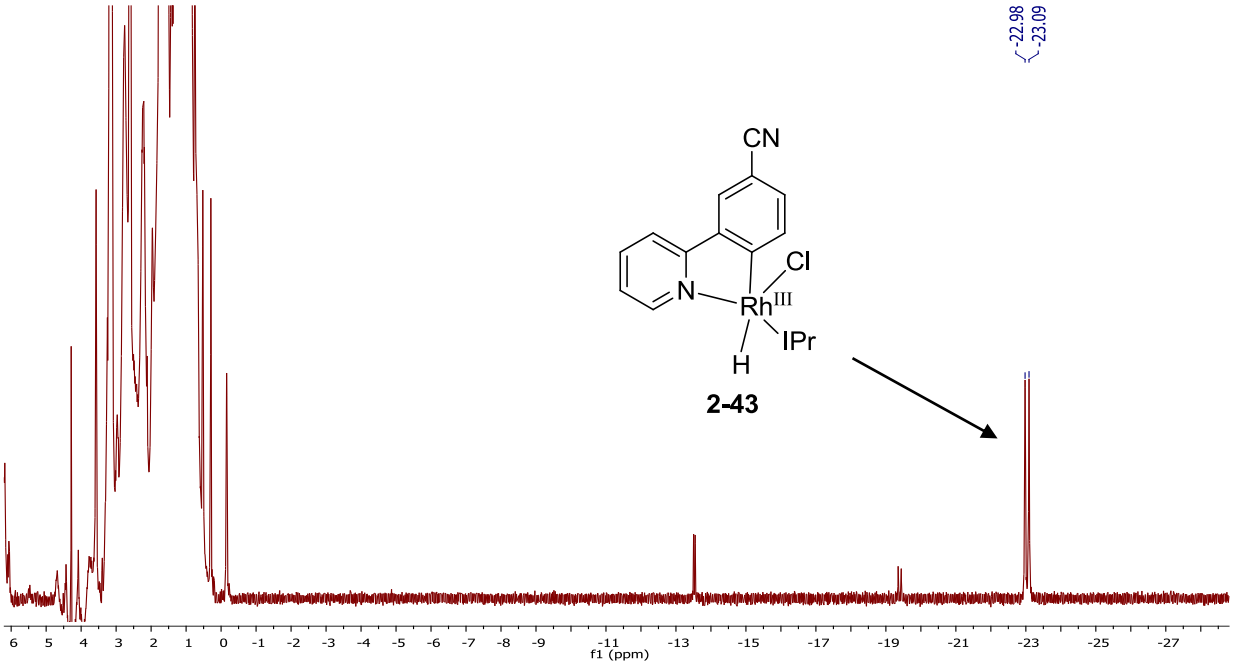

Figure 2-8. Rh^{III}–H formation by mixing **2–20** with 2–(3–nitrile)phenylpyridine producing **2–43**

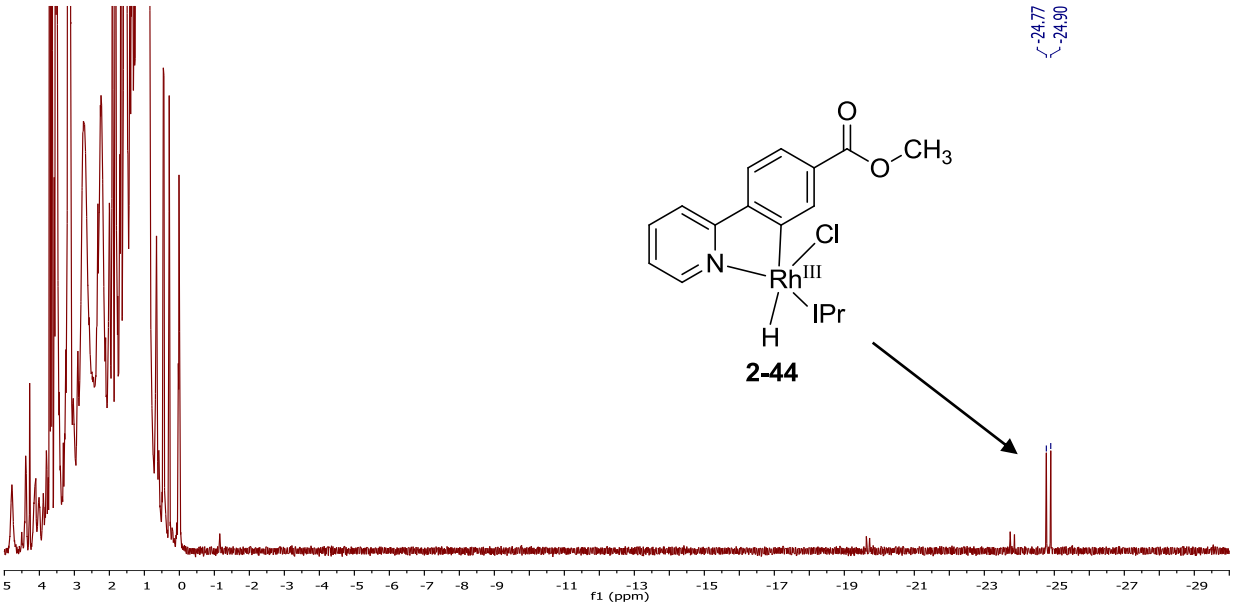

Figure 2-9. Rh–H formation by mixing **2–20** with 2–(4–methoxycarbonyl)phenylpyridine producing **2–44**

2.2.6 Mono–Selectivity of the C–H Borylation

With two vacant *ortho*–positions present in phenylpyridine substrates, the monoborylated product is solely produced with bisborylation completely undetectable by ^{1}H NMR. However, *bis*–substitution is a common side product observed in many catalytic C–H borylation reactions.[51] Monoborylation largely results from coordination of the nitrogen on the pyridine ring with the boron centre in the initial product, preventing further borylation. While pinacol boronate esters typically appear at *circa* δ 30 ppm in ^{11}B NMR, the C–H borylated products shown in Table 2–2 & Table 2–3 all have ^{11}B NMR shifts much further upfield (*circa* δ 13 ppm) indicative of higher coordination at boron.[52] In further support of this, the crystal structure of **2–25** (Figure 2–10)[48] also shows coordination of the nitrogen to the boron centre. As the ^{11}B NMR indicates, the upfield shift present for both the isolated species as well as the species still in the crude mixture in the solution state, it is apparent that the coordination between the nitrogen and boron moieties prevents the bisborylation from occurring providing exclusive selectivity for the monoborylated products under the mild conditions with our dimeric rhodium catalyst, **2–20**.

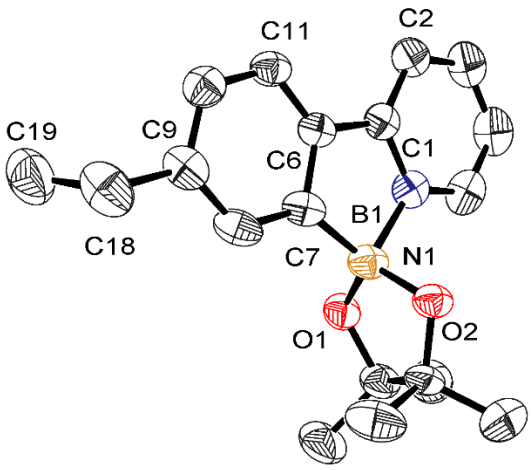

Figure 2-10. X–Ray crystal structure of **2–25**[48]

2.2.7 Mechanism of the Rh–Catalyzed C–H Borylation

A proposed catalytic cycle for the rhodium–catalyzed C–H borylation of 2–Ph–pyr is depicted in Figure 2–11.[48] Initially, the dimeric rhodium complex **2–20** undergoes a salt metathesis with the alkoxide base generating the Rh^{I}–H, **2–J**, which is thought to be the active catalyst in the reaction. Oxidative addition of HBpin produces the $Rh^{III}(H)_2$ species **2–K** which undergoes reductive elimination of $H_{2(g)}$ to generate a Rh^{I}–boryl species **2–L**. Oxidative addition of the 2–Ph–pyr to the active species generates the Rh^{III}–boryl complex **2–M**, which undergoes reductive elimination producing product **2–24** and regenerating the active species **2–J**.

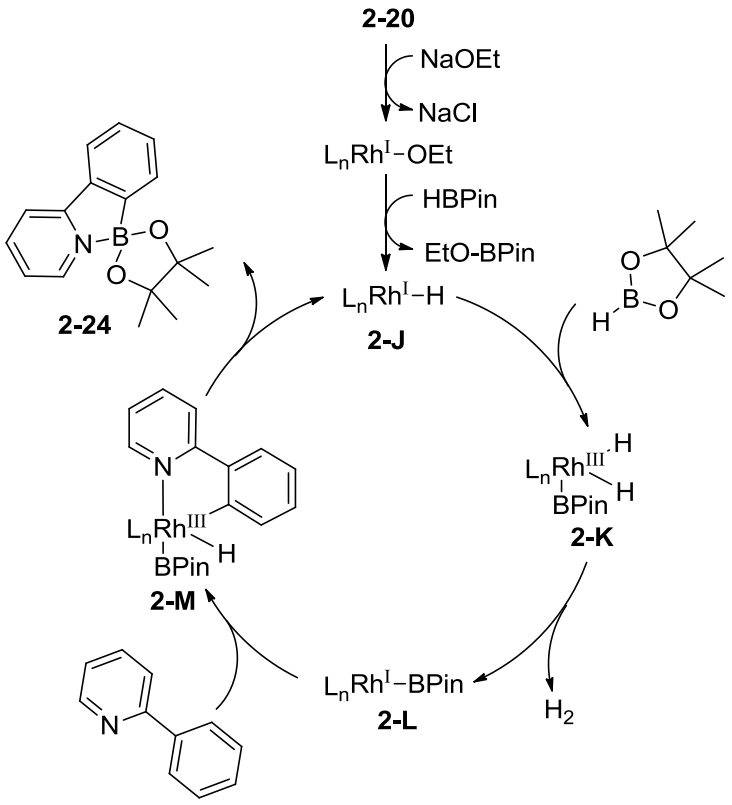

Figure 2-11. Proposed mechanism for the C–H borylation of 2–Ph–pyr catalyzed by **2–20**[48]

2.2.8 Sequential C–H Borylation/Arylation via Suzuki–Miyaura Cross–Coupling

While transition metal–catalyzed cross–couplings have provided advantageous routes for the synthesis of polysubstituted aromatics, the use of prefunctionalized starting materials is still a significant drawback in their synthesis. Ideally, the ability to directly arylate aromatic molecules reducing the need to use aryl halides or organometallic reagents would be much more advantageous.

Transition metal–catalyzed direct C–H arylation has shown to be an attractive and alternative synthetic route to cross–coupling reactions for the synthesis of polysubstituted aromatics.[53-55] Unfortunately, reports to date reveal three major issues with direct C–H arylation reactions. The first such issue deals with the selectivity of the reaction. In the majority of cases, bisarylation of the substrate takes place.[56-61] In order to prevent over arylation, starting materials which contain a steric bias either blocking one of the two *ortho*–positions or a bulky substituent in the *meta*–position are often employed.[62-65] Finally, direct C–H arylation reactions often require forcing conditions (high temperatures and extended reactions times) to promote the reaction.

*2.2.9 Rh–Catalyzed Direct C–H Arylation with **2–20***

Using complex **2–20** as a precatalyst, the direct arylation of 2–Ph–pyr was investigated. Initial studies began with the direct arylation of 2–Ph–pyr using 4–iodoacetophenone to attain selectively the monoarylated product. However, upon reaction with **2–20** in toluene at 120 ^{o}C in the presence of a strong base KO^{t}Bu showed no arylated product formed by GC–MS, though complete consumption of the aryl halide had occurred. As a result, the aryl halide was substituted for 4–iodotoluene, assuming a possible aldol side reaction occurring with the acetophenone substrate. Using 4–iodotoluene and analyzing the reaction by GC–MS, the products of direct C–H arylation of 2–Ph–pyr were observed in moderate conversion (Table 2–4).

Table 2-4. Rh–Catalyzed Direct C–H Arylation of 2–Ph–pyr[a]

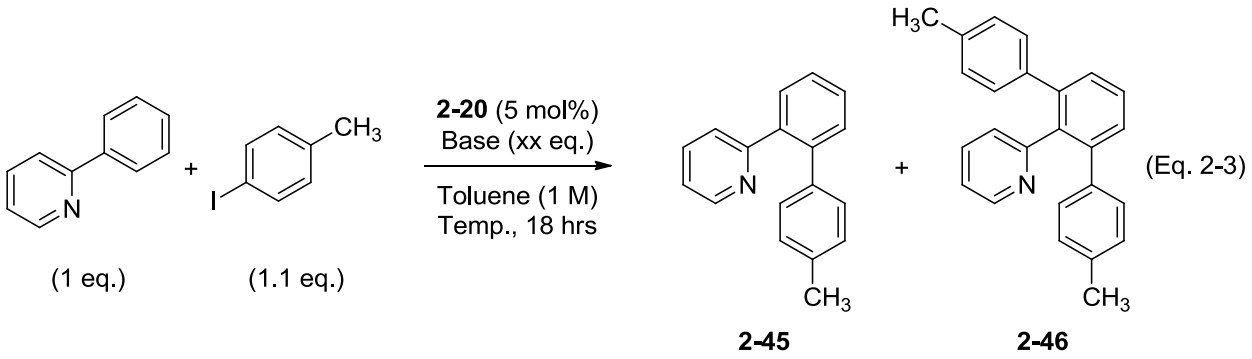

2-45 **2-46**

Entry	Base	Base (Equiv.)	Temperature (°C)	Conversion (%)[b]	2–45 (Ratio %)[c]	2–46 (Ratio %)[c]
1	KO^{t}Bu	2	120	45	20	80
2	KO^{t}Bu	2	80	45	17	83
3	KO^{t}Bu	2	RT	<5	ND[d]	ND[d]
4	K_2CO_3	2	80	<5	100	0
5	K_2CO_3	3	120	25	99	1
6	NaOEt	3	120	40	100	0

[a]Reactions conducted in a pressure tube under a nitrogen atmosphere with 2–Ph–pyr (0.25 mmol), 4–iodotoluene (0.27 mmol) and base (0.5 or 0.75 mmol) with **2–20** (5 mol%) at the indicated temperature in toluene (1 M concentration) for 18 hours. [b]Conversion determined by GC–MS integration of product peaks **2–45** and **2–46** relative to starting material 2–Ph–pyr. [c]Ratios determined by integration of product peaks by GC–MS. [d]ND = not determined.

The direct arylation of 2–Ph–pyr with 4–iodotoluene using strong base at 120 °C yielded the C–H arylated product albeit in a 5:1 ratio of the bisarylated product **2–46** to the monoarylated product **2–45** (Table 2–4, entry 1). Lowering the reaction temperature was found to have negligible effect on the reaction. However, substitution for the weaker base K_2CO_3, and increasing its loading resulted in the exclusive formation of **2–45**, although low conversion was still observed (entry 5). Switching to NaOEt found an increase in the conversion from 2–Ph–pyr with complete selectivity for the **2–45** (entry 6). While the

monoarylated product was achieved with exclusive selectivity using K_2CO_3 and NaOEt, the conversion of 2–Ph–pyr failed to ever reach 50% by GC–MS analysis. The increased loading of aryl iodide was not investigated as usage of 2 equivalents or more would likely increase the potential formation of the bisarylation product **2–46**. While the results showed initial promise, we were deterred from further investigation due to the low activity and poor selectivity of this procedure when compared to other C–H arylation reports.

2.2.10 Sequential C–H Borylation/Arylation via Suzuki–Miyaura Cross–Coupling

Although the direct C–H arylation of 2–Ph–pyr catalyzed by **2–20** failed to go to completion even under forcing conditions, taking advantage of the monoselectivity observed in the C–H borylation reaction could provide another useful route to the desired arylated products. To test this concept, borylated phenyl pyridine **2–24** was subjected to Suzuki–Miyaura cross–coupling.

Using conditions reported by Suginome and coworkers[66] for the cross–coupling of α–(acylamino)benzylboronic ester with arylbromides, a sequential C–H borylation/cross–coupling strategy was investigated (Scheme 2–12). Initially the borylation on 2–Ph–pyr was carried out for 2 hours to produce **2–24**. The crude mixture was then filtered through Celites and the filtrate concentrated. Upon drying, the crude product was introduced back into the glovebox and the reagents for the cross–coupling reaction were added. After reaction for 24 hours at 60 ^{o}C, the product **2–47** was observed by GC–MS with 65% conversion from the starting 2–Ph–pyr. ^{1}H NMR analysis of the crude mixture had also indicated that the desired arylated product had formed from the sequential reaction.

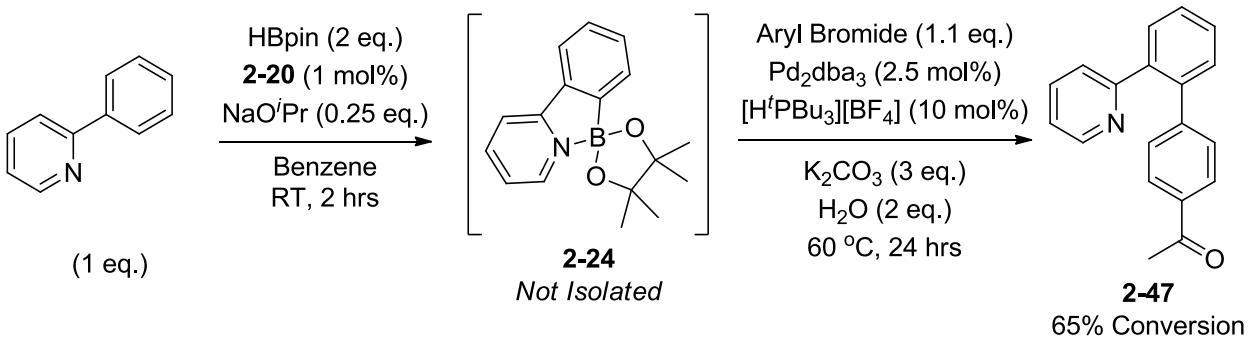

Scheme 2-12. First successful sequential C–H borylation/arylation producing **2–47**

In an attempt to improve the yield of the arylated product **2–47**, screening of the cross–coupling reaction for different phosphines and bases was investigated (Table 2–5). A significant decrease in the isolated yield was observed when the ligand was substituted for other phosphines common in Suzuki–Miyaura cross–coupling reactions (entries 2–4). While SPhos (SPhos = 2–dicyclohexylphosphino–2',6'–dimethoxybiphenyl) showed an improvement in the yield, simply increasing the loading of H_2O to 3 equivalents (entry 9) gave similar results. Likewise, substitution of the base for other carbonate bases showed a decreased reaction yield (entries 7 and 8).

Table 2-5. Ligand and base screening of the Suzuki–Miyaura cross–coupling with **2–24**[a]

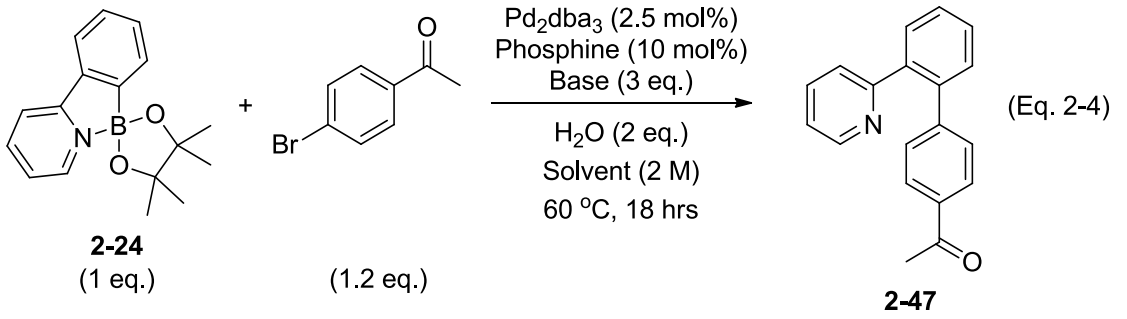

Entry	Base	Ligand	Solvent	Yield (%)[b]
1	K_2CO_3	$[HP^tBu_3][BF_4]$	Toluene	59
2	K_2CO_3	PPh_3	Toluene	22
3	K_2CO_3	PCy_3	Toluene	NR[c]
4	K_2CO_3	P(*o*–tolyl)$_3$	Toluene	NR[c]
5	K_2CO_3	SPhos[d]	Toluene	84
6	K_2CO_3	XPhos[e]	Toluene	33
7	Na_2CO_3	$[HP^tBu_3][BF_4]$	Toluene	62
8	Cs_2CO_3	$[HP^tBu_3][BF_4]$	Toluene	62
9	K_2CO_3	$[HP^tBu_3][BF_4]$	Toluene	82[f,g]

[a]Reactions conducted using **2–24** (0.1 mmol), 4–bromoacetophenone (0.12 mmol), the desired base (0.3 mmol), Pd_2dba_3 (0.0025 mmol) and the desired phosphine (0.01 mmol) in solvent (200μL, 2 M concentration) and H_2O (0.2 mmol) at 60 °C for 18 hours. [b]Isolated yields by silica gel chromatography. [c]NR = no reaction. [d]SPhos = 2–dicyclohexylphosphino–2',6'–dimethoxybiphenyl. [e]XPhos = 2–dicyclohexylphosphino–2',4',6'–triisopropylbiphenyl. [f]0.3 mmol of water used. [g]0.39 mmol scale.

With optimal conditions in hand, we then attempted to carry out the reaction in one pot without changing solvent. Since the cross–coupling reaction requires the use of toluene, the C–H borylation reaction was conducted (Eq. 2–2) using toluene in place of benzene as the solvent. Unfortunately, the reaction only yielded the desired borylated product **2–24** in 43% yield, significantly lower than what was achieved in benzene. However, the simple substitution of benzene in the arylation sequence gave the arylated product **2–47** in 68% isolated yield over the two reaction steps (Scheme 2–13).[48]

Unsurprisingly, an attempt at a one–pot borylation/arylation under a domino process (mixing all reagents at the beginning of the reaction) showed no formation of either the borylated product **2–24** or the arylated product **2–47** by GC–MS, ^{1}H NMR or ^{11}B NMR analyses. It is highly expected that competitive oxidative addition of the arylbromide and 2–Ph–pyr between the dimeric rhodium complex **2–20** and Pd_2dba_3 would occur under such conditions, hindering the borylation reaction.

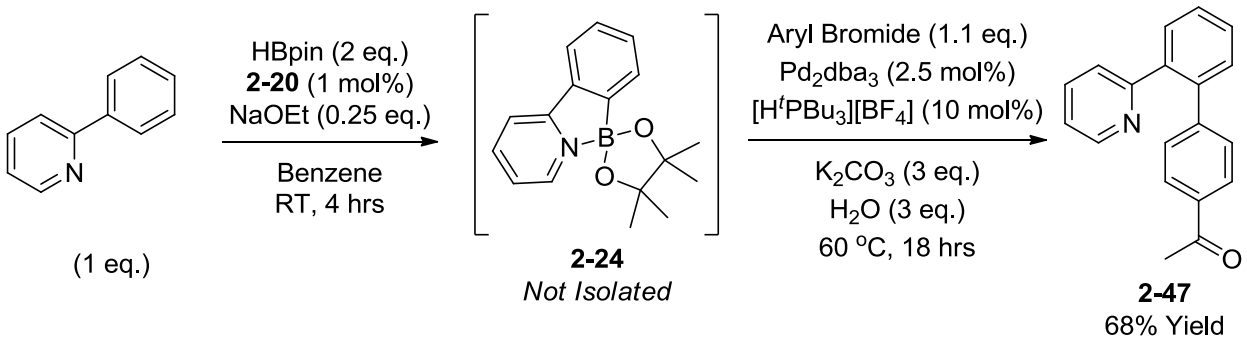

Scheme 2-13. Sequential Rh–catalyzed C–H borylation/Suzuki–Miyaura cross–coupling for a one–pot C–H borylation/arylation of 2–Ph–pyr

With optimized conditions in hand, the one–pot sequential borylation/arylation reaction was investigated for various 2–Ph–pyr substrates and arylbromides (Table 2–6).[48] Sequential C–H borylation/arylation was carried out on a variety of 2–phenylpyridines. These substrates all showed excellent reactivities with yields ranging from 44–68% for the borylated products (**2–47** to **2–54**) over the two step sequential process. Electron donating substituents such as 4–bromoanisole and 4–acetanilide successfully underwent the

sequential reaction albeit with much lower yields (31% and 46% for **2–53** and **2–54** respectively).

Excitingly, although 2–phenylquinoline could not be isolated from the C–H borylation (Table 2–2, entry **2–33**), it could be sequentially cross–coupled to yield the arylated product **2–52** in 50% yield over the two steps. Similarly, a sequential borylation/arylation was attempted on 2–(furan–2–yl)pyridine since its borylation product, **2–42**, could also not be isolated. Unfortunately, no cross–coupled product was attained from the reaction. Similarly, the sequential borylation/arylation was attempted on 2–phenylpyrazole however the cross–coupled product was not observed by GC–MS or ^{1}H NMR, indicating that this may be an inferior directing group for this catalysis.

Table 2-6. Substrate scope for the sequential C–H borylation/arylation[a,b,c]

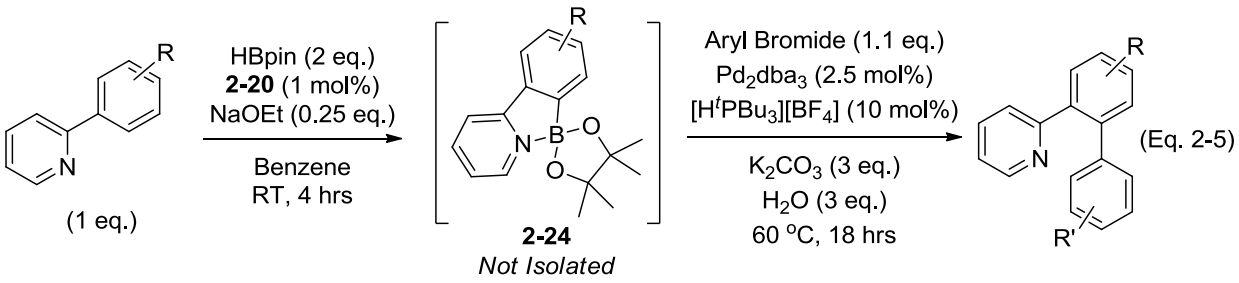

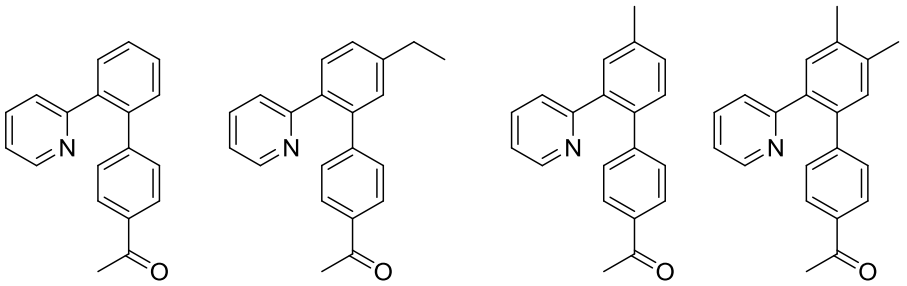

2-47 68%

2-48 66%

2-49 44%

2-50 54%

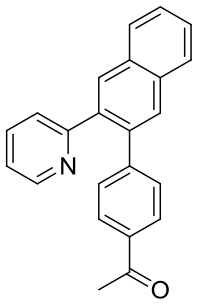

2-51 59%

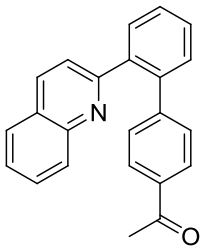

2-52 50%

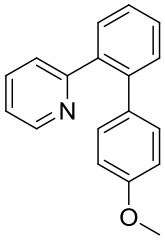

2-53 31%

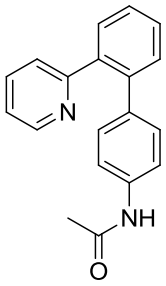

2-54 46%

[a]Reactions conducted with phenylpyridine substrate (0.5 mmol), HBpin (1 mmol), NaOEt (0.125 mmol), 2–20 (0.005 mmol) in benzene (0.1 M) for 4 hours. [b]Arylation reagents arylbromide (0.55 mmol), Pd_2dba_3 (0.0125 mmol), $[HP^tBu_3][BF_4]$ (0.05 mmol), K_2CO_3 (1.5 mmol) and water (1.5 mmol) added directly to crude mixture and stirred at 60 °C for 18 hours. [c]Isolated yields by silica gel chromatography

*2.2.11 Converting the Boronic Ester Product **2–24***

As an extension of the borylation/cross coupling sequence, we briefly investigated the conversion of the C–H borylation product **2–24** to other functional groups. In 2003, Smith and coworkers[67-68] reported conditions for converting pinacol boronate esters to alcohols under mild conditions with Oxone® as the oxidant at room temperature. Using these conditions on the crude C–H borylated mixture, the hydroxyl compound **2–55** was isolated in 35% yield over the two steps (C–H borylation and sequential oxidation) (Scheme 2–14). Additional attempts using stronger oxidizing reagents such as hydrogen peroxide (H_2O_2) failed to produce even trace amounts of the desired compound **2–55**, implying the formation of a pyridine oxides ($R–N^+–O^-$) as possible side reactions complicating the oxidation of the boronate ester.

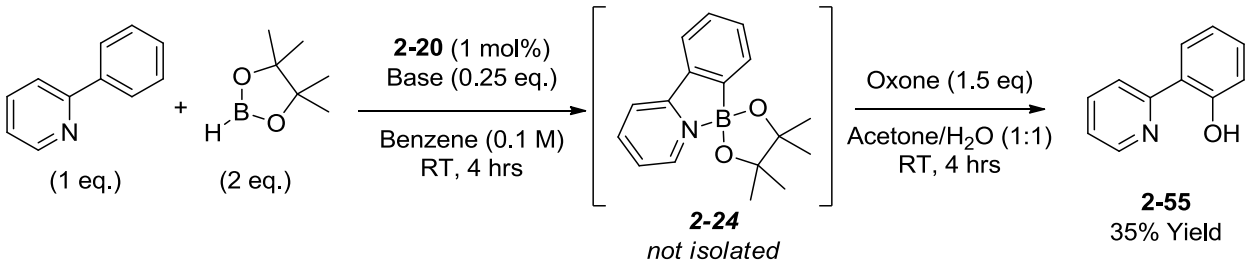

Scheme 2-14. Oxidation of C–H borylated intermediate to 2–(pyrid–2–yl)phenol, **2–55**

In addition to boronic esters, potassium trifluoroborate salts (BF_3K salts) have emerged as air and moisture stable alternatives for boron sources.[69-70] These compounds have shown a broad applicability to a plethora of catalytic reactions and have proven to be viable coupling partners in Suzuki–Miyaura cross–coupling reactions even with less active

aryl chlorides.[71-72] As such, the conversion of boronic acids and boronic esters to their trifluoroborate counterparts is an important process that results in valuable reagents for further manipulations. Potentially, the conversion to the trifluoroborate salt could assist the stabilization of the borylated furyl product, **2–42**, as well as other borylated phenyl pyridine compounds which could not be previously isolated.

Transforming the pinacol boronate ester to the BF_3K salt was investigated with the C–H borylated intermediate. In 2012, Lloyd–Jones[73] reported a mild method for the group conversion of arylboronic acids and arylboronate esters to BF_3K salts. Employing L–(+)–tartaric acid with an aqueous solution of potassium fluoride (KF) resulted in the aryl–BF_3K products with high yields. With this strategy in mind, the sequential BF_3K formation of the C–H borylated intermediate was investigated. Working with the crude reaction mixture, the 2–(2–trifluoroboryl)phenylpyridine **2–56** was synthesized in an overall yield of 46% over the two steps (Scheme 2–15). In both cases, conversion of the borylated phenylpyridine **2–24** to the hydroxyl and trifluoroboronate compounds **2–55** and **2–56** occurred with significantly reduced yields compared with what has been observed with the sequential arylation process. Thus further optimization of these sequential procedures would be required to make them synthetically viable pathways for our system.

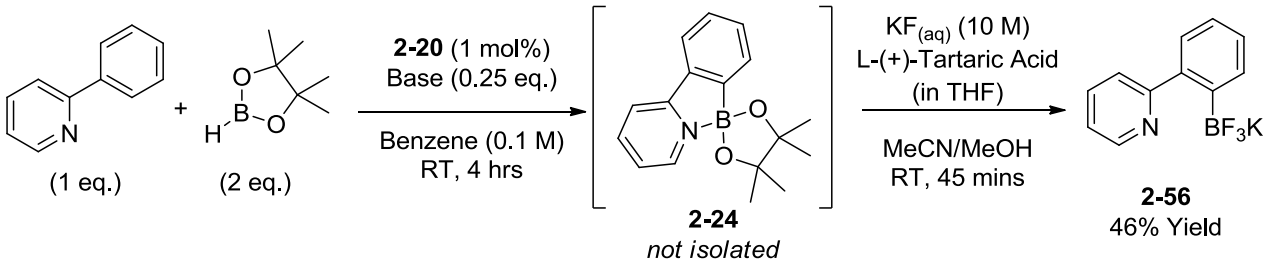

Scheme 2-15. Formation of the BF_3K product **2–56** by C–H borylation and sequential functional group interconversion

2.3 Conclusions and Future Work

Utilizing the dimeric Rh^{I}–NHC complex **2–20**, we have successfully effected the mild C–H borylation of various phenyl pyridine containing substrates. To the best of our knowledge, this is the first directed C–H borylation using a homogenous rhodium system, as previous catalytic attempts using rhodium catalysts have only been successful with heterogeneous silica–supported ligand systems.[74] Interestingly, the reaction is selective for the monoborylated products and can be isolated in moderate to excellent yields. The borylated products can undergo subsequent transformations including oxidation of the boronate ester to form the hydroxyl product **2–55**, or converted to the stable BF_3K salt, **2–56**. Most importantly, a one–pot sequential C–H borylation/Suzuki–Miyaura cross–coupling was developed. Taking advantage of the selective monoborylation from the rhodium–catalyzed process, this overall transformation results in the selective formation of monoarylated products. This borylation/arylation strategy avoids the common bisarylated byproduct or the requirement for steric blocking groups at one of the

ortho–positions which has been commonly encountered in the literature. It is important to note the mild conditions of not only the directed C–H borylation reaction, but the overall two–step process to produce the C–H arylated products, compared to other reported processes.

While the reaction has proven successful for the selective borylation and sequential borylation/arylation, there is still more work to be done to improve the overall utility of the reaction. For example, all the reactions take place in the glovebox/nitrogen atmosphere, it would be beneficial to conduct the reaction under atmospheric conditions using air and moisture stable catalysts. Also looking into borylations with B_2Pin_2 as the boron source can result in more efficient reaction potentially avoiding the formation of the B_2Pin_3 decomposition byproduct, which is commonly encountered with our system. Steering away from phenylpyridine substituents and focusing into other nitrogen heterocycles such as indoles and benzimidazoles as well as other directing groups such as imines, aldimines and amides would improve the overall utility of the process while providing valuable organic products. Subsequently, it would also be useful to investigate other sequential process such as aminations, which would enhance the overall synthetic utility of the methodology developed in our lab. Needless to say, the full scope of the sequential process initiated by the rhodium–catalyzed C–H borylation reaction still remains to be explored.

2.4 References

1. Colby, D. A.; Bergman, R. G.; Ellman, J. A. *Chem. Rev.* **2010**, *110*, 624-655.
2. Cotton, F. A.; Hillard, E. A.; Murillo, C. A. *J. Am. Chem. Soc.* **2002**, *124*, 5658-5660.
3. Gois, P. M. P.; Trindade, A. F.; Veiros, L. F.; André, V.; Duarte, M. T.; Afonso, C. A. M.; Caddick, S.; Cloke, F. G. N. *Angew. Chem. Int. Ed.* **2007**, *46*, 5750-5753.
4. Kim, M.; Kwak, J.; Chang, S. *Angew. Chem. Int. Ed.* **2009**, *48*, 8935-8939.
5. Diamond, S. E.; Szalkiewicz, A.; Mares, F. *J. Am. Chem. Soc.* **1979**, *101*, 490-491.
6. Lim, Y. G.; Kim, Y. H.; Kang, J. B. *J. Chem. Soc., Chem. Commun.* **1994**, 2267-2268.
7. Jun, C. H.; Hong, J. B.; Kim, Y. H.; Chung, K. Y. *Angew. Chem. Int. Ed.* **2000**, *39*, 3440-3442.
8. Murai, S.; Kakiuchi, F.; Sekine, S.; Tanaka, Y.; Kamatani, A.; Sonoda, M.; Chatani, N. *Nature* **1993**, *366*, 529-531.
9. Colby, D. A.; Bergman, R. G.; Ellman, J. A. *J. Am. Chem. Soc.* **2006**, *128*, 5604-5605.
10. Arndtsen, B. A.; Bergman, R. G.; Mobley, T. A.; Peterson, T. H. *Acc. Chem. Res.* **1995**, *28*, 154-162.
11. Bergman, R. G. *Nature* **2007**, *446*, 391-393.
12. Lewis, J. C.; Bergman, R. G.; Ellman, J. A. *Acc. Chem. Res.* **2008**, *41*, 1013-1025.
13. Colby, D. A.; Tsai, A. S.; Bergman, R. G.; Ellman, J. A. *Acc. Chem. Res.* **2012**, *45*, 814-825.
14. O'Malley, S. J.; Tan, K. L.; Watzke, A.; Bergman, R. G.; Ellman, J. A. *J. Am. Chem. Soc.* **2005**, *127*, 13496-13497.
15. Wiedemann, S. H.; Ellman, J. A.; Bergman, R. G. *J. Org. Chem.* **2006**, *71*, 1969-1976.
16. Wilson, R. M.; Thalji, R. K.; Bergman, R. G.; Ellman, J. A. *Org. Lett.* **2006**, *8*, 1745-1747.
17. Fischer, E. O.; Maasböl, A. *Angew. Chem. Int. Ed. Engl.* **1964**, *3*, 580-581.
18. Öfele, K. *J. Organomet. Chem.* **1968**, *12*, 42-43.
19. Wanzlick, H. W.; Schönherr, H. J. *Angew. Chem. Int. Ed. Engl.* **1968**, *7*, 141-142.
20. Igau, A.; Grutzmacher, H.; Baceiredo, A.; Bertrand, G. *J. Am. Chem. Soc.* **1988**, *110*, 6463-6466.
21. Arduengo, A. J.; Harlow, R. L.; Kline, M. *J. Am. Chem. Soc.* **1991**, *113*, 361-363.
22. Dorta, R.; Stevens, E. D.; Scott, N. M.; Costabile, C.; Cavallo, L.; Hoff, C. D.; Nolan, S. P. *J. Am. Chem. Soc.* **2005**, *127*, 2485-2895.
23. Glorius, F. N-Heterocyclic Carbenes in Catalysis-An Introduction. In *N-Heterocyclic Carbenes in Transition Metal Catalysis*, Springer Berlin Heidelberg: **2007**; Vol. 21, pp 1-20.
24. Herrmann, W. A.; Elison, M.; Fischer, J.; Koecher, C.; Artus, G. R. J. *Angew. Chem. Int. Ed.* **1995**, *34*, 2371-2374.
25. Herrmann, W. A.; Köcher, C. *Angew. Chem. Int. Ed. Engl.* **1997**, *36*, 2162-2187.

26. Glorius, F. *N-Heterocyclic Carbenes in Transition Metal Catalysis*. Springer-Verlag: Berlin, **2007**; Vol. 21, p 1-231.
27. Díez-González, S.; Marion, N.; Nolan, S. P. *Chem. Rev.* **2009**, *109*, 3612-3676.
28. Díez-González, S. *N-Heterocyclic Carbenes: From Laboratory Curiosities to Efficient Synthetic Tools*. The Royal Society of Chemistry: Cambridge, **2011**; p 1-442.
29. Kantchev, E. A. B.; O'Brien, C. J.; Organ, M. G. *Angew. Chem. Int. Ed.* **2007**, *46*, 2768-2813.
30. Valente, C.; Çalimsiz, S.; Hoi, K. H.; Mallik, D.; Sayah, M.; Organ, M. G. *Angew. Chem. Int. Ed.* **2012**, *51*, 3314-3332.
31. Grubbs, R. H. *Handbook of Metathesis*. Wiley-VCH: Weinheim, **2003**; Vol. 1-3, p 1-1234.
32. Monfette, S.; Fogg, D. E. *Chem. Rev.* **2009**, *109*, 3783-3816.
33. Praetorius, J. M.; Crudden, C. M. *Dalton Trans.* **2008**, 4079-4094.
34. Chen, A. C.; Ren, L.; Decken, A.; Crudden, C. M. *Organometallics* **2000**, *19*, 3459-3461.
35. Praetorius, J. M.; Kotyk, M. W.; Webb, J. D.; Wang, R.; Crudden, C. M. *Organometallics* **2007**, *26*, 1057-1061.
36. Allen, D. P.; Crudden, C. M.; Calhoun, L. A.; Wang, R. *J. Organomet. Chem.* **2004**, *689*, 3203-3209.
37. Zenkina, O. V.; Keske, E. C.; Wang, R.; Crudden, C. M. *Angew. Chem. Int. Ed.* **2011**, *50*, 8100-8104.
38. Keske, E. C.; Zenkina, O. V.; Asadi, A.; Sun, H.; Praetorius, J. M.; Allen, D. P.; Covelli, D.; Patrick, B. O.; Wang, R.; Kennepohl, P.; James, B. R.; Crudden, C. M. *Dalton Trans.* **2013**, *42*, 7414-7423.
39. Zenkina, O. V.; Keske, E. C.; Wang, R.; Crudden, C. M. *Organometallics* **2011**, *30*, 6423-6432.
40. Dorta, R.; Stevens Edwin, D.; Nolan Steven, P. *J. Am. Chem. Soc.* **2004**, *126*, 5054-5055.
41. Yu, X. Y.; Patrick, B. O.; James, B. R. *Organometallics* **2006**, *25*, 2359-2363.
42. Yu, X. Y.; Patrick, B. O.; James, B. R. *Organometallics* **2006**, *25*, 4870-4877.
43. Yu, X. Y.; Sun, H.; Patrick, B. O.; James, B. R. *Eur. J. Inorg. Chem.* **2009**, *2009*, 1752-1758.
44. Shimada, S.; Batsanov, A. S.; Howard, J. A. K.; Marder, T. B. *Angew. Chem. Int. Ed.* **2001**, *40*, 2168-2171.
45. Clegg, W.; Scott, A. J.; Dai, C.; Lesley, G.; Marder, T. B.; Norman, N. C.; Farrugia, L. J. *Acta Crystallogr., Sect. C: Cryst. Struct. Commun.* **1996**, *52*, 2545-2547.
46. Zenkina, O. V.; Keske, E. C.; Kochhar, G. S.; Wang, R.; Crudden, C. M. *Dalton Trans.* **2013**, *42*, 2282-2293.
47. Kwak, J.; Ohk, Y.; Jung, Y.; Chang, S. *J. Am. Chem. Soc.* **2012**, *134*, 17778-17788.
48. Keske, E. C.; Moore, B. D.; Zenkina, O. V.; Wang, R.; Schatte, G.; Crudden, C. M. *Chem. Commun.* **2014**, *50*, 9883-9886.
49. Hong, K.; Morken, J. P. *J. Am. Chem. Soc.* **2013**, *135*, 9252-9254.
50. Hleba, Y. B. *Ph.D. Dissertation*. Queen's Universty, **2007**.

51. Mkhalid, I. A. I.; Barnard, J. H.; Marder, T. B.; Murphy, J. M.; Hartwig, J. F. *Chem. Rev.* **2010**, *110*, 890-931.
52. Ros, A.; Estepa, B.; López-Rodríguez, R.; Álvarez, E.; Fernández, R.; Lassaletta, J. M. *Angew. Chem. Int. Ed.* **2011**, *50*, 11724-11728.
53. Ackermann, L.; Vicente, R.; Kapdi, A. R. *Angew. Chem. Int. Ed.* **2009**, *48*, 9792-9826.
54. Bouffard, J.; Itami, K. *Top. Curr. Chem.* **2010**, *292*, 231-280.
55. Yamaguchi, J.; Yamaguchi, A. D.; Itami, K. *Angew. Chem. Int. Ed.* **2012**, *51*, 8960-9009.
56. Satoh, T.; Kawamura, Y.; Miura, M.; Nomura, M. *Angew. Chem. Int. Ed. Engl.* **1997**, *36*, 1740-1742.
57. Oi, S.; Watanabe, S. I.; Fukita, S.; Inoue, Y. *Tetrahedron Lett.* **2003**, *44*, 8665-8668.
58. Shabashov, D.; Daugulis, O. *Org. Lett.* **2005**, *7*, 3657-3659.
59. Vogler, T.; Studer, A. *Org. Lett.* **2008**, *10*, 129-131.
60. Zhao, X.; Yu, Z. *J. Am. Chem. Soc.* **2008**, *130*, 8136-8137.
61. Seršen, S.; Kljun, J.; Požgan, F.; Štefane, B.; Turel, I. *Organometallics* **2013**, *32*, 609-616.
62. Oi, S.; Fukita, S.; Inoue, Y. *Chem. Commun.* **1998**, 2439-2440.
63. Bedford, R. B.; Coles, S. J.; Hursthouse, M. B.; Limmert, M. E. *Angew. Chem. Int. Ed.* **2003**, *42*, 112-114.
64. Kalyani, D.; Deprez, N. R.; Desai, L. V.; Sanford, M. S. *J. Am. Chem. Soc.* **2005**, *127*, 7330-7331.
65. Song, W.; Ackermann, L. *Angew. Chem. Int. Ed.* **2012**, *51*, 8251-8254.
66. Ohmura, T.; Awano, T.; Suginome, M. *J. Am. Chem. Soc.* **2010**, *132*, 13191-13193.
67. Maleczka, R. E.; Shi, F.; Holmes, D.; Smith, M. R. *J. Am. Chem. Soc.* **2003**, *125*, 7792-7793.
68. Dai, H. X.; Yu, J. Q. *J. Am. Chem. Soc.* **2012**, *134*, 134-137.
69. Chambers, R. D.; Clark, H. C.; Willis, C. J. *J. Am. Chem. Soc.* **1960**, *82*, 5298-5301.
70. Vedejs, E.; Chapman, R. W.; Fields, S. C.; Lin, S.; Schrimpf, M. R. *J. Org. Chem.* **1995**, *60*, 3020-3027.
71. Molander, G. A.; Canturk, B. *Angew. Chem. Int. Ed.* **2009**, *48*, 9240-9261.
72. Lennox, A. J. J.; Lloyd-Jones, G. C. *Chem. Soc. Rev.* **2014**, *43*, 412-443.
73. Lennox, A. J. J.; Lloyd-Jones, G. C. *Angew. Chem. Int. Ed.* **2012**, *51*, 9385-9388.
74. Kawamorita, S.; Miyazaki, T.; Ohmiya, H.; Iwai, T.; Sawamura, M. *J. Am. Chem. Soc.* **2011**, *133*, 19310-19313.

Chapter 3

Chemoselectivity in Pd–Catalyzed Cross–Coupling of Secondary Boronate Esters

3.1 Introduction

*3.1.1 Synthesis and Reactivity of 1–(1–Phenylethyl)boronic Acid Pinacolate Ester (**3–2**)*

In 2004, Crudden and coworkers[1] reported the regio– and enantio–controlled hydroboration of styrene derivatives with pinacol borane (Scheme 3–1) building on the seminal work of Hayashi and Ito.[2] Amazingly, the regioselectivity of the reaction could be entirely dictated by the nature of the metal catalyst used. For example, the use of an $[Ir(COD)Cl_2]$/DBBP catalytic system (DPPB = 1,4–bisdiphenylphosphinobutane) produced the linear isomer, **3–1**, exclusively in preference to the branched isomer, **3–2**. Alternatively, the hydroboration could be carried out with near exclusive regioselectivity for the branched isomer in a 98:2 branched to linear ratio by employing a cationic rhodium species $[Rh(COD)_2]^+[BF_4]^-$ with DPPB (Scheme 3–1, A). While regioisomers were easily controlled by the substitution of the metal source, the enantioselectivity of the hydroboration for the branched isomer impressively could also be controlled by the ligand (Scheme 3–1, B). Exchanging the phosphine ligand for the chiral ligand (*R*,*S*)–Josiphos

produced the *R*–enantiomer of the branched hydroborated product with good enantioselectivity.

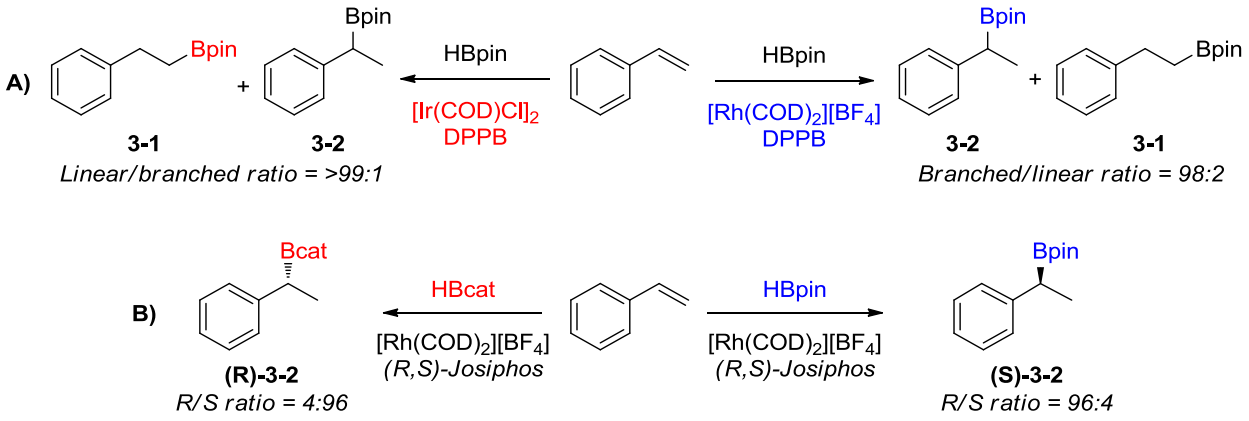

Scheme 3-1. Hydroboration of styrene controlled (**A**) regioselectively and (**B**) enantioselectively

This reaction provides a highly efficient route to enantiomerically pure secondary boronic esters such as **3–2**. As boronic esters are common organometallic substrates for a variety of transition metal–catalyzed reactions,[3] the effective synthesis of such sp^3 organoboronate esters would be of even higher importance if these substrates could also be used for the formation of new C–C bonds.[4] Typically however, sp^3 organoboronic esters are difficult substrates in transition metal–catalyzed reactions. This is chiefly due their sluggish transmetalation to metal centers, as well as side reactions such as β–hydride eliminations which commonly occur on the Pd–alkyl intermediates (Eq. 3–1).[5-6] This is particularly problematic in cases where the organoboronates bear stereochemical

information, as elimination/reinsertion pathways can completely destroy existing chirality in these substrates.[7-8]

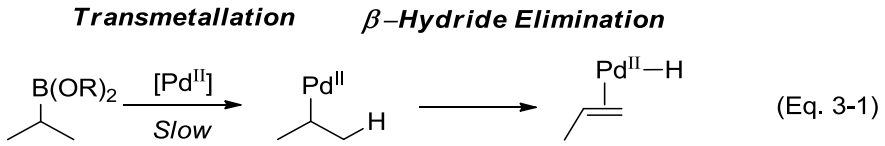

(Eq. 3-1)

In 2009, Crudden and coworkers[9] developed a novel palladium–catalyzed method for the cross–coupling of secondary boronic esters with aryl iodides in high yield. Key to this reaction was the use of stoichiometric amounts of Ag_2O which is thought to aid in transmetalation of the sp^3 boronic ester.[10] Furthermore, the reaction could be carried out using enantiopure secondary boronic esters resulting in a high level of stereoretention (92% for the *R*–enantiomer) after the cross–coupling reaction (Scheme 3–2).

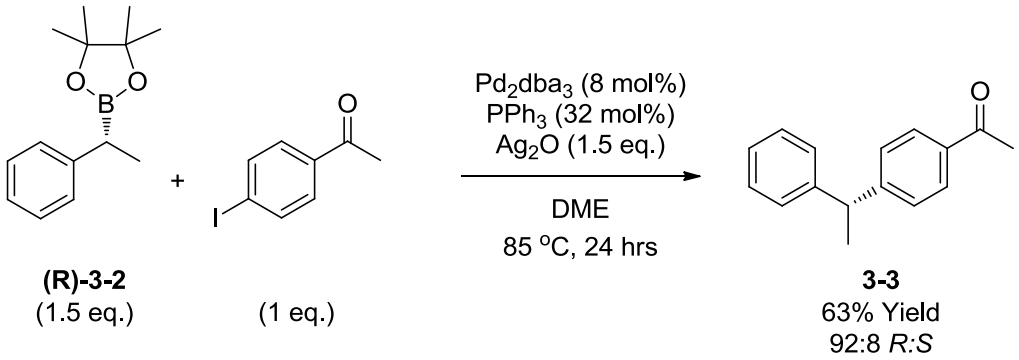

Scheme 3-2. Enantioselective cross–coupling of secondary boronic ester with retention of stereochemistry

The retention of configuration is an interesting observation, as it gives evidence that transmetalation occurs without inversion on a metal center. Similar observations were reported by Jarvo and coworkers[11] in nickel–catalyzed systems. This is in contrast to studies reported by Suginome and coworkers[12] who observed inversion of configuration, however his substrates are amide based and quite distinct from boronic ester **3–2**. In support of the specific functionality on the chiral boronic ester, Hall[13] and Molander[14] also observed inversion of stereochemistry from cross–coupling, while Aggarwal and Crudden observed retention for allylic,[15-16] propargylic[17] and doubly benzylic[18] boronic esters.

Interestingly, it was found that the increases in the phosphine loading resulted in an increase in the yield of the cross–coupling reaction. Unfortunately, this increase came at the expense of the stereoretention which was found to decrease dramatically with the increase in phosphine loadings above 4:1 ratios of PPh_3:Pd.[19] Similarly, increases in water concentration were found to improve the yield of the cross–coupling reaction albeit at a significant expense of the stereoretention of the reaction when concentrations were above 2000 ppm of H_2O.[19]

A plausible catalytic cycle for the cross–coupling reaction is given in Figure 3–1.[20] Oxidative addition of the aryl iodide to the Pd^0 metal centre produces **3–A** followed by addition of Ag_2O which abstracts the iodide and allows for coordination of the –OAg ligand to produce **3–B**. Addition of the enantiopure secondary boronic ester produces intermediate **3–C** with coordination of the silver through the π–system.[19] Coordination of the boronic ester to the oxygen of the –OAg ligand produces **3–D** and allows for

transmetalation to occur to produce intermediate **3–E**. Reductive elimination of this intermediate results in the enantiopure product **3–F**.

In order to source the loss of stereochemistry, key intermediates in the catalytic cycle should be considered. Alternatively, Intermediate **3–E** could possibly undergo competitive β–hydride elimination to form intermediate **3–G** with the olefin undergoing π–coordination to the metal centre. The labile olefin 'ligand' could potentially decomplex from the metal centre and reinsert to the metal complex resulting in racemized intermediate **3–H**, thus losing the stereochemistry obtained from the secondary boronic ester and essentially forming the racemic product **3–I**. Although the additional phosphine used in the reaction should inhibit the β–hydride elimination from **3–E**, this excess phosphine can also promote the decomplexation to **3–H** once the intermediate **3–G** is formed.[20] A similar pathway was observed by Hartwig and coworkers[5] in the cross–coupling of *sec*–butyl boronic esters which were found to produce significant amounts of the corresponding *n*–butyl cross–coupled products. This is not an uncommon pathway seen with large rings as typically β–hydride elimination becomes increasingly competitive with reductive elimination in larger ring systems.[4] Additionally, the competition between the two pathways increases when the adjacent alkyl substituent is primary.

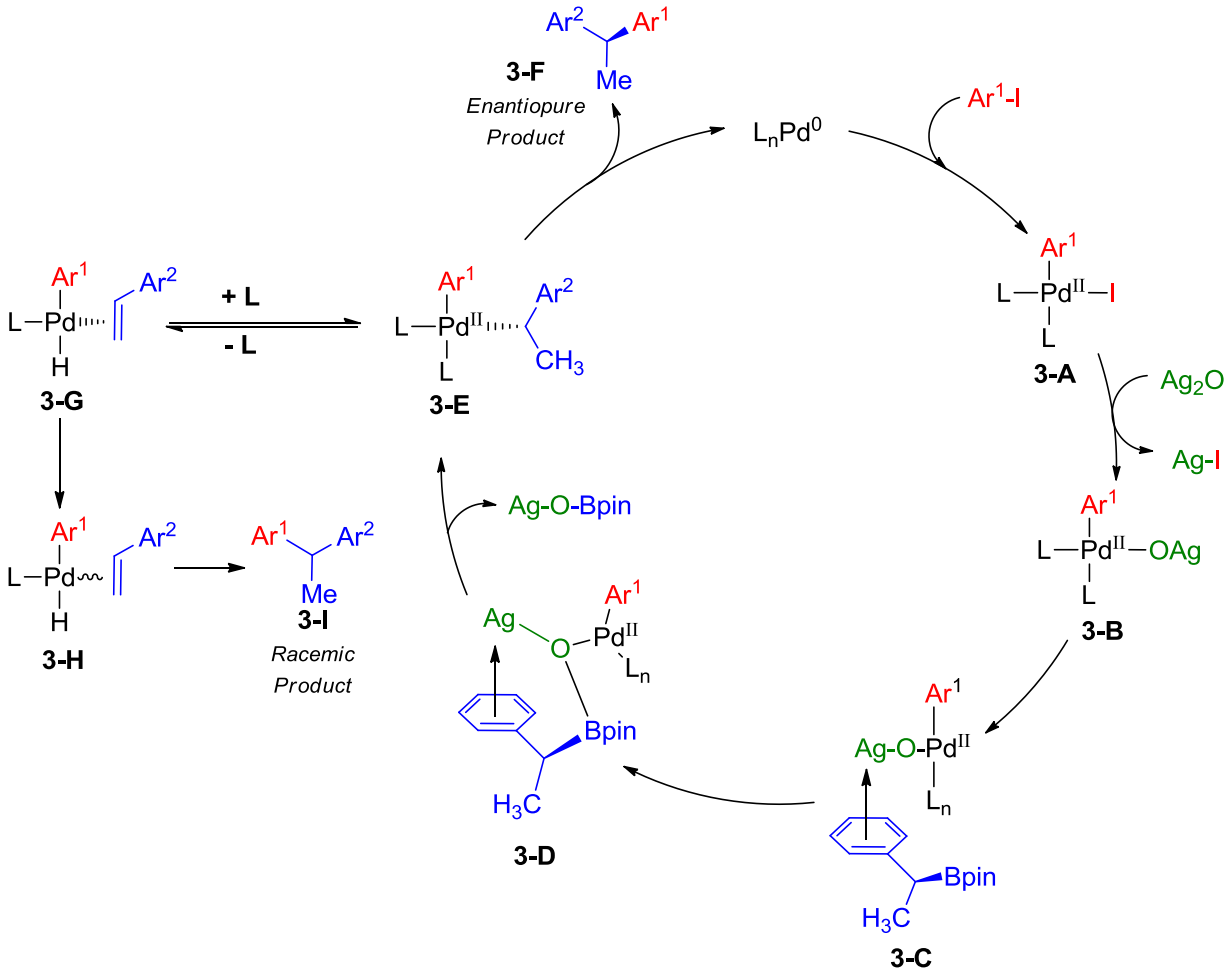

Figure 3-1. Plausible catalytic cycle for enantioselective cross–coupling of secondary boronic esters accounting for possible product racemization

In order to probe the possibility of this decomplexation pathway, the Suzuki–Miyaura reaction was conducted in the presence of 1.5 equivalents of 4–methylstyrene (Scheme 3–3).[4] Theoretically, presence of the alkene would facilitate the formation of the cross–over product **3–5** if the decomplexation pathway were occurring. Interestingly, the cross–over product **3–5** was not observed by gas chromatography–mass spectrometry

(GC–MS). However, the desired the product **3–4** was obtained and isolated in 47% yield by column chromatography. When the loading of styrene was increased to a ten–fold excess relative to the secondary boronic ester, the cross–over product **3–5** was still unobserved by GC–MS. These results suggest that the decomplexation pathway was not taking place in the catalytic cycle even with an increased loading of the phosphine ligand. This racemization could be promoted by K_2CO_3 which can deprotonate minor amounts of Pd–H intermediate **3–G**.[20] However, this deprotonation would prevent an equilibrium from forming between **3–G** and **3–E** and thus prevent the racemic product from forming. This is consistent with a report from Fu and coworkers[21] indicating the ability of Hünig's base (*N*,*N*–diisopropylethylamine) in deprotonating Pd–H bonds, however incorporation of Hünig's base found the enantiospecificity of the reaction to be increased with our system.[19]

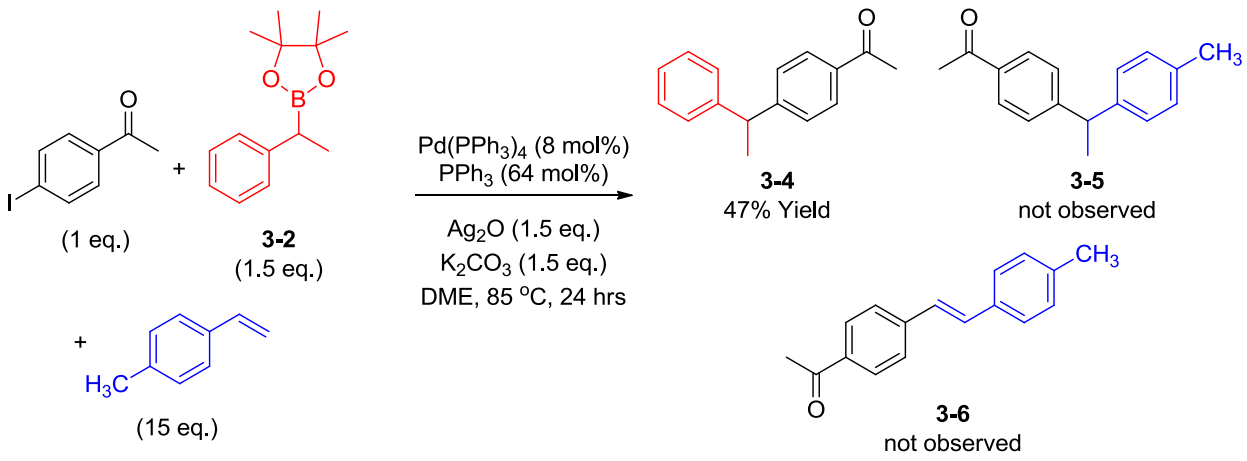

Scheme 3-3. Chemoselective Suzuki–Miyaura cross–coupling of **3–2** in cross–over study with 4–methylstyrene

Interestingly, despite the incorporation of 4–methylstyrene in the reaction mixture the Mizoroki–Heck cross–coupled product **3–6**, which could be obtained by coupling of the styrene with aryl iodide, was also not observed. This unique chemoselectivity was explored by former Crudden group member Aurora Antoft–Finch[22] with various aryl iodides for the selective cross–coupling with the secondary boronic esters in the presence of the styrene. In each case, the Mizoroki–Heck cross–coupled product was not observed and only coupling of the secondary boronic ester was observed. Due to the remarkable chemoselectivity for the secondary boronic ester, we sought to further investigate the conditions of the reaction to determine which reagents were blocking the Mizoroki–Heck reaction from occurring. Likewise, we also sought to investigate conditions to chemoselectively cross–couple the Mizoroki–Heck acceptor in the presence of the aryl secondary boronic ester.

3.1.2 The Mizoroki–Heck Reaction

Similar to the Suzuki–Miyaura reaction, the Mizoroki–Heck cross–coupling reaction has provided chemists with a valuable synthetic tool for the creation of new C–C bonds. In 1971, Tsutomu Mizoroki[23] introduced the first palladium–catalyzed cross–coupling of aryl iodides with vinyl substrates (Scheme 3–4, A). Heck's highly cited 1972 report[24] broadened the scope of the initial coupling reaction to include other aryl halides (bromides and chlorides) as well as olefins such as styrene derivatives and methyl acrylate (Scheme 3–4, B).

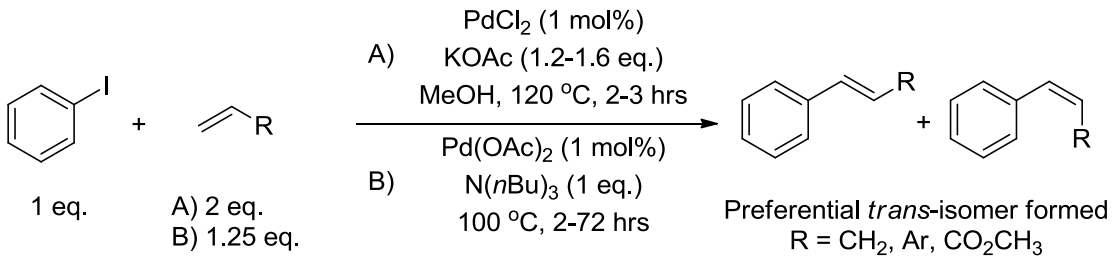

Scheme 3-4. Palladium–catalyzed vinylic cross–couplings with aryl iodides by A) Mizoroki conditions and B) Heck conditions

Currently, the Mizoroki–Heck reaction (similar to the Suzuki–Miyaura reaction) stands as one of the fundamental synthetic tools used for the construction of C–C bonds in pharmaceutical, agrochemical and fine chemical industries.[25-28] The 'traditional' Mizoroki–Heck reaction (intermolecular coupling of aryl halide with a vinyl substrate) has also evolved[29] to include intramolecular[26] and enantioselective examples.[26, 30] Further development has advanced into more complex systems such as dehydrogenative couplings[31] which utilize the activation of C–H bond in place of the aryl halide; as well as oxidative couplings.[32]

3.1.3 Mechanism of the Mizoroki–Heck

From a mechanistic stand point, the Mizoroki–Heck reaction has been widely studied[25, 33-35] and is fairly similar to the Suzuki–Miyaura catalytic cycle. The general catalytic cycle for the Mizoroki–Heck cross–coupling is displayed in Figure 3–2. The catalytically active Pd^0 species **3–J** is generated through ligand dissociation from either a Pd^0 or Pd^{II} precatalyst. Oxidative addition of an aryl halide generates intermediate **3–K**,

followed by migratory insertion of the olefin into the Pd–R bond with *syn*–addition to form **3–L**. This *syn*–addition occurs from an intermediate complex in which the olefin, metal and the R group adopt a co–planar orientation allowing the migratory insertion to occur. Prior to the elimination step in the Mizoroki–Heck cycle, **3–I** undertakes an internal rotation about the C–C bond generating **3–M**. This rotation sets up the *syn*–*β*–hydride elimination to generate the product **3–N** as well as Pd^{II}–H complex **3–O**. Addition of stoichiometric base allows **3–O** to undergo reductive elimination to regenerate the catalytically active Pd^{0} complex **3–J**.

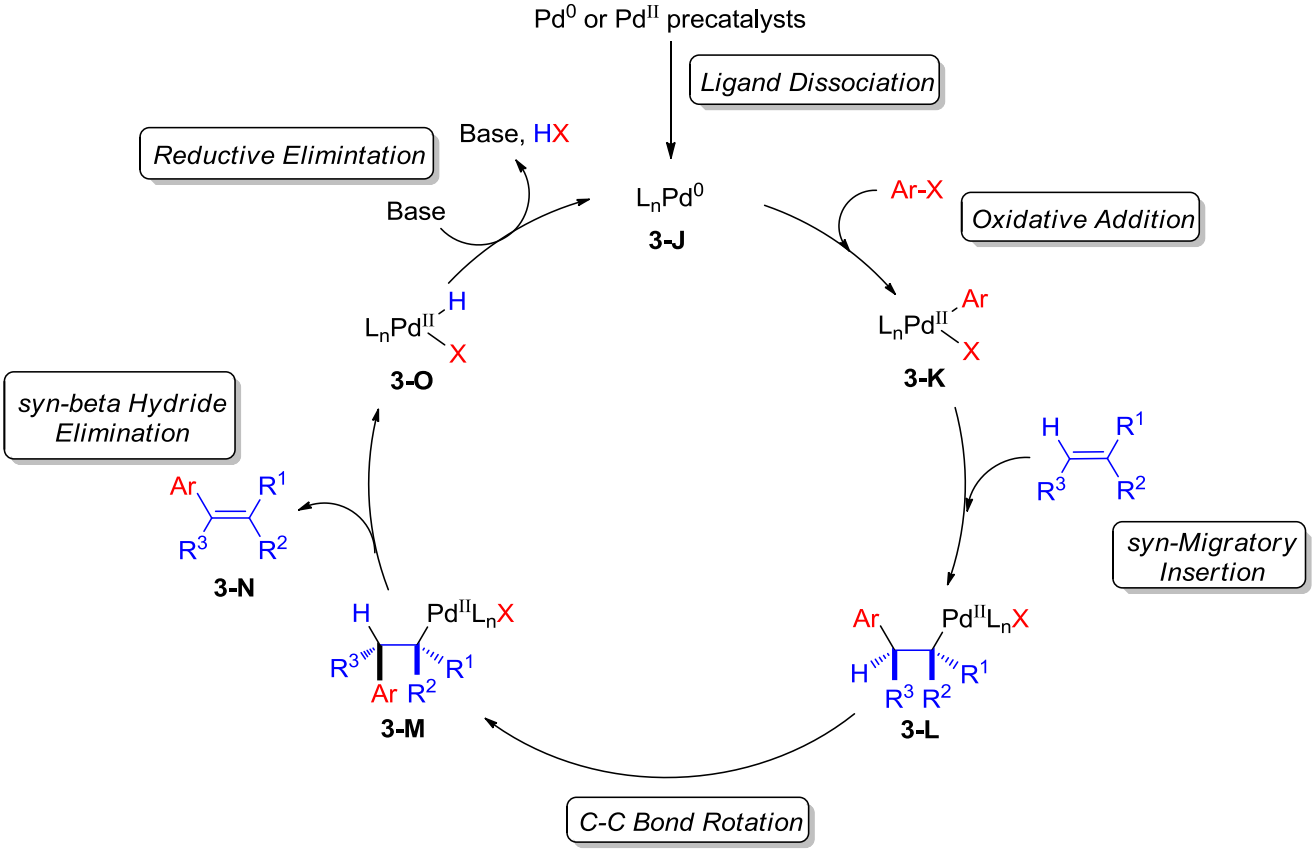

Figure 3-2. General catalytic cycle for Mizoroki–Heck Cross–Coupling

3.2 Results and Discussion

3.2.1 Controlled Mizoroki–Heck Cross–Couplings

In order to test the chemoselectivity of our reaction, we employed methyl acrylate, which is known to be a good acceptor in the Mizoroki–Heck reaction. Under conditions that were otherwise identical to our Suzuki–Miyaura couplings, the reaction was found to be chemoselective, giving the Suzuki–Miyaura cross–coupled product, **3–4**, in 52% isolated yield (Table 3–1, entry 1). In contrast, the Mizoroki–Heck cross–coupled product, **3–7**, was not observed by GC–MS or by the crude ^{1}H NMR. Increasing the loading of the olefin to 10 equivalents was found to have no effect on the reaction (entry 2), similar to the reactivity observed with 4–methylstyrene. Interestingly, even when the temperature increased to 120 °C in DMF, the reaction completely failed, producing neither the Suzuki–Miyaura nor the Mizoroki–Heck product (entry 3). Furthermore, removal of Ag_2O from the reaction produced only trace amounts of the Mizoroki–Heck product by ^{1}H NMR and GC–MS (entry 4). The desired Mizoroki–Heck product, **3–7**, was finally obtained upon further removing the excess phosphine from the reaction yielding the Mizoroki–Heck product in 50% isolated yield (entry 5) from the competition reaction. The conditions for the chemoselective Mizoroki–Heck reaction were also found to be applicable to cinnamate derivatives, though reactivities with these substrates was decreased.[20]

Table 3-1. Intermolecular chemoselective Mizoroki–Heck reactions[a]

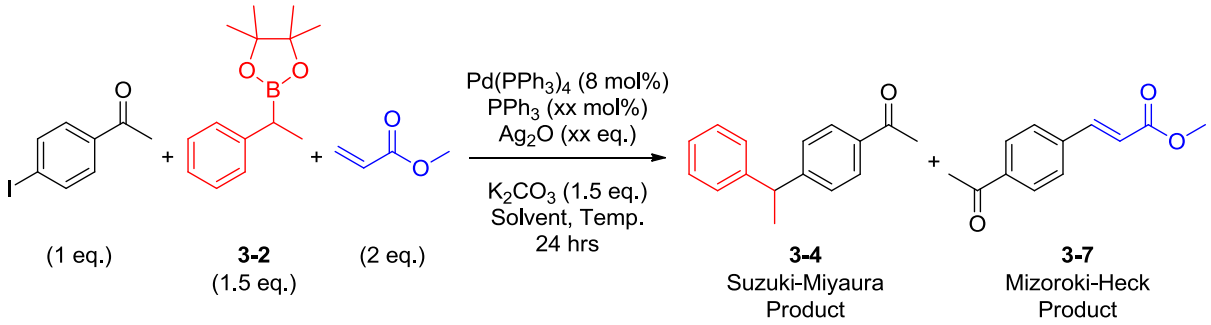

Entry	Ag_2O (equiv.)	PPh_3 (mol%)	Solvent	Temperature (°C)	3–4 (%)[b]	3–7 (%)[b]
1	1.5	32	DME[e]	85	52	NR[g]
2[c]	1.5	32	DME[e]	85	54	NR[g]
3	1.5	32	DMF[f]	120	NR[g]	NR[g]
4	0	32	DMF[f]	120	NR[g]	Trace
5[d]	0	0	DMF[f]	120	NR[g]	50

[a]Reactions conducted using **3–2** (0.75 mmol), methyl acrylate (1 mmol), 4–iodoacetophenone (0.5 mmol), K_2CO_3 (0.75 mmol), $Pd(PPh_3)_4$ (0.041 mmol, 8 mol%) and 350 ppm of H_2O for 24 hours at the indicated temperature. Ag_2O, PPh_3 and solvent were added as indicated. [b]Isolated yields. [c]10 equivalents of methyl acrylate used. [d]Reaction conducted for 15 hours. [e]DME = 1,2–dimethoxyethane. [f]DMF = *N*,*N*–dimethylformamide. [g]NR = no reaction

Removal of the secondary boronic ester from the reaction yielded the Mizoroki–Heck cross–coupled product in 67% isolated yield (Scheme 3–5). Unsurprisingly, the removal of the excess triphenylphosphine helped to promote the formation of the product **3–7**, perhaps because the added phosphine hindered β–hydride elimination from occurring by saturation of the coordination sites with the phosphine ligand. However, it is important to note that Ag_2O, while of crucial importance to the Suzuki–Miyaura coupling of secondary boronic esters, was found to be completely detrimental to the Mizoroki–Heck reaction. While the exact reason for this is not currently known, it could be attributed to a

couple possibilities. For one, Ag_2O is also an oxidant and could be oxidizing the phosphine ligand. While this would open coordination sites on the palladium for the Mizoroki–Heck reaction to proceed, there could be potentially competitive binding from the silver oxide forming a Pd–O–Ag species, which would saturate coordination sites on the meal centre. Alternatively, Ag_2O could bind to the substrate, sequestering the alkene and prevent its coordination with the palladium metal centre which would in turn shut down the Mizoroki–Heck reaction.

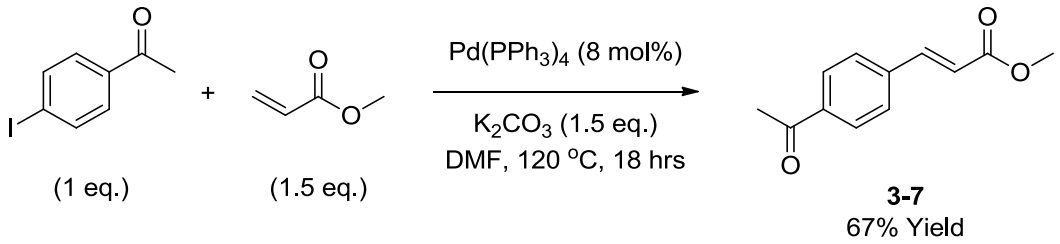

Scheme 3-5. Controlled Mizoroki–Heck reaction with methyl acrylate producing **3–7**

In summary, the conditions of the intermolecular competition reaction between methyl acrylate and the secondary boronic ester can easily be tuned to chemoselectively produce either the either the Suzuki–Miyaura product, **3–4**, or the Mizoroki–Heck product, **3–7**, while leaving the other reagent untouched in the reaction (Scheme 3–6). It is suspected that higher yields were not observed in the Suzuki–Miyaura reaction due to competitive binding of exogenous olefin with the palladium centre hindering oxidative addition of the aryl iodoacetophenone.[36-38]

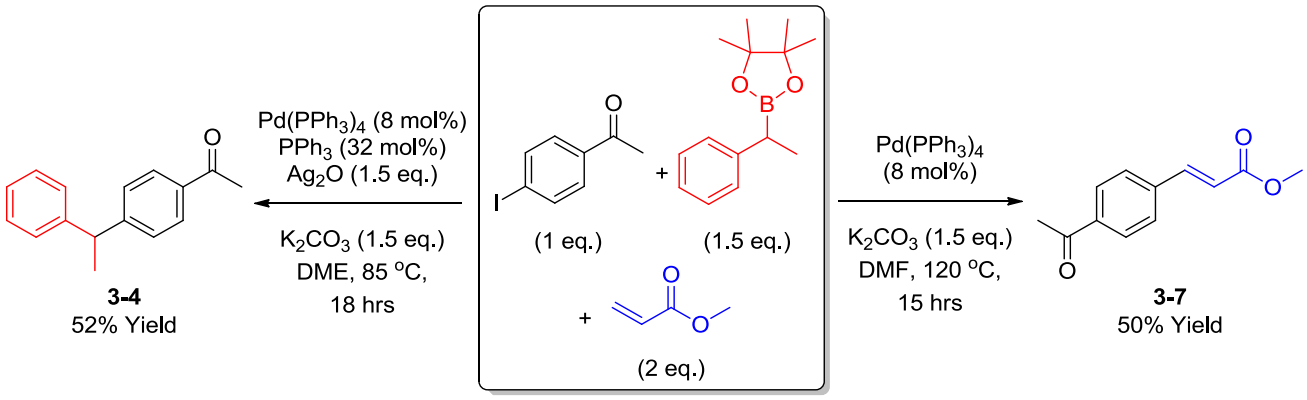

Scheme 3-6. Intermolecular chemoselective cross–coupling summary

3.2.2 Synthesis of Suzuki/Heck Substrate and Intramolecular Chemoselectivity

While intermolecular competition studies revealed that no competitive Mizoroki–Heck cross–coupling occurred under the conditions developed for coupling of the secondary boronic ester, it was imperative to investigate this chemoselective process intramolecularly. Ideally, having a substrate in which a Suzuki–Miyaura acceptor (boronic ester) and Mizoroki–Heck acceptor (vinyl substituent) are both present would provide the optimal challenge to selectivity.[39]

In order to synthesize the Suzuki–Heck substrate **3–10**, a two–step synthesis beginning with 4–bromostyrene as the starting material was envisioned. The two–step process would utilize selective hydroboration to produce the branched organoboronate, followed by cross–coupling of the bromo–substituent to obtain the desired substrate **3–10**.

We attempted the hydroboration of 4–bromostyrene using conditions previously reported by our group[1] with the cationic [Rh(COD)(DPPB)][BF_4] complex. Unfortunately, the high regioselectivity observed with the hydroboration of styrene did not translate to the 4–bromostyrene substrate. Resultantly, the hydroboration produced a mixture of the regioisomers in an 83:17 ratio for the branched (**3–8**) to linear (**3–9**) isomers (Scheme 3–7) as determined by analysis of the crude ^{1}H NMR. The product of the hydroboration was not further isolated due to the selectivity observed.

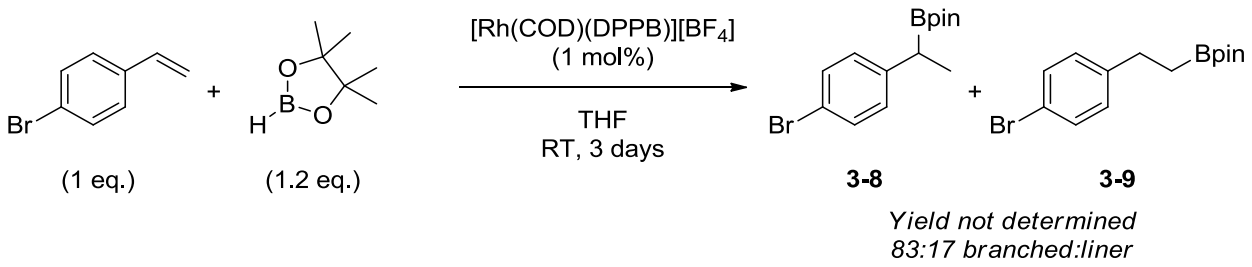

Scheme 3-7. Branched to linear selectivity in the hydroboration of 4–bromostyrene with Crudden conditions

In 2008, Shibata and coworkers[40] utilized the dimeric rhodium species [Rh(COD)OAc]$_2$ with DPPB ligand to generate an *in situ* cationic complex that was shown to be highly active for the hydroboration of olefins, requiring only 40 minutes at room temperature while showing high regioselectivities for the branched isomer in various styrene derivatives. Employing these conditions, the hydroboration of 4–bromostyrene was achieved with a regioselectivity of 93:7 for the branched isomer and produced the desired product **3–8** in 68% yield (Scheme 3–8).

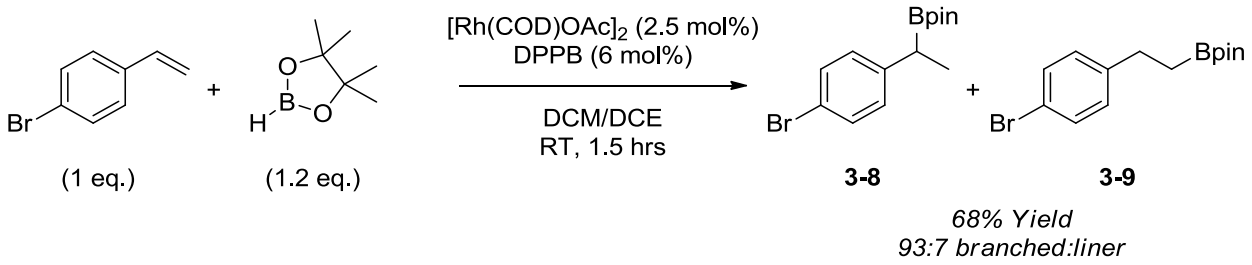

Scheme 3-8. Regioselective synthesis of **3–8**

With the boronic ester in place, we turned our attention to installing the Mizoroki–Heck acceptor, which could be prepared by converting the bromine functional group in the *para*–position on the substrate. Attempts at installing the vinyl component included the cross–coupling of substrate **3–8** with vinyltrimethylsilane, which has proven to be an effective cross–coupling partner for aryl bromides by Hallberg and coworkers.[41-42] While a mixture of isomers were obtained resulting from the scrambling of the TMS group, deprotection of this functional group was found to be problematic. Deprotection of the TMS groups using a tetrabutylammonium fluoride (TBAF) produced a mixture of products including the desired product **3–10**, the protodeboronated product, as well as silylated product as observed by GC–MS of the crude mixture. Thin layer chromatography (TLC) proved to be ineffective for separation of the product mixtures. While TBAF was effective for the deprotection, competitive protodeboronation was problematic and could not be avoided under the conditions used, thus other routes were explored.

In 1978, Plevyak and Heck[43] reported the use of ethylene gas ($H_2C=CH_2$) as the vinyl coupling substrate for the palladium–catalyzed cross–coupling. Ethylene offers an advantageous route to styrene derivatives preventing regioisomers of the olefinic

component while also being a very atom economic[44] alternative. Utilizing conditions similar to Heck's[43] report and Fu's[45] report, we were able to successfully obtain the desired product **3–10** in 66% isolated yield (Scheme 3–9). Analysis of the crude ^{1}H NMR did not indicate formation of the stilbene product which would result from coordination of **3–10** with the catalyst in place of the ethylene substrate. The scope of this reaction is still widely unexplored but provides a nice alternative to present approaches at making styrene compounds.

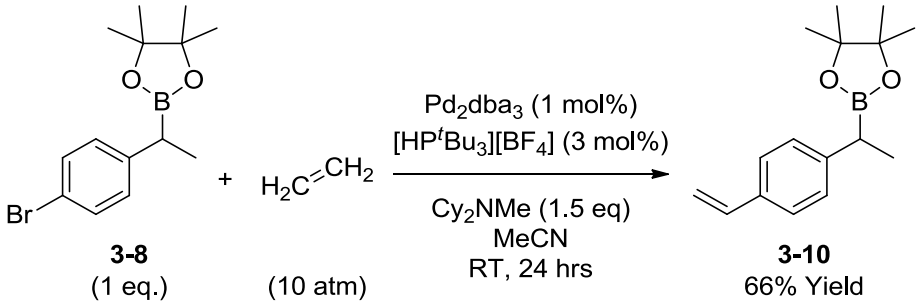

Scheme 3-9. Synthesis of Suzuki/Heck substrate **3–10** *via* Mizoroki–Heck reaction with ethylene

*3.2.3 Chemoselectivity of **3–10***

With the Suzuki/Heck substrate **3–10** in hand, we attempted the conditions which were found to selectively cross–couple the secondary boronic ester for coupling with 4–iodoacetophenone (Scheme 3–10). Gratifyingly, the Suzuki–Miyaura cross–coupling product **3–11** was isolated in 55% yield. Similar to the intermolecular studies, the Mizoroki–Heck product **3–12** was not observable by ^{1}H NMR or GC–MS analysis. The chemoselectivity observed here with preferentially reactivity at the Suzuki–Miyaura

acceptor may circumvent synthetic routes which purposely avoid formation of intermediate products which contain similar reactive sites such as Suzuki–Miyaura and Mizoroki–Heck functionalities. Likewise, this methodology can offer insight into more efficient chemical processes requiring multi–step syntheses.

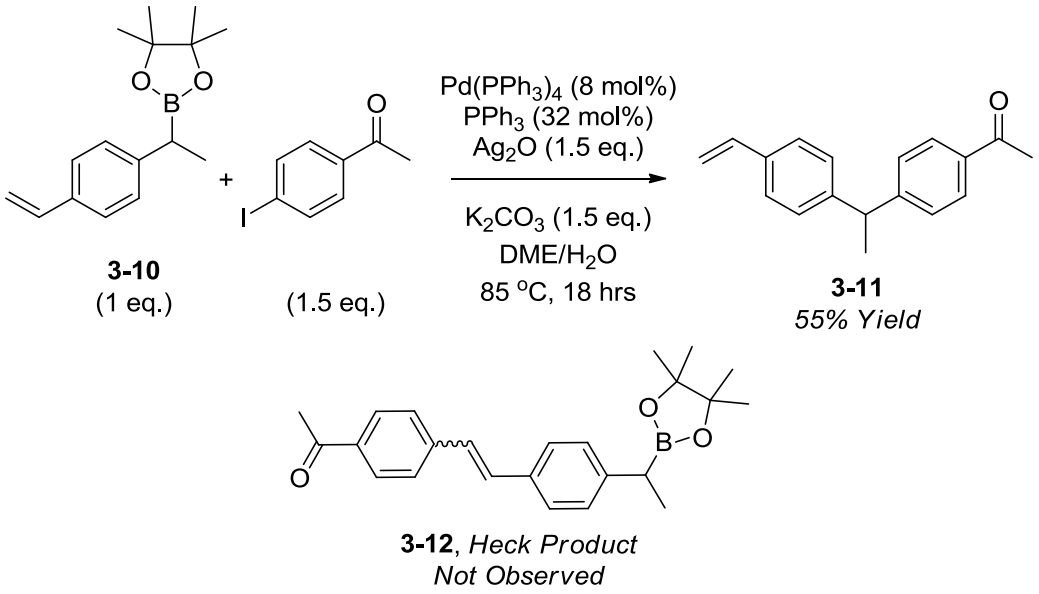

Scheme 3-10. Synthesis of **3–11** by chemoselective cross–coupling of the secondary boronic ester

3.3 Conclusions and Future Work

One thing still to be investigated is the compatibility of the substrate **3–10** to chemoselectively undergo the Mizoroki–Heck reaction without degradation of the secondary boronic ester. With promising results observed in the intermolecular competitions reactions showing the reaction to be selective for the boronic ester or the olefin, the intramolecular competition should be analogous to the intermolecular case. If

true, complete chemoselectivity can be obtained with substrates containing a terminal olefin as well as a secondary boronic ester and prevent the need for protection/deprotection steps or lengthier alternative routes towards total synthesis of natural products, drug candidate molecules and material compounds.

Looking at the chemoselectivity of the reaction with the secondary boronic ester, a sequential Mizoroki–Heck reaction could be conducted further expanding the synthetic methodology scope towards polysubstituted aromatics (Scheme 3–11, Pathway A). Likewise with the olefinic component still present after the cross–coupling of the secondary boronic ester, a diboration (to produce **3–13**) could be carried out followed by further cross–coupling reactions to build large poly–substituted aromatic molecules such as **3–14** (Scheme 3–11, Pathway B). With a diboration to the styrene component, chemoselectively cross–coupling one of the linear or secondary boronic esters would be highly advantageous for synthetic methodologies. While the chemoselective cross–coupling of the secondary boronic ester has been proven by our group intermolecularly,[4, 20] work is ongoing to achieve this feat intramolecularly. Additionally conducting these reactions one–pot with little to no workup in between steps would be an optimal synthetic strategy.

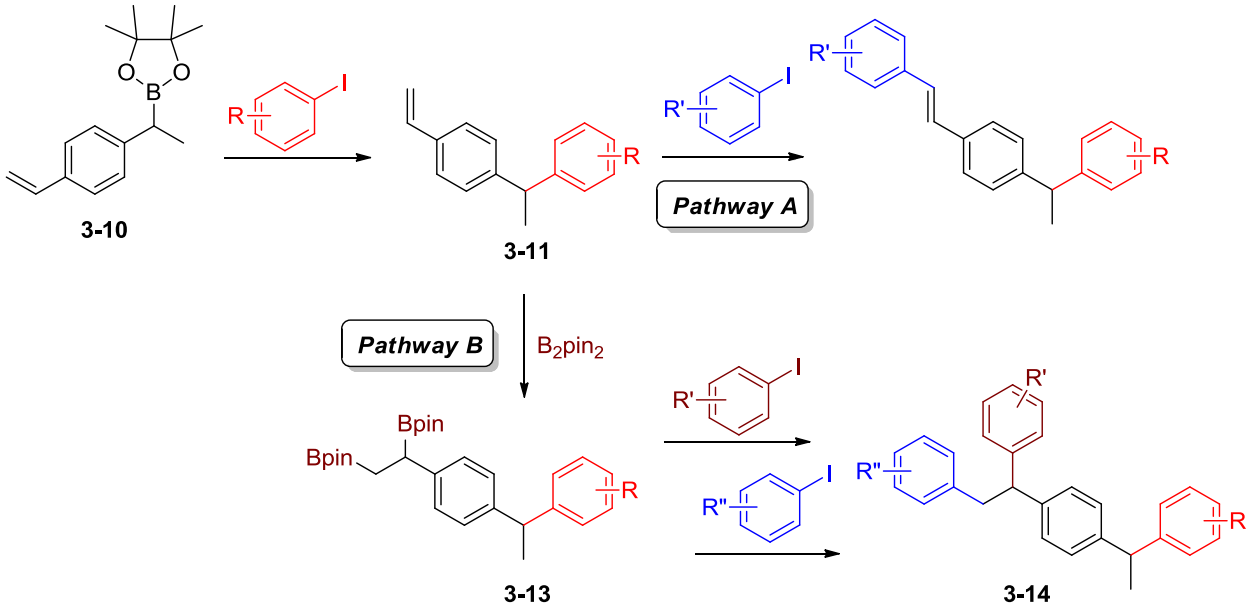

Scheme 3-11. Potential routes to polysubstituted aromatic compounds

3.4 References

1. Crudden, C. M.; Hleba, Y. B.; Chen, A. C. *J. Am. Chem. Soc.* **2004**, *126*, 9200-9201.
2. Hayashi, T.; Matsumoto, Y.; Ito, Y. *J. Am. Chem. Soc.* **1989**, *111*, 3426-3428.
3. Miyaura, N.; Suzuki, A. *Chem. Rev.* **1995**, *95*, 2457-2483.
4. Crudden, C. M.; Glasspoole, B. W.; Lata, C. J. *Chem. Commun.* **2009**, 6704-6716.
5. Kataoka, N.; Shelby, Q.; Stambuli, J. P.; Hartwig, J. F. *J. Org. Chem.* **2002**, *67*, 5553-5566.
6. Han, C.; Buchwald, S. L. *J. Am. Chem. Soc.* **2009**, *131*, 7532-7533.
7. Jana, R.; Pathak, T. P.; Sigman, M. S. *Chem. Rev.* **2011**, *111*, 1417-1492.
8. Glasspoole, B. W.; Keske, E. C.; Crudden, C. M. Stereospecific and stereoselective Suzuki-Miyaura cross-coupling reactions. In *New Trends in Cross-Coupling: Theory and Applications*, Colacot, T. J., Ed. RSC Catalysis: Cambridge, **2014**; pp 519-548.
9. Imao, D.; Glasspoole, B. W.; Laberge, V. S.; Crudden, C. M. *J. Am. Chem. Soc.* **2009**, *131*, 5024-5025.
10. Uenishi, J.; Beau, J. M.; Armstrong, R. W.; Kishi, Y. *J. Am. Chem. Soc.* **1987**, *109*, 4756-4758.
11. Taylor, B. L. H.; Jarvo, E. R. *J. Org. Chem.* **2011**, *76*, 7573-7576.
12. Ohmura, T.; Awano, T.; Suginome, M. *J. Am. Chem. Soc.* **2010**, *132*, 13191-13193.
13. Lee, J. C. H.; McDonald, R.; Hall, D. G. *Nat. Chem.* **2011**, *3*, 894-899.
14. Sandrock, D. L.; Jean-Gérard, L.; Chen, C. Y.; Dreher, S. D.; Molander, G. A. *J. Am. Chem. Soc.* **2010**, *132*, 17108-17110.
15. Glasspoole, B. W.; Ghozati, K.; Moir, J. W.; Crudden, C. M. *Chem. Commun.* **2012**, *48*, 1230-1232.
16. Chausset-Boissarie, L.; Ghozati, K.; LaBine, E.; Chen, J. L. Y.; Aggarwal, V. K.; Crudden, C. M. *Chem. Eur. J.* **2013**, *19*, 17698-17701.
17. Partridge, B. M.; Chausset-Boissarie, L.; Burns, M.; Pulis, A. P.; Aggarwal, V. K. *Angew. Chem. Int. Ed.* **2012**, *51*, 11795-11799.
18. Matthew, S. C.; Glasspoole, B. W.; Eisenberger, P.; Crudden, C. M. *J. Am. Chem. Soc.* **2014**, *136*, 5828-5831.
19. Glasspoole, B. W. *Ph.D. Dissertation*. Queen's University, **2011**.
20. Glasspoole, B. W.; Oderinde, M. S.; Moore, B. D.; Antoft-Finch, A.; Crudden, C. M. *Synthesis* **2013**, *45*, 1759-1763.
21. Hills, I. D.; Netherton, M. R.; Fu, G. C. *Angew. Chem. Int. Ed.* **2003**, *42*, 5749-5752.
22. Antoft-Finch, A. *BSc. Dissertation*. Queen's University, **2012**.
23. Mizoroki, T.; Mori, K.; Ozaki, A. *Bull. Chem. Soc. Jpn.* **1971**, *44*, 581-581.
24. Heck, R. F.; Nolley, J. P. *J. Org. Chem.* **1972**, *37*, 2320-2322.
25. Crisp, G. T. *Chem. Soc. Rev.* **1998**, *27*, 427-436.
26. Dounay, A. B.; Overman, L. E. *Chem. Rev.* **2003**, *103*, 2945-2964.
27. Torborg, C.; Beller, M. *Adv. Syn. Cat.* **2009**, *351*, 3027-3043.

28. Board, J.; Cosman, J. L.; Rantanen, T.; Singh, S. P.; Snieckus, V. *Platinum Metals Rev.* **2013**, *57*, 234-258.
29. Alonso, F.; Beletskaya, I. P.; Yus, M. *Tetrahedron* **2005**, *61*, 11771-11835.
30. Shibasaki, M.; Vogl, E. M.; Ohshima, T. *Adv. Syn. Cat.* **2004**, *346*, 1533-1552.
31. Le Bras, J.; Muzart, J. *Chem. Rev.* **2011**, *111*, 1170-1214.
32. Karimi, B.; Behzadnia, H.; Elhamifar, D.; Akhavan, P. F.; Esfahani, F. K.; Zamani, A. *Synthesis* **2010**, *2010*, 1399-1427.
33. de Meijere, A.; Meyer, F. E. *Angew. Chem. Int. Ed. Engl.* **1995**, *33*, 2379-2411.
34. Beletskaya, I. P.; Cheprakov, A. V. *Chem. Rev.* **2000**, *100*, 3009-3066.
35. Cabri, W.; Candiani, I. *Acc. Chem. Res.* **1995**, *28*, 2-7.
36. Amatore, C.; Jutand, A.; Khalil, F.; M'Barki, M. A.; Mottier, L. *Organometallics* **1993**, *12*, 3168-3178.
37. Amatore, C.; Broeker, G.; Jutand, A.; Khalil, F. *J. Am. Chem. Soc.* **1997**, *119*, 5176-5185.
38. Johnson, J. B.; Rovis, T. *Angew. Chem. Int. Ed.* **2008**, *47*, 840-871.
39. Nicolaou, K. C.; Bulger, P. G.; Sarlah, D. *Angew. Chem. Int. Ed.* **2005**, *44*, 4442-4489.
40. Endo, K.; Hirokami, M.; Shibata, T. *Organometallics* **2008**, *27*, 5390-5393.
41. Hallberg, A.; Westerlund, C. *Chem. Lett.* **1982**, *1982*, 1992-1993.
42. Karabelas, K.; Hallberg, A. *J. Org. Chem.* **1986**, *51*, 5286-5290.
43. Plevyak, J. E.; Heck, R. F. *J. Org. Chem.* **1978**, *43*, 2454-2456.
44. Trost, B. M. *Angew. Chem. Int. Ed. Engl.* **1995**, *34*, 259-281.
45. Littke, A. F.; Fu, G. C. *J. Am. Chem. Soc.* **2001**, *123*, 6989-7000.

Chapter 4

Experimental Section

4.1 General Experimental Conditions

Unless otherwise specified, all manipulations were carried out under an atmosphere of dry argon in oven–dried glassware, or under a nitrogen atmosphere in a glovebox (M. Braun) with oxygen and water levels ≤2 ppm. All solvents were distilled from either calcium hydride (CaH_2) or sodium metal (Na), deoxygenated with a minimum of three freeze–pump–thaw cycles and stored under N_2 over molecular sieves (4 Å) prior to use. Phenyl boronic acids used to synthesize starting materials for C–H borylation reactions were purchased from Frontier Scientific and used without further purification. Pinacolborane (HBpin) was purchased from Sigma Aldrich, purified by bulb–to–bulb distillation and stored at –30 ^{o}C under a nitrogen atmosphere. 2–Phenylpyridine (2–Ph–pyr) was purchased from Sigma Aldrich, distilled from CaH_2 and stored at –30 ^{o}C under a nitrogen atmosphere. Sodium ethoxide (NaOEt) was purchased from Sigma Aldrich stored under a nitrogen atmosphere in the glovebox in the absence of light and used without further purification. Addition of water in Suzuki–Miyaura and sequential arylation reactions was accomplished by bubbling argon (Ar) through distilled water for a minimum of 30 minutes and adding the water to the reaction mixture with a μL glass

syringe by piercing the rubber septa. $RhCl_3 \cdot 3H_2O$, [Rh(COD)dppb][BF_4] and $Pd_2(dba)_3$ were generously donated by Johnson Matthey and used without further purification. [HP^tBu_3][BF_4] was purchased from Alfa Aesar, stored under a nitrogen atmosphere and used without further purification. $Pd(PPh_3)_4$ was purchased from Sigma Aldrich, stored under a nitrogen atmosphere and used without further purification. 1,4–Bis(diphenylphosphino)butane (dppb) was purchased from Sigma Aldrich, recrystallized from hot ethanol and stored under a nitrogen atmosphere. *N*,*N*–Dicyclohexylmethylamine (Cy_2NMe) was purchased from Sigma Aldrich, distilled and stored under a nitrogen atmosphere over molecular sieves (4 Å). 4–Bromostyrene was purchased from Acros, distilled by short path distillation and stored under a nitrogen atmosphere at –30 °C in the absence of light.

Purification of C–H borylation products was achieved by column chromatography using a stationary phase of aluminum oxide purchased from Sigma Aldrich (activated, basic, Brockmann Grade I, 58 Å porosity, pH 9.0–10.0) and eluted with reagent grade hexanes and ethyl acetate (EtOAc). All other products purified by column chromatography were accomplished using flash grade silica gel (Silicycle, 50 μm particle size, 60 Å porosity) and eluted with reagent grade mixtures of hexanes/EtOAc or DCM/MeOH.

NMR spectra were recorded on a Bruker Avance 300, 400 or 500 MHz (^1H) where indicated. Chemical shifts are reported in delta (δ) units, expressed in parts per million (ppm) downfield from tetramethylsilane using residual protonated solvent as an internal standard ($CDCl_3$, δ 7.26 ppm; CD_2Cl_2, δ 5.32 ppm; C_6D_6, δ 7.16 ppm). Boron NMR spectra (^{11}B) were recorded at 128 MHz and 160 MHz and referenced to an external

standard (BF_3·OEt, δ 0 ppm). Fluorine NMR spectra (^{19}F) were recorded at 375 MHz and referenced to an external standard ($CFCl_3$, δ 0 ppm). Elemental analyses were performed using a Thermo Scientific Flash 2000 CHNS Elemental Analyzer. High–resolution mass spectrometry (HRMS) was performed using a Micromass GCT Mass Spectrometer (GC–Time of Flight). Gas chromatography–mass spectrometry (GC–MS) measurements were performed on an Agilent Technologies GC 6850N / MS 5975N VL MSD equipped with Agilent technologies HP–5MS column (length: 30m, 0.25 mm id, 0.25 μm coating thickness) coupled with a quadrupole mass filter. Helium is used as the carrier gas under a constant flow rate of 1.0 mL/min and separation achieved by optimized temperature programs. X–ray data collection was performed on a Bruker SMART APEX II X-ray diffractometer and collected by Dr. Gabrielle Schatte of the Queen's Chemistry department.

4.2 Synthesis of IPr Ligand (2–15) and Dimeric Rh–NHC Complex (2–20)

Synthesis of (1E,2E)–1,2–Bis(2,6–diisopropylphenylimino)ethane:

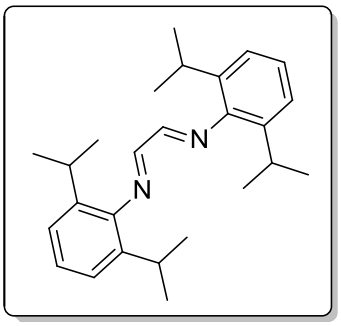

In a 250 mL round bottom flask equipped with a stir bar, 2,6–diisopropylaniline (6.11 g, 34.5 mmol) and glyoxal (40% in water, 1 g, 17.2 mmol) were taken up in 90 mL of absolute ethanol. To the stirring solution, a catalytic amount of formic acid (three drops) was added dropwise from a Pasteur pipette. The reaction was stirred at room temperature for 48 hours and then filtered and washed

with cold ethanol. The filtrate was concentrated to ~40 mL and the solution allowed to stir for an additional 24 hours. The mixture was again filtered and washed with cold ethanol. The crystals were combined and dried under reduced pressure to yield 2.99 g of bright yellow crystals (46% yield). ^{1}H NMR data are cnsistent with those previously reported in the literature.[1] **^{1}H NMR** (400 MHz, $CDCl_3$): δ 8.19 (, *J* = 12.6 Hz, 2H), 7.59 (t, *J* = 7.8 Hz 2H), 7.37 (d, *J* = 7.8 Hz, 4H), 2.46 (septet, *J* = 6.8 Hz, 4H), 1.31 (d, *J* = 7.8 Hz, 12 H), 1.26 (d, *J* = 7.8 Hz, 12H).

Synthesis of 1,3–Bis(2,6–diisopropylphenyl)imidazolium chloride salt:

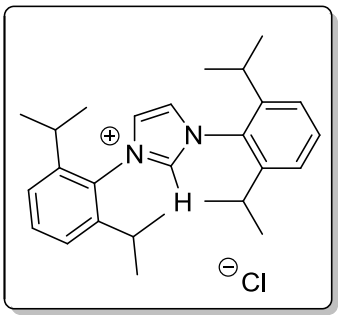

In a 250 mL round bottom flask equipped with a stir bar, (1*E*,2*E*)–1,2–*bis*(2,6–diisopropylphenylimino)ethane (2.27 g, 6.03 mmol) was taken up in 75 mL of ethyl acetate and the flask was placed in an ice water bath. In a separate 50 mL round bottom flask equipped with a stir bar, hydrochloric acid (4M solution in dioxane, 2.34 mL, 9.35 mmol) and paraformaldehyde (0.25 g, 8.20 mmol) were combined and heated to dissolve paraformaldehyde. The paraformaldehyde solution was transferred to a dropping funnel and added dropwise to the stirring solution over one hour. Upon completion of the addition, the flask was sealed with a rubber septum and allowed to stir at room temperature for 3 days. The mixture was then filtered and washed with cold ethyl acetate. The powder product was collected and dried under reduced pressure to yield 1.8 g of a white powder (77% yield). ^{1}H NMR data are consistent with

those previously reported in the literature.[1] **^{1}H NMR** (400 MHz, $CDCl_3$): δ 8.12 (s, 2 H), 7.18–7.21 (m, 6H), 2.96 (septet, *J* = 6.7 Hz, 4H), 1.23 (d, *J* = 6.8 Hz, 24H).

Synthesis of 1,3–Bis(2,6–diisopropylphenyl)–1,3–dihydro–2H–imidazol–2–ylidene (**2–15**):

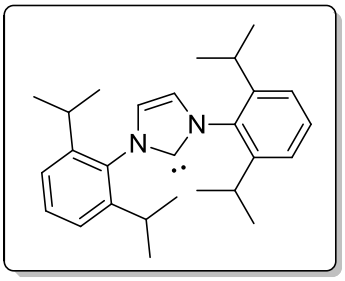

In a nitrogen filled glovebox, 1,3–*bis*(2,6–diisopropylphenyl)imidazolium chloride salt (500 mg, 1.18 mmol) was added to a 100 mL round bottom flask and taken up in 20 mL of THF. In a separate 4 dram scintillation vial, potassium *tert*–butoxide (KO^{t}Bu) (132 mg, 1.18 mmol) was taken up in 10 mL of THF. The KO^{t}Bu solution was then added to the stirring IPr–HCl solution dropwise (addition took approximately 30 minutes). After addition of KO^{t}Bu, the solution was stirred for an additional 1.5 hours in the glovebox producing a translucent dark yellow solution. The solution was then filtered through a fritted funnel. The filtrate was collected and dried under reduced pressure to produce 385 mg of an off-white powder (84% yield). ^{1}H NMR data are consistent with those previously reported in the literature.[1] **^{1}H NMR** (300 MHz, C_6D_6): δ 7.29 (t, *J* = 7.6 Hz, 2 H), 7.18 (d, *J* = 6.9 Hz, 4H), 6.71 (s, 2H), 2.96 (septet, *J* = 6.6 Hz, 4H), 1.40 (d, *J* = 6.7 Hz, 12H), 1.29 (d, *J* = 6.8 Hz, 12H).

Synthesis of $[Rh(C_2H_4)_2Cl]_2$ (**2–19**):

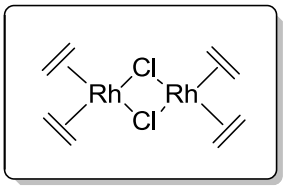

Prepared according to a modified procedure by Cramer.[2] In a 100 mL round bottom flask, a 17:1 MeOH/H_2O solution was degassed by bubbling argon through the mixture for 30 minutes. To a separate 100 mL round bottom flask equipped with a stir bar, $RhCl_3 \cdot 3H_2O$ (500 mg, 1.90 mmol) was added. To this, 18 mL of the MeOH/H_2O solution was added. The flask sealed with a rubber septum and stirred. A balloon filled with ethylene gas was equipped with needle was placed through the septum and bubbled through the solution to purge the system of air. The balloon was filled an additional two times with ethylene gas. Upon mixing, the $[Rh(C_2H_4)_2Cl]_2$ crashed out of the solution as dark red crystals. The mixture was then filtered and rinsed with a minimal amount of ice cold MeOH (~5 mL). The product was dried under reduced pressure for 5 minutes. The product was stored under a nitrogen atmosphere at –30 °C. The reaction yielded 214 mg of a red–orange powder (58% yield). The complex was not further characterized.

Synthesis of $[Rh(IPr)(C_2H_4)Cl]_2$ (**2–20**):[3]

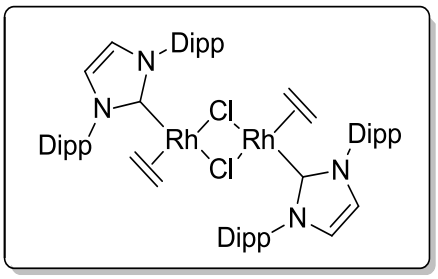

In a nitrogen–filled glovebox, a 4 dram vial equipped with a stir bar was charged with $[Rh(C_2H_4)_2Cl]_2$ (55 mg, 0.14 mmol), which was taken up in THF (10 mL). A solution of *N*,*N*′–bis(2,6–diisopropylphenyl)–imidazol–2–ylidene (110 mg, 0.28 mmol) in THF (10 mL) was added drop–wise to the stirring solution and the mixture was stirred for 3 hours in the glovebox. The reaction was

then filtered through a plug of Celite and the THF was removed *in vacuo*. The residue was triterated with hexanes and isolated in 152 mg as an orange–yellow powder (98% yield). The complex was stored as a powder at –30 °C under nitrogen. ^{1}H NMR data at 273 K are consistent with those which we have previously reported. **^{1}H NMR** (300 MHz, C_6D_6, 273 K): δ 7.33–7.24 (t, *J* = 7.6 Hz, 4H), 7.19 (d, *J* = 6.8 Hz, 8H), 6.34 (s, 4H), 3.16 (septet, *J* = 6.5 Hz, 8H), 2.74 (br s, 4H), 2.24 (br s, 4H), 1.56 (d, *J* = 6.5 Hz, 24H), 1.01 (d, *J* = 6.8 Hz, 24H).

4.3 Synthesis of 2–Phenylpyridine Starting Materials for C–H Borylations

General Procedure: 2–Phenyl pyridines were prepared according to a modified procedure by Qiu and coworkers.[4] To a 100 mL round bottom flask equipped with a stir bar was added 2–bromopyridine (505 μL, 5.34 mmol), boronic acid (6.43 mmol), K_3PO_4 (2.27 g, 10.7 mmol) and $Pd(OAc)_2$ (71 mg, 0.105 mmol, 2 mol%) in air. The mixture was taken up in ethylene glycol (14 mL) and stirred at 80 ^{o}C for 2 hours. The mixture was returned to room temperature, and diluted with EtOAc (10 mL) and transferred to a separatory funnel and washed with brine (10 mL). The organic fractions were combined, dried over sodium sulfate, filtered and then concentrated. The products were purified by column chromatography on silica gel.

Synthesis of 2–(4–Ethylphenyl)pyridine:

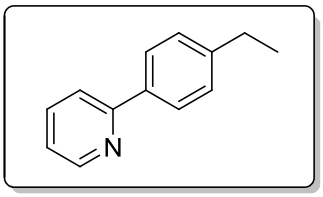

Prepared according to the general procedure using 4–ethylphenylboronic acid (965 mg, 6.43 mmol). The crude mixture was purified by column chromatography on silica with a 9:1 Hexanes:EtOAc eluent mixture to afford 742 mg of a slightly yellow oil (76% yield). ^{1}H NMR data are consistent with those previously reported in the literature.[4] **^{1}H NMR** (400 MHz, $CDCl_3$): δ 8.69 (d, *J* = 4.8 Hz, 1H), 7.93 (d, *J* = 8.2 Hz, 2H), 7.72–7.66 (m, 2H), 7.32 (d, *J* = 8.1 Hz, 2H), 7.19 (td, *J* = 4.9, 3.5 Hz, 1H), 2.71 (q, *J* = 7.6 Hz, 2H), 1.28 (t, *J* = 7.6 Hz, 3H).

Synthesis of 2–(naphthalene–2–yl)pyridine:

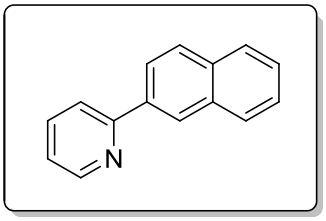

Prepared according to the general procedure using 2–naphthylboronic acid (1.10 g, 6.43 mmol). The crude mixture was purified by column chromatography on silica with a 10:1 Hexanes:EtOAc eluent mixture to afford 810 mg of a white powder (74% yield). ^{1}H NMR data are consistent with those previously reported in the literature.[5] **^{1}H NMR** (500 MHz, $CDCl_3$): δ 8.51 (s, 2H), 7.80 (s, 1H), 7.74 (dd, *J* = 12.5, 7.8 Hz, 2H), 7.28 (dt, *J* = 13.9, 6.9 Hz, 3H), 7.00 (d, *J* = 7.6 Hz, 1H), 6.82 (t, *J* = 7.7 Hz, 1H), 6.43–6.31 (m, 1H).

Synthesis of 2–(Naphthalene–1–yl)pyridine:

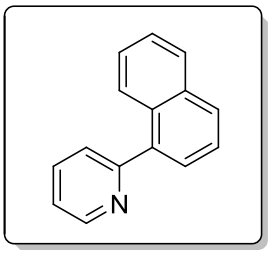

Prepared according to the general procedure using 1–naphthylboronic acid (357 mg, 2.1 mmol). The crude mixture was purified by column chromatography on silica with a 10:1 Hexanes:EtOAc eluent mixture to afford 287 mg of a slightly yellow oil (78% yield). ^{1}H NMR data are consistent with those previously reported in the literature.[6] **^{1}H NMR** (400 MHz, $CDCl_3$): δ 8.81 (d, *J* = 4.8 Hz, 1H), 8.09 (d, *J* = 9.0 Hz, 1H), 7.92 (d, *J* = 8.5 Hz, 2H), 7.83 (td, *J* = 7.7, 1.8 Hz, 1H), 7.66–7.44 (m, 5H), 7.38–7.30 (m, 1H).

Synthesis of 2–((1,1'–Biphenyl)–4–yl)pyridine:

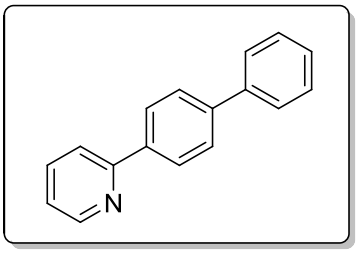

Prepared according to the general procedure using 1,1'–biphenyl–4–ylboronic acid (886 mg, 4.47 mmol). The crude mixture was purified by column chromatography on silica with a 8:2 Hexanes:EtOAc eluent mixture to afford 450 mg of a white crystalline solid (78% yield). ^{1}H NMR data are consistent with those previously reported in the literature.[7] **^{1}H NMR** (300 MHz, $CDCl_3$): δ 8.72 (d, *J* = 5.3 Hz, 1H), 8.08 (d, *J* = 8.0 Hz, 2H), 7.78–7.76 (m, 2H), 7.72 (d, *J* = 8.4 Hz, 2H), 7.66 (d, *J* = 6.8 Hz, 2H), 7.55–7.51 (m, 1H), 7.47 (t, *J* = 7.4 Hz, 2H), 7.38 (d, *J* = 6.7 Hz, 1H).

Synthesis of 2–(Furan–2–yl)pyridine:

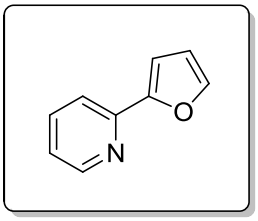

Prepared according to the general procedure using furan–2–ylboronic acid (500 mg, 4.47 mmol). The crude mixture was purified by column chromatography on silica with a 9:1 Hexanes:EtOAc eluent mixture to afford 412 mg of a yellow oil (76% yield). ^{1}H NMR data are consistent with those previously reported in the literature.[8] **^{1}H NMR** (400 MHz, $CDCl_3$): δ 8.44 (d, *J* = 4.0 Hz, 1H), 7.54 (d, *J* = 8.0 Hz, 1H), 7.30 (d, *J* = 3.4 Hz, 1H), 7.09 (s, 1H), 7.05 (t, *J* = 7.8 Hz, 1H), 6.58–6.46 (m, 1H), 6.16 – 6.12 (m, 1H).

Synthesis of 2–(3–nitrile)phenylpyridine:

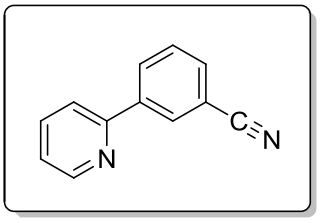

Prepared according to the general procedure using (3–cyanophenyl)boronic acid (378 mg, 2.57 mmol). The crude mixture was purified by column chromatography on silica with a 3:1 Hexanes:EtOAc eluent mixture to afford 272 mg of a brown solid (71% yield). ^{1}H NMR data are consistent with those previously reported in the literature.[9] **^{1}H NMR** (500 MHz, $CDCl_3$): δ 8.69 (d, *J* = 4.0 Hz, 1H), 8.29 (s, 1H), 8.20 (d, *J* = 7.9 Hz, 1H), 7.81–7.78 (m, 1H), 7.71 (d, *J* = 7.9 Hz, 1H), 7.66 (d, *J* = 7.7, 1H), 7.55 (t, *J* = 7.8 Hz, 1H), 7.30 (dd, *J* = 6.6, 4.9 Hz, 1H)

Synthesis of 2–(4–methoxycarbonyl)phenylpyridine:

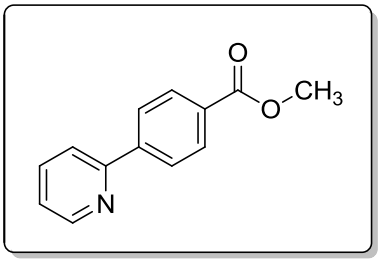

Prepared according to a modified procedure by Cheng and coworkers.[10] To a 100 mL round bottom flask equipped with a stir bar was added 2–bromopyridine (350 μL, 3.67 mmol), (4–methoxycarbonyl)phenylboronic acid (826 mg, 4.59 mmol), K_3PO_4 (1.55 g, 7.31 mmol) and $PdCl_2$ (32 mg, 0.182 mmol, 5 mol%). The mixture was taken up in toluene (18 mL) and stirred at 100 ^oC for 18 hours. The mixture was transferred to a separatory funnel and diluted with brine (25 mL). The mixture was extracted into EtOAc and the organic fractions combined, dried over sodium sulfate and concentrated. The crude mixture was purified by column chromatography on silica with a 4:1 Hexanes:EtOAc eluent mixture to afford 682 mg of a brown solid (87% yield). ^{1}H NMR data are consistent with those previously reported in the literature.[6] **^{1}H NMR** (400 MHz, $CDCl_3$): δ 8.63 (d, *J* = 4.7 Hz, 1H), 8.33 (d, *J* = 8.3 Hz, 2H), 8.18 (d, *J* = 8.2 Hz, 2H), 7.33–7.28 (m, 2H), 7.16 (t, *J* = 7.7 Hz, 1H), 6.79–6.68 (m, 1H), 3.60 (s, 3H).

Synthesis of 2–(3–dimethylamino)phenylpyridine:

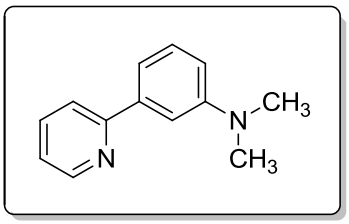

Prepared according to a modified procedure by Cheng and coworkers.[10] To a 100 mL round bottom flask equipped with a stir bar was added 2–bromopyridine (230 μL, 2.42 mmol), (3–dimethylamino)phenylboronic acid (500 mg, 3.03 mmol), K_3PO_4 (1.03 g, 4.85 mmol) and $PdCl_2$ (22 mg, 0.013 mmol, 5 mol%). The mixture was taken up in toluene (10 mL) and stirred at 100 ^oC for 18 hours. The mixture was

transferred to a separatory funnel and diluted with brine (15 mL). The mixture was extracted into EtOAc and the organic fractions combined, dried over sodium sulfate and concentrated. The crude mixture was purified by column chromatography on silica with a 8:2 Hexanes:EtOAc eluent mixture to afford 431 mg of a brown oil (90% yield). ^{1}H NMR data are consistent with those previously reported in the literature.[11] **^{1}H NMR** (500 MHz, $CDCl_3$): δ 8.69 (d, *J* = 4.7 Hz, 1H), 7.73 (dd, *J* = 5.4, 1.3 Hz, 2H), 7.42 (s, 1H), 7.34 (t, *J* = 7.9 Hz, 1H), 7.28 (d, *J* = 7.7 Hz, 1H), 7.21 (td, *J* = 5.3, 3.0 Hz, 1H), 6.82 (dd, *J* = 8.1, 1.9 Hz, 1H), 3.03 (s, 6H).

4.4 Rhodium–Catalyzed C–H Borylations

Synthesis of NaO^{i}Pr Base:

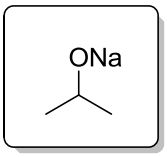

To an oven dried 250 mL Schlenk flask equipped with a stir bar, 50 mL of HPLC grade 2–propanol was added. To the stirring mixture, sodium metal was cut with scissors, added in small portions and was washed with 2 rinses of hexanes and 2 rinses of HPLC grade 2–propanol to remove residual paraffin oil. A total of 200 mg (8.7 mmol) of Na metal was added to the stirring solution and the flask was resealed with a rubber septum equipped with an outlet needle and flushed with argon. The solution was stirred for 18 hours, over which, white crystals slowly crash out of solution. The solvent was concentrated under reduced pressure with gentle heating (40 ^{o}C) product transferred to the glovebox. The reaction yielded 675 mg of a white powder (90% yield) which slowly turned yellow overtime.

Direct Borylation of Benzene (**2–22**):

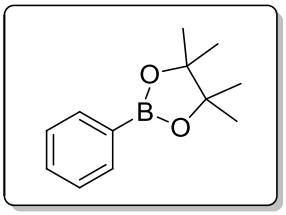

Under a nitrogen atmosphere, a 50 mL Schlenk bomb equipped with a stir bar was charged with $[Rh(IPr)(C_2H_4)Cl]_2$ (4.4 mg, 0.004 mmol, 1 mol%) and HBpin (51 mg, 0.4 mmol). The mixture was taken up in 2 mL of benzene (total concentration of solution = 0.2 M). The flask was capped, removed from the glovebox and stirred at 140 ^oC for 24 hours. The solution was cooled and run through a plug of Celite. ^{11}B NMR of the crude mixture displayed a singlet at δ 30.3 ppm (borylated benzene product) and δ 22 ppm (B_2pin_3 decomposition product). Crude mixture was purified by silica gel chromatography using eluent mixture of 90:10 (hexanes:EtOAc) to afford 46 mg of a white solid (56% yield). **^{1}H NMR** (400 MHz, $CDCl_3$): δ 7.81 (d, *J* = 7.3 Hz, 2H), 7.46 (t, *J* = 7.4 Hz, 1H), 7.37 (t, *J* = 7.4 Hz, 1H), 1.35 (s, 12H). **^{13}C NMR** (100 MHz, $CDCl_3$): δ 134.7, 131.3, 127.7, 83.8, 24.9 (*C–B* bond not observed). **^{11}B NMR** (128 MHz, $CDCl_3$): δ 30.6.

Rh^{III}–H Complex formation with 2–Phenylpyridine (**2–23**):[12]

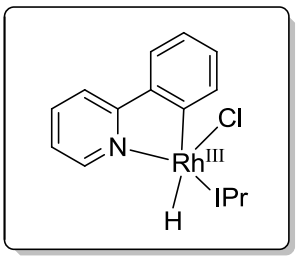

Under a nitrogen atmosphere, a 4 dram scintillation vial equipped with a stir bar was charged with 2–phenylpyridine (4.2 mg, 0.064 mmol) and $[Rh(IPr)(C_2H_4)Cl]_2$ (30 mg, 0.027 mmol). The mixture was taken up in 1 mL of C_6D_6 and stirred in the glovebox for 3 hours at room temperature. The crude mixture was transferred to a J–Young tube and analyzed by ^{1}H NMR. The characteristic Rh^{III}–H is observed as a doublet. The

product was not further purified. **^{1}H NMR** (400 MHz, C_6D_6): δ –24.5 ppm (d, $^1J_{Rh–H}$ = 49.9 Hz).

Rh^{III}–H Complex formation with 2–(3–nitrile)phenylpyridine (**2–43**):

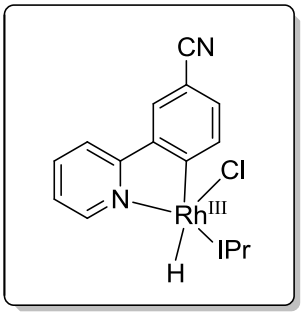

Under a nitrogen atmosphere, a 4 dram scintillation vial equipped with a stir bar was charged with 2–phenylpyridine derivative (5 mg, 0.027 mmol) and $[Rh(IPr)(C_2H_4)Cl]_2$ (15 mg, 0.014 mmol). The mixture was taken up in 1 mL of C_6D_6 and stirred in the glovebox for 3 hours. The crude mixture was transferred to a J–Young tube and analyzed by ^{1}H NMR. The characteristic Rh^{III}–H is observed as a doublet. The product was not further purified. **^{1}H NMR** (400 MHz, C_6D_6): δ –23 ppm (d, $^1J_{Rh–H}$ = 45 Hz).

Rh^{III}–H Complex formation with 2–(4–methoxycarbonyl)phenylpyridine (**2–44**):

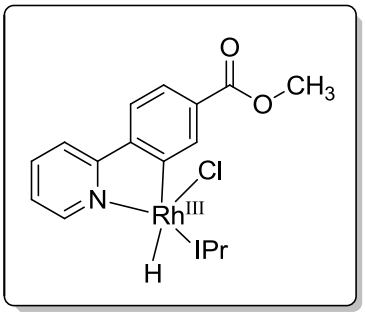

Under a nitrogen atmosphere, a 4 dram scintillation vial equipped with a stir bar was charged with 2–phenylpyridine derivative (5.8 mg, 0.027 mmol) and $[Rh(IPr)(C_2H_4)Cl]_2$ (15 mg, 0.014 mmol). The mixture was taken up in 1 mL of C_6D_6 and stirred in the glovebox for 3 hours. The crude mixture was transferred to a J–Young tube and analyzed by ^{1}H NMR. The characteristic Rh^{III}–H is observed as a doublet. The product was not further purified. **^{1}H NMR** (400 MHz, C_6D_6): δ –24.8 ppm (d, $^1J_{Rh–H}$ = 50 Hz).

***General Procedure for C–H Borylation of 2–Phenylpyridines* (2–24 to 2–42):**[12]

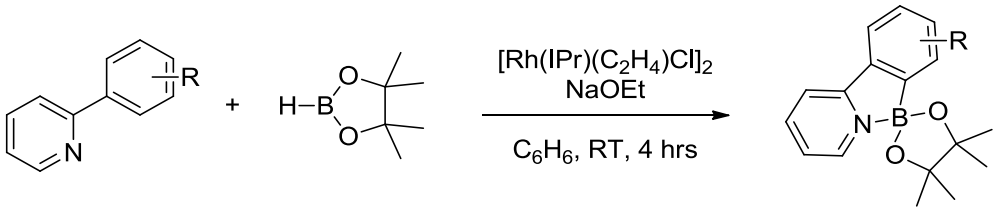

To an oven–dried round bottom flask equipped with a stir bar, NaOEt (8.5 mg, 0.125 mmol) was added. Substrate (0.5 mmol) and catalyst **2–20** (5.55 mg, 0.005 mmol, 1%) were taken up in 4 mL of benzene and added to the round bottom flask. HBpin (128 mg, 1 mmol) was taken up in 0.6 mL of benzene then added to the stirring mixture and the reaction was vigorously stirred for 4 hours. After the elapsed time, the flask was removed from the glovebox and the contents loaded directly onto an alumina column (eluted with ethyl acetate/hexanes mixtures). The organic fractions were then collected and concentrated *in vacuo*.

Synthesis of 2–(2–Boronic acid pinacolate ester)–phenylpyridine (**2–24**):[12]

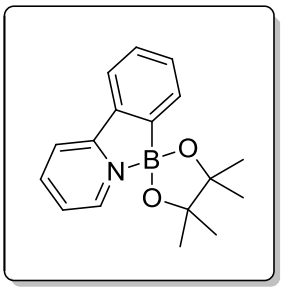

Synthesized according to the general procedure and purified by column chromatography eluting with a 7:3 EtOAc/Hexanes mixture to afford a yellow powder (114 mg, 81% yield). **^{1}H NMR** (400 MHz, $CDCl_3$): δ 8.66 (d, *J* = 5.5 Hz, 1H), 7.95, (td, *J* = 7.8, 1.5 Hz, 1H) 7.79 (d, *J* = 8.0 Hz, 1H), 7.72 (d, *J* = 7.2 Hz, 1H), 7.65 (d, *J* = 7.6 Hz, 1H), 7.41 (td, *J* = 7.3, 0.9 Hz, 1H), 7.35 (dd, *J* = 9.5, 3.4 Hz, 1H), 7.29 (td, *J* = 7.5, 1.1 Hz, 1H), 1.43 (s, 12H) . **^{13}C NMR** (100 MHz, $CDCl_3$): *δ* 156.67, 143.33, 141.92, 137.25, 131.57 (2 Carbons as determined by HSQC), 127.93, 122.79, 121.32, 117.54, 80.33, 27.14 (*C–B* bond not observed). **^{11}B NMR** (128 MHz, $CDCl_3$): δ 13.3.

HRMS(EI) calculated for $C_{17}H_{20}BNO_2$: 281.1587. Found: 281.1599. **(EA)** Anal. Calcd for $C_{17}H_{20}BNO_2$: C, 72.62; H, 7.17; N, 4.98. Found: C, 72.12; H, 6.93; N, 5.27.

2–(4–Ethyl–2–boronic acid pinacolate ester)–phenylpyridine (**2–25**):[12]

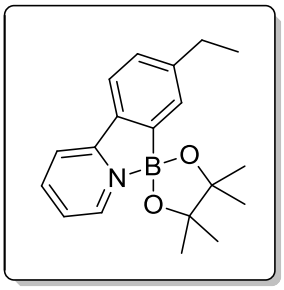

Synthesized according to the general procedure and eluted with 7:3 EtOAc/Hexanes mixture to afford an off–white powder (130 mg, 84% yield). **^{1}H NMR** (500 MHz, $CDCl_3$): δ 8.62 (d, *J* = 4.1 Hz, 1H), 7.90 (t, *J* = 7.0 Hz, 1H), 7.73 (d, *J* = 7.6 Hz, 1H), 7.56 (d, *J* = 7.5 Hz, 1H), 7.52 (s, 1H), 7.30–7.28 (m, 1H), 7.12 (d, *J* = 7.1 Hz, 1H), 2.68 (br q, *J* = 7.3 Hz, 2H), 1.43 (s, 12H), 1.25 (t, *J* = 7.0 Hz, 3H). **^{13}C NMR** (125 MHz, $CDCl_3$): *δ* 156.87, 147.97, 143.21, 141.77, 135.05, 131.27, 127.58, 122.24, 121.36, 117.25, 80.27, 29.45, 27.15, 15.64 (*C–B* bond not observed). **^{11}B NMR** (160 MHz, $CDCl_3$): *δ* 13.3. **HRMS (EI)** calculated for $C_{19}H_{24}BNO_2$: 309.1900. Found: 309.1904. **(EA)** Anal. Calcd for $C_{19}H_{24}BNO_2$: C, 73.80; H, 7.82; N, 4.53. Found: C, 73.34; H, 8.05; N, 4.24.

2–(2–Boronic acid pinacolate ester–5–methyl)phenylpyridine (**2–26**):[12]

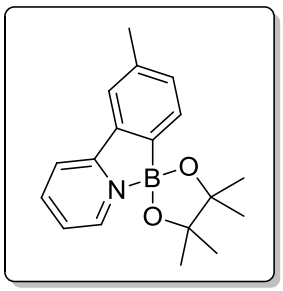

Synthesized according to the general procedure and eluted with 7:3 EtOAc/Hexanes mixture to afford an off–white powder (122 mg, 83% yield). **^{1}H NMR** (400 MHz, $CDCl_3$): δ 8.62 (d, *J* = 5.1 Hz, 1H), 7.89 (t, *J* = 7.6 Hz, 1H), 7.73 (d, *J* = 7.9 Hz, 1H), 7.59 (d, *J* = 7.3 Hz, 1H), 7.44 (s, 1H), 7.29 (t, *J* = 6.3 Hz, 1H), 7.21 (d, *J* = 7.2 Hz, 1H), 2.35 (s, 3H), 1.41 (s, 12H). **^{13}C NMR** (100 MHz, $CDCl_3$): *δ* 156.72, 143.24,

141.68, 137.55, 137.39, 132.43, 131.36, 122.55, 121.90, 117.37, 80.20, 26.98, 21.43 (*C–B* bond not observed). **^{11}B NMR** (128 MHz, $CDCl_3$): δ 13.7. **HRMS (EI)** calculated for $C_{18}H_{22}BNO_2$: 295.1744. Found: 295.1747. **(EA)** Anal. Calcd for $C_{18}H_{22}BNO_2$: C, 73.24; H, 7.51; N, 4.75. Found: C, 73.88; H, 7.98; N, 4.57.

2–(2–Boronic acid pinacolate ester–4,5–dimethyl)phenylpyridine (**2–29**):[12]

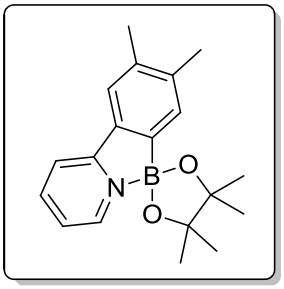

Synthesized according to the general procedure and eluted with 7:3 EtOAc/Hexanes mixture to afford an off–white powder (119 mg, 77% yield). **^{1}H NMR** (500 MHz, $CDCl_3$): δ 8.61 (d, *J* = 5.2 Hz, 1H), 7.88 (t, *J* = 7.6 Hz, 1H), 7.71 (d, *J* = 7.9 Hz, 1H), 7.46 (s, 1H), 7.41 (s, 1H), 7.27 (t, *J* = 6.4 Hz, 1H), 2.31 (s, 3H), 2.28 (s, 3H), 1.43 (s, 12H). **^{13}C NMR** (125 MHz, $CDCl_3$): δ 156.94, 143.20, 141.58, 140.37, 136.06, 135.42, 132.89, 122.48, 122.06, 117.10, 80.17, 27.04, 20.34, 20.06 (*C–B* bond not observed). **^{11}B NMR** (160 MHz, $CDCl_3$): δ 13.9. **HRMS (EI)** calculated for $C_{19}H_{24}BNO_2$: 309.1900. Found: 309.1913. **(EA)** Anal. Calcd for $C_{19}H_{24}BNO_2$: C, 73.80; H, 7.82; N, 4.53. Found: C, 74.19; H, 7.99; N, 4.57.

2–(3–Boronic acid pinacolate ester)naphthalene–2–yl–pyridine (**2–30**):[12]

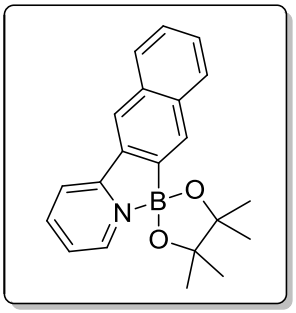

Synthesized according to the general procedure and eluted with 4:1 EtOAc/Hexanes mixture to afford a white powder (131 mg, 79% yield). **^{1}H NMR** (500 MHz, CD_2Cl_2): δ 8.72 (d, J = 5.2 Hz, 1H), 8.21 (s, 1H), 8.13 (s, 1H), 7.99–7.94 (m, 2H), 7.91 (t, J = 9.1 Hz, 2H), 7.53 (t, J = 7.1 Hz, 1H), 7.49 (t, J = 7.2 Hz, 1H), 7.38 (t, J = 5.4 Hz, 1H), 1.49 (s, 12H). **^{13}C NMR** (125 MHz, CD_2Cl_2): δ 156.06, 143.53, 141.98, 136.24, 136.07, 133.67, 130.99, 128.95, 128.71, 127.28, 126.17, 123.70, 121.59, 118.79, 80.65, 27.29 (*C–B* bond not observed). **^{11}B NMR** (160 MHz, CD_2Cl_2): δ 13.4. **HRMS (EI)** calculated for $C_{21}H_{22}BNO_2$: 331.1744. Found: 331.1747. **(EA)** Anal. Calcd for $C_{21}H_{22}BNO_2$: C, 76.15; H, 6.69; N, 4.23. Found: C, 76.53; H, 6.95; N, 4.21.

2–(2–Boronic acid pinacolate ester)naphthalene–1–yl–pyridine (**2–31**):[12]

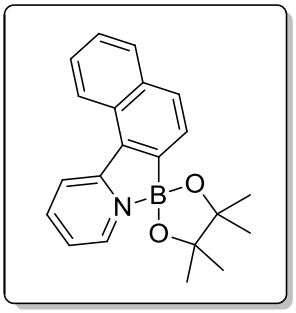

Synthesized according to the general procedure and eluted with 3:2 Hexanes/EtOAc mixture to afford a yellow powder (96 mg, 58% yield). **^{1}H NMR** (500 MHz, $CDCl_3$): δ 8.76 (d, J = 5.0 Hz, 1H), 8.33 (d, J = 8.5 Hz, 1H), 8.28 (d, J = 8.1 Hz, 1H), 7.99 (t, J = 7.7 Hz, 1H), 7.91–7.88 (m, 3H), 7.55 (t, J = 7.6 Hz, 1H), 7.47 (t, J = 7.5 Hz, 1H), 7.37 (t, J = 7.4, 1H), 1.43 (s, 12H). **^{13}C NMR** (125 MHz, $CDCl_3$): δ 157.66, 144.35, 141.56, 134.71, 133.73, 131.63, 129.78, 129.71, 128.52, 127.14, 125.27, 122.92, 121.90, 121.79, 80.77, 27.22 (*C–B* bond not observed). **^{11}B NMR** (160 MHz, $CDCl_3$): δ 14.3. **HRMS (EI)** calculated for $C_{21}H_{22}BNO_2$: 331.1744. Found: 331.1747.

(EA) Anal. Calcd for $C_{21}H_{22}BNO_2$: C, 76.15; H, 6.69; N, 4.23. Found: C, 76.33; H, 6.84; N, 4.44.

2–(1–Boronic acid pinacolate ester–4–methoxy)phenylpyridine (**2–36**):[12]

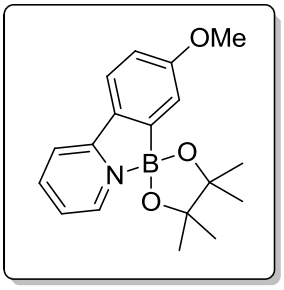

Synthesized according to the general procedure and eluted with 7:3 EtOAc/Hexanes mixture to afford an off–white powder (126 mg, 81% yield). **^{1}H NMR** (500 MHz, $CDCl_3$): δ 8.57 (d, J = 5.2 Hz, 1H), 7.87 (t, J = 7.7 Hz, 1H), 7.65 (d, J = 7.9 Hz, 1H), 7.56 (d, J = 8.3 Hz, 1H), 7.26–7.22 (m, 2H), 6.79 (d, J = 8.1 Hz, 1H), 3.86 (s, 3H), 1.41 (s, 12H). **^{13}C NMR** (125 MHz, $CDCl_3$): δ 162.79, 156.67, 142.97, 141.92, 130.04, 122.83, 121.46, 116.76, 116.37, 113.82, 80.21, 55.38, 27.17 (*C–B* bond not observed). **^{11}B NMR** (160 MHz, $CDCl_3$): δ 12.7. **HRMS (EI)** calculated for $C_{18}H_{22}BNO_3$: 311.1693. Found: 311.1696. **(EA)** Anal. Calcd for $C_{18}H_{22}BNO_3$: C, 69.47; H, 7.13; N, 4.50. Found: C, 69.02; H, 7.09; N, 4.50.

Synthesis of 2–(3–Boronic acid pinacolate ester–furan–2–yl)pyridine (**2–42**):[12]

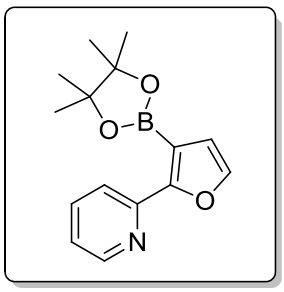

Synthesized according to the general procedure. ^{1}H NMR indicated near quantitative conversion of the starting material 2–(furan–yl)pridine to the product **2–42**, however the final product was not able to be isolated on the alumina column and complete decomposition was observed by ^{11}B and ^{1}H NMR upon attempted purification. Characterization of the crude reaction mixture: **^{1}H NMR** (400 MHz, C_6D_6): δ 8.45 (d, J = 4.5 Hz, 1H), 7.84 (d, J = 8.0 Hz, 1H), 7.16 (peak overlaps with C_6D_6 solvent,

presence confirmed by 2–D COSY NMR), 7.10 (t, J = 6.9 Hz, 1H), 6.70 (d, J = 1.6 Hz, 1H), 6.58–6.54 (m, 1H), 1.23 (s, 12H). **^{13}C NMR** (100 MHz, C_6D_6): δ 158.18, 149.71, 149.24, 142.94, 136.43, 122.31, 121.01, 116.37, 82.88, 24.95, 24.67 (*C–B* bond not observed). **^{11}B NMR** (128 MHz, C_6D_6): δ 30.7. **HRMS (EI)** calculated for $C_{15}H_{18}BNO_3$: 271.1380. Found: 271.1391.

4.5 Direct C–H Arylation & One–Pot Sequential C–H Borylation/Arylation

Attempted Direct Arylation of 2–Phenylpyridine with 4–Iodoacetophenone:

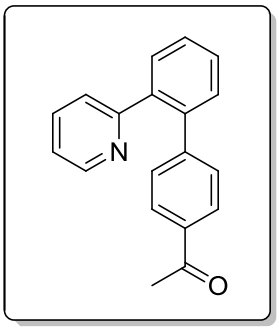

To an oven dried pressure tube equipped with a stir bar was added 2–phenylpyridine (39 mg, 0.25 mmol), 4–iodoacetophenone (68 mg, 0.27 mmol) and KO^{t}Bu (56 mg, 0.5 mmol). $[Rh(IPr)(C_2H_4)Cl]_2$ (14 mg, 0.0125 mmol, 5 mol%) was taken up in 2.5 mL of toluene and added to the pressure tube. The tube was capped, removed from the glovebox and stirred at 120 ^{o}C for 18 hours. After stirring, the mixture was cooled to room temperature and filtered through a pad of silica and washed with excess EtOAc and the filtrate concentrated. Analysis of the mixture by GC–MS indicated only 2–phenylpyridine present in the mixture, no 4–iodoacetophenone, acetophenone (dehalogenated starting material) or product were observed.

Direct Arylation of 2–Phenylpyridine with 4–Iodotoluene (**2–45**):

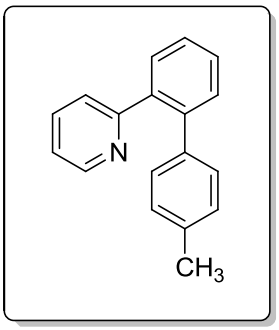

To an oven dried pressure tube equipped with a stir bar was added 2–phenylpyridine (39 mg, 0.25 mmol), 4–iodotoluene (59 mg, 0.27 mmol) and desired base (0.5 or 0.75 mmol). $[Rh(IPr)(C_2H_4)Cl]_2$ (14 mg, 0.0125 mmol, 5 mol) was taken up in 2.5 mL of toluene and added to the pressure tube. The tube was capped, removed from the glovebox and stirred at the indicated temperature (RT, 80 °C or 120 °C) for 18 hours. After stirring, the mixture was cooled to room temperature and filtered through a pad of silica and washed with excess EtOAc and the filtrate concentrated. Conversion to the product was determined by integration of the GC–MS peaks for the combined monoarylated product **2–45** and bisarylated product **2–46**. Ratio of products **2–45** : **2–46** was also determined by integration of the relative peaks by GC–MS. No internal standard was added to the reactions. Under optimal conditions (Table 2–3, Entry 6) exclusive selectivity for the monoarylated product was observed with 40% conversion from the 2–phenylpyridine. The product was not further characterized or isolated.

Suzuki–Miyaura Cross–Coupling with Isolated **2–24**:[12]

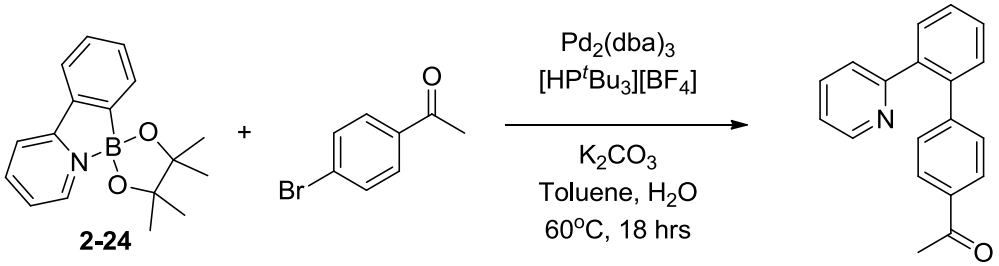

In an oven–dried 50 mL round bottom flask equipped with a stir bar, borylated 2–phenylpyridine (**2–24**) (110 mg, 0.39 mmol) 4–bromoacetophenone (92.7 mg, 0.47 mmol),

K_2CO_3 (161.5 mg, 1.17 mmol), [HP^{t}Bu$_3$][BF_4] (11.3 mg, 0.039 mmol) and $Pd_2(dba)_3$ (9 mg, 0.0098 mmol) were mixed in 4 mL of toluene. The flask was sealed with a rubber septum and removed from the glovebox. Degassed H_2O (21 μL, 1.17 mmol) was added via syringe. The reaction vessel was placed in an oil bath at 60 ^oC and allowed to stir for 18 hours. Afterwards, the mixture was allowed to cool to room temperature and the crude mixture filtered through Celites with EtOAc. The filtrate was concentrated and isolated by column chromatography (4:1 Hexanes/EtOAc) to afford an off–white solid (87 mg, 82% yield). **^{1}H NMR** (400 MHz, $CDCl_3$): δ 8.62 (d, J = 4.3 Hz, 1H), 7.85 (d, J = 8.0 Hz, 2H), 7.73–7.71 (m, 1H), 7.51 (dd, J = 8.7, 5.3 Hz, 2H), 7.47–7.42 (m, 2H), 7.27 (d, J = 8.0 Hz, 2H), 7.15–7.12 (m, 1H), 6.95 (d, J = 7.8 Hz, 1H), 2.59 (s, 3H). **^{13}C NMR** (100 MHz, $CDCl_3$): δ 197.91, 158.97, 149.65, 146.55, 139.73, 139.57, 135.62, 135.43, 130.74, 130.40, 129.97, 128.75, 128.42, 128.25, 125.29, 121.70, 26.70. **HRMS (EI)** calculated for $C_{19}H_{15}NO$: 273.1154. Found: 273.1165.

General Procedure for the One–Pot C–H Borylation/Arylation Reactions:[12]

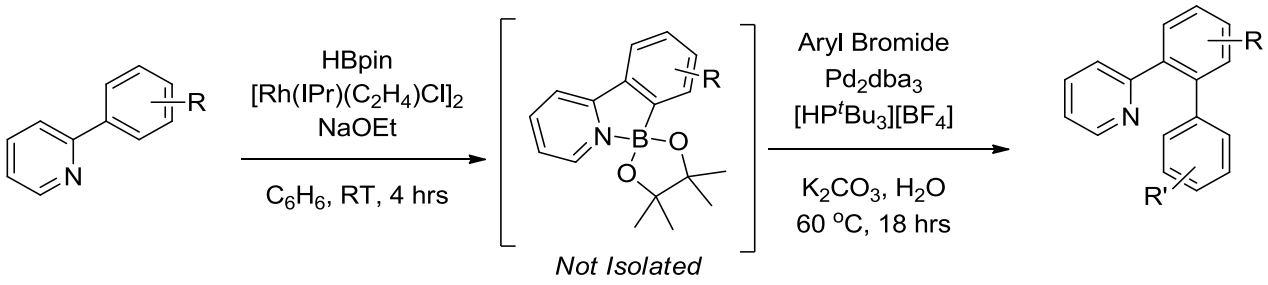

To an oven dried 50 mL round bottom flask equipped with a stir bar, NaOEt (8.5 mg, 0.125 mmol) was added. In separate vials, **2–20** (5.55 mg, 0.005 mmol, 1 mol%) and

phenyl pyridine (0.5 mmol) were each taken up in 2 mL of benzene each and sequentially added to the round bottom flask. HBpin (128 mg, 1 mmol) was taken up in 0.6 mL of benzene and added to the stirring solution (total reaction volume = 4.6 mL, 0.11 M concentration). The flask was sealed with a septum and vigorously stirred in the glovebox for 4 hours. After this time, aryl bromide (0.55 mmol), K_2CO_3 (207 mg, 1.5 mmol), $[HP^tBu_3][BF_4]$ (14.5 mg, 0.05 mmol, 10 mol%) and $Pd_2(dba)_3$ (11.5 mg, 0.0125 mmol, 2.5 mol%) were added to the reaction mixture. The flask was sealed with a rubber septum and removed from the glove box. Degassed H_2O (27 μL, 1.5 mmol) was added through the septum via syringe. The reaction flask was placed in an oil bath at 60 ^oC and the reaction mixture allowed to stir for 18 hours. Afterwards, the mixture was allowed to cool to room temperature and filtered through Celites in EtOAc. The filtrate was concentrated and the product isolated by column chromatography on silica gel.

Synthesis of 2–(2–(4–Acetylphenyl))phenylpyridine (**2–47**):[12]

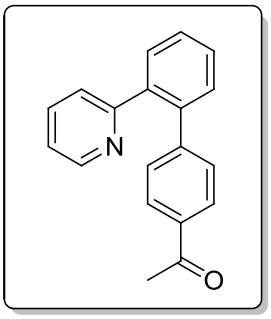

Synthesized according to the general C–H borylation/arylation procedure using 2–phenylpyridine (78 mg, 0.5 mmol, 1 eq) and 4–bromoacetophenone (109 mg, 0.55 mmol, 1.1 eq). Isolated eluting with a 4:1 Hexanes/EtOAc solvent mixture to afford an off–white solid (93 mg, 68% yield). Spectral data are consistent with that reported above.

Synthesis of 2–(2–(4–Acetylphenyl)–4–ethyl)phenylpyridine (**2–48**):[12]

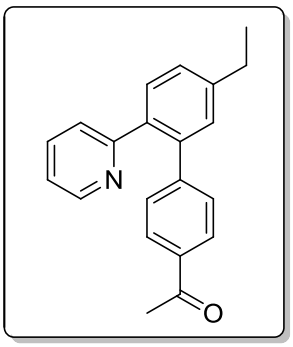

Synthesized according to the general C–H borylation/arylation procedure using 2–(4–ethylphenyl)pyridine (92 mg, 0.5 mmol) and 4–bromoacetophenone (109 mg, 0.55 mmol). The product was isolated by column chromatography eluting with a 98:2 CH_2Cl_2/MeOH solvent mixture to afford a yellow oil (100 mg, 66% yield). **^{1}H NMR** (400 MHz, $CDCl_3$): δ 8.61 (d, J = 4.7 Hz, 1H), 7.84 (d, J = 8.2 Hz, 2H), 7.64 (d, J = 7.9 Hz, 1H), 7.42 (td, J = 7.7, 1.5 Hz, 1H), 7.35 (d, J = 7.8 Hz, 1H), 7.28–7.26 (m, 3H), 7.12 (dd, J = 7.1, 5.1 Hz, 1H), 6.92 (d, J = 7.9 Hz, 1H), 2.77 (q, J = 7.6 Hz, 2H), 2.59 (s, 3H), 1.32 (t, J = 7.6 Hz, 3H), trace hexanes observed at 1.27 ppm. **^{13}C NMR** (100 MHz, $CDCl_3$): δ 198.01, 159.08, 149.63, 146.93, 145.05, 139.57, 137.25, 135.60, 135.45, 130.85, 130.04, 130.01, 128.27, 128.05, 125.33, 121.53, 28.78, 26.73, 15.65. **HRMS (EI)** calculated for $C_{21}H_{19}NO$: 301.1467. Found: 301.1455.

Synthesis of 2–(2–(4–Acetylphenyl)–5–methyl)phenylpyridine (**2–49**):[12]

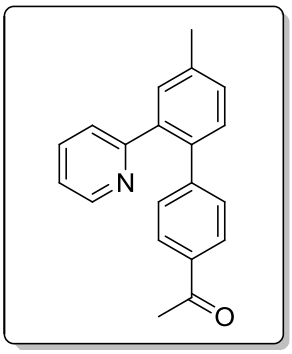

Synthesized according to the general C–H borylation/arylation procedure using 2–(3–methylphenyl)pyridine (85 mg, 0.5 mmol) and 4–bromoacetophenone (109 mg, 0.55 mmol). The product was isolated by column chromatography eluting with a 4:1 Hexanes/EtOAc solvent mixture to afford an off–white solid (62 mg, 44% yield). **^{1}H NMR** (400 MHz, $CDCl_3$): δ 8.62 (d, J = 4.2 Hz, 1H), 7.81 (d, J = 8.4 Hz, 2H), 7.52 (s, 1H), 7.40 (td, J = 7.7, 1.7 Hz, 1H), 7.34–7.29 (m, 2H), 7.23 (d, J = 8.4

Hz, 2H), 7.13–7.10 (m, 1H), 6.89 (d, *J* = 7.9 Hz, 1H), 2.57 (s, 3H), 2.46 (s, 3H). **^{13}C NMR** (100 MHz, $CDCl_3$): δ 197.95, 159.15, 149.68, 146.60, 139.56, 138.40, 136.80, 135.58, 135.34, 131.41, 130.42, 130.01, 129.54, 128.26, 125.41, 121.67, 26.70, 21.25. **HRMS (EI)** calculated for $C_{20}H_{17}NO$: 287.1310. Found: 287.1319.

Synthesis of 2–(2–(4–Acetylphenyl)–4,5–dimethyl)phenylpyridine (**2–50**):[12]

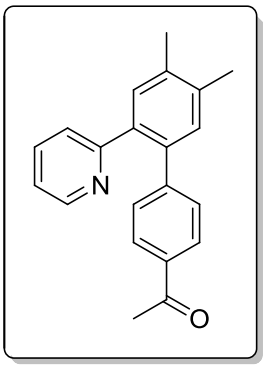

Synthesized according to the general C–H borylation/arylation procedure using 2–(3,4–dimethylphenyl)pyridine (92 mg, 0.5 mmol) and 4–bromoacetophenone (109 mg, 0.55 mmol). The product was isolated by column chromatography eluting with a 3:1 Hexanes/EtOAc solvent mixture to afford an off–white solid (82 mg, 54% yield). **^{1}H NMR** (400 MHz, $CDCl_3$): δ 8.61 (d, *J* = 4.5 Hz, 1H), 7.81 (d, *J* = 8.2 Hz, 2H), 7.49 (s, 1H), 7.37 (t, *J* = 8.4 Hz, 1H), 7.24 (s, 1H), 7.22 (d, *J* = 5.9 Hz, 2H), 7.10–7.07 (m, 1H), 6.86 (d, *J* = 7.9 Hz, 1H), 2.56 (s, 3H), 2.36 (s, 6H). **^{13}C NMR** (100 MHz, $CDCl_3$): δ 197.93, 159.04, 149.61, 146.69, 137.32, 137.18, 137.03, 137.01, 135.48, 135.27, 131.94, 131.69, 129.97, 128.22, 125.38, 121.44, 26.66, 19.62, 19.51. **HRMS (EI)** calculated for $C_{21}H_{19}NO$: 301.1467. Found: 301.1459.

Synthesis of 2–(3–(4–Acetylphenyl)naphthalen–2–yl)pyridine (**2–51**):[12]

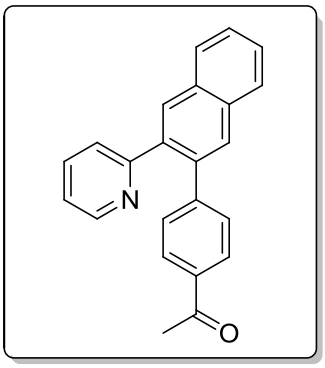

Synthesized according to the general C–H borylation/arylation procedure using 2–(2–naphthyl)pyridine (2 mg, 0.5 mmol) and 4–bromoacetophenone (109 mg, 0.55 mmol). The product was isolated by column chromatography eluting with a 3:1 Hexanes/EtOAc solvent mixture to afford a yellow solid (95 mg, 59% yield). **^{1}H NMR** (400 MHz, $CDCl_3$): δ 8.63 (d, J = 4.3 Hz, 1H), 8.19 (s, 1H), 7.95–7.89 (m, 3H), 7.86 (d, J = 8.1 Hz, 2H), 7.55–7.53 (m, 2H), 7.45 (t, J = 7.6 Hz, 1H), 7.34 (d, J = 8.1 Hz, 2H), 7.16–7.13 (m, 1H), 7.02 (d, J = 7.8 Hz, 1H), 2.59, (s, 3H). **^{13}C NMR** (100 MHz, $CDCl_3$): δ 197.95, 158.94, 149.68, 146.61, 137.72, 137.58, 135.68, 135.47, 133.21, 133.03, 130.46, 130.08, 129.86, 128.36, 128.28, 127.97, 127.13, 126.93, 125.42, 121.76, 26.72. **HRMS (EI)** calculated for $C_{23}H_{17}NO$: 323.1310. Found: 323.1322.

Synthesis of 2–(2–(4–Acetylphenyl)phenyl)quinolone (**2–52**):[12]

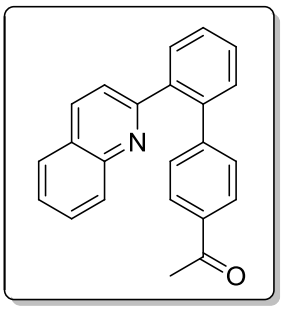

Synthesized according to the general C–H borylation/arylation procedure using 2–phenylquinoline (103 mg, 0.5 mmol) and 4–bromoacetophenone (109 mg, 0.55 mmol). The product was isolated by column chromatography eluting with a 4:1 Hexanes/EtOAc solvent mixture to afford a yellow solid (81 mg, 50% yield). **^{1}H NMR** (400 MHz, $CDCl_3$): δ 8.14 (d, J = 8.4 Hz, 1H), 7.87–7.83 (m, 2H), 7.80 (d, J = 8.4 Hz, 2H), 7.76–7.71 (m, 2H), 7.57–7.52 (m, 3H), 7.51–7.48 (m, 1H), 7.30

(d, J = 8.4 Hz, 2H), 6.96 (d, J = 8.5 Hz, 1H), 2.54 (s, 3H). **^{13}C NMR** (100 MHz, $CDCl_3$): δ 197.92, 159.49, 148.35, 146.37, 140.08, 139.76, 135.62, 135.33, 131.15, 130.46, 130.13, 129.71 (2 carbons as determined by HSQC), 129.13, 128.69, 128.36, 127.64, 126.75, 126.67, 123.42, 26.70. **HRMS (EI)** calculated for $C_{23}H_{17}NO$: 323.1310. Found: 323.1299.

Synthesis of 2–(2–(4–methoxy)phenyl)phenylpyridine (**2–53**):[12]

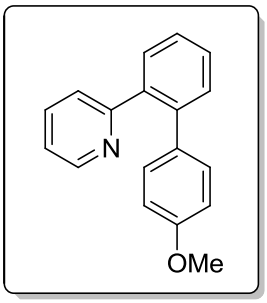

Synthesized according to the general C–H borylation/arylation procedure using 2–phenylpyridine (78 mg, 0.5 mmol) and 4–bromoanisole (103 mg, 0.55 mmol). The product was isolated by column chromatography eluting with a 8:2 Hexanes/EtOAc solvent mixture to afford an off–white solid (41 mg, 31% yield). **^{1}H NMR** (400 MHz, $CDCl_3$): δ 8.70 (d, J = 5.1 Hz, 1H), 8.04 (d, J = 7.1 Hz, 2H), 7.90 (d, broad, J = 0.9 Hz, 1H), 7.66 (d, J = 8.8 Hz, 2H), 7.50 (t, J = 7.3 Hz, 2H), 7.45–7.41 (m, 2H), 7.04 (d, J = 8.8 Hz, 2H), 3.88 (s, 3H). **^{13}C NMR** (100 MHz, $CDCl_3$): δ 160.70, 158.22, 150.20, 148.91, 139.83, 130.95, 129.09, 128.89 (2 Carbons as determined by HSQC), 128.39 (2 Carbons as determined by HSQC), 127.19, 119.86, 118.35, 114.72, 55.57. **HRMS (EI)** calculated for $C_{18}H_{15}NO$: 261.1154. Found: 261.1163.

Synthesis of 2–(2–acetanilide)phenylpyridine (**2–54**):[12]

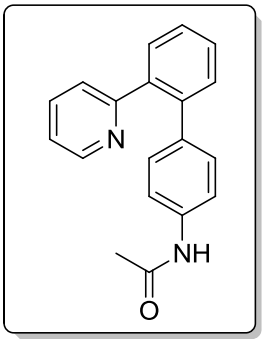

Synthesized according to the general C–H borylation/arylation procedure using 2–phenylpyridine (78 mg, 0.5 mmol, 1 eq) and 4–bromoacetanilide (118 mg, 0.55 mmol, 1.1 eq). The product was isolated by column chromatography eluting with a 3:1 EtOAc/Hexanes solvent mixture to afford an off–white solid (66 mg, 46% yield). **^{1}H NMR** (400 MHz, $CDCl_3$): δ 8.72 (d, J = 5.1 Hz, 1H), 8.04 (d, J = 7.3 Hz, 2H), 7.90 (s, 1H), 7.67 (s, 4H), 7.50 (t, J = 7.3 Hz, 2H), 7.45–7.41 (m, 3H), 2.21 (s, 3H). **^{13}C NMR** (100 MHz, $CDCl_3$): δ 168.49, 158.34, 150.27, 148.62, 139.68, 139.00, 134.32, 129.19, 128.93, 127.87, 127.20, 120.52, 120.33, 119.98, 118.49, 24.83. **HRMS (EI)** calculated for $C_{19}H_{16}N_2O$: 288.1263.

Attempted One–Pot C–H Borylation/Arylation of Pyrazole Derivative:

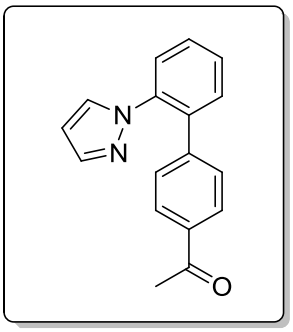

To an oven dried 50 mL Schlenk flask equipped with a stir bar, NaOEt (8.5 mg, 0.125 mmol) was added. In separate vials, **2–20** (5.55 mg, 0.005 mmol, 1 mol%) and 1–phenyl–1H–pyrazole (72 mg, 0.5 mmol) were each taken up in 2 mL of benzene each and sequentially added to the round bottom flask. HBpin (128 mg, 1 mmol) was taken up in 0.6 mL of benzene and added to the stirring solution (total reaction volume = 4.6 mL, 0.11 M concentration). The flask was sealed with a teflon stopper, removed from the glovebox and stirred at 60 ^{o}C for 48 hours. After this time, the flask was reintroduced into the glovebox and the crude mixture transferred to 50 mL round bottom flask and the solvent evaporated under reduced pressure. To the crude mixture, 4–

bromoacetophenone (109 mg, 0.55 mmol), K_2CO_3 (207 mg, 1.5 mmol), $[HP^tBu_3][BF_4]$ (14.5 mg, 0.05 mmol, 10 mol%) and $Pd_2(dba)_3$ (11.5 mg, 0.0125 mmol, 2.5 mol%) were added and taken up in toluene (4.6 mL). The flask was sealed with a rubber septum and removed from the glove box. Degassed H_2O (27 μL, 1.5 mmol) was added through the septum *via* syringe. The reaction flask was placed in an oil bath at 110 ^oC and allowed to stir for 18 hours. Analysis of the crude mixture by ^1H NMR showed no formation to the desired arylated product.

Attempted One–Pot C–H Borylation/Arylation of 2–(Furan–2–yl)pyridine:

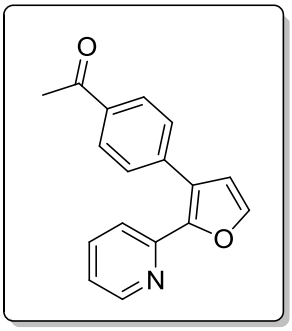

To an oven dried 50 mL round bottom flask equipped with a stir bar, NaOEt (8.5 mg, 0.125 mmol) was added. In separate vials, **2–20** (5.55 mg, 0.005 mmol, 1 mol%) and 2–(furan–2–yl)pyridine (73 mg, 0.5 mmol) were each taken up in 2 mL of benzene each and sequentially added to the round bottom flask. HBpin (128 mg, 1 mmol, 2 eq) was taken up in 0.6 mL of benzene and added to the stirring solution (total reaction volume = 4.6 mL, 0.11 M concentration). The flask was sealed with a Teflon® stopper, removed from the glovebox and stirred at 60 ^oC for 48 hours. After this time, the flask was reintroduced into the glovebox and the crude mixture transferred to 50 mL round bottom flask and the solvent evaporated under reduced pressure. To the crude mixture, 4–bromoacetophenone (109 mg, 0.55 mmol), K_2CO_3 (207 mg, 1.5 mmol), $[HP^tBu_3][BF_4]$ (14.5 mg, 0.05 mmol, 10 mol%) and $Pd_2(dba)_3$ (11.5 mg, 0.0125 mmol, 2.5 mol%) were added and taken up in toluene (4.6 mL). The flask was sealed with a rubber septum and removed from the glove box. Degassed H_2O (27 μL, 1.5

mmol) was added through the septum *via* syringe. The reaction flask was placed in an oil bath at 110 ^{o}C and allowed to stir for 18 hours. Analysis of the crude mixture by ^{1}H NMR showed only trace amounts of the desired arylated product.

4.6 One–Pot Sequential Reactions of 2–Phenylpyrdine

Synthesis of 2–(2–Hydroxy)–phenylpyridine (**2–55**):

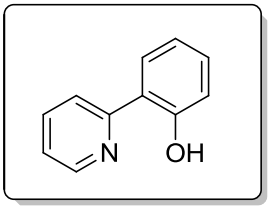

Prepared by a modified procedure by Yu and coworkers.[13] To an oven dried 50 mL round bottom flask equipped with a stir bar, NaO^{i}Pr (10.3 mg, 0.125 mmol) was added. In separate vials, **2–20** (5.55 mg, 0.005 mmol, 1 mol%) and 2–phenylpyridine (77.5 mg, 0.5 mmol) were each taken up in 2 mL of benzene each and sequentially added to the round bottom flask. HBpin (128 mg, 1 mmol, 2 eq) was taken up in 0.6 mL of benzene and added to the stirring solution (total reaction volume = 4.6 mL, 0.11 M concentration). The flask was sealed with a septum and vigorously stirred in the glovebox for 2 hours. The mixture was removed from the glovebox and the solvent evaporated under reduced pressure. To the crude mixture, Oxone® (462 mg, 1.5 mmol) was added and the mixture diluted with acetone (3 mL) and H_2O (3 mL). The solution was allowed to stir for 4 hours at which point the solution was quenched with $NaHSO_3$ (6 mL). The aqueous layer was extracted with ether (3x5 mL) and the organic layers combined, dried over sodium sulphate and filtered. The filtrate was concentrated and isolated by column chromatography on silica gel (4:1 hexanes/ether) to afford a yellow oil (31 mg, 35% yield). ^{1}H NMR data is consistent with that previously reported.[14] **^{1}H NMR** (300 MHz, $CDCl_3$): δ 14.36 (s, 1H),

8.53 (d, *J* = 4.7 Hz, 1H), 7.94 (d, *J* = 8.2 Hz, 1H), 7.88–7.81 (m, 2H), 7.35–7.24 (m, 2H), 7.05 (d, *J* = 8.3 Hz, 1H), 6.92 (dd, *J* =11.0, 4.1 Hz, 1H). **HRMS (EI)** calculated for $C_{11}H_9NO$: 171.0684. Found: 171.0692.

Synthesis of 2–(2–Potassium Trifluoroboro)–phenylpyridine (**2–56**):

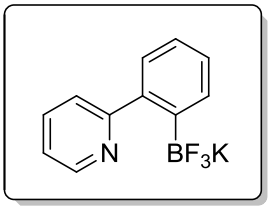

Prepared according to a modified procedure by Lloyd–Jones and coworkers.[15] To an oven dried 50 mL round bottom flask equipped with a stir bar, NaO^{i}Pr (10.3 mg, 0.125 mmol) was added. In separate vials, **2–20** (5.55 mg, 0.005 mmol, 1 mol%) and 2–phenylpyridine (77.5 mg, 0.5 mmol) were each taken up in 2 mL of benzene each and sequentially added to the round bottom flask. HBpin (128 mg, 1 mmol, 2 eq) was taken up in 0.6 mL of benzene and added to the stirring solution (total reaction volume = 4.6 mL, 0.11 M concentration). The flask was sealed with a septum and vigorously stirred in the glovebox for 4 hours. After this time, the flask was removed from the glovebox and the solvent removed *in vacuo*. The crude mixture was dissolved in 4 mL of MeOH and 4 mL of MeCN. To the stirring solution, a 10 mol/L aqueous KF solution (1.02 mL, 10.2 mmol) was added dropwise and the solution stirred for 30 minutes. L–(+)–Tartaric acid (770 mg, 5.13 mmol) was taken up in 3.75 mL of THF in a 4 dram scintillation vial and heated to dissolve the tartaric acid, then added dropwise to the stirring mixture over the course of 5 minutes and stirred an addition 10 minutes. The crude mixture was then filtered through a fritted funnel and washed with 3x10 mL of MeCN. The filtrate was concentrated and isolated by column chromatography on silica gel (2:1 EtOAc/Hexanes) to afford a white

solid (62 mg, 46% yield). **^{1}H NMR** (400 MHz, $CDCl_3$): δ 8.57 (d, J = 5.5 Hz, 1H), 8.15 (td, J = 7.9, 1.5 Hz, 1H), 7.93 (d, J = 8.1 Hz, 1H), 7.77 (t, J = 8.4 Hz, 2H), 7.57–7.47 (m, 2H), 7.43 (t, J = 7.5 Hz, 1H). **^{13}C NMR** (100 MHz, $CDCl_3$): δ 156.2, 143.7, 141.7, 136.7, 132.3, 130.5, 128.9, 123.4, 121.8, 118.1 (*C–B* bond not observed). **^{11}B NMR** (128 MHz, $CDCl_3$): δ 7.5. **^{19}F NMR** (375 MHz, $CDCl_3$): δ –162.9. **HRMS (EI)** calculated for $C_{11}H_8NBF_3^-$ negative polarity: 222.0702. Found: 222.0711.

4.7 Suzuki–Miyaura/Mizoroki–Heck Chemoselectivity Studies

Synthesis of Racemic 1–(1–Phenylethyl)boronic acid pinacolate ester (**3–2**):[16]

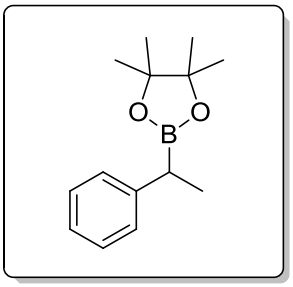

To an oven dried 4 dram scintillation vial equipped with a stir bar, styrene (527 mg, 5.1 mmol) and [Rh(COD)dppb][BF_4] were added and taken up in 3 mL of THF. In a separate vial, HBpin (789 mg, 6.2 mmol) was taken up in 1 mL of THF and added dropwise to the stirring catalyst/styrene solution. The vial was sealed and stirred in the glovebox for 3 days. The crude reaction mixture was removed from the glovebox and filtered through Celite with ether. The product was isolated by column chromatography using silica gel stationary phase and eluted with 95:5 hexanes/EtOAc to afford 843 mg of a clear oil (72% yield). ^{1}H NMR indicated a branched to linear ratio of 98:2. ^{1}H NMR and ^{11}B NMR data is consistent with that previously reported.[16] **^{1}H NMR** (300 MHz, $CDCl_3$): δ 7.31–7.19 (m, 4H), 7.13 (t, J = 6.7 Hz, 1H),

2.44 (q, J = 7.3 Hz, 1H), 1.33 (d, J = 7.5 Hz, 1H). 1.21 (s, 6H), 1.20 (s, 6H). **^{11}B NMR** (128 MHz, $CDCl_3$): δ 33.4.

Intermolecular Chemoselective Suzuki–Miyaura Competition Study:

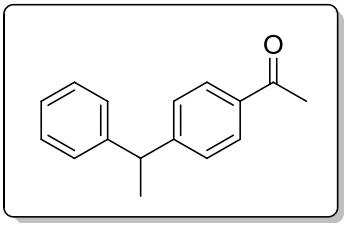

Sample procedure. To an oven dried 2 dram scintillation vial equipped with a stir bar and Teflon® cap were added 4–iodoacetophenone (24 mg, 0.01 mmol), 1–(1–phenylethyl)boronic acid pinacolate ester (34 mg, 0.15 mmol), methyl acrylate (45 mg, 0.53 mmol), Ag_2O (35 mg, 0.15 mmol), K_2CO_3 (21 mg, 0.15 mmol), PPh_3 (8.4 mg 0.032 mmol, 32 mol%) and $Pd(PPh_3)_4$ (9.2 mg, 0.008 mmol, 8 mol%). The crude mixture was taken up in 1.2 mL of DME, capped and removed from the glovebox. Degassed H_2O (7 μL of 4:1 DME/H_2O solution) was added through the septum *via* glass μL syringe. The solution was stirred at 85 ^{o}C for 18 hours. The mixture was filtered through a pipette of Celite and washed with copious amounts of ether. GC–MS and ^{1}H NMR analysis indicated no Mizoroki–Heck coupled product. ^{1}H NMR data are consistent with those which we have previously reported.[17] **^{1}H NMR** (300 MHz, $CDCl_3$): δ 7.88 (d, J = 8.2 Hz, 2H), 7.33–7.27 (m, 4H), 7.22–7.20 (m, 3H), 4.21 (q, J = 7.3 Hz, 1H), 2.57 (s, 3H), 1.66 (d, J = 7.2 Hz, 3H).

Controlled Mizoroki–Heck for Synthesis of (E)–Methyl–3–(4–acety1phenyl)acrylate (**3–7**):[17]

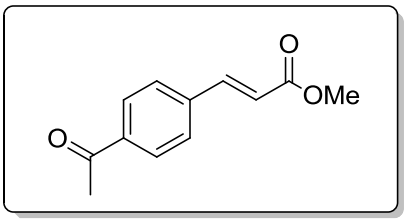

To an oven dried 100 mL Schlenk flask equipped with a stir bar and a Teflon® lined tap were added 4–iodoacetophenone (52 mg, 0.21 mmol), methyl acrylate (28 mg, 0.32 mmol), K_2CO_3 (44 mg, 0.32 mmol) and $Pd(PPh_3)_4$ (19 mg, 0.016 mmol, 8 mol%). The crude mixture was taken up in 3 mL of dimethylformamide (DMF), removed from the glove box and the mixture stirred at 120 ^oC for 18 hours. The flask was cooled to 60 ^oC and the solvent evaporated *in vacuo*. The crude mixture was filtered through Celite and washed with a copious amount of ether and the filtrate concentrated. No Suzuki–Miyaura cross–coupling product was not observed by GC–MS and ^1H NMR analysis. The product was isolated by column chromatography on silica gel with an eluent mixture of 10:1 hexanes/EtOAc to afford 29 mg of a white powder (67% yield). ^1H NMR data were consistent with those previously reported literature.[18] **^1H NMR** (400 MHz, $CDCl_3$): δ 7.96 (d, *J* = 8.3 Hz, 2H), 7.70 (d, *J* = 16.1 Hz, 1H), 7.60 (d, *J* = 8.3 Hz, 2H), 6.52 (d, *J* = 16.0 Hz, 1H), 3.82 (s, 3H), 2.61 (s, 3H).

Chemoselective Mizoroki–Heck Synthesis of (E)–Methyl–3–(4–acety1phenyl)acrylate (**3–7**):[17]

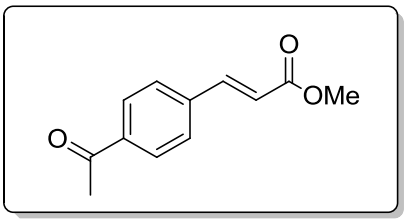

To an oven dried 100 mL Schlenk flask equipped with a stir bar and a Teflon® lined tap were added 1–(1–phenylethyl)boronic acid pinacolate ester (176 mg, 0.75 mmol), methyl acrylate (87 mg, 1.01 mmol), 4–

iodoacetophenone (124 mg, 0.5 mmol), K_2CO_3 (104 mg, 0.75 mmol) and $Pd(PPh_3)_4$ (47 mg, 0.041 mmol, 8 mol%). The crude mixture was taken up in 7.5 mL of dimethylformamide (DMF), removed from the glove box and the mixture stirred at 120 ^oC for 15 hours. The flask was cooled to 60 ^oC and the solvent evaporated *in vacuo*. The crude mixture was filtered through Celite and washed with a copious amount of ether and the filtrate concentrated. No Suzuki–Miyaura cross–coupling product was not observed by GC–MS and ^1H NMR analysis. The product was isolated by column chromatography on silica gel with an eluent mixture of 10:1 hexanes/EtOAc to afford 50 mg of a white powder (49% yield). ^1H NMR data were consistent with those previously reported literature.[18] **^1H NMR** (400 MHz, $CDCl_3$): δ 7.96 (d, *J* = 8.3 Hz, 2H), 7.70 (d, *J* = 16.1 Hz, 1H), 7.60 (d, *J* = 8.3 Hz, 2H), 6.52 (d, *J* = 16.0 Hz, 1H), 3.82 (s, 3H), 2.61 (s, 3H).

Synthesis of $[Rh(COD)Cl]_2$

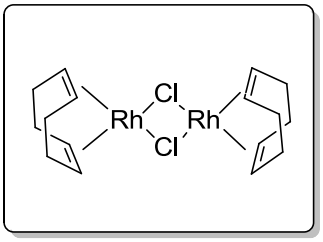

Prepared according to a literature procedure.[19] To a 100 mL two–neck round bottom flask equipped with a stir bar and a reflux condenser was added $RhCl_3 \cdot 3H_2O$ (500 mg, 1.9 mmol), 1,5–cyclooctadiene (0.8 mL, 6.5 mmol) and Na_2CO_3 (205 mg, 1.9 mmol). The mixture was taken up in 5 mL of a degassed 5:1 ethanol/water mixture. The flask was sealed and stirred under reflux for 18 hours. The mixture was then cooled to room temperature and filtered through a Hirsch funnel and washed with a minimal amount of pentane and ice cold 1:5 methanol/water mixture (5 mL). The powder was dried under reduced pressure to yield 330 mg (71% yield) of a greenish/yellow powder. ^1H NMR

data is consistent with that previously reported.[20] **^{1}H NMR** (300 MHz, $CDCl_3$): δ 4.23 (s, 8H), 2.57–2.40 (m, 8H), 1.75 (d, *J* = 8.2 Hz, 8H).

Synthesis of [Rh(COD)OAc]$_2$

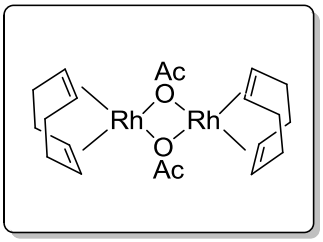

Prepared according to a procedure reported by Chatt and Venanzi.[21] A 50 mL oven dried Schlenk flask equipped with a stir bar was charged with $[Rh(COD)Cl]_2$ (150 mg, 0.3 mmol) and KOAc (150 mg, 1.53 mmol) and taken up in 10 mL of acetone. The flask was sealed and stirred at reflux for 2.5 hours. The crude mixture was filtered through a pipette of Celite and filtrate concentrated under reduced pressure to yield 150 mg (90% yield) of a bright orange powder. ^{1}H NMR consistent with previously reported data.[20] **^{1}H NMR** (400 MHz, $CDCl_3$): δ 4.03 (s, 8H), 2.61 (br s, 8H), 1.72–1.68 (m, 8H), 1.66 (s, 6H).

Hydroboration of 4–Bromostyrene (**3–8**):

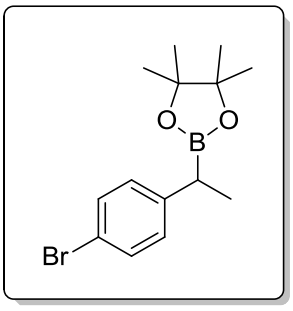

Prepared according to a modified procedure by Shibata and coworkers.[22] To an oven dried 4 dram scintillation vial equipped with a stir bar, $[Rh(COD)OAc]_2$ (34 mg, 0.063 mmol, 2.5 mol%) and freshly recrystallized DPPB (64 mg, 0.15 mmol, 6 mol%) were taken up in 2.5 mL of DCM and allowed to stir in the glovebox for 1 hour. After which, the solvent was removed *in vacuo* and dried thoroughly. To the dried crude mixture was added 4–bromostyrene (458 mg, 2.5 mmol) and HBpin (384 mg, 3 mmol) and the crude mixture taken up in the 2.5 mL of DCE and the mixture

was stirred for 30 minutes. The product formation was monitored by ^{1}H NMR. The mixture was removed from the glovebox and filtered through a pipette of silica gel and washed with 50 mL of diethyl ether. The product was isolated by column chromatography using silica gel stationary phase and eluted with 95:5 hexanes/EtOAc to afford 529 mg of a clear oil (68% yield). ^{1}H NMR analysis confirmed a 93:7 branched to linear ratio of regioisomers and the product was used as is for further reactions. ^{1}H NMR data is consistent with that previously reported.[16] **^{1}H NMR** (300 MHz, $CDCl_3$): δ 7.37 (d, *J* = 8.4 Hz, 2H), 7.09 (d, *J* = 8.3 Hz, 2H), 2.39 (q, *J* = 7.2 Hz, 1H), 1.30 (d, *J* = 7.5 Hz, 3H), 1.20 (s, 6H), 1.19 (s, 6H).

Synthesis of 4–(Ethyl–1–boronic acid pinacolato ester)styrene (**3–10**):

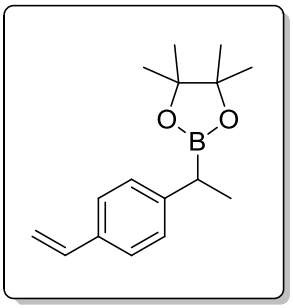

The Mizoroki – Heck reaction was carried out using the arylbromide **3–8** which contained a 93:7 branched to linear ratio of regioisomers. To an oven dried autoclave equipped with a stir bar were added **3–8** (311 mg, 1 mmol), *N*,*N*–dicyclohexylmethylamine (0.32 mL, 1.5 mmol), $[HP^tBu_3][BF_4]$ (8.7 mg, 0.03 mmol, 3 mol%) and Pd_2dba_3 (9.16 mg, 0.01 mmol, 1 mol%). The crude mixture was taken up in 5 mL of acetonitrile and the vessel sealed. The autoclave was hooked up to a cylinder of ethylene gas ($H_2C{=}CH_2$) and the system purged 5 times. The autoclave was then pressurized with 8 atm of ethylene, sealed, and the reaction allowed to stir at room temperature for 24 hours. The autoclave was then vented and the crude mixture passed through a pad of silica and washed with EtOAc and the filtrate concentrated. GC–MS analysis of the crude mixture indicated the desired product had formed. The product was isolated by column chromatography on silica gel with an eluent mixture of 9:1

hexanes/EtOAc to afford 195 mg of a clear oil (66% yield). **^{1}H NMR** (400 MHz, $CDCl_3$): δ 7.32 (d, J = 8.2 Hz, 2H), 7.19 (d, J = 8.2 Hz, 2H), 6.69 (dd, J = 17.6, 10.9 Hz, 1H), 5.69 (dd, J = 17.6, 0.9 Hz, 1H), 5.17 (dd, J = 10.9, 0.9 Hz, 1H), 2.44 (q, J = 7.5 Hz, 1H), 1.34 (d, J = 7.6 Hz, 2H), 1.22 (s, 6H), 1.21 (s, 6H). **^{11}B NMR** (128 MHz, $CDCl_3$): δ 33.1. **^{13}C NMR** (100 MHz, $CDCl_3$): δ 137.0, 131.4, 129.7, 128.0, 126.3, 112.6, 83.5, 31.7, 24.73 24.70, 17.0.

Synthesis of 1–(4–Styrenyl)–1–(acetylphenyl)ethane (**3–11**):

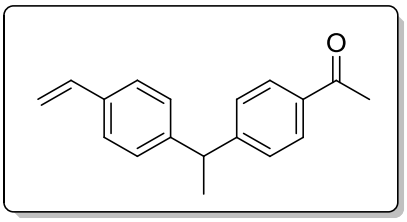

To an oven dried 50 mL round bottom flask equipped with a stir bar were added 4–iodoacetophenone (47 mg, 0.19 mmol), 4–(ethyl–1–boronic acid pinacolato ester)styrene (78 mg, 0.30 mmol), Ag_2O (72 mg, 0.31 mmol), K_2CO_3 (42 mg, 0.30 mmol), PPh_3 (16 mg, 0.063 mmol, 32 mol%) and $Pd(PPh_3)_4$ (19 mg, 0.016 mmol, 8 mol%). The crude mixture was taken up in 4.1 mL of DME, sealed with a rubber septa and removed from the glovebox. Degassed H_2O (7 μL of a 5:1 DME/H_2O solution) was added through the rubber septa via glass μL syringe. The reaction mixture was stirred at 85 °C for 24 hours, then cooled to room temperature and filtered through Celites with copious amounts of ether. The filtrate was concentrated and the product was isolated by column chromatography on silica gel with an eluent mixture of 9:1 hexanes/EtOAc to afford 25 mg of a clear oil (55% yield). ^{1}H NMR was consistent with that which we have previously reported.[17] **^{1}H NMR** (400 MHz, $CDCl_3$): δ 7.88 (d, *J* = 8.4 Hz, 2H), 7.34 (d, *J* = 8.2 Hz, 2H), 7.31 (d, *J* = 8.2 Hz, 2H), 7.16 (d, *J* = 8.2 Hz, 2H), 6.68

(dd, *J* = 17.6, 10.9 Hz, 1H), 5.70 (dd, *J* = 17.6, 0.7 Hz, 1H), 5.21 (dd, *J* = 10.9, 0.6 Hz, 1H), 4.12 (q, *J* = 7.2 Hz, 1H), 2.57 (s, 3H), 1.65 (d, *J* = 7.2 Hz, 3H).

4.8 References

1. Bantreil, X.; Nolan, S. P. *Nat. Protocols* **2011**, *6*, 69-77.
2. Cramer, R. *Inorg. Synth.* **1974**, *15*, 14-16.
3. Zenkina, O. V.; Keske, E. C.; Wang, R.; Crudden, C. M. *Organometallics* **2011**, *30*, 6423-6432.
4. Liu, C.; Han, N.; Song, X.; Qiu, J. *Eur. J. Org. Chem.* **2010**, *2010*, 5548-5551.
5. Dick, G. R.; Woerly, E. M.; Burke, M. D. *Angew. Chem. Int. Ed.* **2012**, *51*, 2667-2672.
6. Yang, J.; Liu, S.; Zheng, J. F.; Zhou, J. *Eur. J. Org. Chem.* **2012**, *2012*, 6248-6259.
7. Deng, J. Z.; Paone, D. V.; Ginnetti, A. T.; Kurihara, H.; Dreher, S. D.; Weissman, S. A.; Stauffer, S. R.; Burgey, C. S. *Org. Lett.* **2008**, *11*, 345-347.
8. Ge, S.; Hartwig, J. F. *Angew. Chem. Int. Ed.* **2012**, *51*, 12837-12841.
9. Luzung, M. R.; Patel, J. S.; Yin, J. *J. Org. Chem.* **2010**, *75*, 8330-8332.
10. Wang, W.; Luo, F.; Zhang, S.; Cheng, J. *J. Org. Chem.* **2010**, *75*, 2415-2418.
11. Yoshikai, N.; Asako, S.; Yamakawa, T.; Ilies, L.; Nakamura, E. *Chem. Asian J.* **2011**, *6*, 3059-3065.
12. Keske, E. C.; Moore, B. D.; Zenkina, O. V.; Wang, R.; Schatte, G.; Crudden, C. M. *Chem. Commun.* **2014**, *50*, 9883-9886.
13. Dai, H. X.; Yu, J. Q. *J. Am. Chem. Soc.* **2012**, *134*, 134-137.
14. Chen, X.; Hao, X. S.; Goodhue, C. E.; Yu, J. Q. *J. Am. Chem. Soc.* **2006**, *128*, 6790-6791.
15. Lennox, A. J. J.; Lloyd-Jones, G. C. *Angew. Chem. Int. Ed.* **2012**, *51*, 9385-9388.
16. Crudden, C. M.; Hleba, Y. B.; Chen, A. C. *J. Am. Chem. Soc.* **2004**, *126*, 9200-9201.
17. Glasspoole, B. W.; Oderinde, M. S.; Moore, B. D.; Antoft-Finch, A.; Crudden, C. M. *Synthesis* **2013**, *45*, 1759-1763.
18. He, Z.; Kirchberg, S.; Fröhlich, R.; Studer, A. *Angew. Chem. Int. Ed.* **2012**, *51*, 3699-3702.
19. Giordano, G.; Crabtree, R. H.; Heintz, R. M.; Forster, D.; Morris, D. E. *Inorg. Synth.* **1979**, *19*, 218-220.
20. van der Zeijden, A. A. H.; van Koten, G.; Nordemann, R. A.; Kojic-Prodic, B.; Spek, A. L. *Organometallics* **1988**, *7*, 1957-1966.
21. Chatt, J.; Venanzi, L. M. *J. Chem. Soc.* **1957**, 4735-4741.
22. Endo, K.; Hirokami, M.; Shibata, T. *Organometallics* **2008**, *27*, 5390-5393.

Appendix

Spectroscopic Data for C–H Borylation &

Sequential Arylation Products

400 MHz, ^{1}H NMR, $CDCl_3$

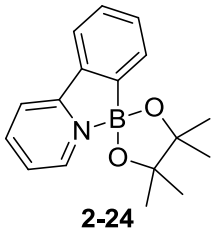

2-24

100 MHz, ^{13}C NMR, $CDCl_3$

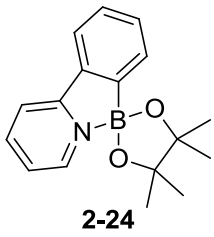

2-24

125 MHz, ^{11}B NMR, $CDCl_3$

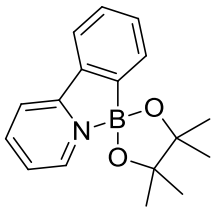

2-24

500 MHz, ^{1}H NMR, $CDCl_3$

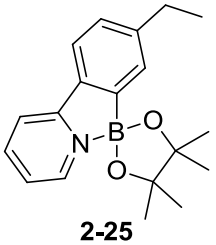

2-25

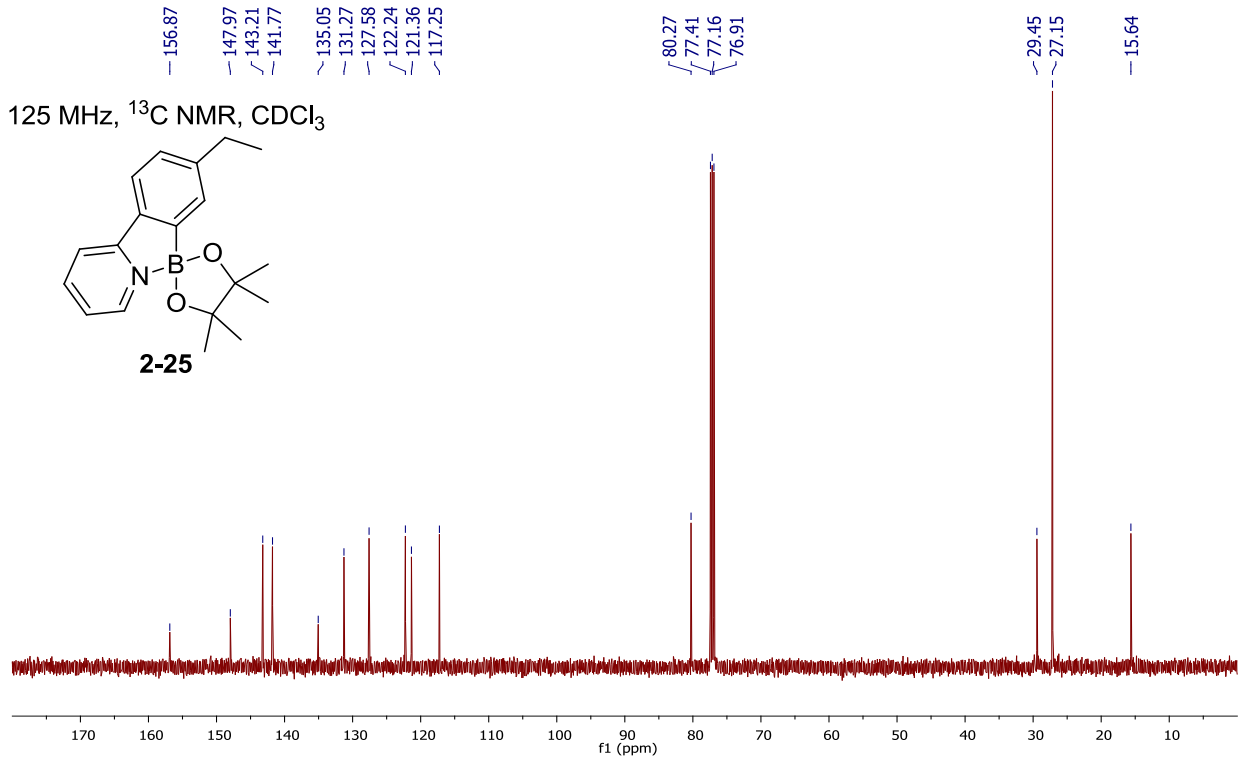
156.87
147.97
143.21
141.77
135.05
131.27
127.58
122.24
121.36
117.25
80.27
77.41
77.16
76.91
29.45
27.15
15.64
125 MHz, ^{13}C NMR, CDCl$_3$
N
B
O
O
2-25
170 160 150 140 130 120 110 100 90 80 70 60 50 40 30 20 10
f1 (ppm)

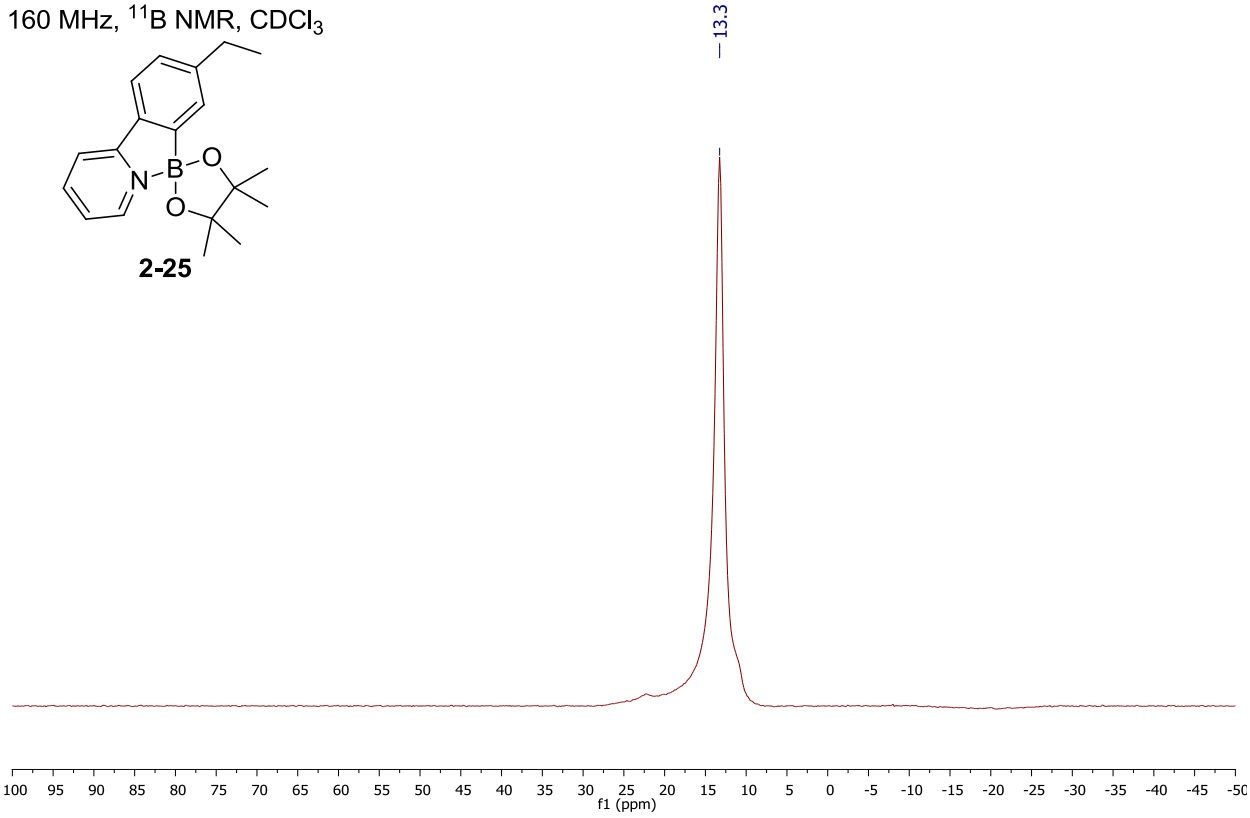
160 MHz, ^{11}B NMR, CDCl$_3$
13.3
N
B
O
O
2-25
100 95 90 85 80 75 70 65 60 55 50 45 40 35 30 25 20 15 10 5 0 -5 -10 -15 -20 -25 -30 -35 -40 -45 -50
f1 (ppm)

400 MHz, ^{1}H NMR, $CDCl_3$

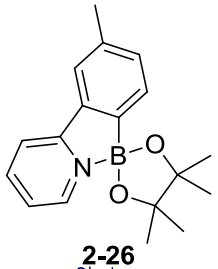

2-26

100 MHz, ^{13}C NMR, $CDCl_3$

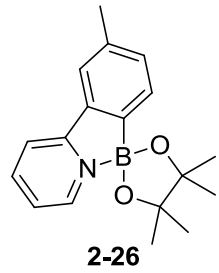

2-26

128 MHz, ^{11}B NMR, $CDCl_3$

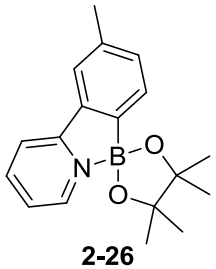

2-26

500 MHz, ^{1}H NMR, $CDCl_3$

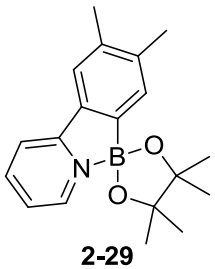

2-29

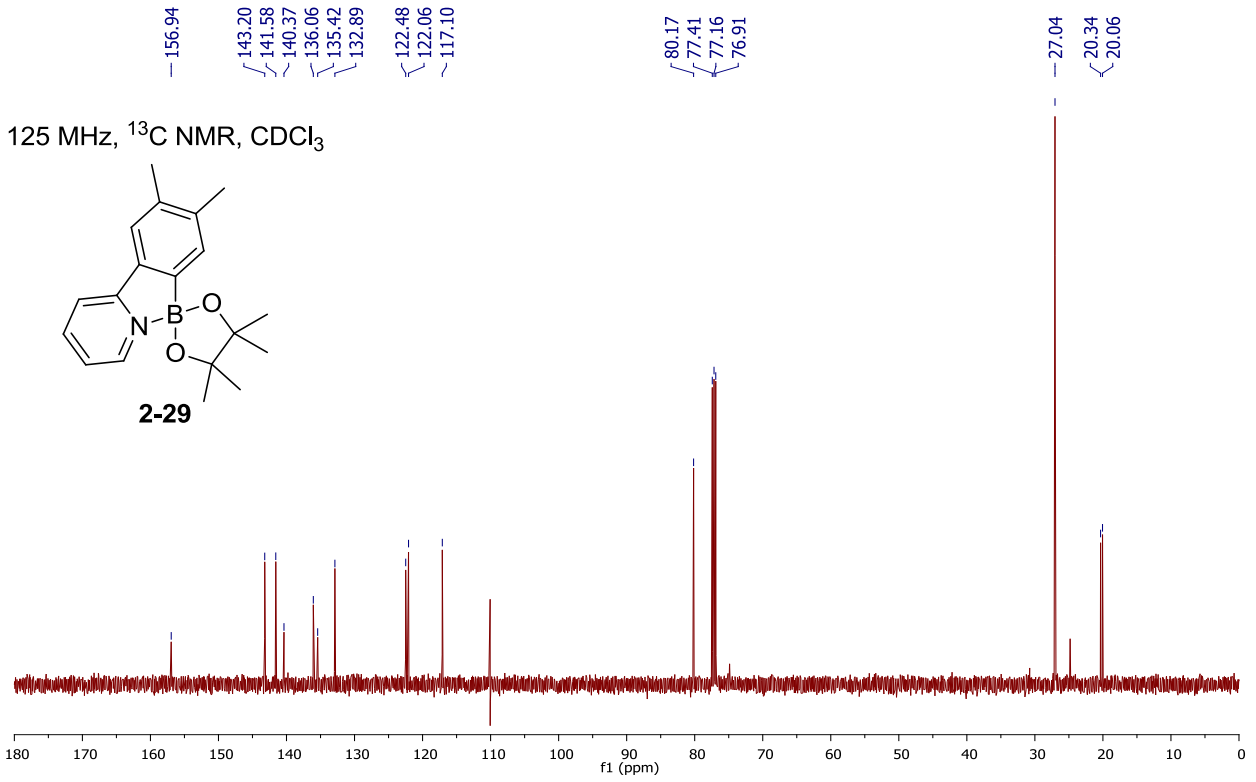
156.94
143.20
141.58
140.37
136.06
135.42
132.89
122.48
122.06
117.10
80.17
77.41
77.16
76.91
27.04
20.34
20.06
125 MHz, 13C NMR, CDCl3
N
B
O
O
2-29
f1 (ppm)

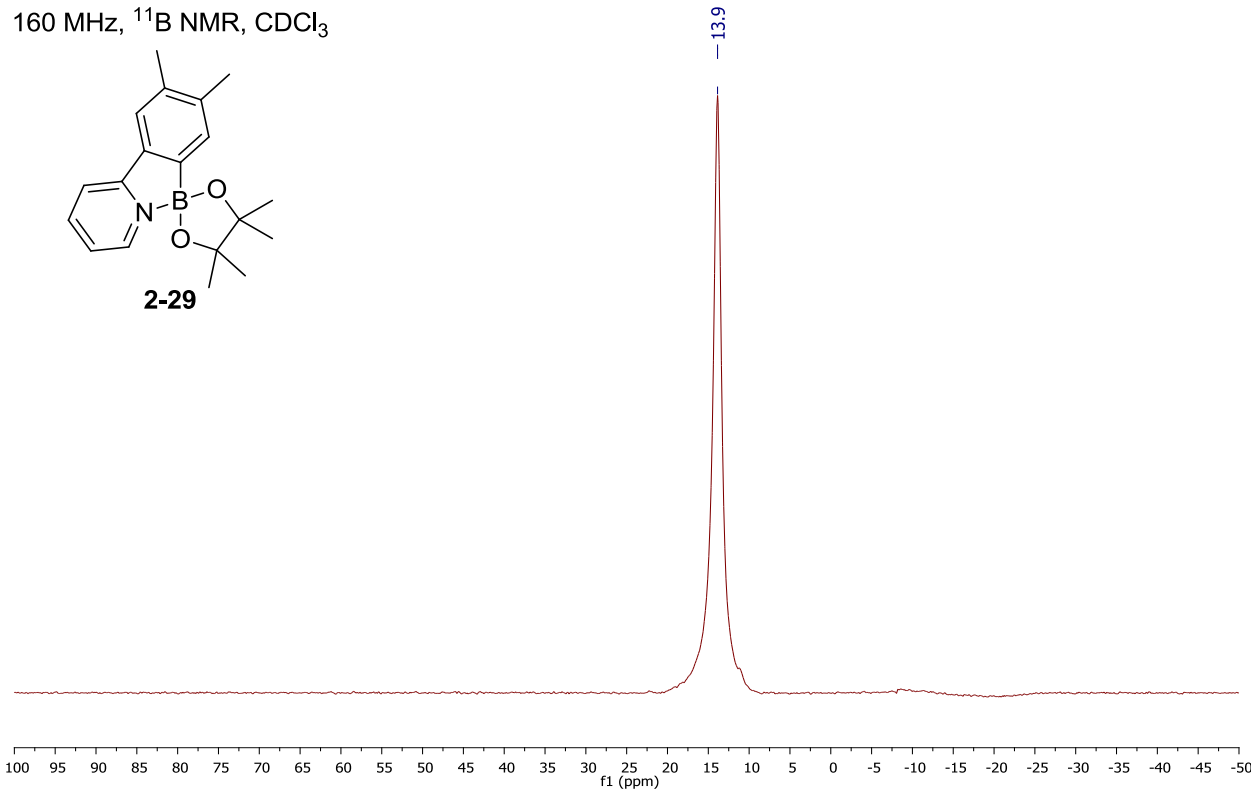
160 MHz, 11B NMR, CDCl3
13.9
N
B
O
O
2-29
f1 (ppm)

500 MHz, ^{1}H NMR, CD_2Cl_2

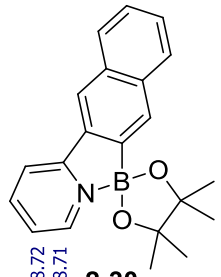

2-30

125 MHz, ^{13}C NMR, CD_2Cl_2

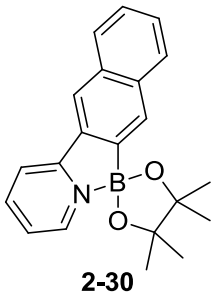

2-30

128 MHz, ^{11}B NMR, CD_2Cl_2

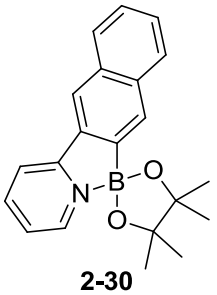

2-30

500 MHz, ^{1}H NMR, $CDCl_3$

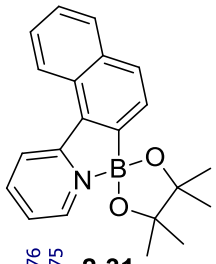

2-31

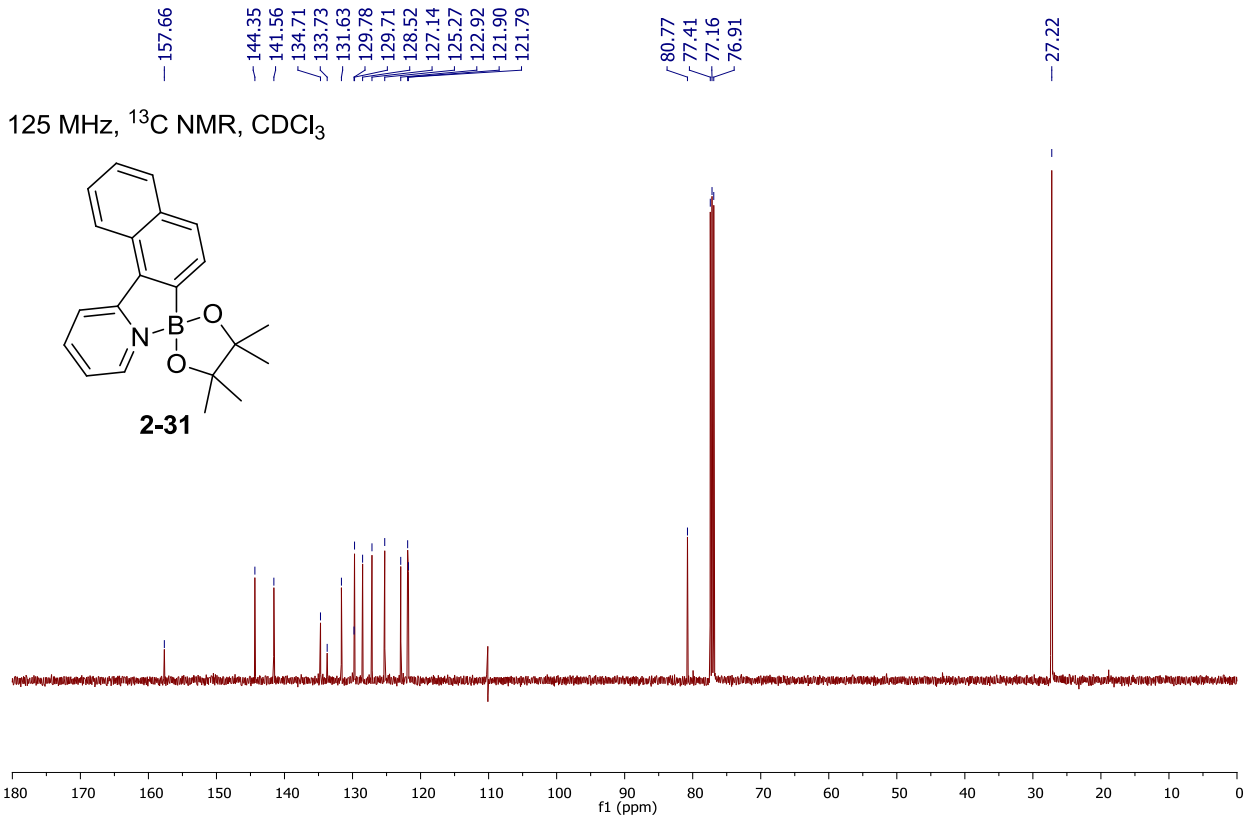
157.66
144.35
141.56
134.71
133.73
131.63
129.78
129.71
128.52
127.14
125.27
122.92
121.90
121.79
80.77
77.41
77.16
76.91
27.22
125 MHz, 13C NMR, CDCl3
N
B
O
O
2-31
f1 (ppm)

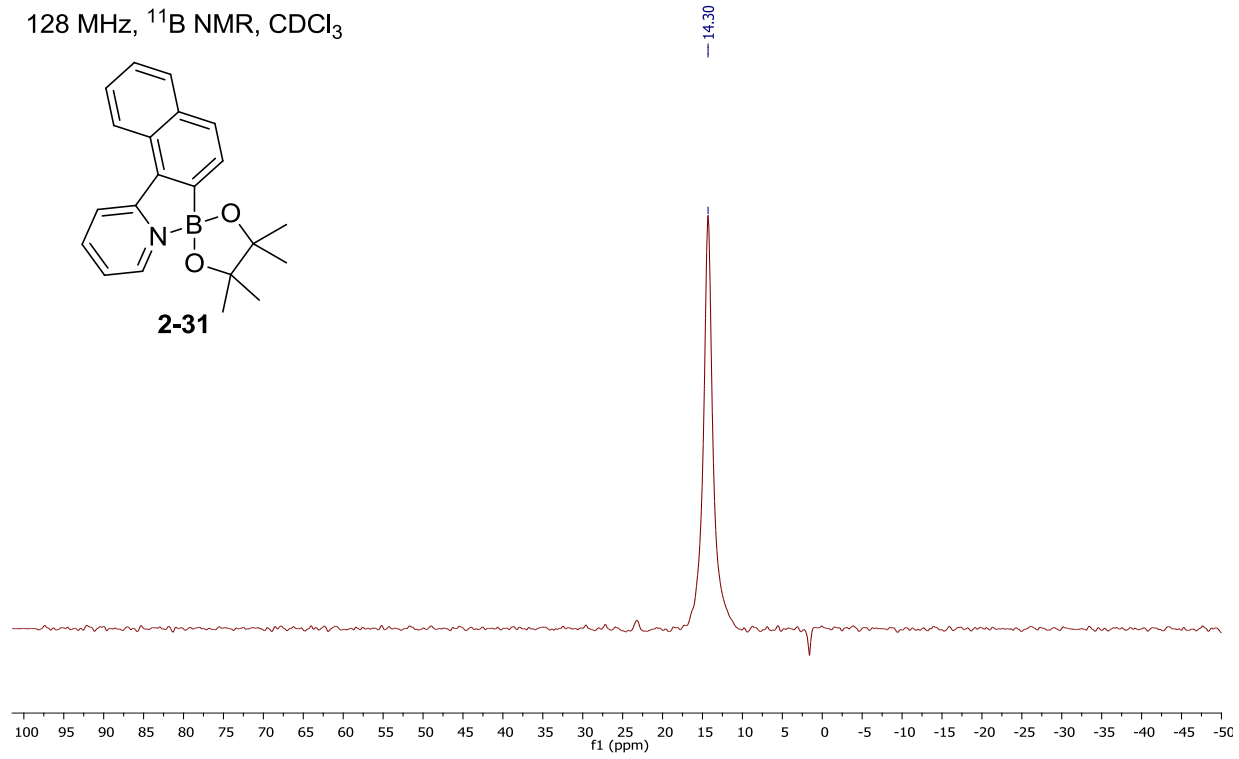
14.30
128 MHz, 11B NMR, CDCl3
N
B
O
O
2-31
f1 (ppm)

500 MHz, ^{1}H NMR, $CDCl_3$

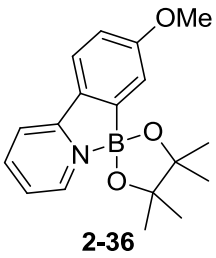

2-36

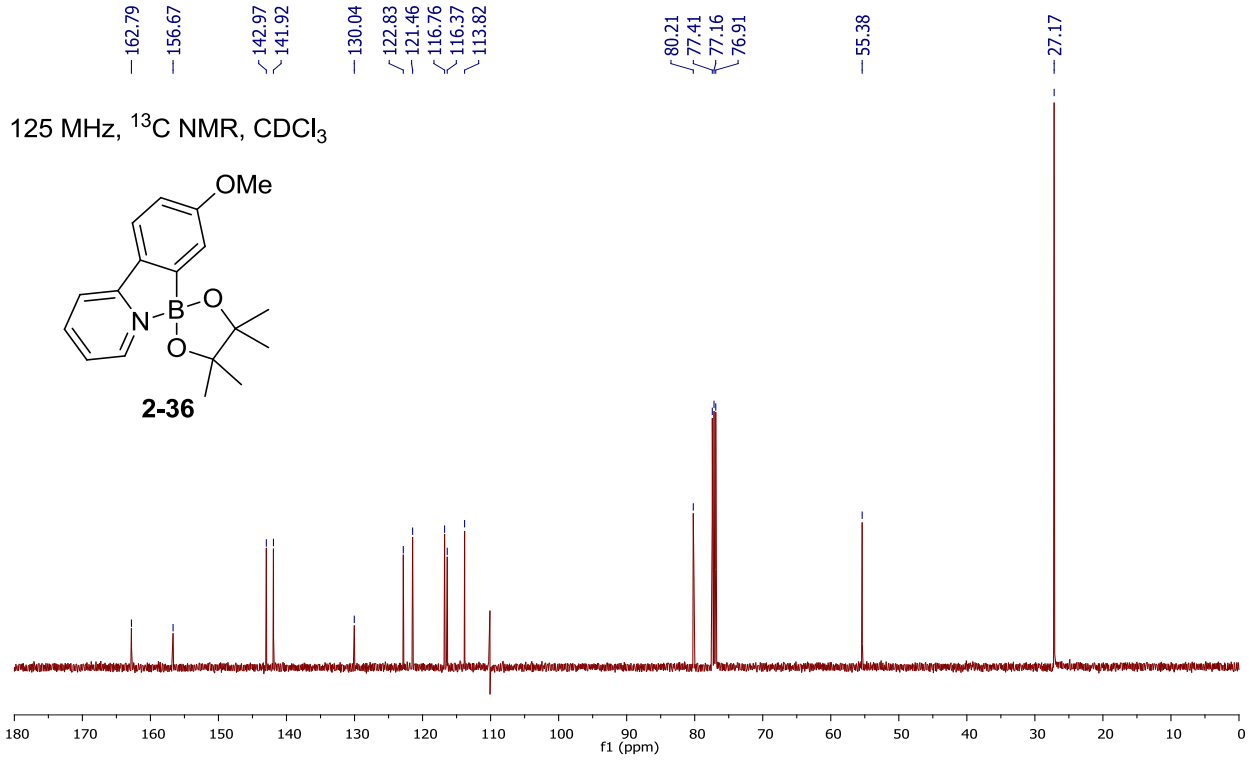

125 MHz, ^{13}C NMR, $CDCl_3$

2-36

128 MHz, ^{11}B NMR, $CDCl_3$

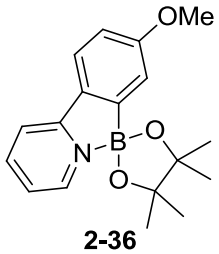

2-36

400 MHz, ^{1}H NMR, C_6D_6

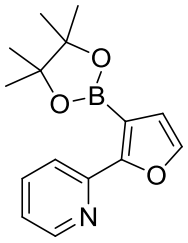

2-42

100 MHz, ^{13}C NMR, C_6D_6

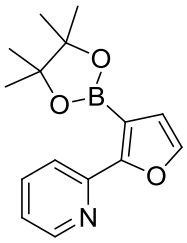

2-42

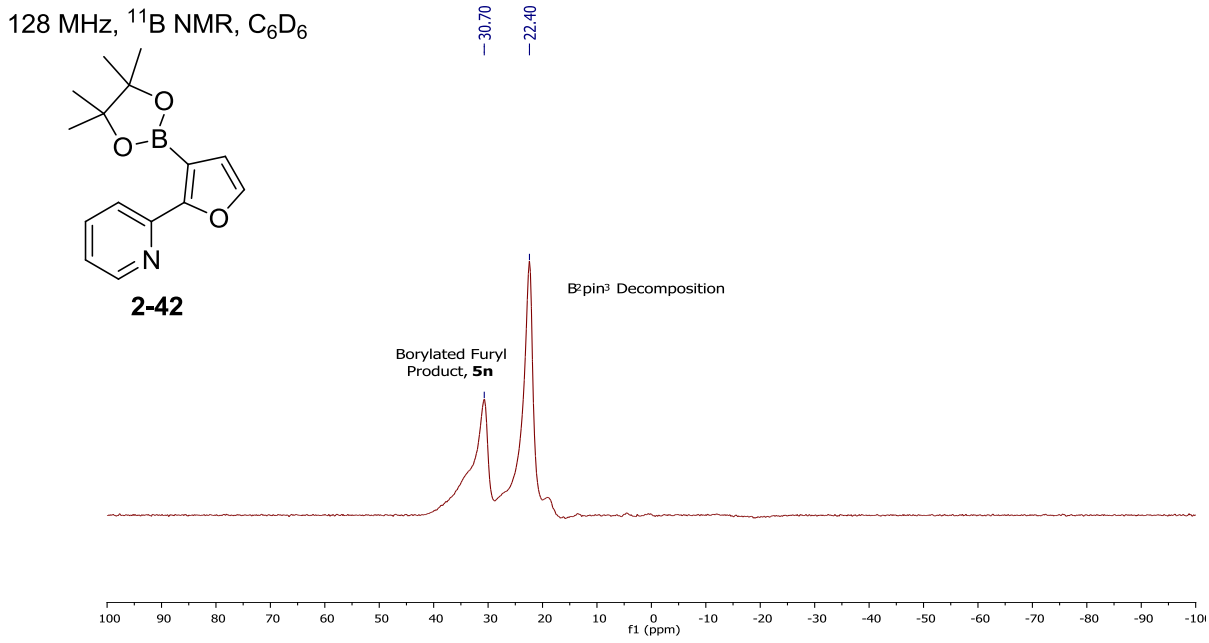

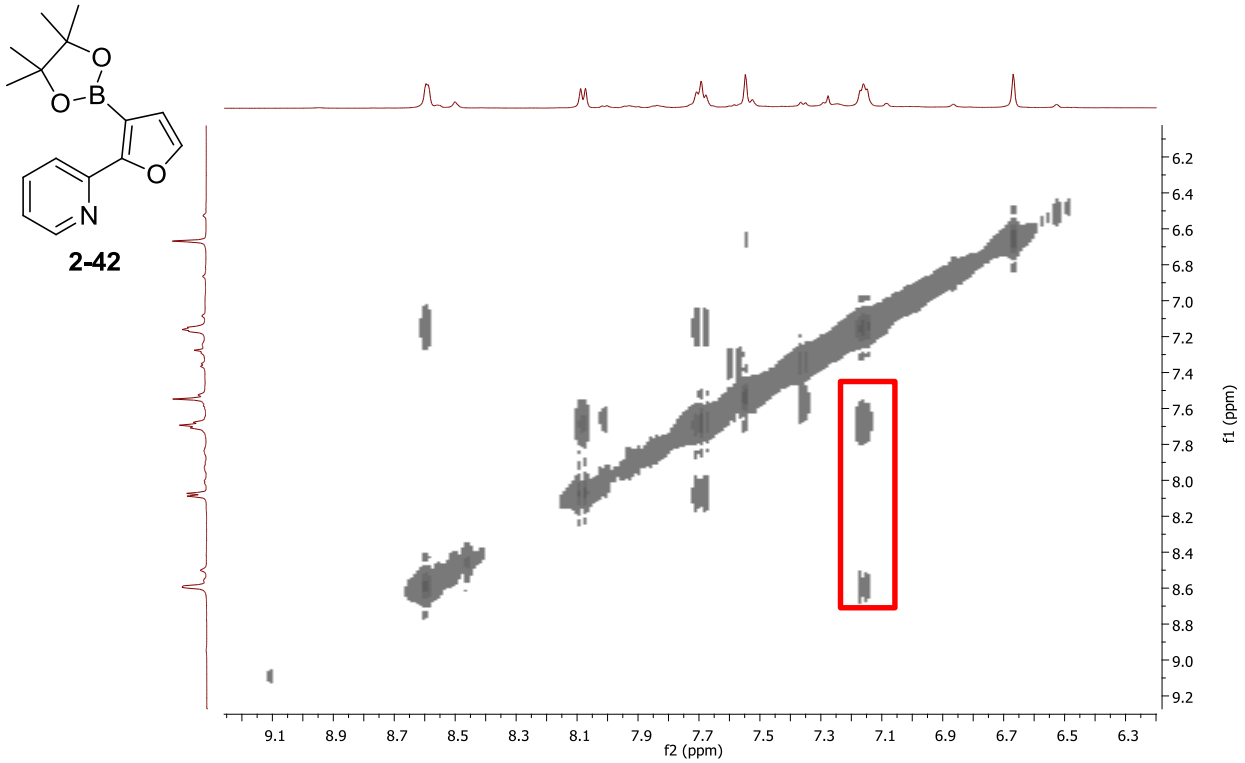

2–D COSY NMR of 2–(3–boronic acid pinacolate ester–furan–2–yl)pyridine derivative. The box highlights the presence of the proton at C5 on the furyl ring which was hidden as a result of the solvent. Further supporting formation of the C–H borylation product **2–42**.

400 MHz, ^{1}H NMR, $CDCl_3$

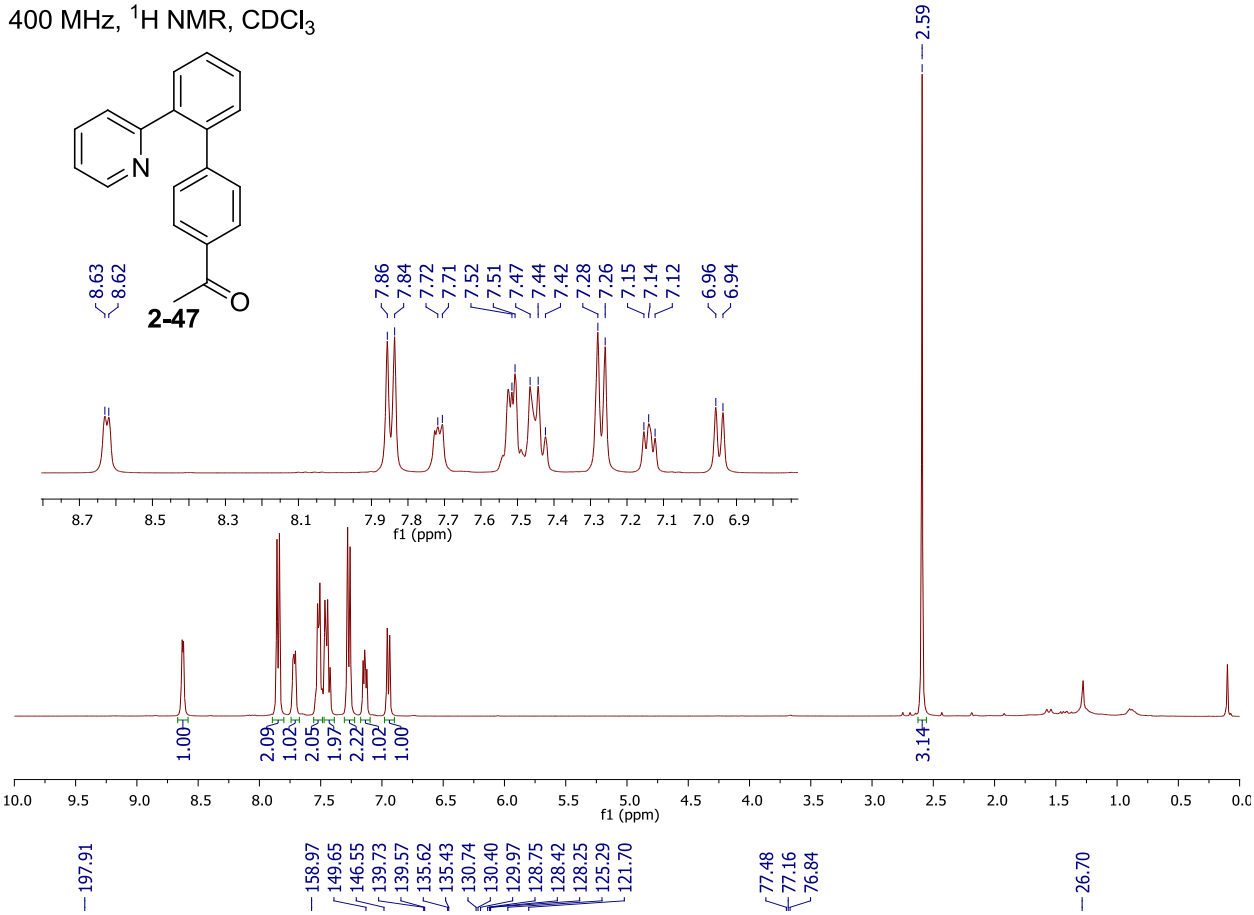

100 MHz, ^{13}C NMR, $CDCl_3$

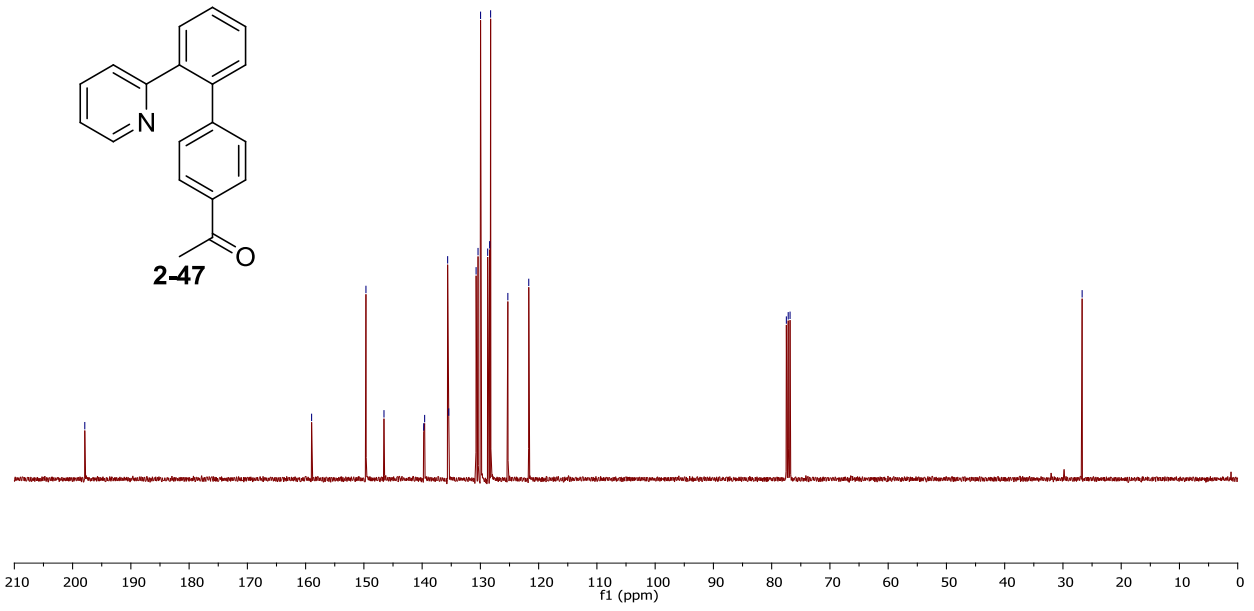

400 MHz, ^{1}H NMR, $CDCl_3$

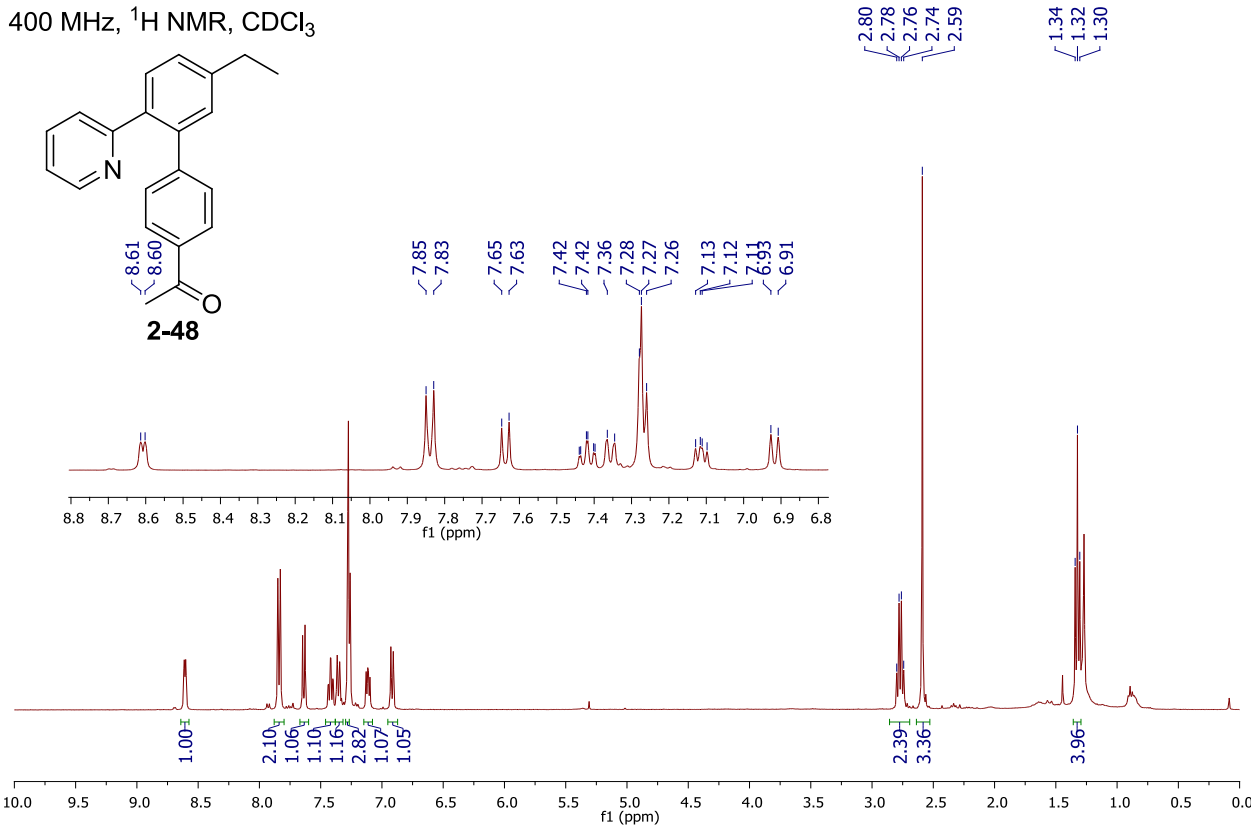

100 MHz, ^{13}C NMR, $CDCl_3$

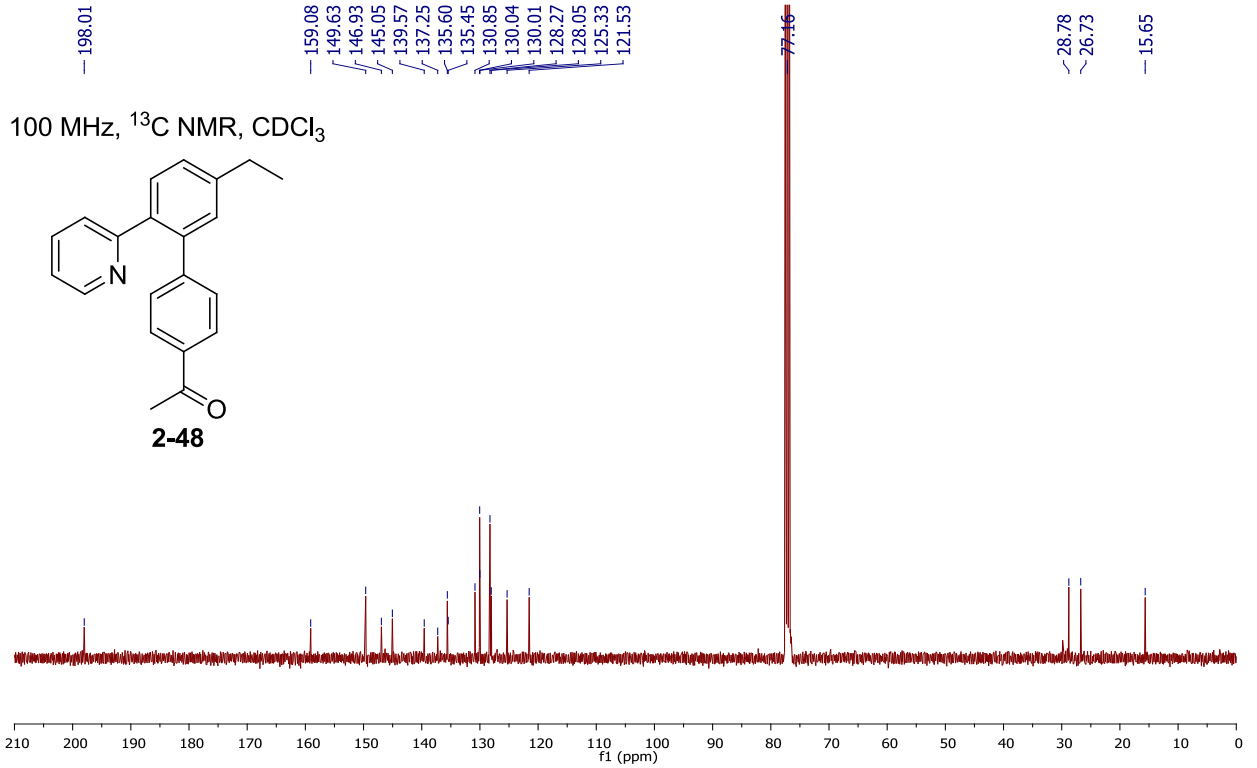

400 MHz, ^{1}H NMR, $CDCl_3$

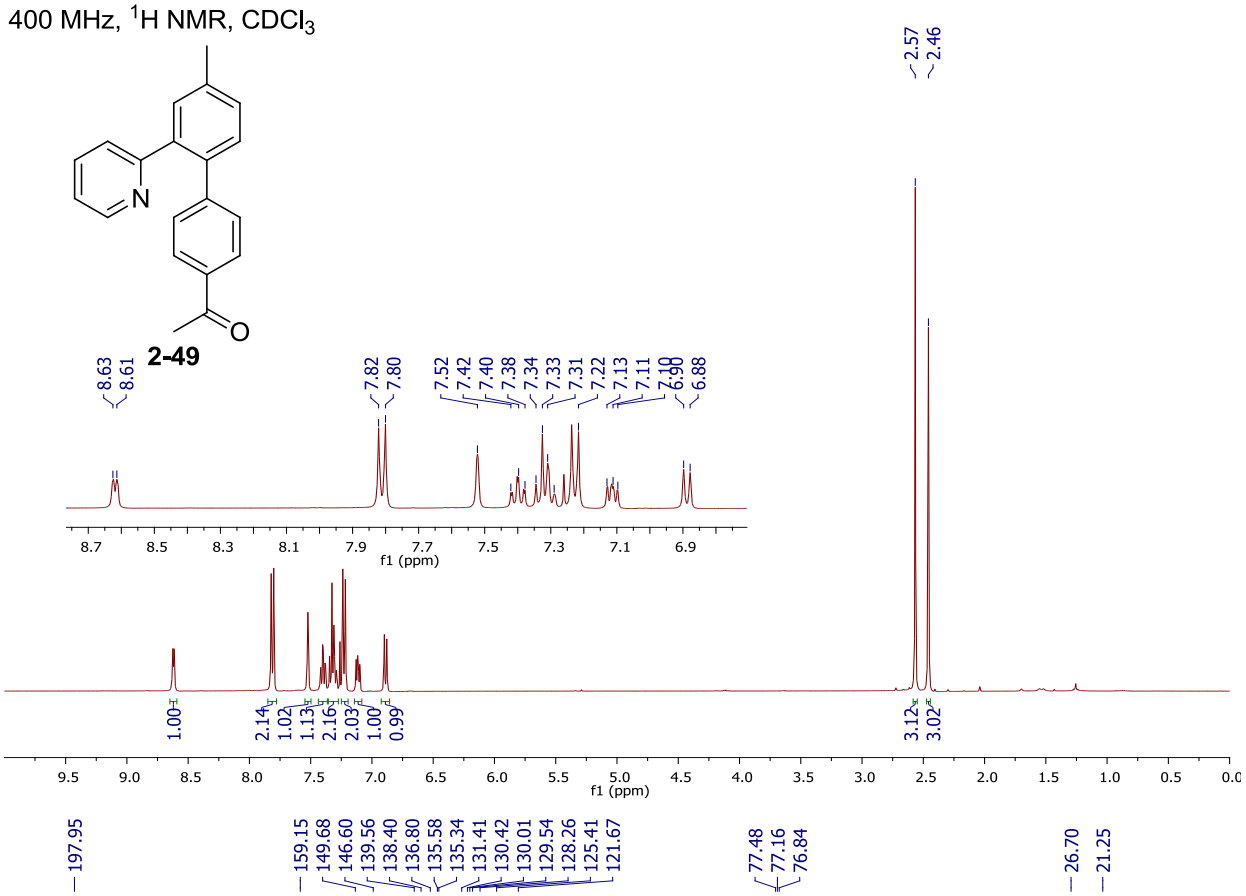

100 MHz, ^{13}C NMR, $CDCl_3$

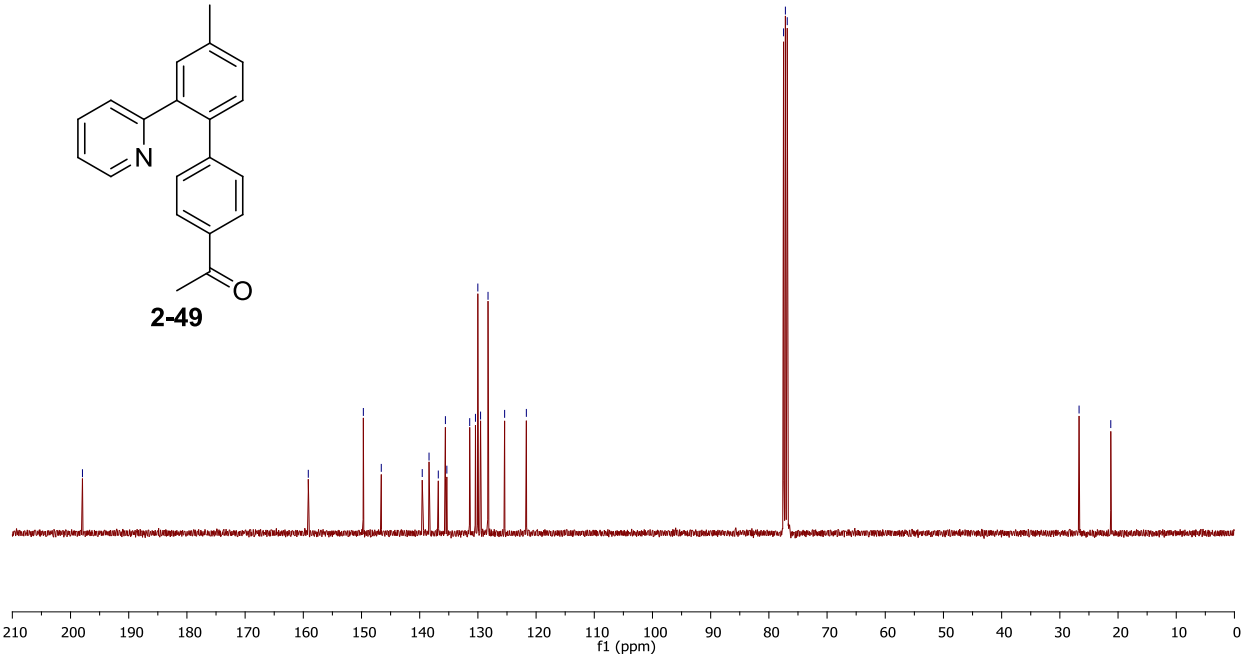

400 MHz, ^{1}H NMR, $CDCl_3$

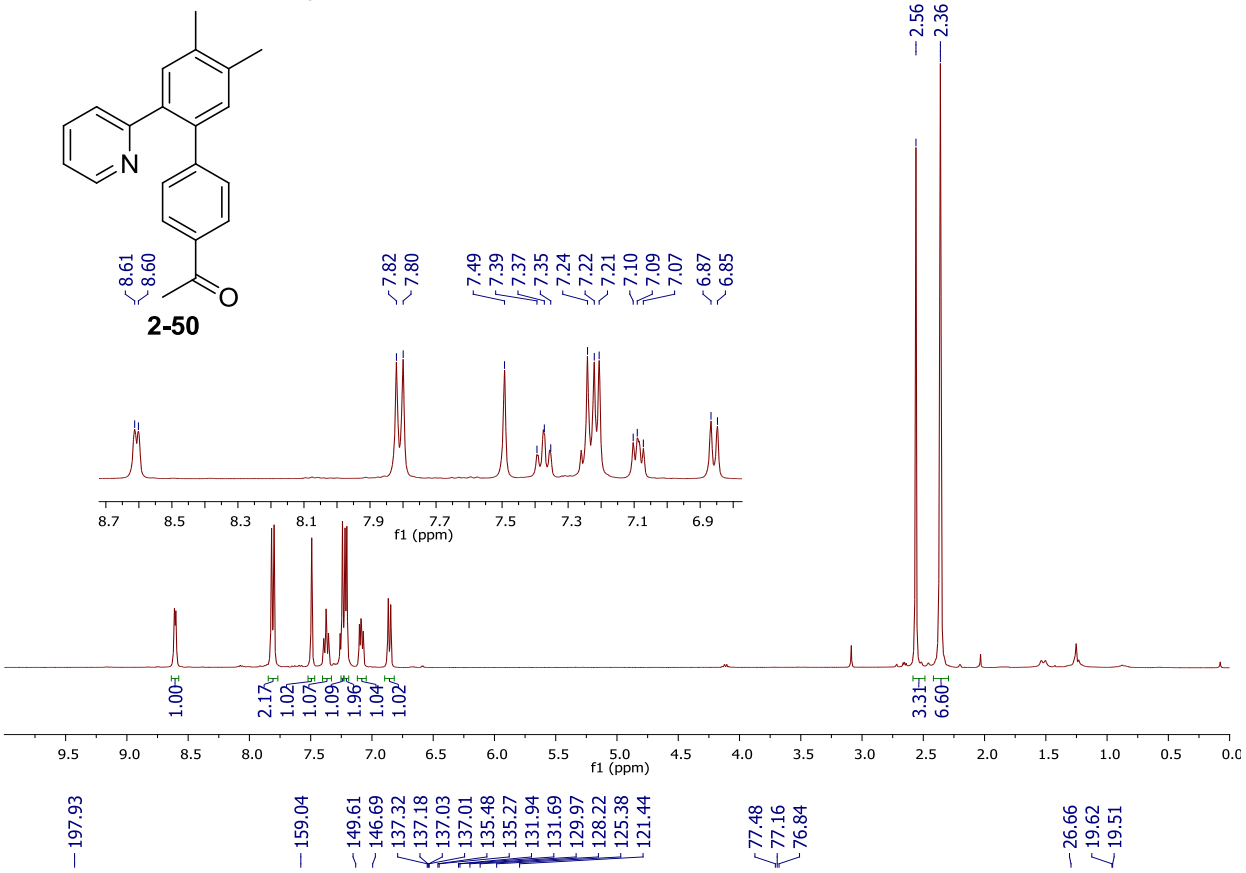

100 MHz, ^{13}C NMR, $CDCl_3$

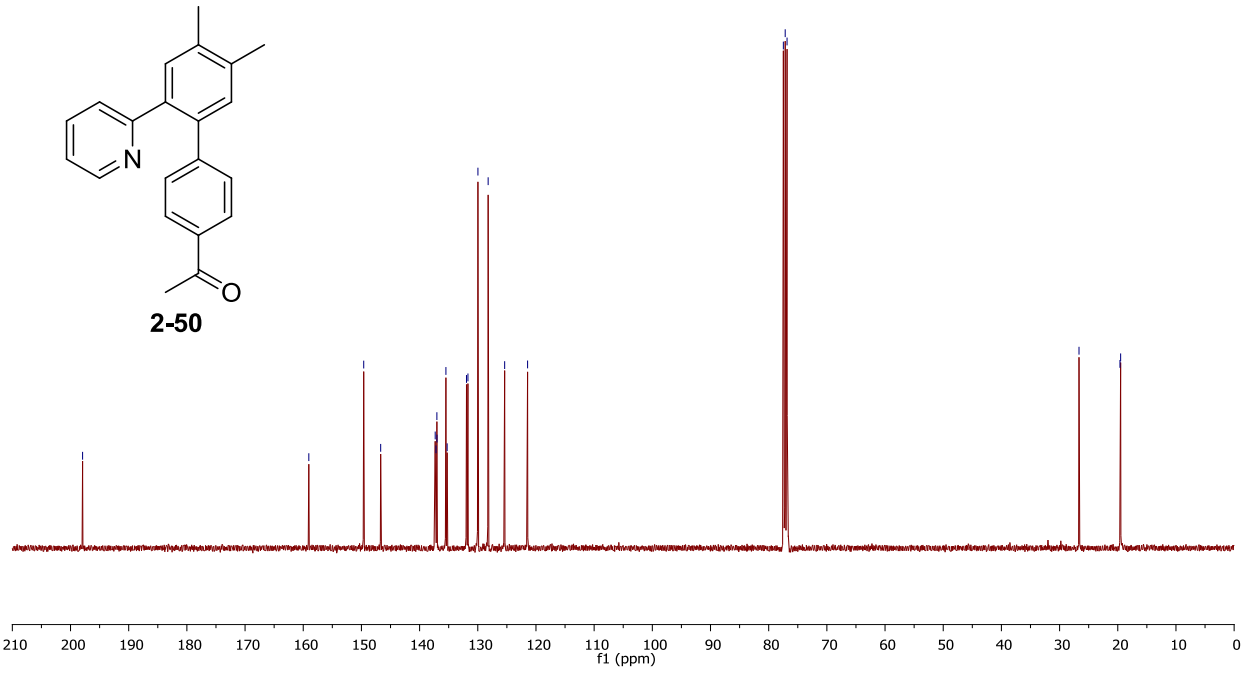

400 MHz, ^{1}H NMR, $CDCl_3$

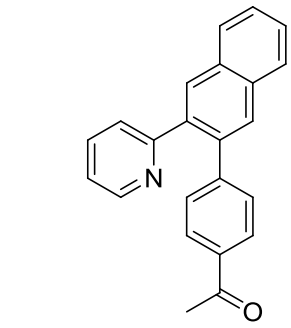

2-51

100 MHz, ^{13}C NMR, $CDCl_3$

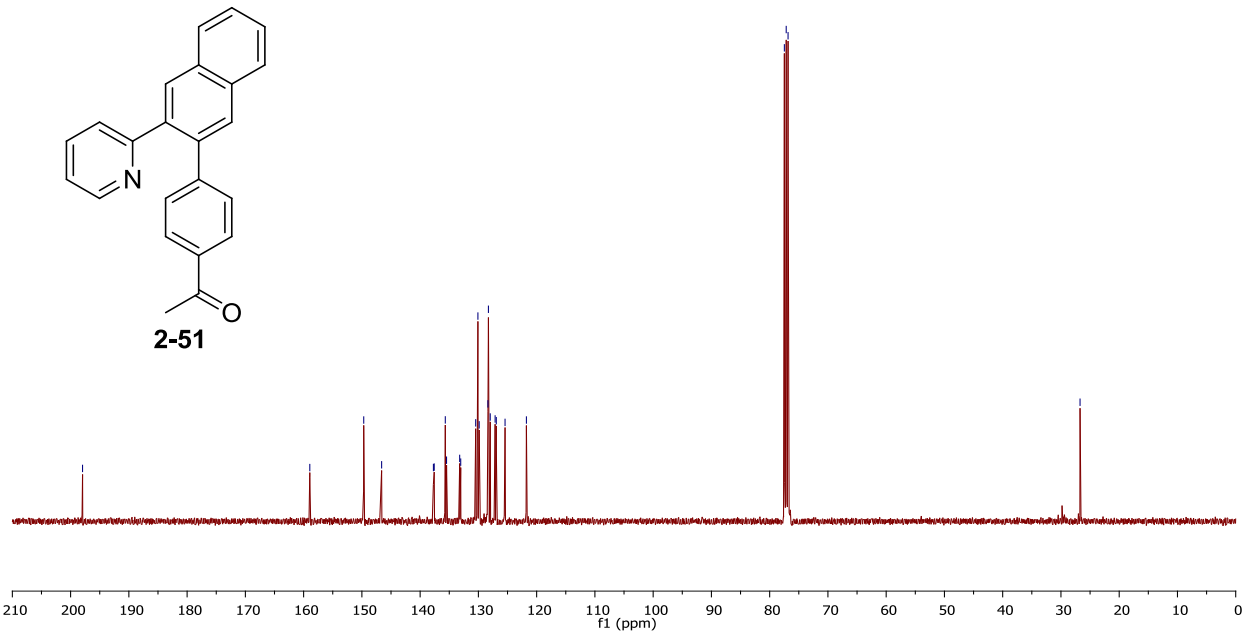

400 MHz, ^{1}H NMR, $CDCl_3$

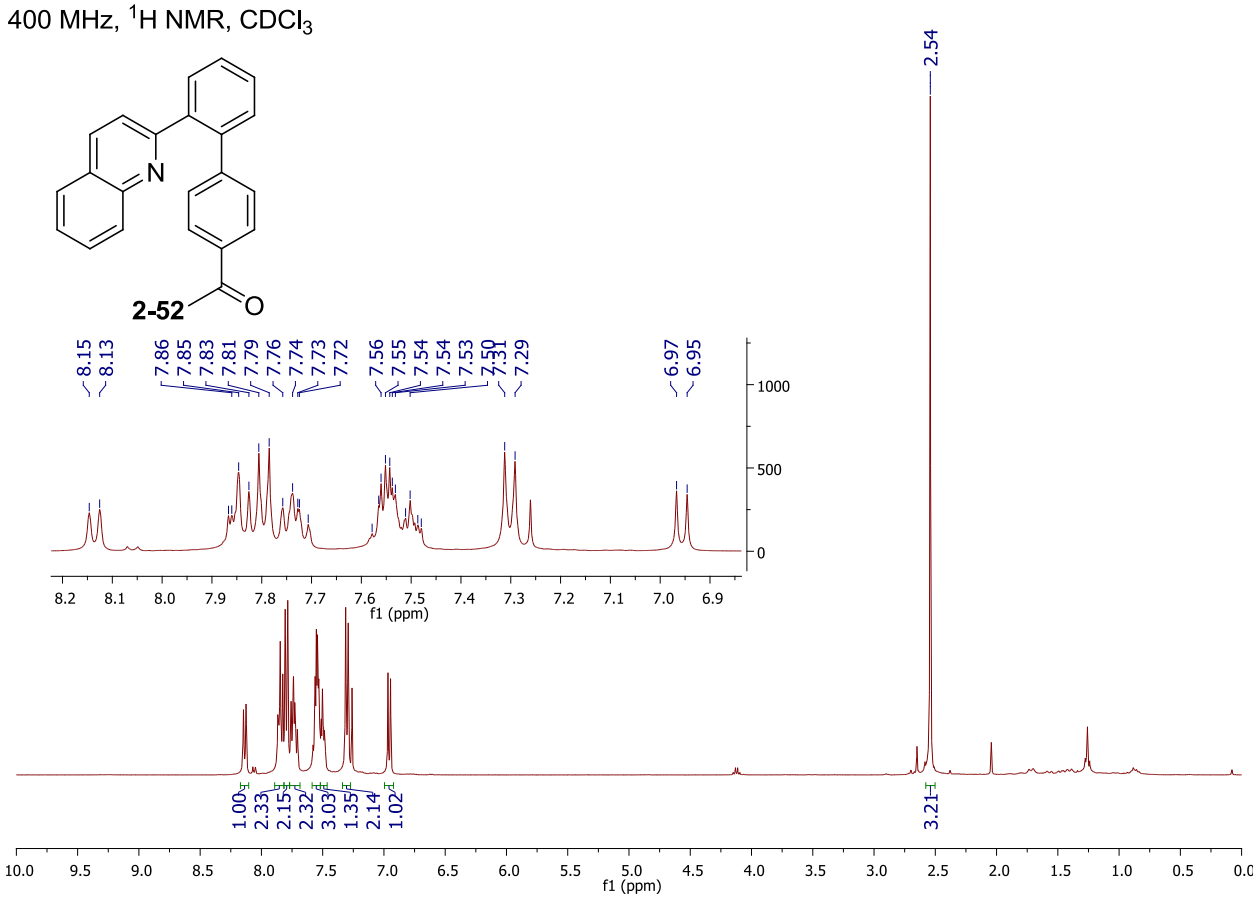

100 MHz, ^{13}C NMR, $CDCl_3$

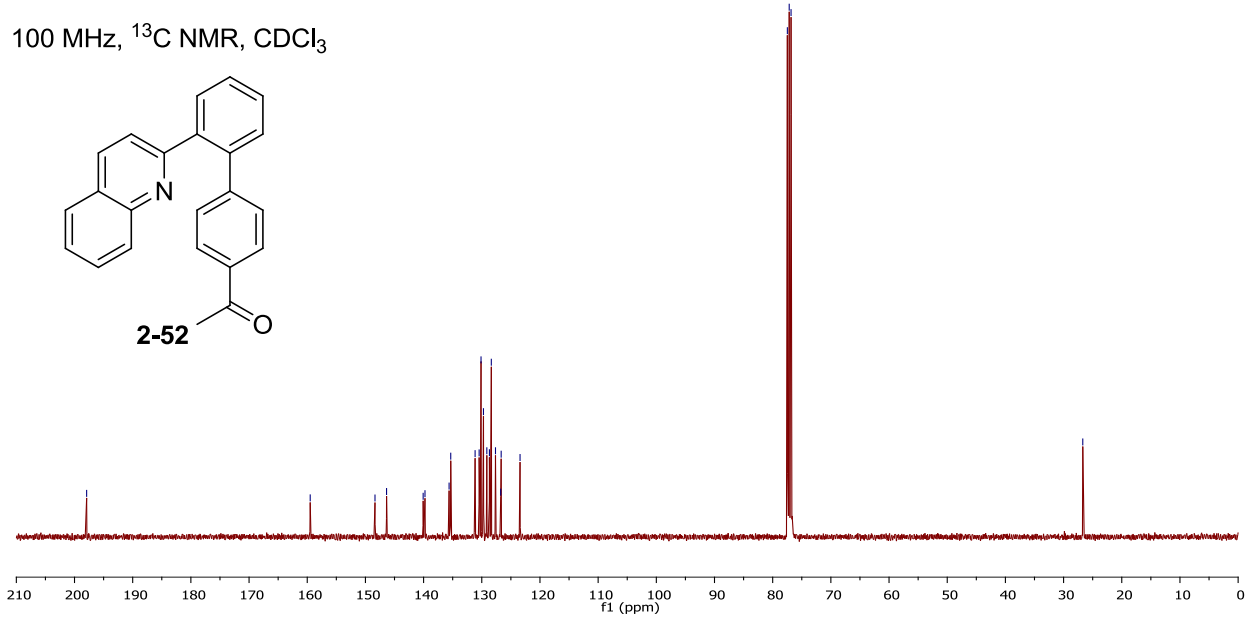

400 MHz, ^{1}H NMR, $CDCl_3$

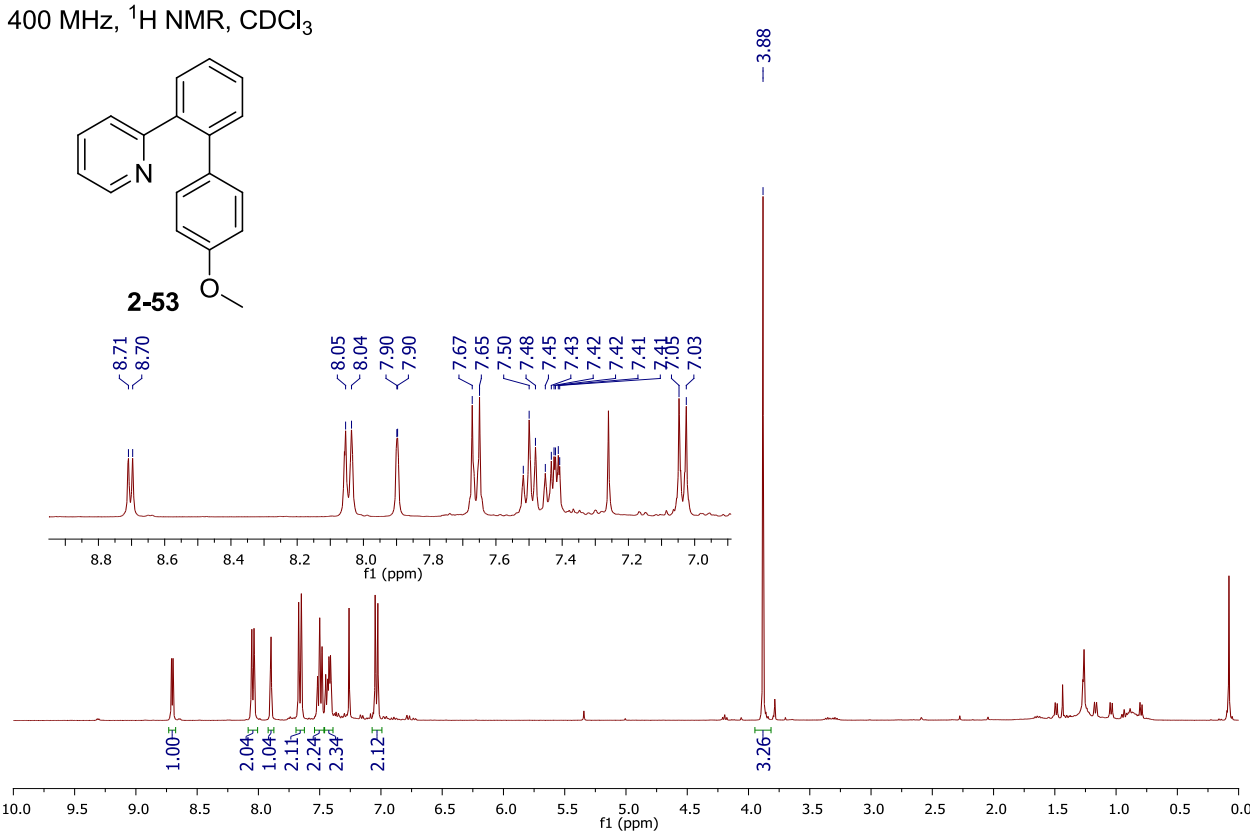

100 MHz, ^{13}C NMR, $CDCl_3$

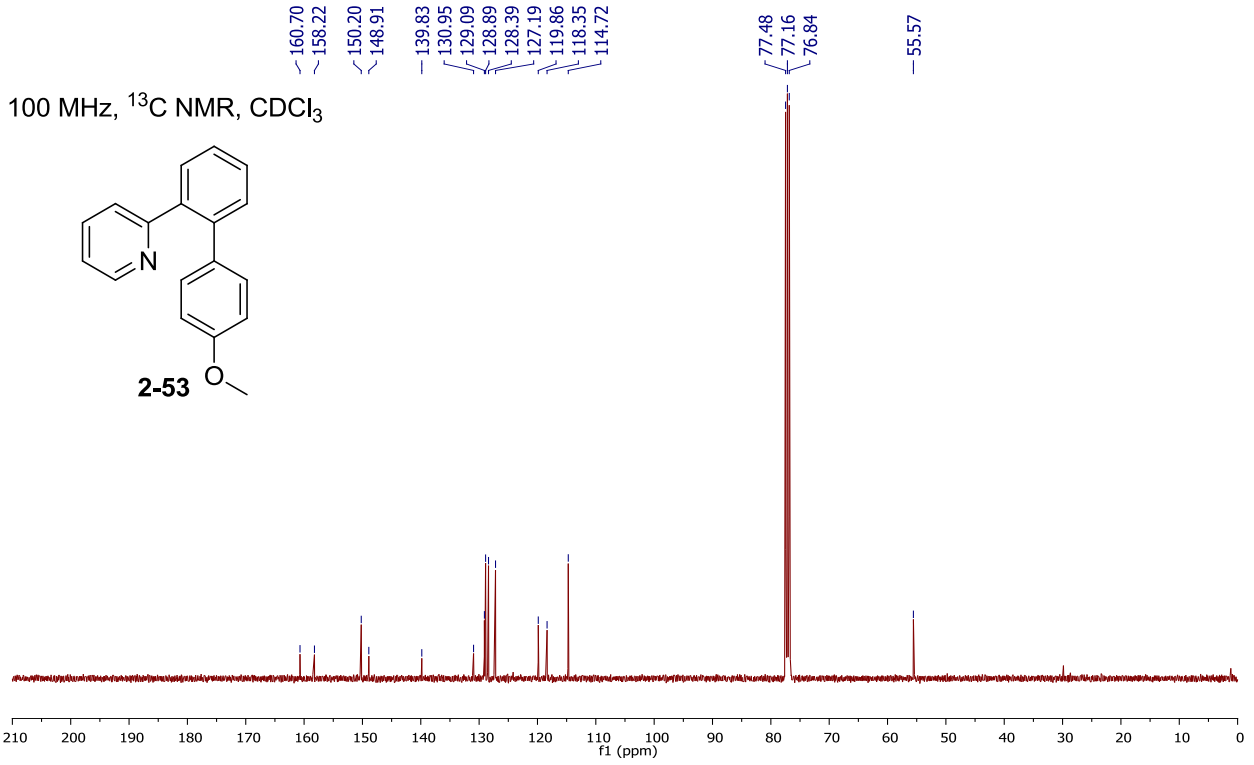

400 MHz, ^{1}H NMR, $CDCl_3$

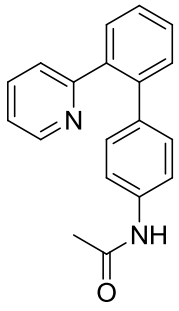

2-54

100 MHz, ^{13}C NMR, $CDCl_3$

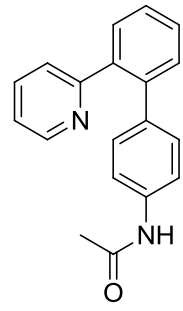

2-54